Experimental and Computational Investigation of Tacrine-Based Inhibitors of Acetylcholinesterase

Larry Douglas Williams, Jr.

Dissertation submitted to the faculty of the Virginia Polytechnic Institute and State University in partial fulfillment of the requirements for the degree of

Doctor of Philosophy
In
Chemistry

Paul R. Carlier, Chair
T. Daniel Crawford
Felicia Etzkorn
David G. I. Kingston
James M. Tanko

October 28, 2008
Blacksburg, Virginia

Keywords: Tacrine, acetylcholinesterase, bump-hole, density functional theory, coalescence

Copyright 2008, Larry Williams

Experimental and Computational Investigation of Tacrine-Based Inhibitors of Acetylcholinesterase

Larry Douglas Williams, Jr.

Abstract

Acetylcholinesterase (AChE) terminates cholinergic neurotransmission by catalyzing the hydrolysis of the neurotransmitter acetylcholine (ACh). Inhibition of AChE has proven an effective treatment for the memory loss exhibited by early stage Alzheimer's disease (AD) patients; four AChE inhibitors (AChEI) have been approved by the FDA for this purpose. The first AChEI approved for the palliative treatment of AD-related memory loss was 9-amino-1,2,3,4-tetrahydroacridine (tacrine).

Inhibition of AChE may present either therapeutic or toxic effects depending upon the dose administered. With the goal of discovering safe and effective pesticides to control the population of *Anopheles gambiae*, a malaria-transmitting mosquito indigenous to Sub-Saharan Africa, the reoptimization of the tacrine pharmacophore was undertaken. Because the optimized drug would necessarily be a poor inhibitor for human AChE (*h*AChE), initial ligand design focused on modification to tacrine known to negatively impact the inhibition potency for *h*AChE. Ultimately, an AChEI was discovered, which exhibited micromolar inhibition of *Anopheles gambiae* AChE (*Ag*AChE) and essentially no potency for *h*AChE. Two units of this lead compound were tethered through an alkyl chain to yield a nanomolar inhibitor of *Ag*AChE that was more than 1,100-fold selective for the mosquito enzyme over *h*AChE.

Dimerization of an active inhibitor is an effective strategy to increase the potency and selectivity of AChEI, and many examples of tacrine hetero- and homodimers complexed to AChE can be found in the RCSB Protein Data Bank (PDB). The bond formed between the exocyclic amine moiety and the heterocyclic ring system of tacrine is analogous to an amide bond when tacrine is protonated. Therefore, the rotational profile of protonated *N*-alkyltacrine should exhibit a conformational profile in which dihedral angles significantly out of the plane formed by the ring system are associated with high energies relative to those when the dihedral angles are nearly coplanar with the ring system. The barrier of rotation ($\Delta G^{\ddagger}$) produced by this phenomenon in two tacrine derivatives and two quinoline derivatives was experimentally

determined using dynamic ^{1}H NMR. These values were compared to density functional theory (DFT) derived values for the same phenomenon. Furthermore, since the $\Delta G^{\ddagger}$ proved to be impossible to experimentally determine for the optimal model compound for the active site portion of tacrine dimers, *N*-methyltacrine, the DFT method employed for modeling the $\Delta G^{\ddagger}$ of the tacrine and quinoline analogs was used to computationally derive the entire rotational conformation diagram of *N*-methyltacrine. The calculated values were then used to comment on the relative energies of adopting certain conformations found in the X-ray crystal structures of dimer/AChE complexes.

Acknowledgements

I would like to begin by expressing my heartfelt gratitude for my advisor, Dr. Paul R. Carlier. He has constantly shown me the importance of a skeptical approach to science, a skill that will continue to serve me well in the coming days. Likewise, I would like to acknowledge the dedication and assistance of my advisory committee, Dr. T. Daniel Crawford, Dr. Felicia Etzkorn, Dr. David G. I. Kingston, and Dr. James M. Tanko.

The mosquito project was a multidisciplinary endeavor, and very many people were directly involved in its successes. First, Dr. Jeff R. Bloomquist and Dr. Troy D. Anderson of the Department of Entomology have my gratitude for generating the bioassay data for my compounds. Next, I would like to thank Dr. Sally L. Paulson, Ania Wysinski, Dr. Eric Wong, and Ranginee Choudhury for generously providing *Ag*AChE. Finally, I would like to thank Deborah W. Carlier for being the glue that held the project together.

Research in the Carlier group is never in isolation. I would like to thank all of the members, past and present, who have impacted my graduate career. I am especially indebted to Dr. Ella Clement, Dr. H. Jason Harmon, Dr. Danny Hsu, and Dr. Dawn M. Wong for many helpful discussions.

I would like to thank Bill Bebout for performing mass spectroscopy for my compounds. Tom Glass and Hugo Azurmendi provided copious assistance in the NMR lab, for which I am grateful. My research was funded through the Department of Chemistry and the Foundation for the National Institute Health Grand Challenges in Global Health (GCGH-1497).

I would like to acknowledge my parents, Larry and Cheryl, for encouragement through the years. Finally, I would like to thank my generous and thoughtful wife, Sharlene Williams. Without her patience and encouragement, I would not have come so far.

Dedication

To my wife, the love of my life.

Table of Contents

Abstract ii
Acknowledgements iv
Dedication v
Table of Contents vi
List of Figures viii
List of Schemes x
List of Tables xi
List of Abbreviations xii

Chapter 1 . 9-Amino-1,2,3,4-tetrahydroacridine and its Analogs as Acetylcholinesterase Catalytic Active Site Inhibitors 1

1.1 Structure and function of acetylcholinesterase 1
1.2 Approved therapeutic AChEI 3
1.3 Historical perspective of the discovery and clinical use of tacrine 7
1.4 Bivalent inhibitor studies 9
1.5 Crystallographic evidence for CAS preference 15
1.6 Modifications undertaken to improve AChE/BuChE selectivity 20
1.7 Conclusions 26
References for Chapter 1 26

Chapter 2 . Bump-Hole Optimization of Tacrine Produces a Potent, Species-Selective Inhibitor of *Ag*AChE 33

2.1 Introduction 33
2.2 Results and Discussion 33
2.2.1 Initial considerations in ligand design 33
2.2.2 Inhibitor design and synthesis 36
2.2.3 Dimerization of the lead compound 44
2.3 Conclusion 50
References for Chapter 2 51

Chapter 3 . Experimental Procedures for Bump-Hole Optimized AChEI 54

3.1 General information 54
3.2 Synthesis of tacrine derivatives via the Friedländer Condensation 55
3.3 Synthesis of Bump-Hole optimized tacrine dimers 63
3.3.1 Synthesis of 2,12-dichloro-6,7,8,9,10,11-hexahydrocycloocta[*b*]quinoline 63
3.3.2 Synthesis of the amino-terminated *N*-alkyltacrine derivatives 64
3.3.3 Synthesis of bump-hole optimized tacrine dimers 70
3.4 Computational details 76
3.4.1 Conformational analysis calculation 76
3.4.2 DFT optimization of MMFF generated conformations 78

References for Chapter 3 81

Chapter 4 . Computational and Experimental Studies of Conformational Energies of Tacrine Analogs 84

4.1 Introduction and motivation 84
4.2 Determination of Rotational Barriers 87
4.2.1 Experimentally determined rotational barriers 87
4.2.2 Calculated rotational barriers 91
4.3 Calculation of the rotational potential energy surface of *N*-methyltacrine 96
4.4 Relationship to virtual ligand screening and conclusion 107
References for Chapter 4 108

Chapter 5 . Experimental and Computational Procedures for Tacrine Derivative Rotational Barriers 112

5.1 Experimental Details 112
5.1.1 Synthetic details 112
5.1.2 Calibration for variable temperature ^{1}H NMR 112
5.2 Computational details 114
5.2.1 Conformational energy calculations 114
5.2.1.1 Cartesian coordinates for constrained optimization calculations of $16{\cdot}H^{+}$ 115
5.2.1.2 Cartesian coordinates for constrained optimization calculations of 17 170
5.2.1.3 Tabulation of energies obtained in the constrained optimizations 235
5.2.2 Calculation of rotational barriers. 242
5.2.2.1 Cartesian coordinates for calculated rotational barriers 242
5.2.2.2 Tabulation of calculated rotational barrier results 264
References for Chapter 5 264

Chapter 6 . Conclusions and Future Directions 266

6.1 Re-optimization of the tacrine pharmacophore 266
6.2 Rotational barriers of *N*-alkyltacrines 267
References for Chapter 6 268

List of Figures

Figure 1.1. X-ray crystal structure of acetylcholine docked to native *Tc*AChE (PDB ID 2ACE) 2
Figure 1.2. Schematic of *Tc*AChE which emphasizes the catalytic gorge 3
Figure 1.3. FDA approved AChEI for the treatment of Alzheimer's related dementia..... 3
Figure 1.4. X-ray crystal structure of E2020 **2** complexed to *Tc*AChE (PDB ID 1EVE) 4
Figure 1.5. X-ray crystal structure of galanthamine **3** complexed to *Tc*AChE (PDB ID 1DX6) . 5
Figure 1.6. X-ray crystal structure of Rivastigmine **4** complexed to *Tc*AChE (PDB ID 1GQR). 6
Figure 1.7. X-ray crystal structure of Tacrine **1** complexed to *Tc*AChE (PDB ID 1ACJ) 7
Figure 1.8. Sarin..... 8
Figure 1.9. 9-Amino-1,2,3,4-tetrahydroacridin-1-ol, velnacrine 9
Figure 1.10. Tacrine homodimers 10
Figure 1.11. Tether-length dependence of tacrine homodimers. 11
Figure 1.12. X-ray crystal structure of **7g** complexed with *Tc*AChE (PDB ID 2CKM) 12
Figure 1.13. X-ray crystal structure of **7e** complexed with *Tc*AChE (PDB ID 2CMF) 13
Figure 1.14. Heterodimeric tacrine inhibitors of AChE..... 14
Figure 1.15. Substituents (R) of tacrine based AChEI **12** – **16** complexed to AChE. 15
Figure 1.16. Overlay of *Dm*AChE complex with *N*-benzyltacrines **12** and **13** 16
Figure 1.17. Sharpless's ligand set for i*n situ* click chemistry 17
Figure 1.18. Overlay of *Mm*AChE complex with *in situ* click chemistry products..... 18
Figure 1.19. Huperzine A (**21**) and soman (**22**) 18
Figure 1.20. Tetrahydroquinolone 19
Figure 1.21. Overlay of *Tc*AChE complexed with bivalent inhibitors (*R*)-**15** and (±)-**15**..... 19
Figure 1.22. Overlay of *Tc*AChE complexed with various bivalent inhibitors 20
Figure 1.23. Inhibitors from the Kaul study..... 21
Figure 1.24. Tacrine analogs differing only by the size of the cycloalkyl ring 22
Figure 1.25. Modified tacrines optimized for *in vivo* pharmacological profiles..... 22
Figure 1.26. Tacrine derivatives described by Gregor et al and Recanatini et al 23
Figure 1.27. Tacrine derivative homodimers from the study of Hu et al..... 25
Figure 2.1. Tacrine 33
Figure 2.2. Alignment of *Torpedo californica*, human, and *Anopheles gambiae* AChE..... 34
Figure 2.3. Full-length protein as encoded for by *Ag ace*-1 and the W38 construct 35
Figure 2.4. Bump-hole optimized modified 7-chlorotacrine **8c**..... 42
Figure 2.5. Correlation between assay results versus W38 construct and homogenate..... 43
Figure 2.6. Ground state structures of protonated **8c** as calculated using B3LYP/6-31G* 44
Figure 2.7. Ground state structure of protonated **8c** conformation **A** 44
Figure 2.8. Combined dose-response curves for bump-hole optimized tacrine dimer **20h** 49
Figure 2.9. Tether-length dependence of bump-hole optimized tacrine dimers **20c** – **l** 50
Figure 4.1. Structure of tacrine (**1**) and resonance in protonated *N*-alkyltacrines (**2**·H^+) 84
Figure 4.2. Substituents (R) of *N*-alkyltacrine based ligands **3** – **11** complexed to AChE..... 86
Figure 4.3. Ground state and C-N bond rotation transition structures of a simple amide 87
Figure 4.4. Free base structures of compounds studied by variable temperature ^{1}H NMR..... 88
Figure 4.5. Variable temperature ^{1}H NMR of 4-aminoquinaldine HCl (**12**·HCl) 89
Figure 4.6. Variable temperature ^{1}H NMR of tacrine HCl (**1**·HCl)..... 90
Figure 4.7. Variable temperature ^{1}H NMR of 9-azetidinyl substituted tacrine TFA (**13**·TFA).. 90

Figure 4.8. Variable temperature ^{1}H NMR of *N*,*N*-dimethylquinoline HCl (**14**·HCl)..... 90
Figure 4.9. Schematic of ground state destabilization of 15·H^+ relative to 1·H^+ 91
Figure 4.10. Protonated *N*-methyltacrine (**16**·H^+) and its formamide complex (**17**) 91
Figure 4.11. Calculated structures for protonated tacrine **1**·H^+ 93
Figure 4.12. Calculated structures for protonated 4-aminoquinaldine **12**·H^+ 93
Figure 4.13. Calculated structures for protonated 9-azetidinylsubstituted tacrine **13**·H^+ 94
Figure 4.14. Calculated structures for protonated *N*,*N*-dimethylquinoline **14**·H^+ 94
Figure 4.15. Calculated structures for protonated *N*-methyltacrine **16**·H^+ 96
Figure 4.16. Conformational diagram of protonated *N*-methyltacrine **16**·H^+ 97
Figure 4.17. Calculated structures for protonated *N*-methyltacrine **16**·H^+ at $\theta = 250°$..... 98
Figure 4.18. Conformational diagram of protonated 4-aminoquinaldine **12**·H^+ 100
Figure 4.19. Conformational diagram of protonated tacrine **1**·H^+ 101
Figure 4.20. Conformational diagram of protonated 9-azetidinyl substituted tacrine **13**·H^+.... 102
Figure 4.21. Conformational diagram of protonated *N*,*N*-dimethylquinoline **14**·H^+ 103
Figure 4.22. Conformational diagram of protonated *N*,*N*-dimethyltacrine **15**·H^+ 104
Figure 4.23. Composite curves of **16**·H^+ and **17** 105
Figure 5.1. Calibration curve used for all variable temperature ^{1}H NMR experiments 113

List of Schemes

Scheme 1.1. Catalytic cycle of acetylcholinesterase 1
Scheme 2.1. The Ellman Assay 35
Scheme 2.2. Friedländer condensation reaction scheme 36
Scheme 2.3. Schematic of double mutant strategy of tacrine modification 37
Scheme 2.4. Synthesis of 9-chloro-1,2,3,4-tetrahydroacridine **15** and tacrine homodimers..... 45
Scheme 2.5. Synthesis of ring expanded modified 7,9-dichlorotacrine **18**. 46
Scheme 2.6. Synthesis of bump-hole optimized tacrine homodimers **20c** – **l**..... 47
Scheme 2.7. Synthesis of *N*-methyl bridged bump-hole optimized tacrine dimer **22** 48
Scheme 4.1. Inversion of benzodiazepines as investigated by Lam and Carlier..... 92
Scheme 4.2. Schematic of constrained optimization results for **16**·H^+ 99

List of Tables

Table 1.1. Inhibition data of tacrine **1** and four tacrine homodimers **7g – j** 10
Table 1.2. Inhibition data of tacrine **1** and tacrine homodimers **7b – j** 11
Table 1.3. Inhibition data of tacrine **1** and tacrine heterodimers **8 – 11** 14
Table 1.4. Inhibition data of tacrine **1** and **27 – 30** 22
Table 1.5. Inhibition data for **1** and **31 – 39** 23
Table 1.6. Basicity, concentration of conjugate acid, and relative potency for **36** and **37** 23
Table 1.7. Inhibition data of tacrine **1** and Cl-substituted analogs **34**, **36**, **40**, and **41** 24
Table 1.8. Inhibition data of tacrine **1** and various 6- and 7-substituted analogs 24
Table 1.9. Inhibition data of tacrine **1** and various tacrine derivative homodimers 25
Table 2.1. Cycloalkyl ring size, yields, and *in vitro* pharmacology of **1b – c** 38
Table 2.2. Substituents, cycloalkyl ring size, yields, and *in vitro* pharmacology of **1a – 3c** 39
Table 2.3. Substituents, cycloalkyl ring size, yields, and pharmacology of **1a – c** and **4a – 6c** . 40
Table 2.4. Substituents, cycloalkyl ring size, yields, and pharmacology of **1a – c** and **7a – c** ... 41
Table 2.5. Substituents, cycloalkyl ring size, yields, and pharmacology of **1a – c**, **8a – 12c** 42
Table 2.6. Electronic energy, ZPVE, and relative energy of three minima of **8c** 44
Table 2.7. Percent yields of the amino-terminated *N*-alkyltacrine derivatives **19c – l** and **21** ... 47
Table 2.8. Alkyl chain size, yields, and *in vitro* pharmacology of optimized tacrine dimers 49
Table 3.1. Electronic energy, ZPVE, and relative energy of three minima of **8c** 81
Table 4.1. Experimental and computed C-N rotation barriers for salts of **1** and **12-15** 88
Table 4.2. Substituents, coalescence temperatures, and inversion barriers of benzodiazepines. 92
Table 4.3. Comparison of observed dihedral angles θ of *N*-alkyltacrines 106
Table 5.1. Temperature calibrations from the variable temperature ^{1}H NMR experiments. 114
Table 5.2. Energies resulting from the constrained optimization of **16**·H^+ 235
Table 5.3. Energies resulting from the constrained optimization of **12**·H^+ 236
Table 5.4. Energies resulting from the constrained optimization of **1**·H^+ 237
Table 5.5. Energies resulting from the constrained optimization of **13**·H^+ 238
Table 5.6. Energies resulting from the constrained optimization of **14**·H^+ 239
Table 5.7. Energies resulting from the constrained optimization of **15**·H^+ 240
Table 5.8. Energies resulting from the constrained optimization of **17** 241
Table 5.9. Energies, thermodynamic factors, and calculated barriers for tacrine derivatives .. 264
Table 5.10. Energies, thermodynamic factors, and barriers for solvated tacrine derivatives ... 264

List of Abbreviations

ACh	Acetylcholine
AChE	Acetylcholinesterase
AChEI	Acetylcholinesterase inhibitors
AD	Alzheimer's disease
Ag	Anopheles gambiae
ALT	Alanine aminotransferase
ATCh	Acetylthiocholine
BChE	Butyrylcholinesterase
CAS	Catalytic active site
DFT	Density functional theory
Dm	Drosophila melanogaster
Ee	Electrophorus electricus
*h*AChE	Human AChE
Md	Musca domestica
Mm	Mus musculus
MMFF	Molecular mechanics force field
PAS	Peripheral anionic site
PCM	Polarized continuum solvation model
PDB	Protein Data Bank
Tc	Torpedo californica
T_c	Coalescence temperature
THA	Tacrine

Chapter 1. 9-Amino-1,2,3,4-tetrahydroacridine and its Analogs as Acetylcholinesterase Catalytic Active Site Inhibitors.

1.1 Structure and function of acetylcholinesterase

Acetylcholinesterase (AChE) is a member of the serine hydrolase family of enzymes. Its primary function is to terminate cholinergic neurotransmission at the post-synaptic neuron by hydrolyzing acetylcholine (ACh) to choline and acetic acid (Scheme 1.1). As a serine hydrolase, AChE performs its catalytic function through the concerted action of a triad of glutamate, histidine, and serine residues.[1] The first step of the hydrolysis is attack of the activated serine residue on the carbonyl carbon of ACh, the result of which is an acetylated enzyme and choline. A water molecule near the active site de-acetylates the serine residue, thereby completing the catalytic cycle.

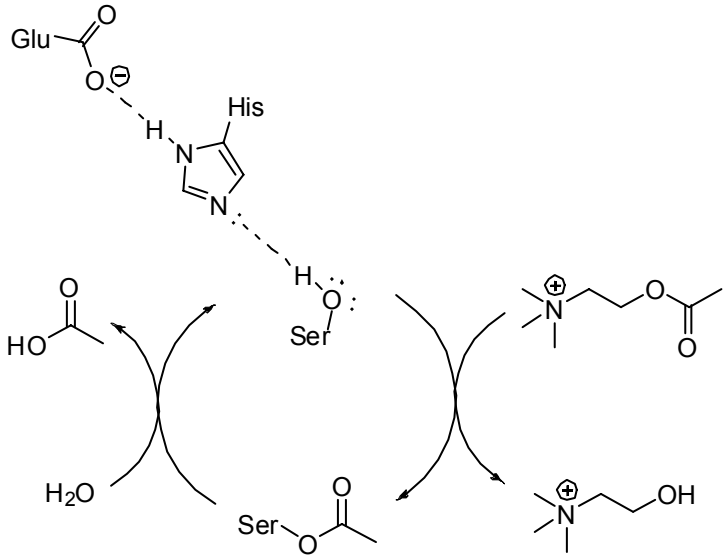

Scheme 1.1. Catalytic cycle of acetylcholinesterase

The crystal structure of native *Torpedo californica* AChE (*Tc*AChE) was solved in 1991 by Sussman, Silman, and co-workers (PDB ID 1ACE).[2] Because 1ACE was subsequently shown to contain decamethonium, a known inhibitor of AChE used to elute the protein from the affinity column used for purification,[3] a new inhibitor-free structure was published in 1996 (PDB ID 2ACE, Figure 1.1).[4] The substrate, ACh, was manually docked into this structure of native *Tc*AChE. The crystal structures (1ACE and 2ACE) confirmed the conclusions from mutagenesis experiments which predicted that His440[5] and Ser200[6] (*Tc*AChE numbering) were involved in the enzymatic hydrolysis, and provided the identity of the final residue of the catalytic triad,

Glu327. Interestingly, the catalytic triad was shown to reside at the bottom of an approximately 20 Å gorge, the mouth of which contained a region of aromatic residues, such as Trp279. The region proximal to Trp279 is often referred to as the peripheral anionic site (PAS), and the region proximal to the catalytic triad is often referred to as the catalytic active site (CAS). This gorge arrangement is now known to be highly conserved in the animal kingdom due to the publication of crystal structures of AChE from human (*h*AChE),[7] *Drosophila melanogaster* (fruit fly, *Dm*AChE),[8] *Mus musculus* (mouse, *Mm*AChE),[9] and *Electrophorus electricus* (electric eel, *Ee*AChE).[10] Figure 1.2 provides a highly simplified schematic of *Tc*AChE which emphasizes the catalytic gorge and the presence of a peripheral site.

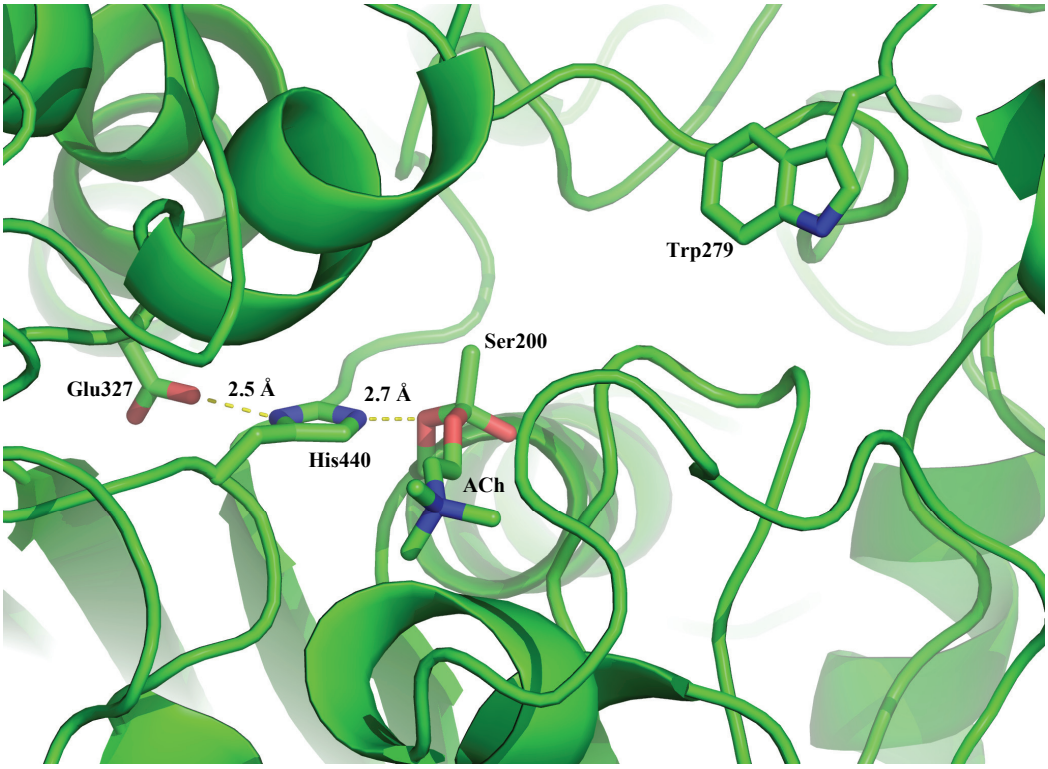

Figure 1.1. X-ray crystal structure of acetylcholine docked to native *Tc*AChE (PDB ID 2ACE) with a crystallographic resolution of 2.5Å. Residue numbering given for *Tc*AChE. Figure generated with PyMol.[11] Key: green = carbon and cartoon representation of the enzyme, red = oxygen, blue = nitrogen. Hydrogen bonding between catalytic triad residues shown as dashed yellow lines with interatomic distances given above.

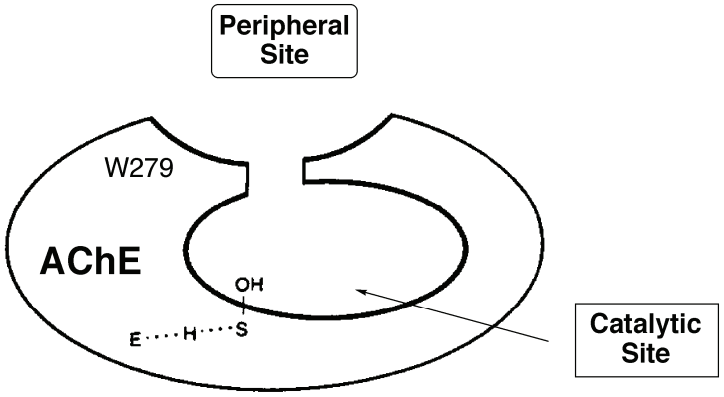

Figure 1.2. Schematic of *Tc*AChE which emphasizes the catalytic gorge

1.2 Approved therapeutic AChEI

The inhibitors of AChE can present either therapeutic or toxic effects depending on the dose administered. Four AChE inhibitors (AChEI) are currently approved for the palliative treatment of Alzheimer's disease (AD) related dementia (Figure 1.3). Tacrine **1** was the first compound approved for the treatment of AD, and subsequently Donepezil **2**, Galanthamine **3**, and Rivastigmine **4**, have all achieved various levels of clinical use for easing the effects of dementia in the first six months following diagnosis.[12] However, none of these medications have shown good long-term tolerability or efficacy over a wide range of patients.

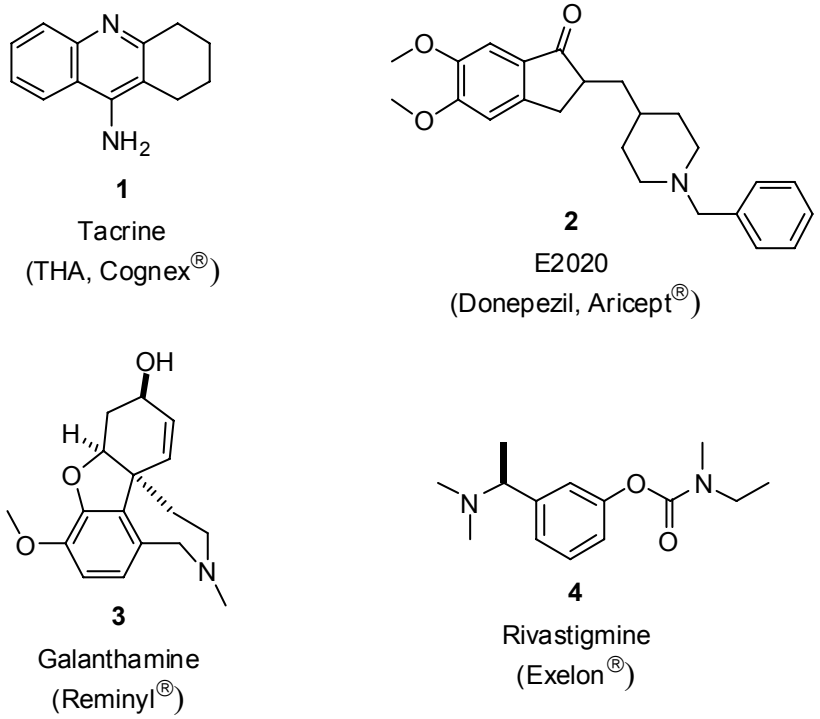

Figure 1.3. FDA approved AChEI for the treatment of Alzheimer's related dementia

Donepezil **2** exhibits a dissociation constant, K_I, of 3.1 nM for *Tc*AChE, and is thus a very potent inhibitor of the enzyme.[13] Protein crystallography has explained this high potency by demonstrating that **2** binds the enzyme over the entire length of the catalytic gorge (Figure 1.4).[10] Beginning at the PAS, the indanone moiety binds the enzyme through π-stacking interactions with Trp279. In the middle of the gorge, the piperidine moiety binds the enzyme through a cation-π interaction with the phenyl ring of Phe330. Finally, the phenyl moiety of E2020 binds the CAS through parallel π-π stacking interactions with the indole of Trp84.

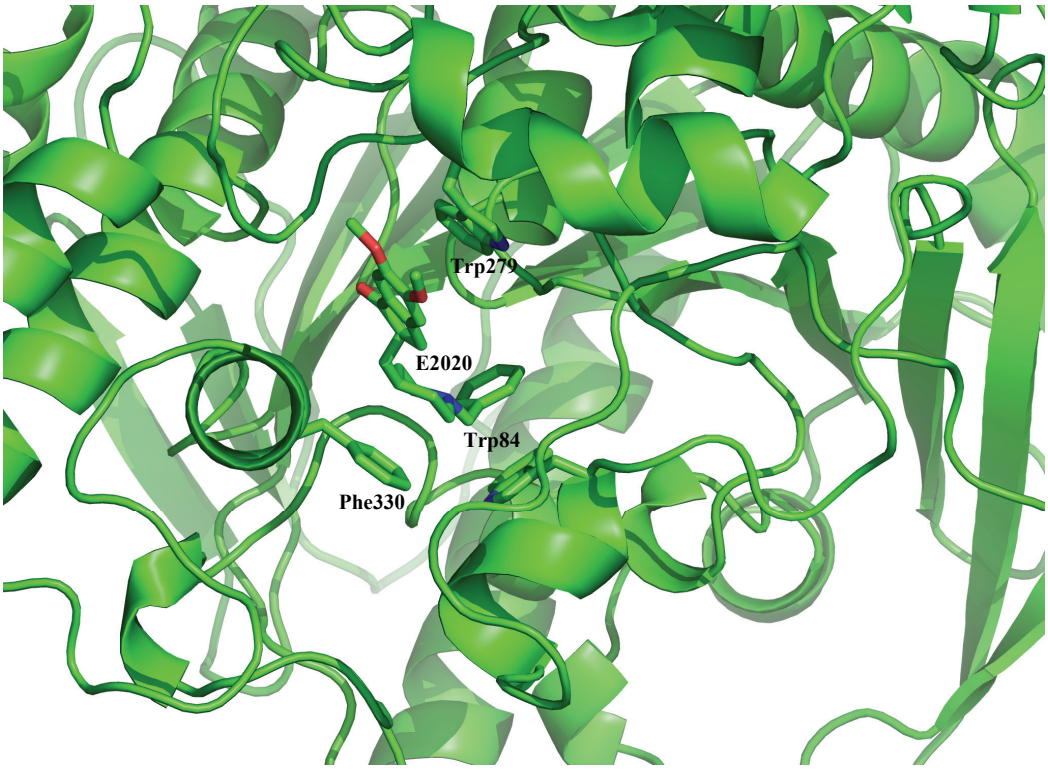

Figure 1.4. X-ray crystal structure of E2020 **2** complexed to *Tc*AChE (PDB ID 1EVE) with a crystallographic resolution of 2.5 Å. Residue numbering given for *Tc*AChE. Figure generated with PyMol.[11] Key: green = carbon and cartoon representation of the enzyme, red = oxygen, blue = nitrogen.

Galanthamine **3** has been shown to possess an IC_{50} of 360 nM for *Ee*AChE.[14] Subsequent crystal structures of the galanthamine/*Tc*AChE complex (Figure 1.5) showed that the inhibitor binds the enzyme through a series of energetically small interactions near the CAS.[15] Using **2** as an analogy, one might expect that the benzene moiety or tertiary amine of **3** would form a π-stacking interaction with Trp84. On the contrary, one finds an interaction between the cyclohexenol moiety's π-bond and the tryptophan residue. Furthermore, a hydrogen-bonding interaction is formed between the hydroxyl group of **3** and Glu199. Interactions are also formed between the inhibitor and Phe290. It has been suggested that the number of protein/ligand

interactions and the relative rigidity of **3** combine to produce the relatively tight binding exhibited by this inhibitor.[15]

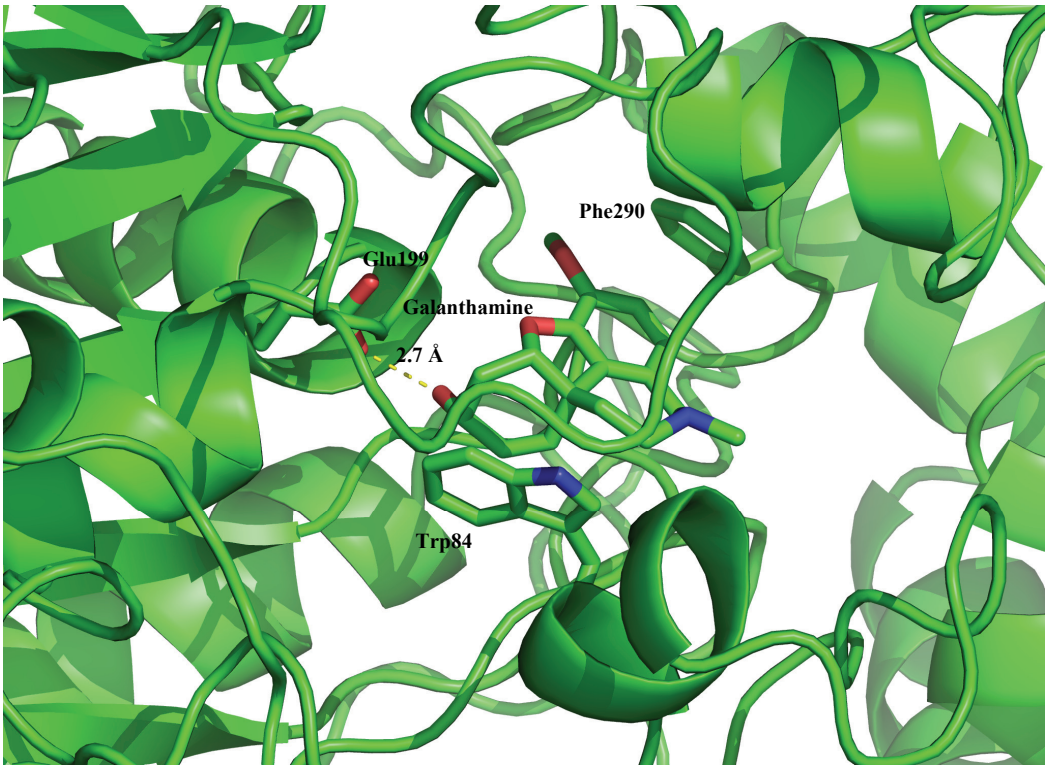

Figure 1.5. X-ray crystal structure of galanthamine **3** complexed to *Tc*AChE (PDB ID 1DX6) with a crystallographic resolution of 2.3 Å. Residue numbering given for *Tc*AChE. Figure generated with PyMol.[11] Key: green = carbon and cartoon representation of the enzyme, red = oxygen, blue = nitrogen.

The IC_{50} of Rivastigmine **4** has been determined to be 1535 nM for *h*AChE.[16] Crystallography has shown that the inhibitory action of **4** is the covalent modification of AChE through the carbamylation of Ser200, part of the catalytic triad (Figure 1.6).[17] The crystal structure of the Rivastigmine/*Tc*AChE complex shows interactions between the aryl leaving group of the inhibitor and Trp84. Furthermore, the carbamate moiety of the inhibitor is seen attached to Ser200 at the carbonyl carbon. Therefore, unlike in the case of the other approved AChEI, **4** is a covalent inhibitor of AChE. Since the carbonyl group is eventually hydrolyzed from Ser200, rivastigmine (and other aryl carbamates) is considered a "pseudo-irreversible" inhibitor. This pseudo-irreversible inhibition allows measurement of steady-state inhibition using IC_{50} values; a truly irreversible inhibitor would not give a meaningful IC_{50} value.

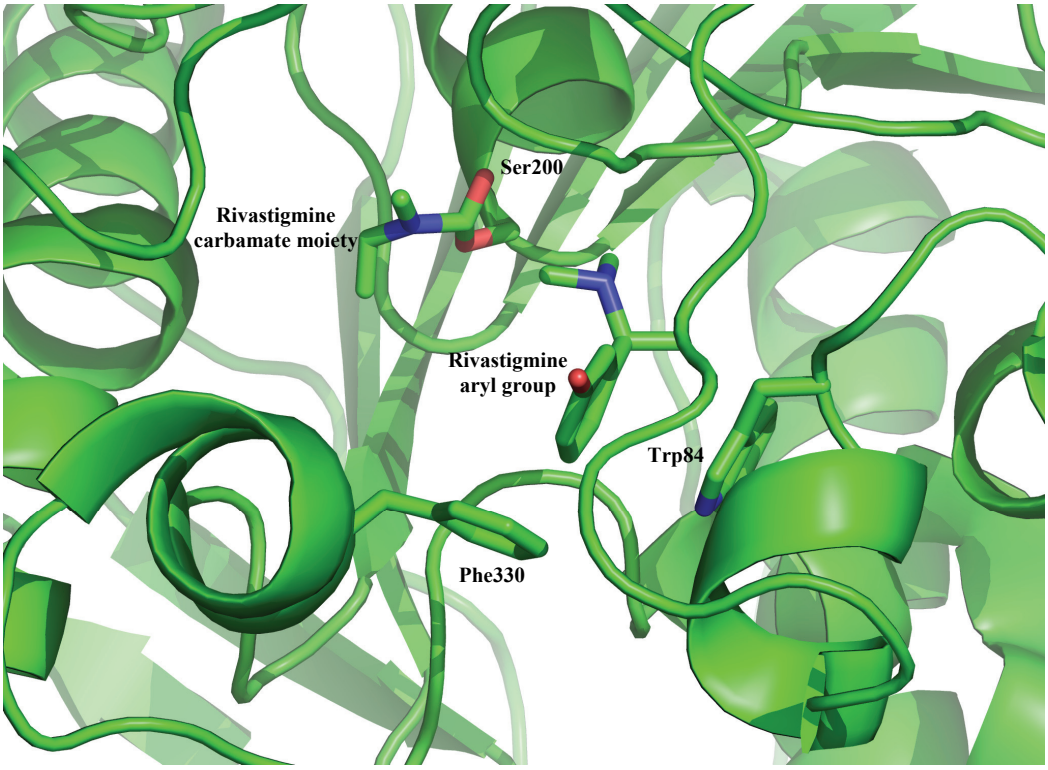

Figure 1.6. X-ray crystal structure of Rivastigmine **4** complexed to *Tc*AChE (PDB ID 1GQR) with a crystallographic resolution of 2.2 Å. Residue numbering given for *Tc*AChE. Figure generated with PyMol.[11] Key: green = carbon and cartoon representation of the enzyme, red = oxygen, blue = nitrogen.

The final inhibitor approved for the treatment of AD related dementia we will discuss is tacrine **1**. The IC_{50} of this inhibitor for rat AChE is 590 nM.[18] Crystallography has shown that this molecule binds the CAS through π-stacking and hydrogen-bonding interactions (Figure 1.7);[19] a double π-stacking interaction is formed between Trp84, the inhibitor, and Phe330, while hydrogen bonding is present between the cyclic nitrogen of tacrine and His440, as evidenced by a 3.2 Å distance between the residue and inhibitor. It is likely that the aromatic (aminoquinoline) portion of **1** is largely responsible for the binding of the drug to AChE, while the cyclohexyl portion has been implicated in blocking the approach of ACh to the active site.[20,21] The remainder of this work will focus on the inhibitory effects of tacrine, and modifications that have been performed on the inhibitor in order to achieve an improved pharmacological profile.

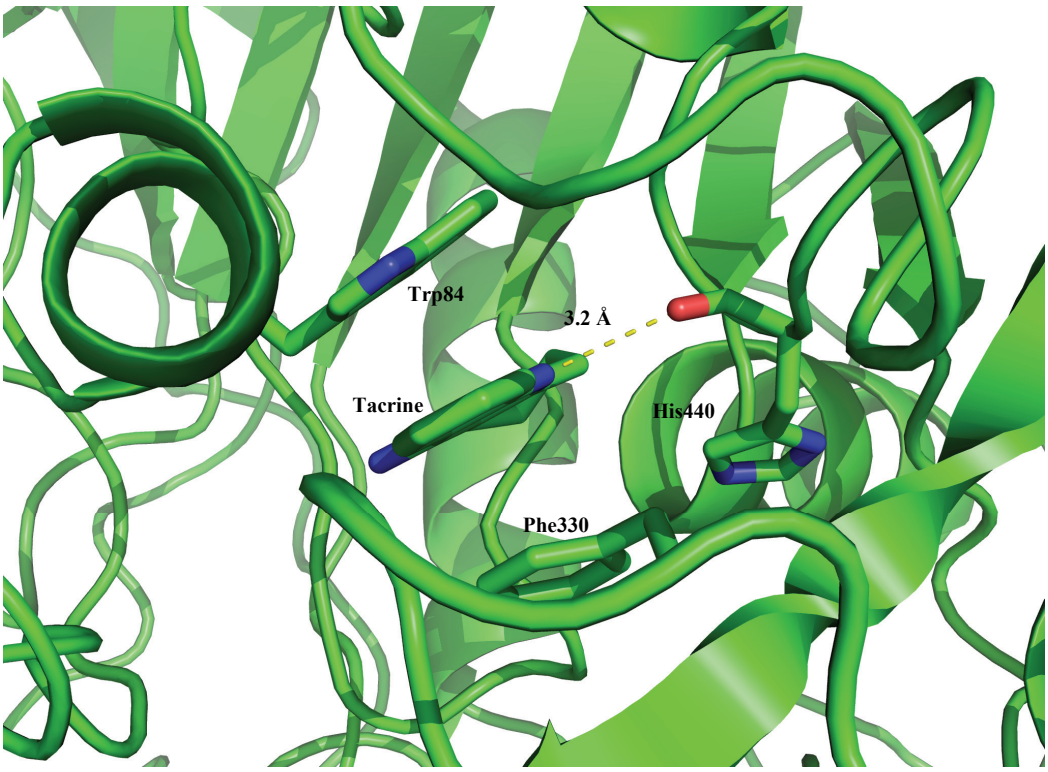

Figure 1.7. X-ray crystal structure of Tacrine **1** complexed to *Tc*AChE (PDB ID 1ACJ) with a crystallographic resolution of 2.8 Å. Residue numbering given for *Tc*AChE. Figure generated with PyMol.[11] Key: green = carbon and cartoon representation of the enzyme, red = oxygen, blue = nitrogen.

1.3 Historical perspective of the discovery and clinical use of tacrine

The first synthesis of tacrine was reported in 1945 by Albert and Gledhill.[22] Working in Australia, these researchers were attempting to discover antibacterial agents to be used on the battle fields of World War II. Soon after the publication of the 1945 paper, penicillin became more economical, leading to the demise of the acridines as antibiotics. However, tacrine was first described as an anticholinesterase in 1953.[23] Since that time, much research has been conducted to elucidate the mechanism by which tacrine inhibits acetylcholinesterase. This section focuses on the historical aspects of the discovery and development of tacrine for clinical applications.

In 1961, Heilbronn[24] showed that tacrine is a reversible inhibitor of both AChE and another biologically important cholinesterase, butyrylcholinesterase (BChE). In her study, the researcher provided evidence that tacrine acts through mixed inhibition in which competitive inhibition dominates at higher substrate concentrations, and noncompetitive inhibition dominates at lower substrate concentrations. Also, Heilbronn reported her studies with sarin (**5**, Figure 1.8). Both of the cholinesterases were incubated with sarin, an irreversible anticholinesterase. When

the experiment was performed in the presence of tacrine, the sarin could not bind as efficiently as it did when no tacrine was present. This dichotomy suggested that tacrine may be used as a prophylactic treatment for irreversible cholinesterase inhibition. Fricke et al.[25] examined this effect in more detail in the early 1990's and found that because there is a sizeable overlap between the dose required for prophylaxis and that which causes behavioral toxicity, tacrine would not be a suitable nerve agent toxicity pretreatment.

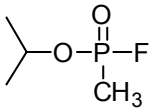

5

Figure 1.8. Sarin

The field of tacrine research met with some controversy due to the work of Summers and coworkers[26] whose preliminary report claimed that tacrine may be used as a palliative treatment for AD-related dementia. Summers had previously used tacrine for the treatment of overdose coma and delirium.[27] In the controversial AD study, seventeen patients with moderate to severe AD began the nonblinded Phase I. In this phase, subjects who received tacrine exhibited a marked decrease in dementia symptoms. Phase II was a controlled, double-blind, crossover study of 14 subjects. Again, subjects who received tacrine exhibited a marked decrease in dementia symptoms. However, the group to which the placebo was administered showed no significant symptomatic change versus the control group to which no drug was administered. The reported Phase III results were based on 12 subjects. In this phase, tacrine was administered over an average of nearly 13 months. In that time, subjects exhibited symptomatic improvement and a lack of tacrine-related side effects.

Soon after the Summers study was published, the editors of the New England Journal of Medicine began to receive letters critical of the simplicity of the Summers study, but no arguments that the study was so flawed as to be unpublishable.[28] In 1992 – 1994, several studies published in the course of a multicenter study demonstrated the effectiveness and relative safety of tacrine as an AD treatment.[29-32] Interestingly, the FDA halted clinical trials of tacrine on October 23, 1987 because of liver toxicity exhibited by eight of the first 41 patients who received the drug.[33] Eventually, the multicenter study was allowed to progress, and it was concluded that tacrine in high doses (i.e., 160 mg/day) could induce a significant improvement on tests designed

to measure the progression of dementia.[31] Tacrine received FDA approval for AD related dementia in 1993.

One of the studies that emanated from the large multicenter study focused on the hepatotoxic effects of tacrine.[34] In that study, 2446 suspected AD patients who were at least 50 years old were given tacrine and monitored for the elevation of serum alanine aminotransferase (ALT) levels. This elevation of ALT levels is symptomatic of hepatotoxicity. While nearly half of the patients experienced ALT levels greater than the upper limit of normal, discontinuation of the treatment allowed the ALT levels to return to normal. Furthermore, 88% of those patients who discontinued the tacrine treatment were able to resume long-term treatment with tacrine after ALT levels returned to normal. It is important to note that no deaths directly attributable to the tacrine treatment occurred over the course of the long-term study.

As a possible amelioration of the liver toxicity effect, Shutske and coworkers[35,36] examined a series of 9-amino-1,2,3,4-tetrahydroacridin-1-ols (e.g. **6**, velnacrine, Figure 1.9), compounds which were physiological metabolites of tacrine but did not possess the high lipophilicity (and the resulting tissue accumulation effects) that plagued the drug. The results showed that **6** was an order of magnitude less effective than tacrine for inhibition of mouse AChE (IC_{50} = 4.8 μM and 0.31 μM, respectively) but exhibited a similar pharmacological profile. However, oral toxicity of **6** in mice was much improved versus that of tacrine (LD_{50} = 136 mg/kg and 39.8 mg/kg, respectively). Interest in velnacrine waned after the FDA approval of tacrine, and this metabolite has not enjoyed clinical use.

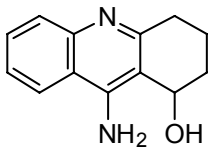

6

Figure 1.9. 9-Amino-1,2,3,4-tetrahydroacridin-1-ol, velnacrine

1.4 Bivalent inhibitor studies

The rationale, design, and synthesis of bivalent inhibitors of AChE have been reviewed by Du and Carlier.[12] This section will primarily focus on bivalent inhibitors in which tacrine or an analog binds the CAS.

The presence of two distinct ligand binding sites on AChE has been known for many years.[2] Using SYSDOC, an automated docking program developed in house, Pang and coworkers[37] showed that tacrine could bind the CAS at His440 as well as the PAS at Trp279. Following this study, Pang used his SYSDOC program to predict tacrine homodimer **7i** (Figure 1.10) would have a quite high affinity for AChE.[18] Indeed, upon the successful synthesis and assay of homodimer **7i** and three analogs (**7g**, **7h**, and **7j**, Table 1.1), the researchers discovered that homodimer **7i** (IC_{50} = 0.77 nM) was more than 750 times more potent for rat brain AChE than was the tacrine monomer **1** (IC_{50} = 590 nM). Interestingly, homodimer **7g** exhibited an IC_{50} value of 0.40 nM for rat brain AChE, making this drug nearly 1500 times more potent than tacrine monomer **1**. Furthermore, because BChE does not possess a PAS analogous to AChE, the homodimers exhibited notable selectivities for AChE over BChE (cf. **7g** selectivity = 980).

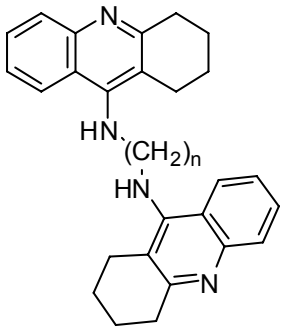

7b-j

Figure 1.10. Tacrine homodimers (homolog lettering scheme for all bivalent inhibitors: a, n = 1; b, n = 2; c, n = 3; d, n = 4; e, n = 5; f, n = 6; g, n = 7; h, n = 8; i, n = 9; j, n = 10).

Table 1.1. Inhibition data of tacrine **1** and four tacrine homodimers **7g – j** from the initial study of Pang et al.[18]

Inhibitor	Rat brain AChE IC_{50} (nM)[a]	Rat serum BChE IC_{50} (nM)	Selectivity for AChE[b]
THA **1**	590 ± 37	44 ± 2.0	0.1
7g	0.40 ± 0.025 (1500x)	390 ± 66	980
7h	0.66 ± 0.20 (890x)	340 ± 13	520
7i	0.77 ± 0.11 (770x)	190 ± 30	250
7j	3.1 ± 0.75 (190x)	440 ± 100	140

[a] Numbers in parentheses correspond to the potency enhancement of the dimers versus **1**. This potency enhancement is defined as IC_{50} **1** / IC_{50} **7**. [b] Selectivity for AChE is defined as BChE IC_{50} / AChE IC_{50}.

Following this study, working in collaboration with Pang, the Carlier group synthesized and assayed a wider range of tacrine homodimers (**7b – j**).[38] The researchers discovered a tether-length dependence, with the optimal compound being **7g** (Table 1.2).[39] At shorter tether lengths, a sharp decline in potency was observed (Figure 1.11). This tether length dependence supported

the conclusion of Pang and Carlier that the longer chain homodimers bind the CAS and PAS simultaneously. Subsequently, **7e** and **7g** were co-crystallized with *Torpedo californica* AChE (*Tc*AChE).[40] Compound **7g** exhibited dual-site binding, with one tacrine unit binding at His440 and one tacrine unit binding in a dual π-stacking interaction with Tyr70 and Trp279 (Figure 1.12). On the other hand, the tether length of compound **7e** precluded the interaction with Tyr70, while allowing an interaction only at Trp279 at the PAS and His440 at the CAS (Figure 1.13).

Table 1.2. Inhibition data of tacrine **1** and tacrine homodimers **7b – j** from the study of Carlier et al.[38]

Inhibitor	Rat brain AChE IC_{50} (nM)[a]	Rat serum BChE IC_{50} (nM)	Selectivity for AChE[b]
THA **1**	223 ± 11	92 ± 2	0.4
7b	711 ± 25 (0.31x)	102 ± 4	0.14
7c	254 ± 55 (0.88x)	152 ± 17	0.60
7d	157 ± 23 (1.4x)	252 ± 9	1.60
7e	28 ± 5 (8.0x)	329 ± 21	11.8
7f	3.8 ± 0.4 (59x)	119 ± 6	31.3
7g	1.5 ± 0.3 (150x)	149 ± 23	99.3
7h	7.8 ± 0.9 (29x)	105 ± 13	13.5
7i	31 ± 3 (7.2x)	155 ± 25	5.0
7j	40 ± 6 (5.6x)	167 ± 12	4.2

[a] Numbers in parentheses correspond to the potency enhancement of the dimers versus **1**. This potency enhancement is defined as IC_{50} **1** / IC_{50} **7**. [b] Selectivity for AChE is defined as BChE IC_{50} / AChE IC_{50}.

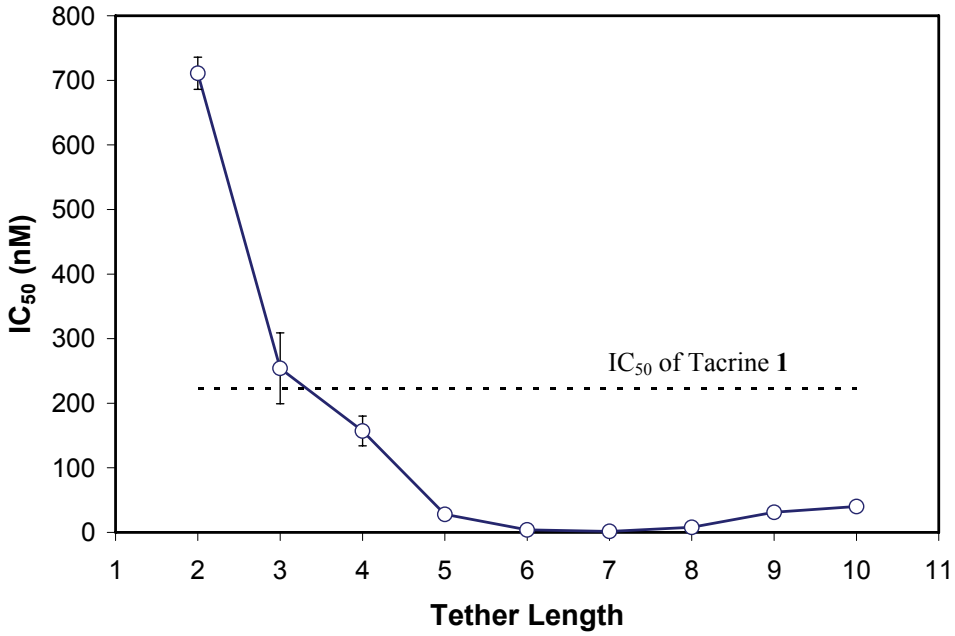

Figure 1.11. Tether-length dependence of tacrine homodimers.

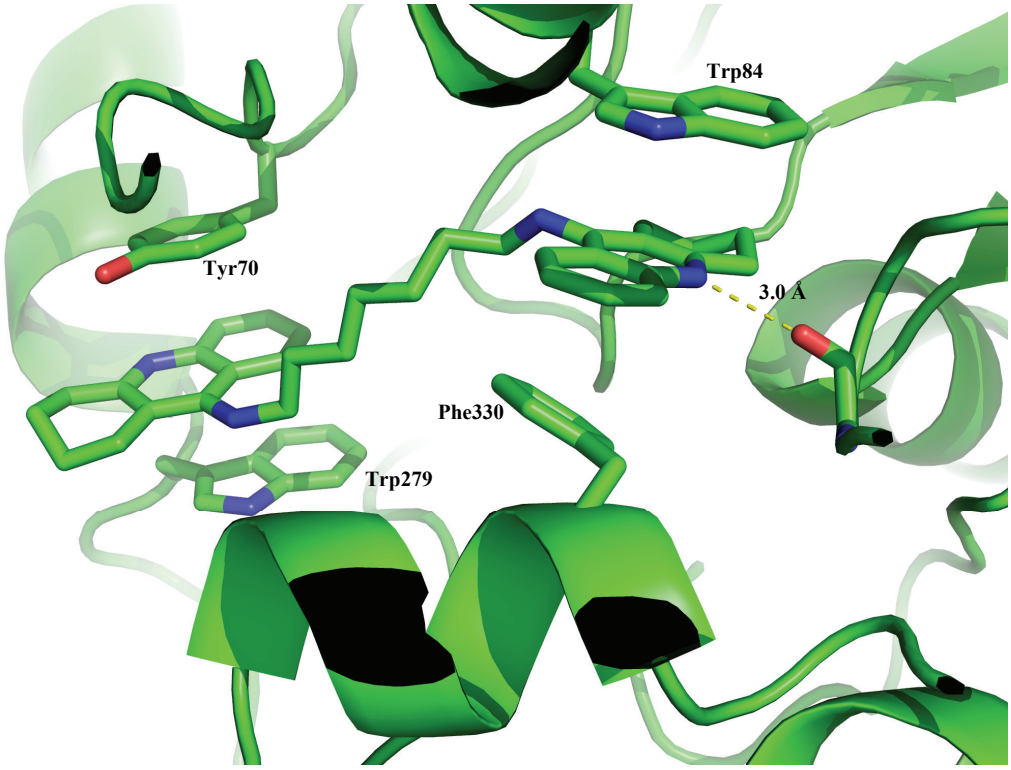

Figure 1.12. X-ray crystal structure of **7g** complexed with *Tc*AChE (PDB ID 2CKM) exhibiting dual site binding. The crystallographic resolution is 2.15 Å. Figure generated with PyMol.[11] Key: green = carbon and cartoon representation of the enzyme, red = oxygen, blue = nitrogen.

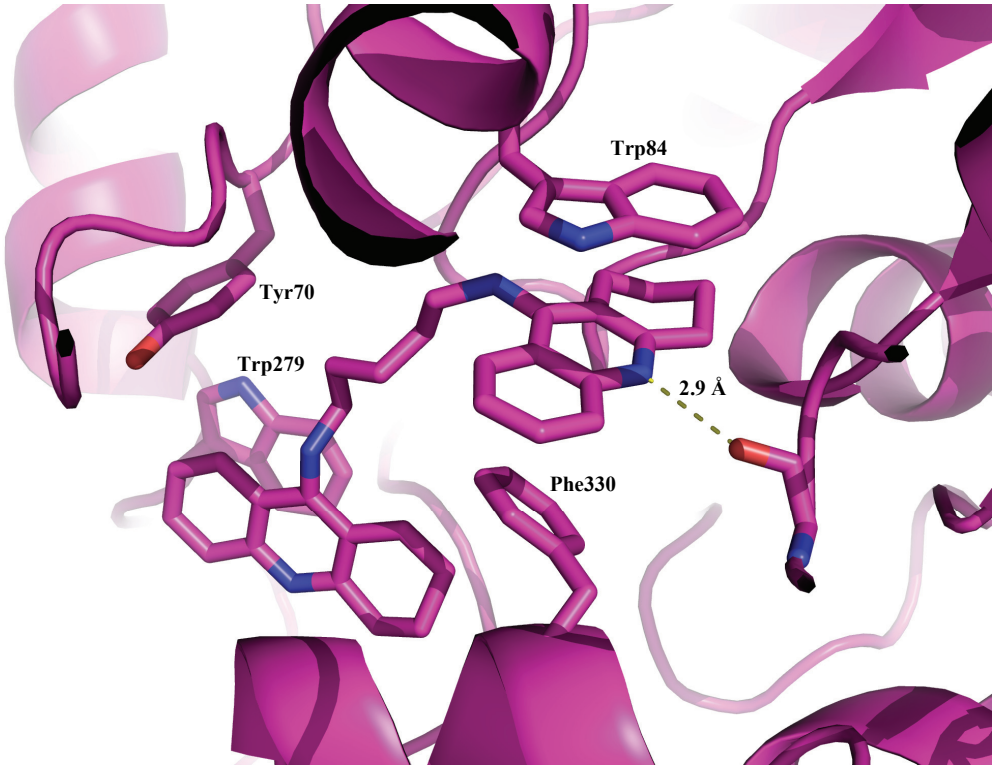

Figure 1.13. X-ray crystal structure of **7e** complexed with *Tc*AChE (PDB ID 2CMF) exhibiting dual site binding. The crystallographic resolution is 2.5 Å. Figure generated with PyMol.[11] Key: magenta = carbon and cartoon representation of the enzyme, red = oxygen, blue = nitrogen.

Carlier and co-workers also studied heterodimers of tacrine and various unsubstituted and substituted amines (Figure 1.14).[41] Again, the researchers found a tether-length dependence for optimal potency (Table 1.3), further suggesting dual-site binding of the ligands. Interestingly, the hydrophobicity of the (presumably) PAS portion of the bivalent ligand was of great importance. Carlier and coworkers found that in the n = 8 dimer (**8h**, **9h**, **10h**, **11h**, and **7h**) series, the potency increased in the order ammonia < dimethylamine < 4-aminopyridine < 4-aminoquinoline < tacrine. While the implications of this finding are outside the scope of this work, the further understanding of the hydrophobicity requirement of PAS ligands has significantly aided in the design of novel PAS selective ligands.

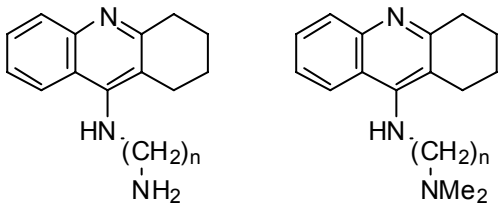

8g-j,l

9g-j,l

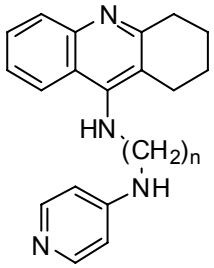

10g-j,l

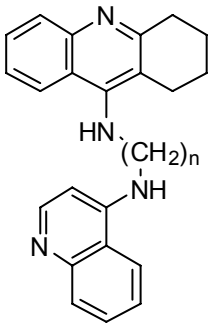

11g-i

Figure 1.14. Heterodimeric tacrine inhibitors of AChE (homolog lettering scheme for all bivalent inhibitors: a, n = 1; b, n = 2; c, n = 3; d, n = 4; e, n = 5; f, n = 6; g, n = 7; h, n = 8; i, n = 9; j, n = 10).

Table 1.3. Inhibition data of tacrine **1** and tacrine heterodimers **8** – **11** from the study of Carlier et al.[41]

Inhibitor	Rat brain AChE IC_{50} (nM)[a]	Rat serum BChE IC_{50} (nM)	Selectivity for AChE[b]
THA **1**	223 ± 11	92 ± 2	0.4
8g	319 ± 13 (0.70x)	357 ± 6	1.1
8h	89.4 ± 6.2 (2.5x)	202 ± 10	2.3
8i	131 ± 8 (1.7x)	687 ± 68	5.2
8j	147 ± 6 (1.5x)	682 ± 82	4.6
8l	180 ± 19 (1.2x)	791 ± 66	4.4
9g	52 ± 4 (4.3x)	143 ± 7	2.7
9h	47 ± 1 (4.7x)	170 ± 1	3.6
9i	71 ± 3 (3.1x)	237 ± 17	3.4
9j	45 ± 1 (5.0x)	581 ± 22	13
9l	264 ± 1 (0.84x)	695 ± 36	2.6
10g	12.8 ± 4 (17x)	302 ± 28	24
10h	13.6 ± 3.9 (16x)	157 ± 9	12
10i	83.6 ± 8.8 (2.7x)	200 ± 11	2.4
10j	176 ± 26 (1.3x)	427 ± 44	2.4
10l	261 ± 16 (0.85x)	377 ± 30	1.4
11g	10.1 ± 1.4 (22x)	110 ± 4	11
11h	8.8 ± 1.3 (25x)	126 ± 17	14
11i	38.7 ± 5.7 (5.8x)	156 ± 13	4.0

[a] Numbers in parentheses correspond to the potency enhancement of the dimers versus **1**. This potency enhancement is defined as IC_{50} **1** / IC_{50} **8** – **11**. [b] Selectivity for AChE is defined as BChE IC_{50} / AChE IC_{50}.

1.5 Crystallographic evidence for CAS preference

Protein X-ray crystallography has proven to be useful in understanding how tacrine binds to acetylcholinesterase. Since Sussman, Silman, and coworkers published the tacrine/*Tc*AChE complex structure in 1994[19] (vide supra), it has been known that tacrine binds AChE near the active site residues that comprise the catalytic triad, effectively blocking the ability of ACh to bind the enzyme. Furthermore, tethering one unit of tacrine to a molecule capable of binding at the PAS has proven a highly effective means to achieve high inhibition potency for AChE (vide supra). The most potent of these bivalent inhibitors have been studied extensively using X-ray crystallography. In the following section, we will discuss several crystal structures of AChE complexed with the inhibitors of Figure 1.15 as well as the implications of these structures for AChEI design.

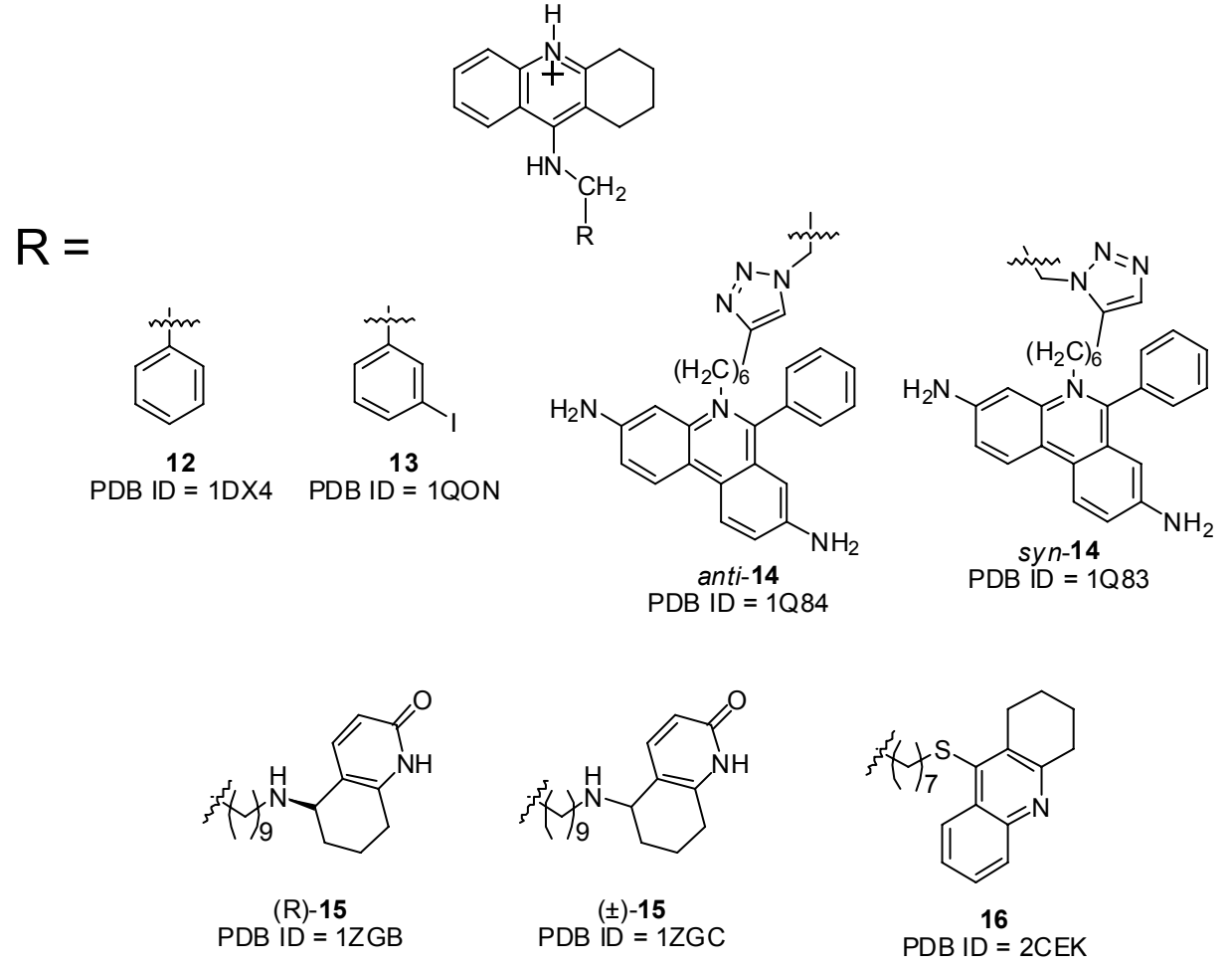

Figure 1.15. Substituents (R) of tacrine based AChEI **12** – **16** complexed to AChE found in the PDB (PDB ID given below each structure).

N-Benzyltacrine **13** is a potent inhibitor of insect AChE, with a reported K_I of 1.09 nM for *Musca domestica* AChE.[8,42] The crystal structures of *Dm*AChE complexed with **13** and its unsubstituted analog **12** were published in 2000.[8] Figure 1.16 shows an overlay of the two structures. The **13** complex structure, just as that of **1** (Figure 1.7, supra), exhibits a dual π-stacking interaction between the tacrine moiety of the ligand and two aromatic residues proximal to the catalytic site (i.e. Trp83 and Tyr370, *Dm* residue numbering). However, in the **12** complex structure, the Tyr370 interaction is removed due to the change in orientation of the Tyr370 side chain. In both structures, the distance between the carbonyl O of the catalytic His480 and the cyclic N of the tacrine unit is 3.7 Å, a distance which precludes one from unequivocally stating that a hydrogen bond is formed between the ligand and enzyme but is suggestive of the interaction.

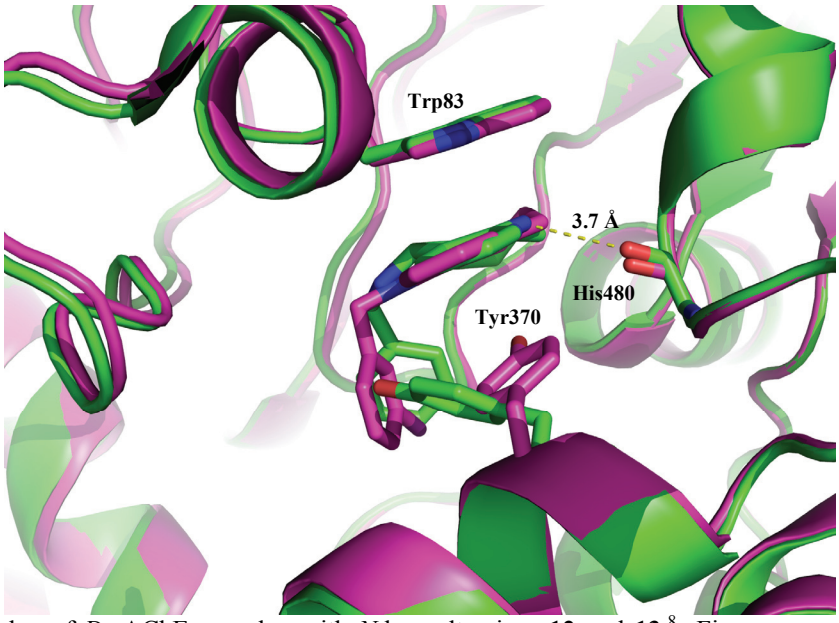

Figure 1.16. Overlay of *Dm*AChE complex with *N*-benzyltacrines **12** and **13**.[8] Figure generated with PyMol.[11] Key: green = PDB ID 1DX4 (ligand **12**), magenta = PDB ID 1QON (ligand **13**).

Sharpless, Finn, Carlier, Taylor, and co-workers, in 2002 used the tacrine moiety in a trial of the *in situ* click chemistry concept.[9,43] In this experiment, the researchers used *Electrophorus electricus* AChE as a template for building its own inhibitor. This was accomplished by incubating a series of acetylene substituent-bearing compounds with AChE in the presence of a series of azide substituent-bearing compounds (Figure 1.17). It is interesting to note that out of the 49 inhibitors that could have been formed, only one was detected in significant quantities: *syn*-**14**, the cycloaddition adduct of **17b** and **20f**). When tested for anticholinesterase activity in

both mouse and *Electrophorus electricus* AChE, this compound exhibited femtomolar dissociation constants, making *syn*-**14** one of the highest affinity ligands on record for AChE. The crystal structure of the *syn*-**14** complex with *Mm*AChE was solved to 2.7 Å resolution, and that of the *anti*-**14** complex was solved to 2.5 Å resolution (Figure 1.18).[9] Just as with the **13** complex structure, a dual π-stacking interaction is exhibited between two aromatic residues of the enzyme (i.e. Trp86 and Tyr337, mouse numbering) and the tacrine moiety of the *anti*-**14** ligand. However, the conformation adopted by the triazole moiety of *syn*-**14** does not allow Tyr337 to adopt a conformation suitable for π-stacking. In both cases, a hydrogen-bond is evidenced by a distance of about 3.0 Å between the cyclic N of the tacrine moiety and the carbonyl O of the catalytic His447.

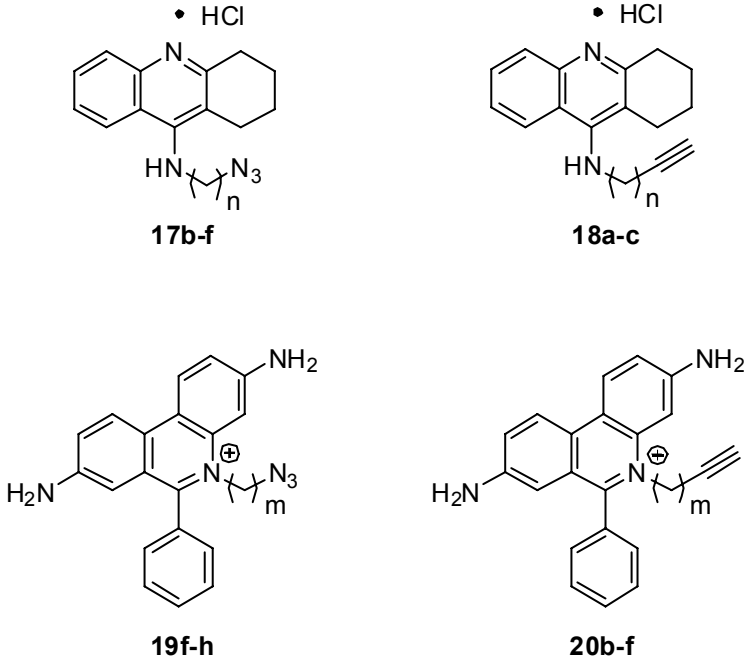

Figure 1.17. Sharpless's ligand set for i*n situ* click chemistry (homolog lettering scheme for all bivalent inhibitors: a, m = n = 1; b, m = n = 2; c, m = n = 3; d, m = n = 4; e, m = n = 5; f, m = n = 6; g, m = n = 7; h, m = n = 8).[43]

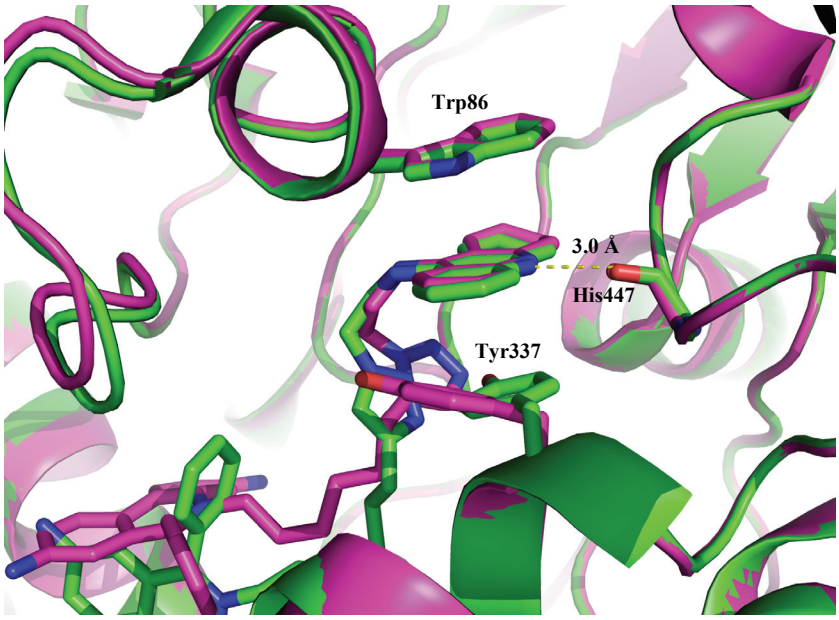

Figure 1.18. Overlay of *Mm*AChE complex with *in situ* click chemistry products *anti*-**9** and *syn*-**9**.[9] Figure generated with PyMol.[11] Key: green = PDB ID 1Q84 (ligand *anti*-**9**), magenta = PDB ID 1Q83 (ligand *syn*-**9**).

Huperzine A (**21**, Figure 1.19), isolated from the club moss *Huperzia serrata*, is a blood-brain-barrier permeable alkaloid.[44-46] The drug is marketed in this country as a dietary supplement and is sold in China as a treatment for AD-related dementia.[44] Furthermore, **21** has been used as a prophylactic treatment for mammalian nerve poisoning induced by soman (**22**, Figure 1.19), a functional analog of sarin **5**.[47-50]

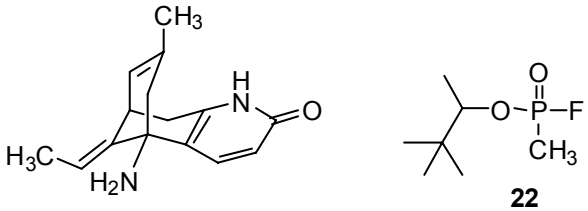

21 **22**

Figure 1.19. Huperzine A (**21**) and soman (**22**)

Protein X-ray crystallography experiments have demonstrated that **21** binds the CAS of AChE preferentially.[4] However, in 1994, Pang and Kozikowski[37] used their SYSDOC computational method to predict that **21** would have some small affinity for the PAS. Motivated by this report, Carlier et al.[45] developed a more synthetically accessible fragment of **21** (**23**, 5-amino-5,6,7,8-tetrahydroquinolin-2-one, tetrahydroquinolone, Figure 1.20) and formed heterodimers of the fragment tethered to tacrine through alkyl chains of various lengths (e.g. **15**, Figure 1.15). The optimal dimer, (±)-**15**, possessed a 10-carbon linker and exhibited an 8.8 nM IC_{50} for rat AChE.

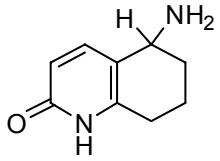

23

Figure 1.20. Tetrahydroquinolone

In 2005, Sussman et al.[51] resolved the crystal structures of the racemic tacrine/tetrahydro-quinolinone decyl linked heterodimer, (±)-**15**, complexed with *T. californica* AChE (Figure 1.21). Interestingly, trigonal AChE crystals selectively complexed the *R*-enantiomer, while orthorhombic crystals exhibited no such selectivity. Upon further investigation, it was determined that in the trigonal form, a proximal symmetry-related *T. californica* AChE molecule occluded the gorge entrance. Residues from this proximal AChE molecule formed hydrogen bonds with the *R*-enantiomer, an arrangement which could not occur with the *S*-enantiomer. However, when the crystals were in the orthorhombic form, the active site gorge was much more open, leading to no selectivity.

Examining the tacrine unit of the protein/ligand complex, one finds a double π-stacking interaction that is analogous to the previously discussed tacrine complexes. In *Tc*AChE, the aromatic residues involved with the π-stacking are Trp84 and Phe330. Furthermore, a hydrogen bond is formed between the carbonyl O of His440 and the cyclic N of the tacrine moiety, suggesting that tacrine is protonated in its bound state.

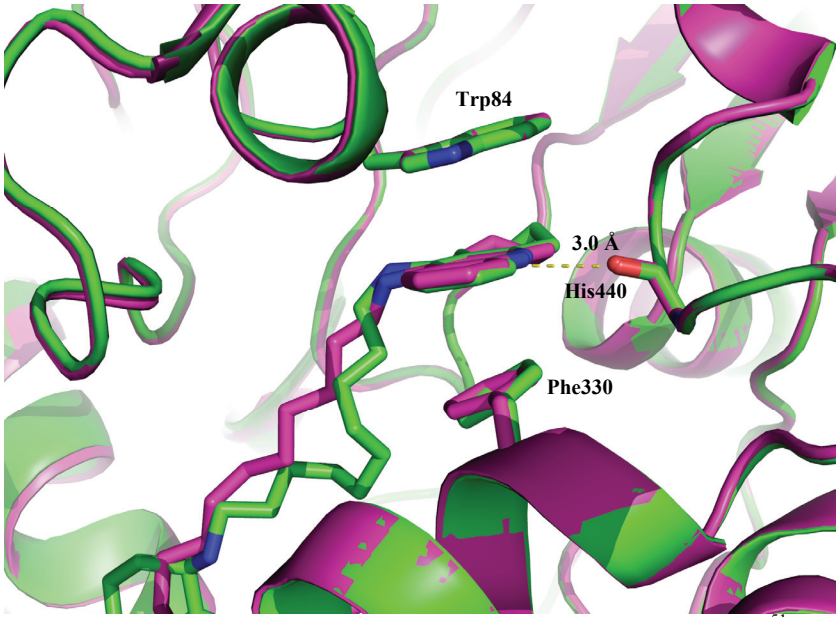

Figure 1.21. Overlay of *Tc*AChE complexed with bivalent inhibitors (*R*)-**15** and (±)-**15**.[51] Figure generated with PyMol.[11]. Key: green = PDB ID 1ZGB (ligand (*R*)-**15**), magenta = PDB ID 1ZGC (ligand (±)-**15**).

As mentioned previously, many bivalent inhibitors comprised of tacrine tethered to another tacrine or a similar heterocyclic moiety have been reported in the literature (e.g. **7** – **11**).[18,38,41,52] Crystal structures of *Tc*AChE complexed with **7e**, **7g**,[40] **8h**, **11h**,[40,53] and **16**[52] have been solved to a resolution of between 2.15 – 2.50 Å (Figure 1.22). Common to all of these structures is the fact that the alkyl tether spans the entire length of the gorge, allowing interactions with the enzyme at both the PAS and CAS. Near the CAS, all five structures exhibit the double π-stacking interaction with Trp84 and Phe330, as well as the hydrogen bonding interaction with the carbonyl O of His440.

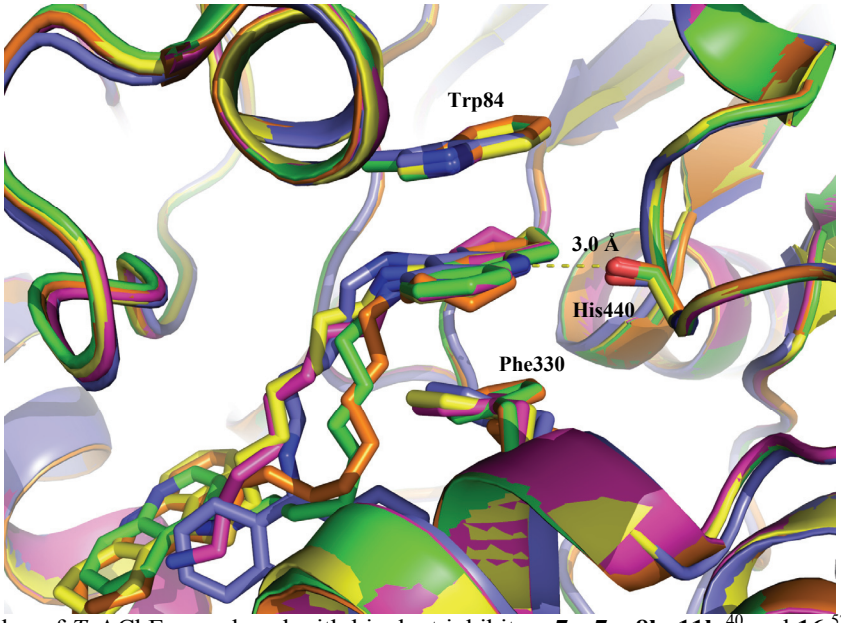

Figure 1.22. Overlay of *Tc*AChE complexed with bivalent inhibitors **7e**, **7g**, **8h**, **11h**,[40] and **16**.[52] Figure generated with PyMol.[11] Key: blue = PDB ID 2CMF (ligand **7e**), yellow = PDB ID 2CKM (ligand **7g**), magenta = PDB ID 1UT6 (ligand **8h**), green = PDB ID 1ODC (ligand **11h**), orange = PDB ID 2CEK (ligand **16**).

1.6 Modifications undertaken to improve AChE/BuChE selectivity

As previously mentioned, tacrine is a non-selective inhibitor of both AChE and BChE. It was once believed that the promiscuity of tacrine might be responsible for the hepatotoxic effects exhibited in patients to whom tacrine was administered. For that reason, much of the research performed in an attempt to perfect the tacrine pharmacophore centered on modifying tacrine in such a way that the drug became highly selective for AChE. This section will focus on the systematic modifications to tacrine that eventually led to improved potency and selectivity of the drug for AChE.

Early work with tacrine led researchers to believe that the inhibition potency of the drug toward the cholinesterases was greatly dependent upon the basicity of tacrine. In 1962, Kaul[54]

investigated the effects of basicity and heteroaromatic ring structure on the inhibitory potency of tacrine and three similar compounds (Figure 1.23): 4-aminopyridine (**24**), 4-aminoquinoline (**25**), and tetrahydroacridine (**26**). Tacrine **1**, **24**, and **25** exhibit similar basicities, but Kaul found that the potencies of **24** and **25** to inhibit AChE were much less than that of **1**. This loss in potency was subsequently duplicated by Carlier et al.[41] Furthermore, the basicity of **26** ($pK_a \approx 5.0$) being significantly different than that of **1** ($pK_a = 9.4$), Kaul expected different inhibitory potencies to be exhibited by the two drugs. However, he reported that there was only a slight difference between the inhibition potencies of **26** and **1**. In the light of subsequent studies (discussed below), this is a very curious finding. Yet to our knowledge, no further research has been conducted on AChE inhibition by **26**. Kaul concluded that the cyclohexyl ring of **1** was important for anticholinesterase activity, and as mentioned previously, the cyclohexyl ring has been implicated in blocking ACh from gaining access to the CAS.[21]

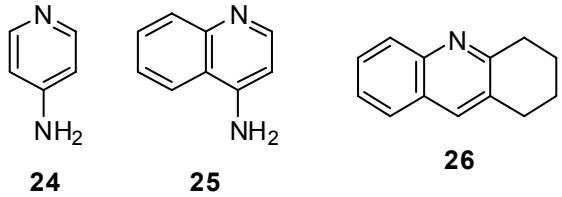

Figure 1.23. Inhibitors from the Kaul study.[54]

Inspired by Kaul's 1962 study, Harvey and coworkers[21] systematically examined the effect of modifying the cyclohexyl ring of **1**. The researchers were interested in the discovery of a single compound to inhibit both AChE and neuronal reuptake of 5-hydroxytryptamine, another neurochemical believed to be involved in the pathology of AD. Assays of **1** and **27** – **30** (Figure 1.24) showed that the size of the cycloalkyl ring in tacrine analogues has an influence on AChE inhibition potency (Table 1.4). Tacrine **1**, **27**, and **28** exhibited similar potencies for AChE. However, inclusion of an eight-membered ring in place of the cyclohexyl moiety of **1** (see **29**) drastically decreased the potency. Harvey and coworkers attributed this reduction in anticholinesterase activity to the increased bulkiness and flexibility of **29** relative to **1**. Furthermore, the bridge of **30** provided a 3-fold decrease in AChE inhibitory potency. These data suggest, once again, that increased bulkiness of the cycloalkyl portion of the inhibitors is detrimental to anticholinesterase activity.

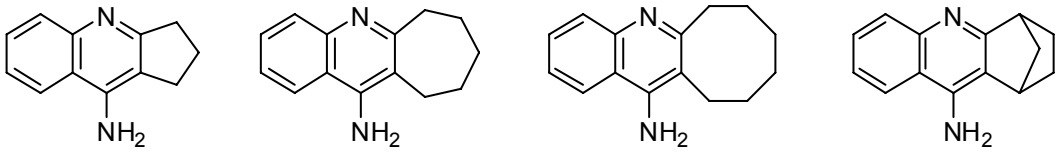

27 **28** **29** **30**

Figure 1.24. Tacrine analogs differing only by the size of the cycloalkyl ring

Table 1.4. Inhibition data of tacrine **1** and **27** – **30** from the study of Harvey et al.[21]

Inhibitor	Rat brain AChE IC_{50} (nM)	Human plasma BChE IC_{50} (nM)	Selectivity for AChE[a]
27	56 ± 4	52 ± 8	0.93
THA **1**	78 ± 1	25 ± 2	0.32
28	39 ± 8	14 ± 2	0.36
29	9,100 ± 600	2,300 ± 80	0.25
30	240 ± 30	41 ± 5	0.17

[a] Selectivity for AChE is defined as BChE IC_{50} / AChE IC_{50}.

With the goal of producing inhibitors with more advantageous *in vivo* pharmacological profiles, Desai, Lipinski, and coworkers[55] synthesized and assayed tacrine-based AChEI with varying pK_a values (**31** – **39**, Figure 1.25, Table 1.5). Changes in pK_a of the conjugate acids did produce differences in AChE IC_{50} values. In all examined cases, except for inhibitors **38** and **39**, a decrease in basicity corresponded to a decrease in AChE inhibitory potency. For instance, the difference in pK_a of the conjugate acids for **36** and **37** is 2.7 units; **36**, with its greater basicity, was 8 times more potent for hAChE than **37**. Using the Henderson-Hasselbalch equation,[56] it can be determined that under assay conditions, 98 % of **36** exists as the conjugate acid (HA). Furthermore, only 11 % of **37** exists as the conjugate acid. Table 1.6 shows that the concentration of the conjugate acid in both cases corresponds well to the relative potency of the inhibitors. These data suggest that it is the protonated form of the tacrine derivative that acts as an AChEI. Thus tacrine and its derivatives, when protonated, better mimic the cationic substrate, ACh.

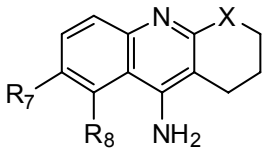

1, 31-39

Figure 1.25. Modified tacrines optimized for *in vivo* pharmacological profiles.[55] See Table 1.5 for substituents.

Table 1.5. Inhibition data for **1** and **31** – **39** from the study of Desai et al.[55]

Inhibitor	X	R_7	R_8	pK_a	Human Erythrocyte AChE IC_{50} (nM)
THA **1**	CH_2	H	H	9.8	143 ± 40
31	O	H	H	7.8	266 ± 91
32	CH_2	H	F	9.1	78 ± 30
33	O	H	F	6.9	335 ± 150
34	CH_2	Cl	H	–	3680 ± 1740
35	O	Cl	H	–	9810 ± 3020
36	CH_2	H	Cl	9.3	39 ± 15
37	O	H	Cl	6.6	313 ± 220
38	CH_2	H	OMe	10.4	615 ± 159
39	O	H	OMe	8.1	606 ± 111

Table 1.6. Basicity, concentration of conjugate acid in solution, and relative potency for **36** and **37**

AChEI	pK_a	[HA][a]	Relative [HA][b]	Relative potency[b]
36	9.3	0.98	1	1
37	6.6	0.11	0.11	0.12

[a] Calculated from the Henderson-Hasselbalch equation. [b] Calculated by the formula: Value for X / Value for **36**, where X is **36** or **37** depending on the relative value sought.

Gregor and coworkers[57] examined tacrine substituted with Cl at the 5-, 6-, 7-, and 8-position (Figure 1.26). Modest selectivity for AChE inhibition versus BChE inhibition was obtained with 6-chloro substituted tacrine **41** (Table 1.7). Furthermore, **41** was determined to be 19-fold more potent for AChE inhibition versus **1**. Interestingly, 7-chloro substituted tacrine **34** was a strongly potent inhibitor of BChE, providing a greater than 1000-fold selectivity for BChE inhibition. This selectivity suggests that while the CAS of both AChE and BChE appear to be similar, there are subtle differences which may be utilized between the two enzymes to effect pronounced inhibitory selectivity.

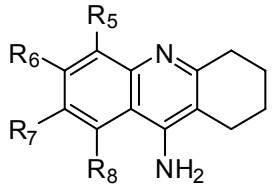

1, 34, 36, 40-51

Figure 1.26. Tacrine derivatives described by Gregor et al.[57] and Recanatini et al.[58] See Table 1.7 and Table 1.8 for the substituents.

Table 1.7. Inhibition data of tacrine **1** and Cl-substituted analogs **34**, **36**, **40**, and **41** from the study of Gregor et al.[57]

Inhibitor	R_5	R_6	R_7	R_8	Human erythrocyte AChE IC_{50} (nM)	Horse serum BChE IC_{50} (nM)	Selectivity for AChE[a]
THA **1**	H	H	H	H	33.5 ± 0.9	5.17 ± 0.44	0.15
34	H	H	Cl	H	743 ± 43	0.7 ± 0.2	0.0009
36	H	H	H	Cl	9.4 ± 0.1	12.7 ± 1.4	1.4
40	Cl	H	H	H	68.9 ± 0.2	45.0 ± 2.89	0.65
41	H	Cl	H	H	1.8 ± 0.3	7.93 ± 1.09	4.4

[a] Selectivity for AChE is defined as BChE IC_{50} / AChE IC_{50}.

Recanatini and coworkers[58] further studied the structure-activity relationships (SAR) of substituted tacrines. In their study, the researchers examined 12 derivatives of tacrine substituted at either the 6- or 7-position (Figure 1.26, Table 1.8). Several patterns emerged from the Recanatini data as well as the earlier Gregor data. First, 6-substitution is generally advantageous for human AChE inhibition. For example, addition of a Cl-substituent at the 6-position, as in **41**, provides a 25-fold increase in potency relative to **1**. On the other hand, 7-substituents generally decrease the potency of the inhibitors. At one extreme of this effect, Recanatini and coworkers described **45**, with a methyl group at the 7-position, which exhibits a 32-fold decrease in potency relative to **1**. Furthermore, the effects of 6- and 7-substitution tend to cancel one another, as is evidenced by the nearly identical inhibitory potencies of 6,7-dichloro-substituted tacrine **50** and **1**. These data may provide a means to design highly potent and selective inhibitors, based on the tacrine pharmacophore, which potentially could replace **1** for clinical use as a treatment for AD.

Table 1.8. Inhibition data of tacrine **1** and various 6- and 7-substituted analogs from the study of Recanatini et al.[58]

Inhibitor	R_5	R_6	R_7	R_8	Human erythrocyte AChE IC_{50} (nM)
THA **1**	H	H	H	H	250 ± 10
34	H	H	Cl	H	550 ± 20
41	H	Cl	H	H	9.9 ± 0.3
42	H	Br	H	H	66 ± 9
43	H	F	H	H	87 ± 1
44	H	CH_3	H	H	100 ± 10
45	H	H	CH_3	H	8,100 ± 600
46	H	NO_2	H	H	28 ± 1
47	H	H	NO_2	H	3,000 ± 200
48	H	H	NH_2	H	3,800 ± 200
49	H	OCH_3	H	H	350 ± 10
50	H	Cl	Cl	H	470 ± 20
51	H	OCH_3	OCH_3	H	5,200 ± 100

The SAR presented above along with the dimerization strategy have been exploited by Hu and coworkers[59] to produce highly potent and selective tacrine derivative homodimers (Figure 1.27, Table 1.9). The researchers found that all of the homodimers were more potent than **1** toward AChE inhibition. Furthermore, 6-chloro substituted tacrine dimers **56f** – **h** were extremely potent and selective for AChE inhibition. Ultimately, Hu and coworkers discovered a homodimer **56g** that possessed an IC_{50} value of 0.07 nM and was greater than 370-fold selective for AChE versus BChE. These data point to an additive effect of modifications to tacrine that can profoundly impact the pharmacological profile.

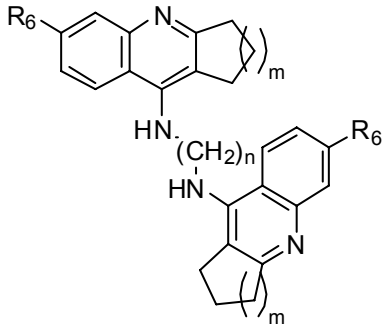

52-57

Figure 1.27. Tacrine derivative homodimers from the study of Hu et al.[59]

Table 1.9. Inhibition data of tacrine **1** and various tacrine derivative homodimers from the study of Hu et al.[59] (homolog lettering scheme for all bivalent inhibitors: a, n = 1; b, n = 2; c, n = 3; d, n = 4; e, n = 5; f, n = 6; g, n = 7; h, n = 8; i, n = 9; j, n = 10).

Inhibitor	R_6	m	Rat Brain AChE IC_{50} (nM)	Human serum BChE IC_{50} (nM)	Selectivity for AChE[a]
THA **1**	H	2	333 ± 39	89 ± 7	0.3
52f	H	1	115 ± 34	273 ± 38	2.4
52g	H	1	75 ± 11	328 ± 40	4.4
52h	H	1	22 ± 4	165 ± 21	7.5
53f	H	2	1.4 ± 0.1	83 ± 19	59
53g	H	2	0.2 ± 0.1	54 ± 14	221
53h	H	2	1.6 ± 0.7	53 ± 17	33.1
54f	F	2	0.9 ± 0.3	45 ± 21	50
54g	F	2	0.6 ± 0.1	257 ± 35	428
54h	F	2	0.7 ± 0.2	164 ± 32	234
56f	Cl	2	0.6 ± 0.3	312 ± 72	520
56g	Cl	2	0.07 ± 0.01	26 ± 1	371
56h	Cl	2	0.3 ± 0.2	194 ± 64	647
57f	H	3	2.5 ± 0.7	3.3 ± 1.4	1.2
57g	H	3	2.7 ± 0.4	2.6 ± 1.3	1.6
57h	H	3	1.6 ± 0.4	3.8 ± 0.3	1.5

[a] Selectivity for AChE is defined as BChE IC_{50} / AChE IC_{50}.

1.7 Conclusions

Tacrine **1** is one of four AChEI approved for the palliative treatment of AD-related dementia. Much research has been conducted to modify **1** to improve the pharmacological profile of the drug. This review has discussed the reported SAR of tacrine and its analogs in relation to mammalian AChE inhibition. The effects of including substitutions on the benzyl moiety of 1 and tethering a ligand to tacrine and its analogs through an alkyl chain was discussed in relation to the optimization of mammalian AChE inhibitory potency.

Chapters 2 and 3 of this work will build on the reported SAR of tacrine and its analogs and disclose our efforts to discover a potent, species-selective inhibitor of AChE from the malaria vector mosquito *Anopheles gambiae*. Chapters 4 and 5 will discuss our efforts to model and experimentally verify rotational barriers in *N*-alkylated tacrine derivatives. We will show that these rotational barriers have significant implications on virtual ligand screening efforts and the ability to predict potent tacrine-related inhibitors of AChE through *in silico* methods.

References for Chapter 1

1. Tõugu, V. Acetylcholinesterase: Mechanism of Catalysis and Inhibition. *Curr. Med. Chem. - Central Nervous System Agents* **2001,** 1, 155-170.

2. Sussman, J. L.; Harel, M.; Frolow, F.; Oefner, C.; Goldman, A.; Toker, L.; Silman, I. Atomic Structure of Acetylcholinesterase from *Torpedo californica*: A Prototypic Acetylcholine-Binding Protein. *Science* **1991,** 253, 872-879.

3. Axelsen, P. H.; Harel, M.; Silman, I.; Sussman, J. L. Structure and dynamics of the active-site gorge of acetylcholinesterase - synergistic use of molecular-dynamics simulation and X-ray crystallography. *Protein Sci.* **1994,** 3, 188-197.

4. Raves, M. L.; Harel, M.; Pang, Y. P.; Silman, I.; Kozikowski, A. P.; Sussman, J. L. Structure of Acetylcholinesterase Complexed with the Nootropic Alkaloid, (±)-Huperzine A. *Nat. Struct. Mol. Biol.* **1997,** 4, 57-63.

5. Gibney, G.; Camp, S.; Dionne, M.; MacPhee-Quigley, K.; Taylor, P. Mutagenesis of essential functional residues in acetylcholinesterase. *Proc. Natl. Acad. Sci. U. S. A.* **1990,** 87, 7546-7550.

6. MacPhee-Quigley, K.; Taylor, P.; Taylor, S. Primary structures of the catalytic subunits from two molecular forms of acetylcholinesterase. A comparison of NH2-terminal and active center sequences. *J. Biol. Chem.* **1985,** 260, 12185-12189.

7. Kryger, G.; Harel, M.; Giles, K.; Toker, L.; Velan, B.; Lazar, A.; Kronman, C.; Barak, D.; Ariel, N.; Shafferman, A.; Silman, I.; Sussman, J. L. Strucutres of Recombinant Native and E202Q Mutant Human Acetylcholinesterase Complexed with the Snake-Venom Toxin Fasciculin-II. *Acta Crystallogr., Sect. D* **2000,** D56, 1385-1394.

8. Harel, M.; Kryger, G.; Rosenberry, T. L.; Mallender, W. D.; Lewis, T.; Fletcher, R. J.; Guss, J. M.; Silman, I.; Sussman, J. L. Three-dimensional structures of Drosophila melanogaster acetylcholinesterase and of its complexes with two potent inhibitors. *Protein Sci.* **2000,** 9, 1063-1072.

9. Bourne, Y.; Kolb, H. C.; Radic, Z.; Sharpless, K. B.; Taylor, P.; Marchot, P. Freeze-Frame Inhibitor Captures Acetylcholinesterase in a Unique Conformation. *Proc. Natl. Acad. Sci. U. S. A.* **2004,** 101, 1449-1454.

10. Kryger, G.; Silman, I.; Sussman, J. L. Strucutre of Acetylcholinesterase Complexed with E2020 (Aricept(R)): Implications for the Design of New Anti-Alzheimer's Drugs. *Structure* **1999,** 7, 297-307.

11. DeLano, W. L. *The PyMol Molecular Graphics System*, 1.0r2; DeLano Scientific LLC: San Carlos, CA, 2007.

12. Du, D.-M.; Carlier, P. R. Development of Bivalent Acetylcholinesterase Inhibitors as Potential Therapeutic Drugs for Alzheimer's Disease. *Curr. Pharm. Des.* **2004,** 10, 3141-3156.

13. Saxena, A.; Fedorko, J. M.; Vinayaka, C. R.; Medhekar, R.; Radic, Z.; Taylor, P.; Lockridge, O.; Doctor, B. P. Aromatic Amino-Acid Residues at the Active and Peripheral Anionic Sites Control the Binding of E2020 (Aricept®) to Cholinesterases. *Eur. J. Biochem.* **2003,** 270, 4447-4458.

14. Mary, A.; Renko, D. Z.; Guillou, C.; Thal, C. Potent Acetylcholinesterase Inhibitors: Design, Synthesis, and Structure–Activity Relationships of Bis-Interacting Ligands in the Galanthamine Series *Bioorg. Med. Chem.* **1998,** 6, 1835-1850.

15. Greenblatt, H. M.; Kryger, G.; Lewis, T.; Silman, I.; Sussman, J. L. Structure of acetylcholinesterase complexed with (-)-galanthamine at 2.3 Å resolution. *FEBS Lett.* **1999,** 463, 321-326.

16. Bolognesi, M. L.; Bartolini, M.; Cavalli, A.; Andrisano, V.; Rosini, M.; Minarini, A.; Melchiorre, C. Design, synthesis, and biological evaluation of conformationally restricted rivastigmine analogues. *J. Med. Chem.* **2004,** 47, 5945-5952.

17. Bar-On, P.; Millard, C. B.; Harel, M.; Dvir, H.; Enz, A.; Sussman, J. L.; Silman, I. Kinetic and Structural Studies on the Interaction of Cholinesterases with the Anti-Alzheimer Drug Rivastigmine. *Biochemistry* **2002,** 41, 3555-3564.

18. Pang, Y.-P.; Quiram, P.; Jelacic, T.; Hong, F.; Brimijoin, S. Highly Potent, Selective, and Low Cost Bis-tetrahydroaminacrine Inhibitors of Acetylcholinesterase. *J. Biol. Chem.* **1996,** 271, 23646-23649.

19. Harel, M.; Schalk, I.; Ehret-Sabatier, L.; Bouet, F.; Goeldner, M.; Hirth, C.; Axelsen, P. H.; Silman, I.; Sussman, J. L. Quaternary Ligand Binding to Aromatic Residues in the Active-Site Gorge of Acetylcholinesterase. *Proc. Natl. Acad. Sci. U. S. A.* **1993,** 90, 9031-9035.

20. Silman, I.; Harel, M.; Axelsen, P.; Raves, M.; Sussman, J. L. Three-dimensional structures of acetylcholinesterase and of its complexes with anticholinesterase agents. *Biochem. Soc. Trans.* **1994,** 22, 745-749.

21. McKenna, M. T.; Proctor, G. R.; Young, L. C.; Harvey, A. L. Novel tacrine analogues for potential use against Alzheimer's disease: Potent and selective acetylcholinesterase inhibitors and 5-HT uptake inhibitors. *J. Med. Chem.* **1997,** 40, 3516-3523.

22. Albert, A.; Gledhill, W. Improved syntheses of aminoacridines. IV. Substituted 9-aminoacridines. *J. Soc. Chem. Ind.* **1945,** 64, 169-172.

23. Shaw, F. H.; Bentley, G. A. The pharmacology of some new anticholinesterases. *Aust. J. Exp. Biol. Med. Sci.* **1953,** 31, 573-576.

24. Heilbronn, E. Inhibition of cholinesterases by tetrahydroaminacrin. *Acta Chem. Scand.* **1961,** 15, 1386-1390.

25. Fricke, R. F.; Koplovitz, I.; Scharf, B. A.; Rockwood, G. A. Efficacy of Tacrine as a Nerve Agent Pretreatment. *Drug Chem. Toxicol.* **1994,** 17, 15 - 34.

26. Summers, W. K.; Majovski, L. V.; Marsh, G. M.; Tachiki, K.; Kling, A. Oral tetrahydroaminoacridine in long-term treatment of senile dementia, Alzheimer type. *N. Engl. J. Med.* **1986,** 315, 1241-1245.

27. Summers, W. K.; Kaufman, K. R.; Altman, F.; Fischer, J. M. THA - A Review of the Literature and its Use in Treatment of Five Overdose Patients. *Clin. Toxicol.* **1980,** 16, 269-281.

28. Relman, A. S. Tacrine as a treatment for Alzheimer's dementia. *N. Engl. J. Med.* **1991,** 324, 349-352.

29. Davis, K. L.; Thal, L. J.; Gamzu, E. R.; Davis, C. S.; Woolson, R. F.; Gracon, S. I.; Drachman, D. A.; Schneider, L. S.; Whitehouse, P. J.; Hoover, T. M.; et al. A double-blind, placebo-controlled multicenter study of tacrine for Alzheimer's disease. The Tacrine Collaborative Study Group. *N. Engl. J. Med.* **1992,** 327, 1253-1259.

30. Farlow, M.; Gracon, S. I.; Hershey, L. A.; Lewis, K. W.; Sadowsky, C. H.; Dolan-Ureno, J. A controlled trial of tacrine in Alzheimer's disease. The Tacrine Study Group. *JAMA, J. Am. Med. Assoc.* **1992,** 268, 2523-2529.

31. Knapp, M. J.; Knopman, D. S.; Solomon, P. R.; Pendlebury, W. W.; Davis, C. S.; Gracon, S. I. A 30-week randomized controlled trial of high-dose tacrine in patients with Alzheimer's disease. The Tacrine Study Group. *JAMA, J. Am. Med. Assoc.* **1994,** 271, 985-991.

32. Wilcock, G. K.; Surmon, D. J.; Scott, M.; Boyle, M.; Mulligan, K.; Neubauer, K. A.; O'Neill, D.; Royston, V. H. An Evaluation of the Efficacy and Safety of Tetrahydroaminoacridine (THA) without Lecithin in the Treatment of Alzheimer's Disease. *Age Ageing* **1993,** 22, 316-324.

33. Marx, J. L. Alzheimer's Drug Trial Put on Hold. *Science* **1987,** 238, 1041-1042.

34. Watkins, P. B.; Zimmerman, H. J.; Knapp, M. J.; Gracon, S. I.; Lewis, K. W. Hepatotoxic effects of tacrine administration in patients with Alzheimer's disease. *JAMA, J. Am. Med. Assoc.* **1994,** 271, 992-998.

35. Shutske, G. M.; Pierrat, F. A.; Kapples, K. J.; Cornfeldt, M. L.; Szewczak, M. R.; Huger, F. P.; Bores, G. M.; Haroutunian, V.; Davis, K. L. 9-Amino-1,2,3,4-Tetrahydroacridin-1-ols - Synthesis and Evaluation as Potential Alzheimers-Disease Therapeutics. *J. Med. Chem.* **1989,** 32, 1805-1813.

36. Shutske, G. M.; Pierrat, F. A.; Cornfeldt, M. L.; Szewczak, M. R.; Huger, F. P.; Bores, G. M.; Haroutunian, V.; Davis, K. L. (+/-)-9-Amino-1,2,3,4-Tetrahydroacridin-1-ol - A Potential Alzheimer's-Disease Therapeutic of Low Toxicity. *J. Med. Chem.* **1988,** 31, 1278-1279.

37. Pang, Y. P.; Kozikowski, A. P. Prediction of the Binding Sites of Huperzine A in Acetylcholinesterase by Docking Studies. *J. Comput.-Aided Mol. Des.* **1994,** 8, 669-681.

38. Carlier, P. R.; Han, Y. F.; Chow, E. S.-H.; Li, C. P.-L.; Wang, H.; Lieu, T. X.; Wong, H. S.; Pang, Y.-P. Evaluation of Short-tether Bis-THA AChE Inhibitors. A Further Test of the Dual Binding Site Hypothesis. *Bioorg. Med. Chem.* **1999,** 7, 351-357.

39. While exact IC_{50} values differed between the Pang 1996 study and the Carlier and Pang 1999 study, the relative trends were identical. Variation in the absolute IC_{50} values between different labs is common because of experimental variation.

40. Rydberg, E. H.; Brumshtein, B.; Greenblatt, H. M.; Wong, D. M.; Shaya, D.; Williams, L. D.; Carlier, P. R.; Pang, Y. P.; Silman, I.; Sussman, J. L. Complexes of alkylene-linked tacrine dimers with *Torpedo californica* acetylcholinesterase: Binding of bis(5)-tacrine produces a dramatic rearrangement in the active-site gorge. *J. Med. Chem.* **2006,** 49, 5491-5500.

41. Carlier, P. R.; Chow, E. S.-H.; Han, Y.; Liu, J.; Yazal, J. E.; Pang, Y.-P. Heterodimeric Tacrine-Based Acetylcholinesterase Inhibitors: Investigating Ligand-Peripheral Site Interactions. *J. Med. Chem.* **1999,** 42, 4225-4231.

42. All efforts to duplicate this K_I in our laboratory have been unsuccessful.

43. Lewis, W. G.; Green, L. G.; Grynszpan, F.; Radic, Z.; Carlier, P. R.; Taylor, P.; Finn, M. G.; Sharpless, K. B. Click Chemistry In Situ: Acetylcholinesterase as a Reaction Vessel for the Selective Assembly of a Femtomolar Inhibitor from an Array of Building Blocks. *Angew. Chem., Int. Ed.* **2002,** 41, 1053-1057.

44. Jiang, H.; Luo, X.; Bai, D. Progress in Clinical, Pharmacological, Chemical and Structural Biological Studies of Huperzine A: A Drug of Traditional Chinese Medicine Origin for the Treatment of Alzheimer's Disease. *Curr. Med. Chem.* **2003,** 10, 2231-2252.

45. Carlier, P. R.; Du, D.-M.; Han, Y.; Liu, J.; Pang, Y.-P. Potent, Easily Synthesized Huperzine A-Tacrine Hybrid Acetylcholinesterase Inhibitors. *Bioorg. Med. Chem. Lett.* **1999,** 9, 2335-2338.

46. Camps, P.; Achab, R. E.; Görbig, D. M.; Morral, J.; Muñoz-Torrero, D.; Badia, A.; Baños, J. E.; Vivas, N. M.; Barril, X.; Orozco, M.; Luque, F. J. Synthesis, *in Vitro* Pharmacology, and Molecular Modeling of Very Potent Tacrine-Huperzine A Hybrids as Acetylcholinesterase Inhibitors of Potential Interest for the Treatment of Alzheimer's Disease. *J. Med. Chem.* **1999,** 42, 3227-3242.

47. Ainge, G. D.; Lorimer, S. D.; Gerard, P. J.; Ruf, L. D. Insecticidal Activity of Huperzine A from the New Zealand Clubmoss, Lycopodium varium. *J. Agric. Food Chem.* **2002,** 50, 491-494.

48. Lallement, G. Pretreatment of organophosphate poisoning: potential importance of huperzine A. *Ann. Pharm. Fr.* **2000,** 58, 13-17.

49. Lallement, G.; Veyret, J.; Masqueliez, C.; Aubriot, S.; Burckhart, M. F.; Baubichon, D. Efficacy of huperzine in preventing soman-induced seizures, neuropathological changes and lethality. *Funda. Clin. Pharmacol.* **1997,** 11, 387-394.

50. Ashani, Y.; Grunwald, J.; Alkalai, D.; Cohen, G.; Raveh, L. Studies with huperzine A, a new candidate in the research of prophylaxis against nerve agents. *Med. Def. Biosci. Rev., Proc.* **1996,** 1, 105-110.

51. Haviv, H.; Wong, D. M.; Greenblatt, H. M.; Carlier, P. R.; Pang, Y.-P.; Silman, I.; Sussman, J. L. Crystal Packing Mediates Enantioselective Ligand Recognition at the Peripheral Site of Acetylcholinesterase. *J. Am. Chem. Soc.* **2005,** 127, 11029-11036.

52. Colletier, J. P.; Sanson, B.; Nachon, F.; Gabellieri, E.; Fattorusso, C.; Campiani, G.; Weik, M. Conformational Flexibility in the Peripheral Site of Torpedo californica Acetylcholinesterase Revealed by the Complex Structure with a Bifunctional Inhibitor. *J. Am. Chem. Soc.* **2006,** 128, 4526-4527.

53. Wong, D. M.; Greenblatt, H. M.; Dvir, H.; Carlier, P. R.; Han, Y.-F.; Pang, Y.-P.; Silman, I.; Sussman, J. L. Acetylcholinesterase Complexed with Bivalent Ligands Related to Huperzine A: Experimental Evidence for Species-Dependent Protein-Ligand Complementarity. *J. Am. Chem. Soc.* **2003,** 125, 363-373.

54. Kaul, P. N. Enzyme inhibiting action of tetrahydroaminoacridine and its structural fragments. *J. Pharm. Pharmacol.* **1962,** 14, 243-248.

55. Desai, M. C.; Thadeio, P. F.; Lipinski, C. A.; Liston, D. R.; Spencer, R. W.; Williams, I. H. Physical parameters for brain uptake: optimizing log P, log D and pKa of THA. *Bioorg. Med. Chem. Lett.* **1991,** 1, 411-414.

56. $pH = pK_a + \log ([A^-] / [HA])$

57. Gregor, V. E.; Emmerling, M. R.; Lee, C.; Moore, C. J. The synthesis and *in vitro* Acetylcholinesterase and Butyrylcholinesterase inhibitory activity of tacrine (Cognex) derivatives. *Bioorg. Med. Chem. Lett.* **1992,** 2, 861-864.

58. Recanatini, M.; Cavalli, A.; Belluti, F.; Piazzi, L.; Rampa, A.; Bisi, A.; Gobbi, S.; Valenti, P.; Andrisano, V.; Bartolini, M.; Cavrini, V. SAR of 9-Amino-1,2,3,4-tetrahydroacridine-Based Acetylcholinesterase Inhibitors: Synthesis, Enzyme Inhibitory Activity, QSAR, and Structure-Based CoMFA of Tacrine Analogues. *J. Med. Chem.* **2000,** 43, 2007-2018.

59. Hu, M.-K.; Wu, L.-J.; Hsiao, G.; Yen, M.-H. Homodimeric Tacrine Congeners as Acetylcholinesterase Inhibitors. *J. Med. Chem.* **2002,** 45, 2277-2282.

Chapter 2. Bump-Hole Optimization of Tacrine Produces a Potent, Species-Selective Inhibitor of *Ag*AChE

2.1 Introduction

Chapter 1 described structure-activity studies directed at enhancing potency and selectivity of tacrine derivatives for mammalian acetylcholinesterase (AChE) to develop treatments for dementia. Inhibitors of AChE (AChEI) can present either therapeutic or toxic effects depending upon the dose administered. With the goal of developing new insecticides to control the malaria-transmitting mosquito, *Anopheles gambiae* (*Ag*), the tacrine pharmacophore (Figure 2.1) was reoptimized to attain high selectivity and potency for inhibition of mosquito AChE. The goal was to capitalize on variations in the active site sizes and shapes resulting from amino acid variations between human and *Anopheles gambiae* AChE (*Ag*AChE) using a modified bump-hole strategy.[1]

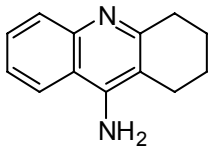

1a

Figure 2.1. Tacrine

2.2 Results and Discussion

2.2.1 Initial considerations in ligand design

To begin, the sequence alignment of *h*AChE with *Ag*AChE (Figure 2.2) was examined to identify easily accessible differences between AChE from each of the species.[2] It is important to note that there are two genes which code for *Ag*AChE (*ace*-1 and *ace*-2),[3] but expression in *Ag* has only been demonstrated for one gene (*ace*-1).[4] All analyses discussed below were conducted on the expressed *Ag*AChE, encoded for by the *ace*-1 gene, within the catalytic subunits of the enzymes. The most striking difference between *h*AChE and *Ag*AChE is the replacement of Phe295 of the human enzyme for Cys286 in the mosquito enzyme. This difference has been noted by Radić[5] and Pezzementi[6], and could provide a means to covalently modify the mosquito enzyme selectively. However, all efforts in our group to date have failed to effect covalent

modification of the mosquito enzyme, suggesting that the thiol of Cys286 is not accessible. Nevertheless, the *h*AChE and *Ag*AChE sequences are only 49% identical and 65% similar within the catalytic subunit, suggesting that highly species-selective inhibitors may be developed.

	Catalytic Triad			Oxyanion Hole		Choline-binding Site	
	200	327	440	116	201	84	330
Tc	TIFGE**S**AGGAS	**E**	**H**	YGGGF	**A**	W	FF
	203	334	447	119	204	86	337
human	TLFGE**S**AGAAS	**E**	**H**	YGGGF	**A**	W	YF
	199	325	439	116	200	84	328
Ag ace-1	TLFGE**S**AGAVS	**E**	**H**	FGGGF	**A**	W	YF

	Acyl Pocket			Peripheral Site				
	233	288	290	70	72	121	279	334
Tc	W	F	F	Y	D	Y	W	YG
	236	295	297	72	74	124	286	341
human	W	F	F	Y	D	Y	W	YG
	232	286	288	70	72	121	280	332
Ag ace-1	W	C	F	I	D	Y	W	YY

Figure 2.2. Alignment of *Torpedo californica*, human, and *Anopheles gambiae* AChE. SwissProt codes: ACES_TORCA (*Tc*), ACES_HUMAN (human), ACE1_ANOGA (*Ag ace*-1). Residues marked in bold are essential for catalysis. By convention, residue numbering is based on that of the catalytic subunit of mature *Tc*AChE, as defined by the X-ray crystal structure of the native enzyme (PDB ID 2ACE[7]).

Bioassays of the inhibitors described below were performed by Dr. Troy Anderson (Bloomquist group, Department of Entomology) using the method of Ellman and coworkers.[8] The colorimetric assay takes advantage of the ability of AChE to hydrolyze acetylthiocholine (ATCh, Scheme 2.1), a substrate analogue. The thiocholine hydrolysis product then reacts with colorless DTNB to form the yellow TNB anion. Two *Ag*AChE enzyme sources were used to characterize all compounds. The first was whole mosquito homogenate from adult, non-blood fed females, provided by Professor Sally Paulson (Department of Entomology). The use of *Ag* homogenate was necessitated by a patent application by Myléne Weill,[9] which claimed the use of recombinant *Ag*AChE for insecticide discovery. Although this application is now no longer active in the US and Europe, at the beginning of our research, it was necessary to protect our research against possible patent infringement. Therefore, *Ag* homogenate was the primary screen for discovery. However, since *Ag* homogenate could contain additional ATCh-hydrolyzing enzymes, IC_{50} values versus *Ag* homogenate may reflect several inhibition phenomena. Thus, an assay of some recombinant *Ag*AChE was necessary. Eventually, we were able to utilize a second source of mosquito enzyme, a recombinant full length *Ag*AChE provided by Professor Eric Wong (Department of Animal and Poultry Science). As shown in Figure 2.3, the full length *Ag*AChE precursor protein contains an *N*-terminal signal peptide (aa1-38), a fragment (aa39-61) that is not seen in *Tc*, mouse, or *h*AChE, a 540-residue catalytic subunit (aa162-701), and a *C*-

terminal peptide (aa702-737). Throughout this chapter, by convention, our discussion of the main catalytic subunit of *Ag*AChE and specific residues will be numbered based on the mature form of *Tc*AChE, beginning at residue aa162 in the full length *Ag*AChE precursor sequence. Thus the main catalytic subunit of *Ag*AChE (Asp1-Pro540) corresponds to aa162-701, and Gly119 is actually aa280 in the full length protein. This construct included a *C*-terminal 6X-His tag (for Ni affinity column purification) and V5 epitope and was expressed in *Drosophila melanogaster* S2 cells (W38, Figure 2.3). Unfortunately, purification of the W38 strain via the 6X-His tag could not be accomplished. Although purification by procainamide affinity column (Dawn Wong, Samantha Casterlow, unpublished) did prove possible, this method was throughput limiting. Thus the W38 recombinant *Ag*AChE was used in the form of cell lysate. All appropriate controls were taken to show that non-transfected *Drosophila* S2 cells did not possess any significant ATCh-hydrolyzing activity.

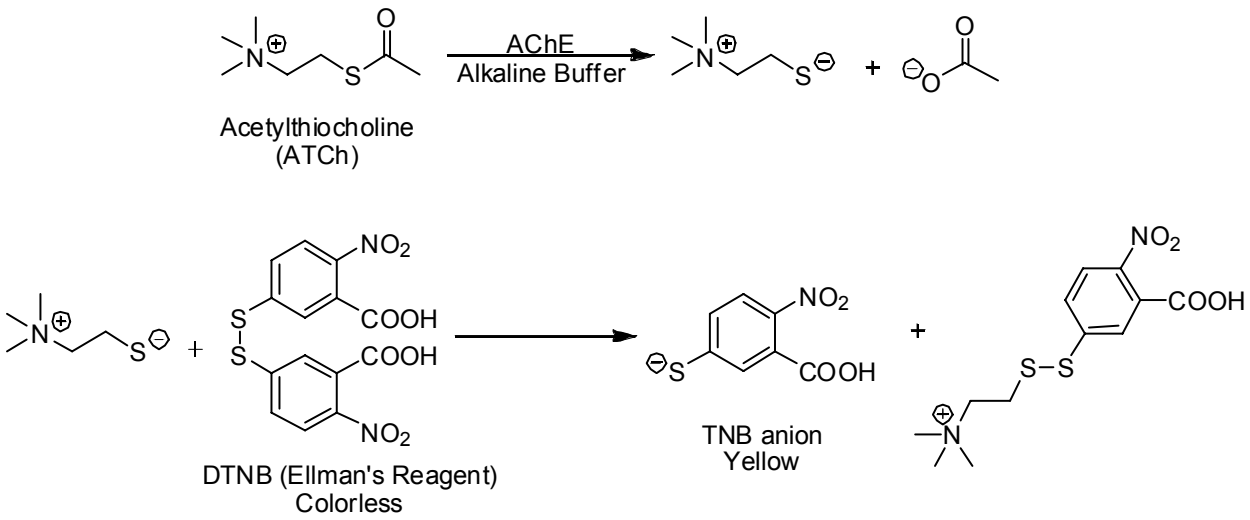

Scheme 2.1. The Ellman Assay.[8] The concentration of TNB anion is measured using UV-vis spectroscopy.

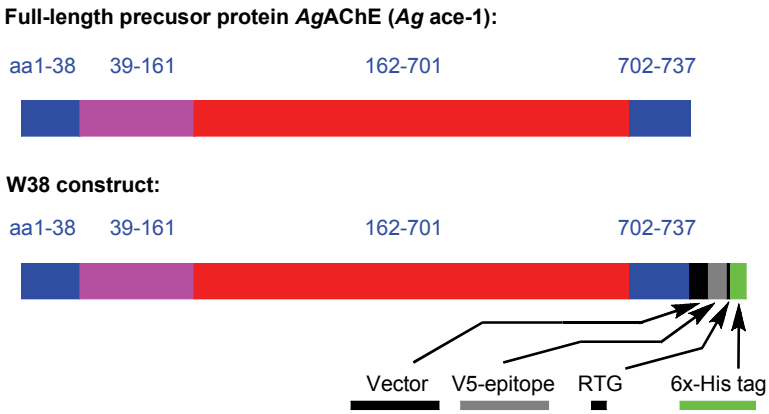

Figure 2.3. Full-length protein as encoded for by *Ag ace*-1 and the W38 construct developed as a source of pure enzyme.

2.2.2 Inhibitor design and synthesis

The initial inhibitor design approach was based on the bump-hole strategy of Schreiber[10] as reviewed by Koh.[1] In this modified strategy, the human enzyme was viewed as the wild type and the mosquito enzyme as the mutant for which a high affinity functionally orthogonal ligand was desired. As the inhibitors were assayed, the goal was to systematically include a "bump" in a ligand which could fill a "hole" in *Ag*AChE that was not present in *h*AChE. In such a manner, it should be possible to find a highly selective inhibitor of *Ag*AChE.

Inhibitor design was based on the wealth of literature discussing the SAR of tacrine and its analogs. As discussed in Chapter 1, many modifications of tacrine have been reported to increase the ligand's affinity for mammalian AChE.[11-13] Those modifications known to be detrimental to ligand binding to mammalian AChE were used as a starting point for further ligand design. For instance, expansion of the cyclohexyl moiety of **1a** to an 8-membered ring as in **1c** has been shown to cause a 100-fold decrease in inhibition potency.[11] Furthermore, 7-substitution (Scheme 2.2) has been known to negatively impact the inhibition potency of the ligands.[12-14]

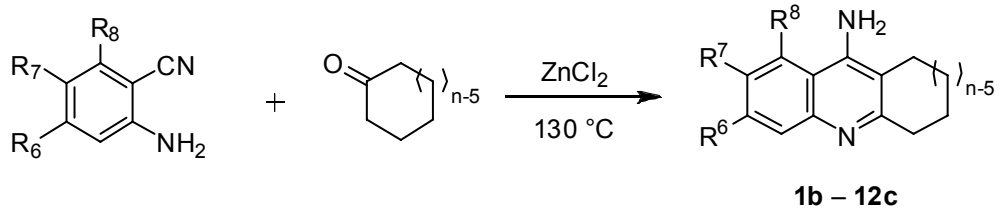

1b – 12c

Scheme 2.2. Friedländer condensation reaction scheme for the synthesis of tacrine derivatives **1b** – **12c**.

Friedländer condensations[12] (Scheme 2.2) of substituted anthranilonitriles and cycloalkanones were carried out to develop a focused library of 36 tacrine derivatives. Substitution at the 6-, 7-, and 8-positions was examined, as well as the effect of varying the ring size from 6-, 7-, and 8-membered rings in a double mutant strategy (Scheme 2.3). The condensations were performed at 130 °C in the presence of $ZnCl_2$. All products were recrystallized from hot ethanol. In general, the isolated yields of the condensation products were quite good. The low yields reported for **4a**, **6a**, **7a**, **7c**, **9c**, and **12a**, were not optimized, and may be attributed to lack of solubility in ethanol during recrystallization, as a pre-nucleation filtration was performed during purification.

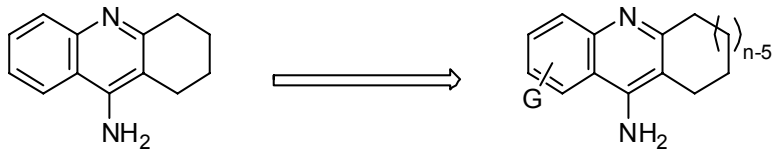

Scheme 2.3. Schematic of double mutant strategy of tacrine modification

As previously stated, the compounds were assayed versus *h*AChE, as well as homogenate *Ag*AChE, and the W38 *Ag*AChE construct, using the Ellman method.[8] The goal for the Friedländer condensation products was to produce an inhibitor with high selectivity for *Ag*AChE. It was known that tacrine **1a** was non-selective to mildly selective for human enzyme, and three scenarios were envisioned whereby modifications to tacrine could cause selectivity for the mosquito enzyme. First, the ideal scenario was that substitution could increase potency for *Ag*AChE while reducing potency for *h*AChE (scenario 1). A second scenario was that substitution would greatly increase the potency for *Ag*AChE but only mildly increase the potency for *h*AChE (scenario 2). Finally, the third scenario was that substitution would reduce the potency in both *Ag*AChE and *h*AChE, with the most severe reduction observed for the human enzyme (scenario 3).

Examining the size of the cycloalkyl moiety first (Table 2.1), one finds that, in general, compounds bearing 7-membered rings are equally potent or more potent than the 6-membered ring homologs for human enzyme. This trend matches the results reported by Harvey and coworkers[11] that showed **1a** exhibited an IC_{50} of 78 nM for rat brain AChE, while **1b** exhibited an IC_{50} of 39 nM for the same enzyme source. In our studies, using *h*AChE, **1a** exhibited a 260 nM IC_{50}, while **1b** exhibited a 13 nM IC_{50}. In the mosquito enzymatic assays, the same trend was observed. Using the W38 construct, **1b** exhibited more than double the potency of **1a**. Further expansion of the cycloalkyl moiety caused a dramatic loss in potency for the human enzyme, an effect first noted by Harvey and coworkers.[11] In our assay, **1c** exhibited a 3,600 nM IC_{50} for human enzyme; the potency of **1c** was nearly 14-fold less than that of **1a** and 280-fold less than that of **1b**. In the mosquito enzymatic assays, a similar effect was observed. For instance, **1c** was 11-fold and 25-fold less potent than **1a** and **1b**, respectively, for the W38 construct. In summary, modification of the cycloalkyl moiety generally exhibited the third scenario presented above; decreases in potency in one enzymatic species were concomitant with decreases in the other species.

Table 2.1. Cycloalkyl ring size (n), yields and *in vitro* pharmacology of tacrine derivatives **1b – c**

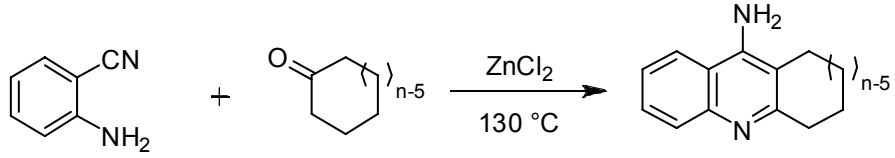

1b – c

Compound	R^6	R^7	R^8	n	% Yield	*h*AChE [a] IC_{50} (nM)	*Ag*AChE [b] *ace-1* IC_{50} (nM)	*Ag*AChE [c] homogenate IC_{50} (nM)
1a	H	H	H	6	na[d]	260	250 (1.0x)	550 (0.47x)
1b	H	H	H	7	86	13	110 (0.12x)	100 (0.13x)
1c	H	H	H	8	40	3,600	2,800 (1.3x)	4,800 (0.75x)

[a] Recombinant human enzyme purchased from Sigma, 2,530 U/mg. [b] W38, see Section 2.2.1; values in parenthesis are IC_{50} ratios (*h*AChE/*Ag*AChE). [c] Enzyme source is non-blood fed G3 strain *Anopheles gambiae* homogenate; values in parenthesis are IC_{50} ratios (*h*AChE/*Ag*AChE). [d] Purchased from Aldrich.

The first set of substitutions we will examine are those at the 6-position (Table 2.2, **2a** – **3c**). Because it was known that 6-substitution greatly enhances potency against *h*AChE, the hope was that even greater potency enhancements would be realized for *Ag*AChE (scenario 2). As expected, we found that 6-substitution caused large enhancements in potency for the human enzyme. For instance, **2a** exhibited an IC_{50} value of 6 nM, while unsubstituted tacrine **1a** only exhibited an IC_{50} value of 260 nM. However, when assayed against the mosquito enzyme, the 6-substituted analogs did not possess a remarkable potency enhancement in comparison to the unsubstituted compounds. From the two sets of 6-substituted compounds examined, it was concluded that other substitution patterns were required in order to gain high species selectivity.

Table 2.2. Substituents (R^6 – R^8), cycloalkyl ring size (n), yields, and *in vitro* pharmacology of tacrine derivatives **1a – 3c**

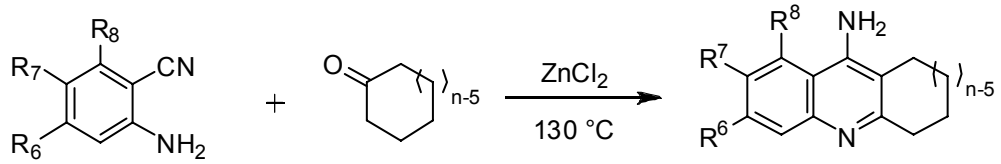

1b – 12c

Compound	R^6	R^7	R^8	n	% Yield	*h*AChE [a] IC_{50} (nM)	*Ag*AChE [b] *ace-1* IC_{50} (nM)	*Ag*AChE [c] homogenate IC_{50} (nM)
1a	H	H	H	6	na[d]	260	250 (1.0x)	550 (0.47x)
1b	H	H	H	7	86	13	110 (0.12x)	100 (0.13x)
1c	H	H	H	8	40	3,600	2,800 (1.3x)	4,800 (0.75x)
2a	Cl	H	H	6	67	6	160 (0.038x)	610 (0.0098x)
2b	Cl	H	H	7	65	1.3	280 (0.0046x)	260 (0.005x)
2c	Cl	H	H	8	62	700	3,900 (0.18x)	1,400 (0.5x)
3a	Me	H	H	6	81	10	380 (0.026x)	290 (0.035x)
3b	Me	H	H	7	56	9	340 (0.026x)	270 (0.033x)
3c	Me	H	H	8	65	1,100	3800 (0.29x)	5,800 (0.19x)

[a] Recombinant human enzyme purchased from Sigma, 2,530 U/mg. [b] W38, see Section 2.2.1; values in parenthesis are IC_{50} ratios (*h*AChE/*Ag*AChE). [c] Enzyme source is non-blood fed G3 strain *Anopheles gambiae* homogenate; values in parenthesis are IC_{50} ratios (*h*AChE/*Ag*AChE). [d] Purchased from Aldrich.

The next set of substitutions we will examine are those at the 8-position (Table 2.3, **4a** – **6c**). From the report of Desai and coworkers,[14] it was known that 8-fluorotacrine **6a** exhibited slightly higher potency for human erythrocyte AChE than did tacrine **1a**. Furthermore, 8-chlorotacrine **4a** has been reported by both Desai and coworkers[14] and Gregor and coworkers[13] to be slightly more potent than **1a** for human erythrocyte AChE. No remarkable potency enhancements in either human or mosquito enzyme for compounds substituted at the 8-position were discovered in our studies. The most pronounced response was 8-fluorotacrine **6a**. This inhibitor exhibited a 4-fold potency enhancement, versus **1a**, for the human enzyme. Unfortunately, there was a concomitant 2-fold loss of potency for **6a** against the mosquito enzyme.

Table 2.3. Substituents (R^6 – R^8), cycloalkyl ring size (n), yields, and *in vitro* pharmacology of tacrine derivatives **1a** – **c** and **4a** – **6c**

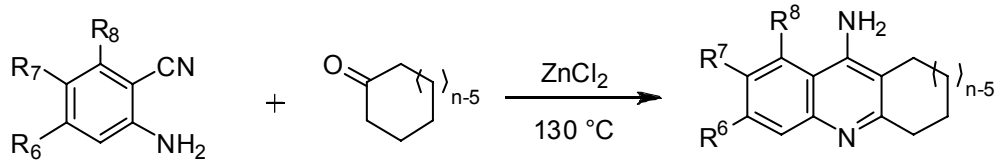

1b – 12c

Compound	R^6	R^7	R^8	n	% Yield	*h*AChE [a] IC_{50} (nM)	*Ag*AChE [b] *ace-1* IC_{50} (nM)	*Ag*AChE [c] homogenate IC_{50} (nM)
1a	H	H	H	6	na[d]	260	250 (1.0x)	550 (0.47x)
1b	H	H	H	7	86	13	110 (0.12x)	100 (0.13x)
1c	H	H	H	8	40	3,600	2,800 (1.3x)	4,800 (0.75x)
4a	H	H	Cl	6	40	330	140 (2.4x)	150 (2.2x)
4b	H	H	Cl	7	98	110	160 (0.69x)	160 (0.69x)
4c	H	H	Cl	8	74	1,500	880 (1.7x)	730 (2.1x)
5a	H	H	Me	6	93	180	270 (0.67x)	360 (0.50x)
5b	H	H	Me	7	89	91	360 (0.25x)	360 (0.25x)
5c	H	H	Me	8	78	2,100	2,700 (0.78x)	2,300 (0.91x)
6a	H	H	F	6	17	59	510 (0.12x)	450 (0.13x)
6b	H	H	F	7	87	130	460 (0.28x)	430 (0.30x)
6c	H	H	F	8	83	3,100	6,400 (0.48x)	8,400 (0.37x)

[a] Recombinant human enzyme purchased from Sigma, 2,530 U/mg. [b] W38, see Section 2.2.1; values in parenthesis are IC_{50} ratios (*h*AChE/*Ag*AChE). [c] Enzyme source is non-blood fed G3 strain *Anopheles gambiae* homogenate; values in parenthesis are IC_{50} ratios (*h*AChE/*Ag*AChE). [d] Purchased from Aldrich.

Disubstitution at the 6- and 7-positions was examined with dimethoxytacrines **7a** – **7c** (Table 2.4). Mild selectivity for mosquito enzyme was observed with **7a**, as the potency for human enzyme decreased relative to that for **1a** and was essentially unchanged relative to **1a** for mosquito enzyme. This species-selective response matched the third scenario envisioned to produce species selective ligands, albeit to an insignificant degree. Interestingly, expansion of the cyclohexyl ring as in **7b** (IC_{50} > 10,000 nM) and **7c** (IC_{50} = 8,200 nM) produced ligands with very poor inhibition potency for *Ag*AChE.

Table 2.4. Substituents (R^6 – R^8), cycloalkyl ring size (n), yields, and *in vitro* pharmacology of tacrine derivatives **1a** – **c** and **7a** – **c**

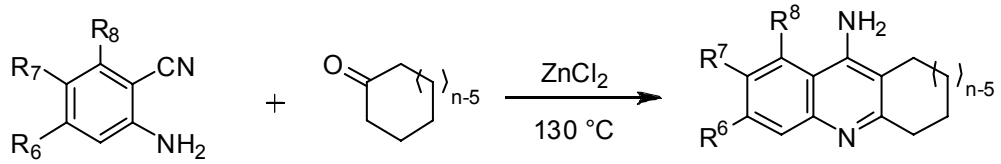

1b – 12c

Compound	R^6	R^7	R^8	n	% Yield	*h*AChE [a] IC_{50} (nM)	*Ag*AChE [b] *ace-1* IC_{50} (nM)	*Ag*AChE [c] homogenate IC_{50} (nM)
1a	H	H	H	6	na[d]	260	250 (1.0x)	550 (0.47x)
1b	H	H	H	7	86	13	110 (0.12x)	100 (0.13x)
1c	H	H	H	8	40	3,600	2,800 (1.3x)	4,800 (0.75x)
7a	MeO	MeO	H	6	37	1,000	300 (3.3x)	370 (2.7x)
7b	MeO	MeO	H	7	72	2,500	>10,000	16,000 (0.16x)
7c	MeO	MeO	H	8	21	1,500	8,200 (0.18)	8,800 (0.17x)

[a] Recombinant human enzyme purchased from Sigma, 2,530 U/mg. [b] W38, see Section 2.2.1; values in parenthesis are IC_{50} ratios (*h*AChE/*Ag*AChE). [c] Enzyme source is non-blood fed G3 strain *Anopheles gambiae* homogenate; values in parenthesis are IC_{50} ratios (*h*AChE/*Ag*AChE). [d] Purchased from Aldrich.

Finally, 7-substitution was examined with compounds **8a** – **12c** (Table 2.5). As expected from literature precedent,[12,13,15] 7-substitution was detrimental to *h*AChE inhibition potency. For instance, **8a** was nearly 27-fold less potent than **1a** for human enzyme inhibition. Interestingly, the decrease in potency was not as pronounced for *Ag*AChE inhibition; the potency decrease for **8a** versus **1a** was only 6-fold against the homogenate mosquito enzyme. This effect corresponds to the third scenario presented above in which potencies versus both *h*AChE and *Ag*AChE were reduced, but the reduction was more prevalent in the human enzyme. Ultimately, modified 7-chlorotacrine **8c** (Figure 2.4), which exhibited moderate potency of 3,000 nM for the W38 *Ag*AChE construct and no measurable potency for the human enzyme, was selected as the bump-hole optimized ligand. Selectivity of **8c** for inhibition of *Ag*AChE versus *h*AChE ranges from 51- to 100-fold, depending on the source of *Ag*AChE (homogenate or recombinant). This selectivity apparently results from synergism between the 8-membered ring and the Cl substituent. Removal of either feature from the pharmacophore led to a decrease in species selectivity. Compound **8c** thus became the lead compound for further optimization.

Table 2.5. Substituents (R^6 – R^8), cycloalkyl ring size (n), yields, and *in vitro* pharmacology of tacrine derivatives **1a** – **c** and **8a** – **12c**

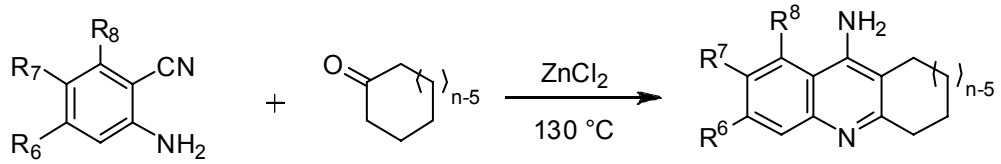

1b – 12c

Compound	R^6	R^7	R^8	n	% Yield	*h*AChE [a] IC_{50} (nM)	*Ag*AChE [b] *ace-1* IC_{50} (nM)	*Ag*AChE [c] homogenate IC_{50} (nM)
1a	H	H	H	6	na[d]	260	250 (1.0x)	550 (0.47x)
1b	H	H	H	7	86	13	110 (0.12x)	100 (0.13x)
1c	H	H	H	8	40	3,600	2,800 (1.3x)	4,800 (0.75x)
8a	H	Cl	H	6	78	7,000	2,000 (3.5x)	3,200 (2.2x)
8b	H	Cl	H	7	87	6,900	1,900 (3.6x)	2,500 (2.8x)
8c	H	Cl	H	8	53	~300,000	3,000 (100x)	5,900 (51x)
9a	H	Me	H	6	92	4,400	3,800 (1.2x)	4,000 (1.1x)
9b	H	Me	H	7	61	17,000	3,500 (4.9x)	2,700 (6.3x)
9c	H	Me	H	8	23	4,500	3,500 (1.3x)	3,800 (1.2x)
10a	H	NO_2	H	6	70	210	3,100 (0.068x)	3,600 (0.058x)
10b	H	NO_2	H	7	51	5,600	6,500 (0.86x)	14,000 (0.40x)
10c	H	NO_2	H	8	74	400	4,200 (0.095x)	4,300 (0.09x)
11a	H	F	H	6	83	500	890 (0.56x)	340 (1.5x)
11b	H	F	H	7	97	320	440 (0.73x)	250 (1.3x)
11c	H	F	H	8	91	3,400	7,900 (0.43x)	3,200 (1.1x)
12a	H	Br	H	6	95	1,100	3,900 (0.28x)	6,000 (0.18x)
12b	H	Br	H	7	94	1,900	3,200 (0.59x)	5,000 (0.38x)
12c	H	Br	H	8	97	2,100	3,000 (0.70x)	4,400 (0.48x)

[a] Recombinant human enzyme purchased from Sigma, 2,530 U/mg. [b] W38, see Section 2.2.1; values in parenthesis are IC_{50} ratios (*h*AChE/*Ag*AChE). [c] Enzyme source is non-blood fed G3 strain *Anopheles gambiae* homogenate; values in parenthesis are IC_{50} ratios (*h*AChE/*Ag*AChE). [d] Purchased from Aldrich.

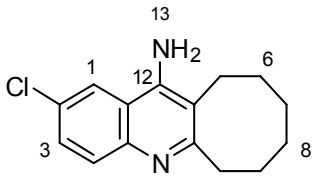

8c

Figure 2.4. Bump-hole optimized modified 7-chlorotacrine **8c**.

Because two sources of *Ag*AChE were utilized in our investigation, it is reasonable to inquire whether the two sources have similar inhibition profiles. If *Ag* homogenate contains only one kinetically significant ATCh-hydrolyzing enzyme, one would expect trends in inhibition potency among the 36 tacrine analogues to match that of the recombinant *Ag*AChE. Thus, a plot was prepared of the logarithm of the IC_{50} of all 36 inhibitors against the W38 construct AChE

versus the logarithm of the analogous IC_{50} against *Ag* homogenate (Figure 2.5). From the correlation value (R^2 = 0.89), one could reasonably conclude that the two enzymatic sources exhibited similar behavior. As a result, it is unlikely that there are additional ATCh-hydrolyzing species in the homogenate mixture. Therefore, the activity observed against Ag homogenate is attributable to AChE, and not other unidentified enzymes.

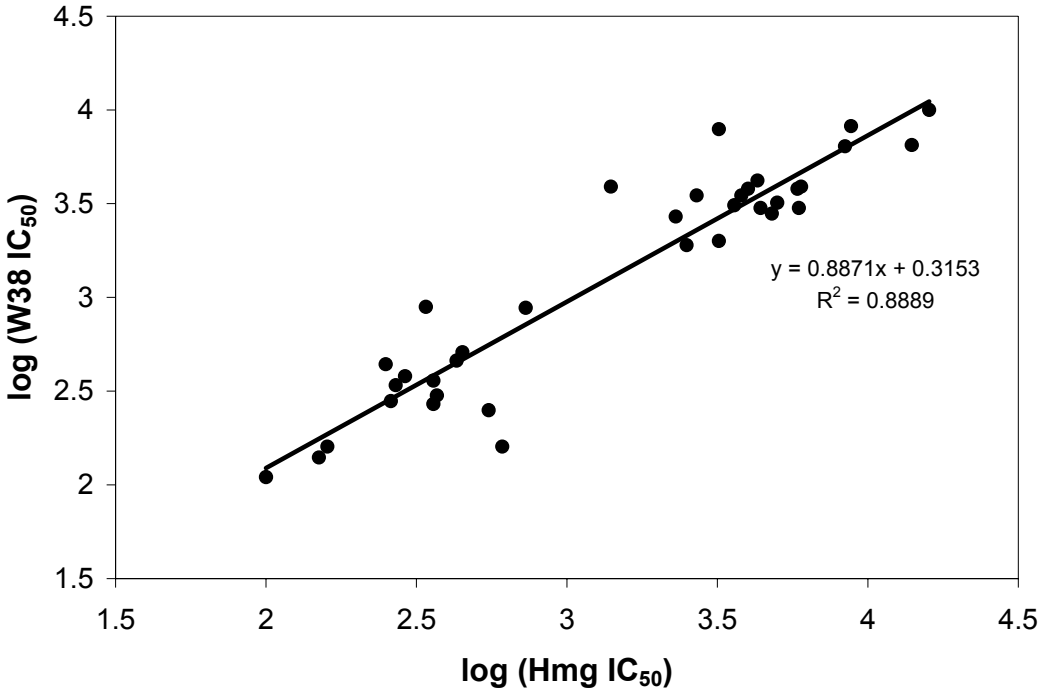

Figure 2.5. Correlation between assay results versus W38 construct and homogenate (Hmg) sources of *Ag*AChE.

To explore the likely conformation of the saturated ring moiety of **8c**, a conformational analysis was performed using the MMFF94[16] method on the protonated inhibitor. This calculation located three minima (within 9.1 kcal/mol), which were subsequently optimized using B3LYP/6-31G*. An overlay of the structures (Figure 2.6) showed that the heteroaromatic portion of all three conformations was identical; however, the saturated moiety of each conformation was different in each structure. For simplicity, the lowest energy ground state conformation is reproduced in Figure 2.7. Interestingly, the lowest energy ground state structure (Table 2.6) exhibits a conformation in which C7 is spatially closer to the aryl system, while C8 is spatially farther away. In the other two conformations, this relationship is reversed; C8 is spatially closer to the aryl system and C7 is farther away.

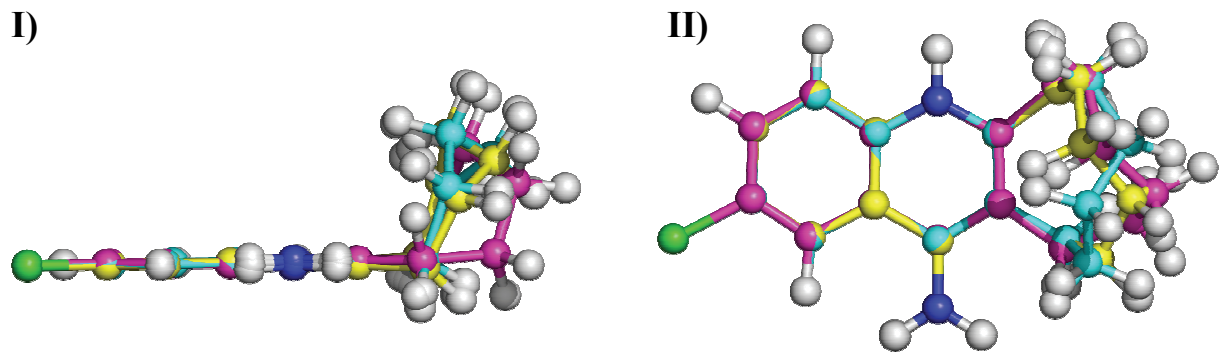

Figure 2.6. Ground state structures of protonated **8c** as calculated using B3LYP/6-31G*. Key: Aqua (conformation **A**) = Gold (conformation **B**) = Magenta (conformation **C**) = Carbon; White = Hydrogen; Blue = Nitrogen; Green = Chlorine. **I**) View looking down the C12-N13 bond. **II**) View looking from above the plane of the heteroaromatic ring system. Figures generated with PyMol.[17]

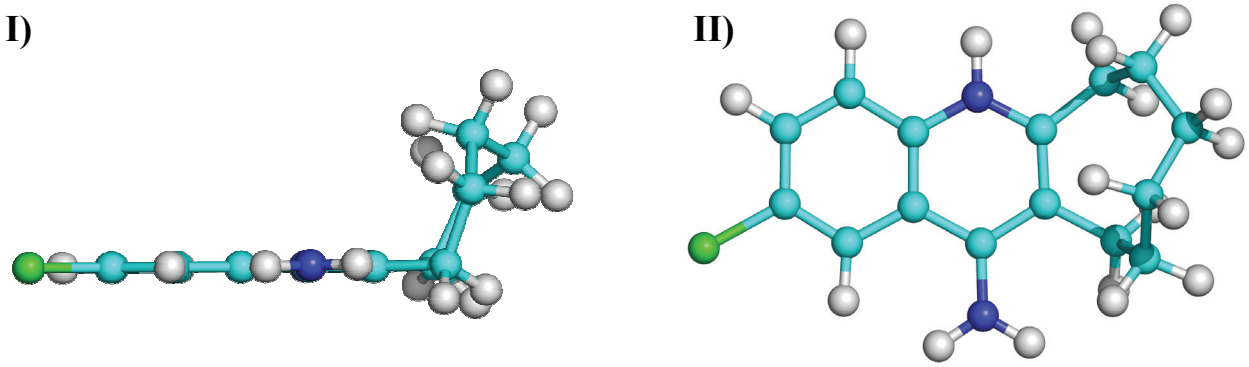

Figure 2.7. Ground state structure of protonated **8c** conformation **A** as calculated using B3LYP/6-31G*. Key: Aqua (conformation **A**) = Carbon; White = Hydrogen; Blue = Nitrogen; Green = Chlorine. **I**) View looking down the C12-N13 bond. **II**) View looking from above the plane of the heteroaromatic ring system. Figures generated with PyMol.[17]

Table 2.6. Electronic energy (E_h), ZPVE, and relative energy of three minima of **8c**. Energies are relative to conformation **A**. Conformations are defined in Figure 2.6.

Conformation	Energy (E_h) [a]	Scaled [b] ZPVE (E_h)	Rel. Energy (kcal/mol)
A	-1151.965517	0.302905	0.0
B	-1151.964661	0.302832	0.5
C	-1151.959110	0.303264	4.2

[a] Calculated using B3LYP/6-31G*. [b] Frequencies were scaled by a factor of 0.9804.

2.2.3 Dimerization of the lead compound

The rationale, design, and synthesis of bivalent inhibitors of AChE have been reviewed by Du and Carlier.[18] Since the initial work of Pang[19] and Carlier,[20,21] it has been known that it is possible to tether a CAS-selective ligand to a PAS-active ligand through an alkyl chain of appropriate length, to effect highly potent inhibition. The design, synthesis, and pharmacology

of tacrine homodimers **16b – l** were reviewed in Chapter 1. As the highly species selective ligand **8c** had been discovered, syntheses of dimers of **8c**, following the same general pathway as reported by Carlier and coworkers (Scheme 2.4),[20] were performed to increase the inhibition potency of the pharmacophore. First, the synthesis of *N*-(2-carboxy)aryl imine **17** (Scheme 2.5) was conducted. Contrary to the reported spiro-carbinolamine ester **13**, which is expected to exist in solution in equilibrium with *N*-(2-carboxy)aryl imine **14**,[20] compound **17** was determined to be the predominant species in our synthesis based on ^{1}H NMR spectroscopy (carboxylic acid ^{1}H at δ 11.57 ppm). This conclusion was confirmed with IR spectroscopy by comparing the spectrum of **17** with that of **13**; vacuum dried **17** exhibited a broad OH stretch at 3363 cm^{-1}, while **13** did not exhibit a similar stretch. Next, **17** was reacted with $POCl_3$ to afford the ring expanded modified 7,9-dichlorotacrine **18**. The preceding scheme may be used conveniently in large scale syntheses, as purification was performed without chromatography and the yield over both steps was a reasonable 59%.

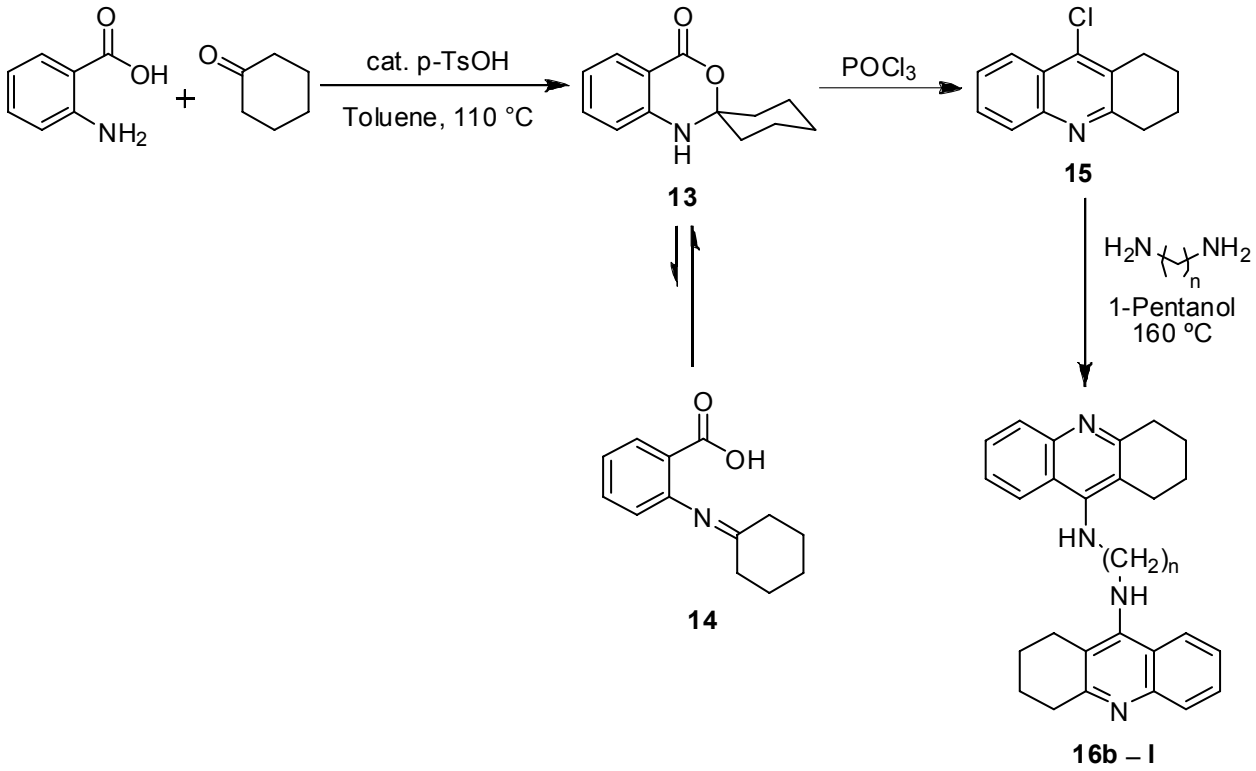

Scheme 2.4. Synthesis of 9-chloro-1,2,3,4-tetrahydroacridine **15** and tacrine homodimers **16b – l**.[20]

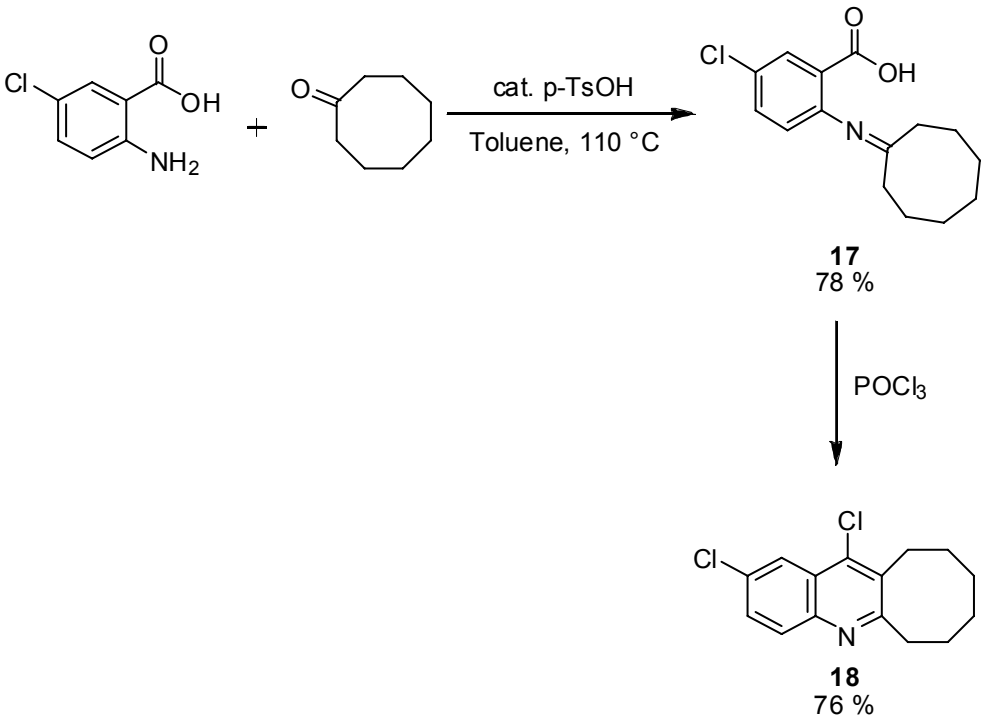

Scheme 2.5. Synthesis of ring expanded modified 7,9-dichlorotacrine **18**.

To synthesize bump-hole optimized tacrine dimers **20c** – **l** (Scheme 2.6), **18** and the appropriate 1,n-diamine were refluxed in 1-pentanol for 48 h. This process was analogous to the reported synthesis of tacrine homodimers **16b** – **l**. However, all efforts to synthesize **20c** – **l** using this protocol proved ineffective due to the incomplete conversion of starting materials. To attempt higher conversion in a reasonable time, the reaction temperature was raised by refluxing in phenol or 1-octanol. However, the use of both of these solvents caused the formation of numerous undesired side products. Ultimately, **20c** – **l** were synthesized over two steps starting with **18**. In the first step, 1 equiv of **18** was allowed to react with a large excess (e.g. 5 equiv) of the appropriate 1,n-diamine to form amino-terminated *N*-alkyltacrine derivatives **19c** – **l** in 37 – 88% yield (Table 2.7). Efforts to increase the reaction time led to the formation of undesired side products. Upon purification of the amino-terminated *N*-alkyltacrine derivatives **19c** – **l** by chromatography in mixtures of methanol and dichloromethane, the products were allowed to react with an excess (e.g. 2.5 equiv) of ring expanded modified 7,9-dichlorotacrine **18** to form bump-hole optimized tacrine homodimers **20c** – **l**. These compounds were purified by recrystallization from hot methanol and water mixtures to afford pure homodimers in 30 – 80% yield. This two step process takes advantage of Le Chatelier's Principle by providing an abundance of starting material to drive the reaction to completion. We also used the two step

process to synthesize **22** (Scheme 2.7) in an attempt to increase *Ag*AChE inhibition potency. Incorporation of an –N(Me)- unit into the alkylene tether has been shown to increase potency for mammalian AChE, presumably through interactions in the mid-gorge region of the enzyme.[22]

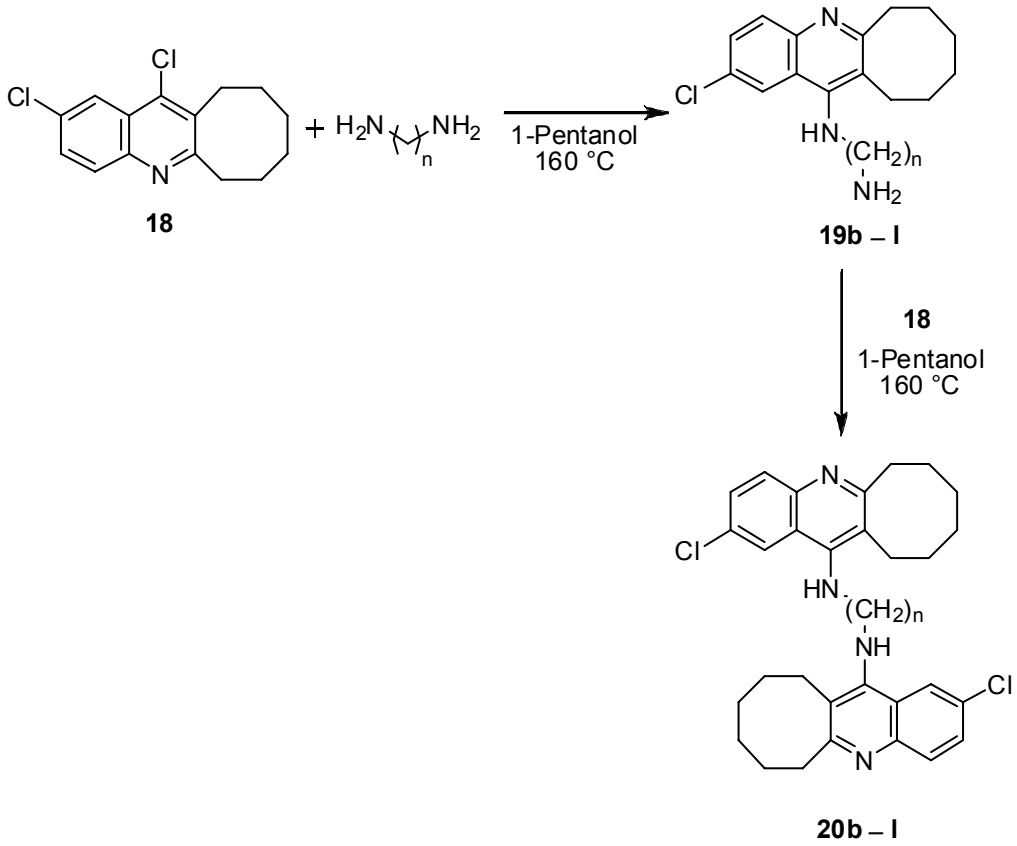

Scheme 2.6. Synthesis of bump-hole optimized tacrine homodimers **20c** – **l** (homolog lettering scheme for all bivalent inhibitors: c, n = 3; d, n = 4; e, n = 5; f, n = 6; g, n = 7; h, n = 8; i, n = 9; j, n = 10; l, n = 12).

Table 2.7. Percent yields of the amino-terminated *N*-alkyltacrine derivatives (**19c** – **l** and **21**)

Compound	n	% Yield
19c	3	66
19d	4	88
19e	5	78
19f	6	82
19g	7	63
19h	8	56
19i	9	66
19j	10	53
19l	12	37
21	–	86

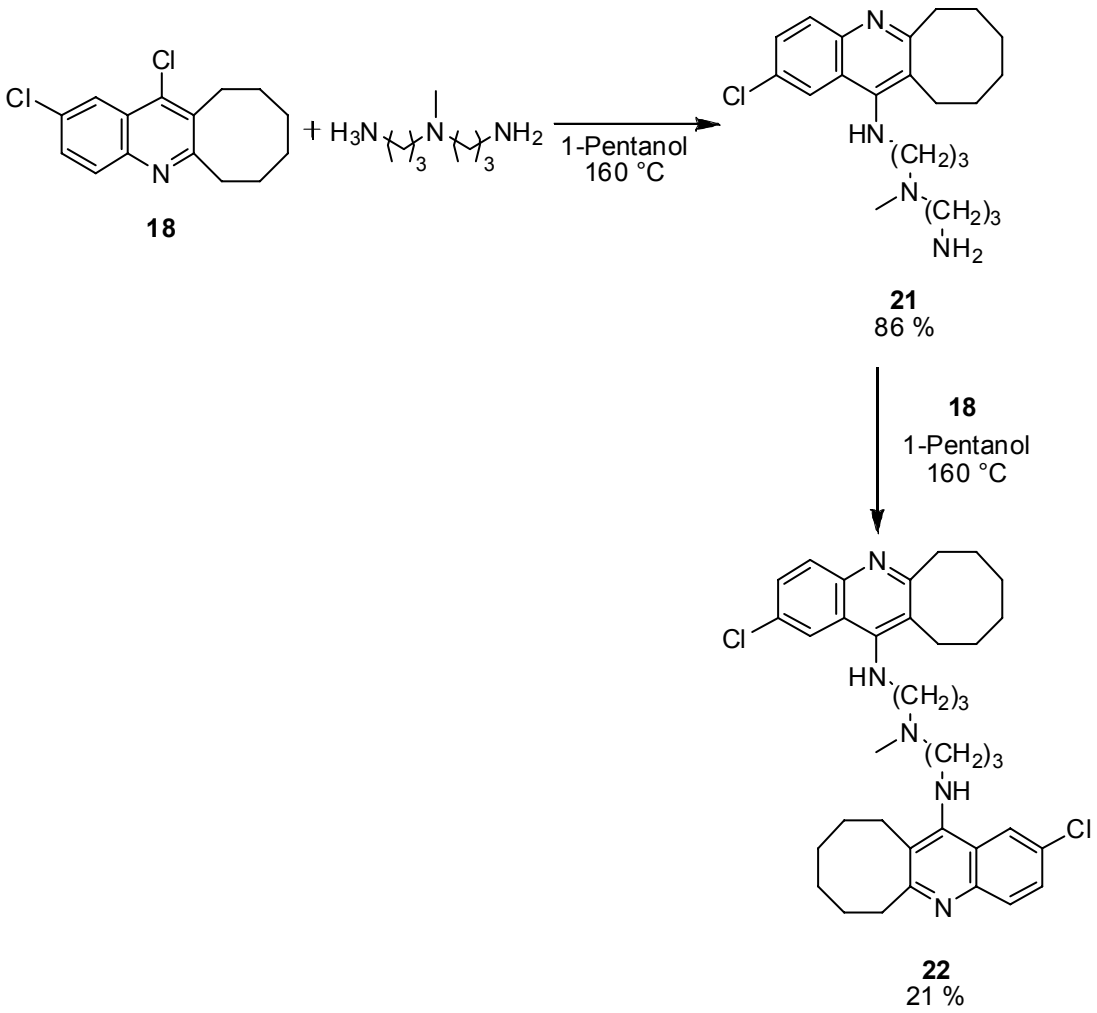

Scheme 2.7. Synthesis of *N*-methyl bridged bump-hole optimized tacrine dimer **22**.[22]

Dimerization of the lead compound proved to be an effective means to produce a highly potent and species selective inhibitor of *Ag*AChE (Table 2.8). The optimal dimer was determined to be octylene-linked bump-hole optimized tacrine dimer **20h** (Figure 2.8). This dimer possessed an IC_{50} of 18 nM for the W38 *Ag*AChE construct and an IC_{50} of >10,000 nM for the human enzyme, yielding a greater than 560-fold selectivity for the mosquito enzyme. Dimerization of **2c** to **20h** increased *Ag*AChE inhibition potency 170- to 650-fold, depending on the source of enzyme. In contrast, dimerization of **2c** to **20g** increased *h*AChE potency only 83-fold. As shown in Figure 2.8, at around 1 μM concentrations of **20h**, *h*AChE still retains 80% of its catalytic activity while the *Ag* homogenate enzyme is completely inactive. Interestingly, the hexylene- and heptylene-linked dimers also exhibited high potency and selectivity for the mosquito enzyme. However, shorter length tethers (i.e. **20c**) and longer length tethers (**20i** –**l**) gave significantly lower inhibition potencies and selectivities. The presence of an optimal tether

length for dual site binding of tacrine dimers has previously been reported,[19,20] and the data for **20c – l** further support the dual-binding site hypothesis (Figure 2.9).

Table 2.8. Alkyl chain size (n), yields, and *in vitro* pharmacology of bump-hole optimized tacrine homodimers

Compound	n	% Yield	*h*AChE [a] IC_{50} (nM)	*Ag*AChE *ace-1* [b] IC_{50} (nM)	*Ag*AChE homogenate [c] IC_{50} (nM)
8c	–	53	~300,000	3,000 (100x)	5,900 (51x)
20c	3	60	3,300	410 (8.0x)	530 (6.2x)
20d	4	50	1,500	9.9 (150x)	15 (100x)
20e	5	80	1,100	48 (23x)	170 (6.5x)
20f	6	69	1,300	4.3 (300x)	21 (62x)
20g	7	52	3,600	19 (190x)	5.0 (720x)
20h	8	36	>10,000	18 (>560x)	9.1 (>1,100x)
20i	9	71	>100,000	1,900 (>53x)	4,800 (>21x)
20j	10	48	>100,000	1,700 (>59x)	690 (>140x)
20l	12	31	>10,000	2,600 (>3.8x)	>10,000 (~1x)
22	–	21	880	80 (11x)	210 (4.2x)

[a] Recombinant human enzyme purchased from Sigma, 2,530 U/mg. [b] W38, see Section 2.2; values in parenthesis are IC_{50} ratios (*h*AChE/*Ag*AChE). [c] Enzyme source is non-blood fed G3 strain *Anopheles gambiae* homogenate; values in parenthesis are IC_{50} ratios (*h*AChE/*Ag*AChE).

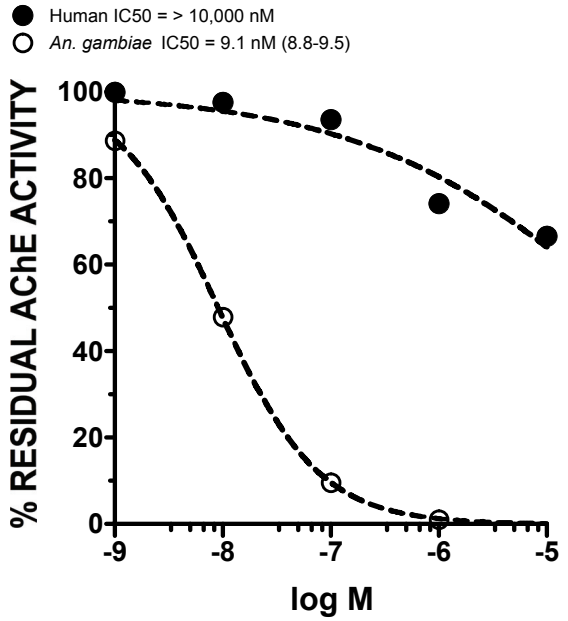

Figure 2.8. Combined dose-response curves for bump-hole optimized tacrine dimer **20h** inhibition of *h*AChE and Ag homogenate AChE

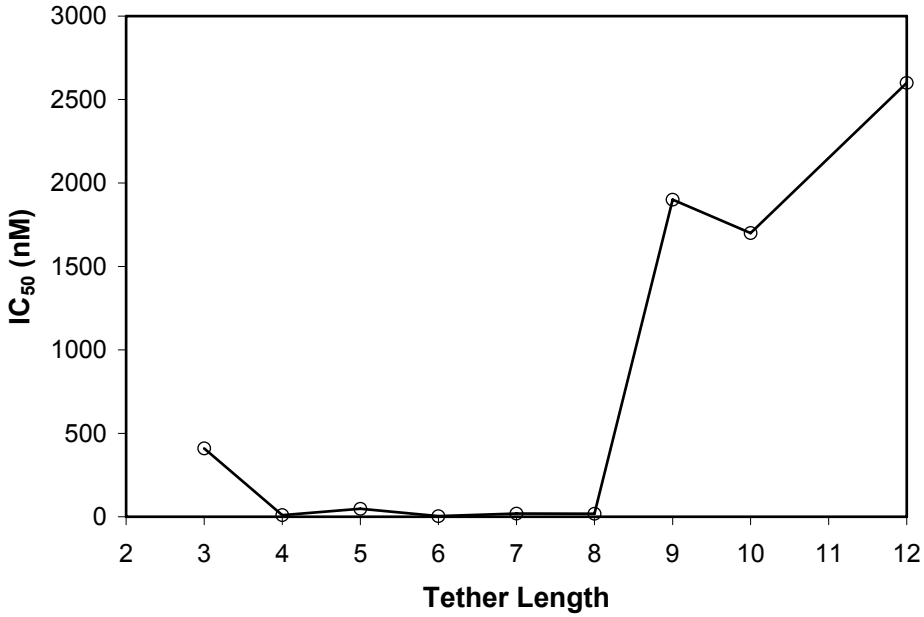

Figure 2.9. Tether-length dependence of bump-hole optimized tacrine dimers **20c –l**

Finally, we examined the relative performance of **22** and **20g**; recall that **22** features an -N(Me)- unit in place of the central methylene in the heptylene chain of **20g**. As anticipated based on the work of Campiani and coworkers[22] on dimeric tacrines, incorporation of the -N(Me)- unit improves *h*AChE inhibition potency. However, because this substitution causes a slight decrease in *Ag*AChE inhibition potency, **22** offers lower selectivity than **20g**.

2.3 Conclusion

Based on the known SAR of tacrine-based AChE inhibitors, a series of modified tacrines were synthesized and assayed for *h*AChE and *Ag*AChE inhibition. Of the 36 compounds assayed, one, **8c**, exhibited moderate (IC_{50} = 3,000 nM) inhibition potency and good selectivity (51 – 100x) for *Ag*AChE. Following the discovery of **8c**, homodimers were prepared incorporating the pharmacophore. Upon assay of the 11 dimers prepared, three were found to exhibit high potency and species selectivity for the mosquito enzyme. Hexylene-linked modified tacrine dimer **20f** exhibited an IC_{50} value for *Ag*AChE of 4.3 – 21 nM and 62 – 300-fold selectivity, depending on the enzyme source. Dimer **20g** exhibited inhibition potencies for *Ag*AChE similar to those of **20f** (5.0 – 19 nM), but was slightly more selective for the mosquito enzyme (190 – 720-fold). Finally, the optimal dimer, **20h**, exhibited IC_{50} values for *Ag*AChE of 9.1 – 18 nM with 560 – 1,100-fold selectivity.

References for Chapter 2

1. Koh, J. T. Engineering Selectivity and Discrimination into Ligand-Receptor Interfaces. *Chemistry & Biology* **2002,** 9, 17-23.

2. Carlier, P. R.; Anderson, T. D.; Wong, D. M.; Hsu, D. C.; Hartsel, J.; Ma, M.; Wong, E. A.; Choudhury, R.; Lam, P. C. H.; Totrov, M. M.; Bloomquist, J. R. Towards a species-selective acetylcholinesterase inhibitor to control the mosquito vector of malaria, Anopheles gambiae. *Chem.-Biol. Interact.* In Press.

3. Weill, M.; Fort, P.; Berthomieu, A.; Dubois, M. P.; Pasteur, N.; Raymond, M. A Novel Acetylcholinesterase Gene in Mosquitoes Codes for the Insecticide Target and is Non-Homologous to the *ace* Gene in *Drosophila*. *Proc. R. Soc. Lond. B* **2002,** 269, 2007-2016.

4. Bourguet, D.; Roig, A.; Toutant, J.-P.; Arpagaus, M. Analysis of Molecular Forms and Pharmacological Properties of Acetylcholinesterase in Several Mosquito Species. *Neurochem. Int.* **1997,** 31, 65-72.

5. Radic, Z.; Taylor, P. Structure and Function of Cholinesterases. In *Toxicology of Organophosphate and Carbamate Compounds*, Gupta, R. C., Ed. Elsevier: Amsterdam, 2006; pp 161-186.

6. Pezzementi, L.; Rowland, M.; Wolfe, M.; Tsigelny, I. Inactivation of an invertebrate acetylcholinesterase by sulfhydryl reagents: the roles of two cysteines in the catalytic gorge of the enzyme. *Invert. Neurosci.* **2006,** 6, 47-55.

7. Raves, M. L.; Harel, M.; Pang, Y. P.; Silman, I.; Kozikowski, A. P.; Sussman, J. L. Structure of Acetylcholinesterase Complexed with the Nootropic Alkaloid, (±)-Huperzine A. *Nat. Struct. Mol. Biol.* **1997,** 4, 57-63.

8. Ellman, G. L.; Courtney, K. D.; Valentino Andres, J.; Featherstone, R. M. A New and Rapid Colorimetric Determination of Acetylcholinesterase Activity. *Biochem. Pharmacol.* **1961,** 7, 88-95.

9. Weill, M. Novel Acetylcholinesterase Gene Responsible for Insecticide Resistance and Applications Thereof. Appl. EP20030760744 June 19, 2003.

10. Belshaw, P. J.; Schoepfer, J. G.; Liu, K.-Q.; Morrison, K. L.; Schreiber, S. L. Rational Design of Orthogonal Receptor-Ligand Combinations. *Angew. Chem., Int. Ed.* **1995,** 34, 2129-2132.

11. McKenna, M. T.; Proctor, G. R.; Young, L. C.; Harvey, A. L. Novel tacrine analogues for potential use against Alzheimer's disease: Potent and selective acetylcholinesterase inhibitors and 5-HT uptake inhibitors. *J. Med. Chem.* **1997,** 40, 3516-3523.

12. Recanatini, M.; Cavalli, A.; Belluti, F.; Piazzi, L.; Rampa, A.; Bisi, A.; Gobbi, S.; Valenti, P.; Andrisano, V.; Bartolini, M.; Cavrini, V. SAR of 9-Amino-1,2,3,4-tetrahydroacridine-Based Acetylcholinesterase Inhibitors: Synthesis, Enzyme Inhibitory Activity, QSAR, and Structure-Based CoMFA of Tacrine Analogues. *J. Med. Chem.* **2000,** 43, 2007-2018.

13. Gregor, V. E.; Emmerling, M. R.; Lee, C.; Moore, C. J. The synthesis and *in vitro* Acetylcholinesterase and Butyrylcholinesterase inhibitory activity of tacrine (Cognex) derivatives. *Bioorg. Med. Chem. Lett.* **1992,** 2, 861-864.

14. Desai, M. C.; Thadeio, P. F.; Lipinski, C. A.; Liston, D. R.; Spencer, R. W.; Williams, I. H. Physical parameters for brain uptake: optimizing log P, log D and pKa of THA. *Bioorg. Med. Chem. Lett.* **1991,** 1, 411-414.

15. Desai, M. C. Tricyclic 4-aminopyridine derivatives for treatment of Alzheimer's disease, and their pharmaceutical compositions, preparation, and intermediates. 88-309040 311303, September 29, 1989.

16. Halgren, T. A. Merck molecular force field. I. Basis, form, scope, parameterization, and performance of MMFF94. *J. Comput. Chem.* **1996,** 17, 490-519.

17. DeLano, W. L. *The PyMol Molecular Graphics System*, 1.0r2; DeLano Scientific LLC: San Carlos, CA, 2007.

18. Du, D.-M.; Carlier, P. R. Development of Bivalent Acetylcholinesterase Inhibitors as Potential Therapeutic Drugs for Alzheimer's Disease. *Curr. Pharm. Des.* **2004,** 10, 3141-3156.

19. Pang, Y.-P.; Quiram, P.; Jelacic, T.; Hong, F.; Brimijoin, S. Highly Potent, Selective, and Low Cost Bis-tetrahydroaminacrine Inhibitors of Acetylcholinesterase. *J. Biol. Chem.* **1996,** 271, 23646-23649.

20. Carlier, P. R.; Han, Y. F.; Chow, E. S.-H.; Li, C. P.-L.; Wang, H.; Lieu, T. X.; Wong, H. S.; Pang, Y.-P. Evaluation of Short-tether Bis-THA AChE Inhibitors. A Further Test of the Dual Binding Site Hypothesis. *Bioorg. Med. Chem.* **1999,** 7, 351-357.

21. Carlier, P. R.; Chow, E. S.-H.; Han, Y.; Liu, J.; Yazal, J. E.; Pang, Y.-P. Heterodimeric Tacrine-Based Acetylcholinesterase Inhibitors: Investigating Ligand-Peripheral Site Interactions. *J. Med. Chem.* **1999,** 42, 4225-4231.

22. Campiani, G.; Fattorusso, C.; Butini, S.; Gaeta, A.; Agnusdei, M.; Gemma, S.; Persico, M.; Catalanotti, B.; Savini, L.; Nacci, V.; Novellino, E.; Holloway, H. W.; Greig, N. H.; Belinskaya, T.; Fedorko, J. M.; Saxena, A. Development of Molecular Probes for the Identification of Extra Interaction Sites in the Mid-Gorge and Peripheral Sites of Butyrylcholinesterase (BuChE). Rational Design of Novel, Selective, and Highly Potent BuChE Inhibitors. *J. Med. Chem.* **2005,** 48, 1919-1929.

Chapter 3. Experimental Procedures for Bump-Hole Optimized AChEI

3.1 General information

9-amino-1,2,3,4-tetrahydroacridine (**1a**) was obtained from Sigma-Aldrich as the HCl salt (monohydrate). All reagents were used as received from the commercial source. All anthranilonitriles, cycloalkanones, and aminobenzoic acids were purchased from commercial sources except 2-amino-5-methylbenzonitrile, which is available in mg-quantities. The compound was prepared in low yield following a modified literature procedure (details below), and all analytical data matched the published values[1] ^{1}H and ^{13}C NMR spectra were recorded at 400 MHz and 100 MHz, or 500 MHz and 125 MHz, respectively. Exact mass spectra were obtained using FAB in the positive ion mode with NBA and PEG as the matrix. Elemental analyses were preformed by the combustion method for C, H, and N. The analytical data of all novel compounds are given below. The following compounds were known in the literature, and all analyses matched the published values: **1b – c**,[2] **2a**,[3] **3a**,[3] **4a**,[4] **4b**,[5] **5a**,[6] **6a**,[4] **6b**,[6] **7a**,[3] **8a**,[3] **9a**,[3] **9b**,[7] **10a**,[3] **10b**,[8] **11a**,[9] **12a**,[10]

Synthesis of 2-amino-5-methylbenzonitrile: To a 50 mL round-bottomed flask, equipped with a stir bar and condenser, were added 2-bromo-4-methylaniline (5.74 g, 30.8 mmol), copper cyanide (5.53 g, 61.7 mmol), and 20 mL DMF. The reaction was stirred at 170 °C for 18 h under a nitrogen atmosphere. The hot reaction mixture was poured over ice (approximately 50 g), and 8.04 g ferric chloride were added. After allowing the mixture to stir for 5 h, the product was extracted from the aqueous phase with chloroform (3 x 250 mL). The combined organic layers were washed with water (2 x 100 mL) and dried over sodium sulfate. An emulsion was observed during the extractions and water washes. The resulting brown oil was chromatographed using 7:3 hexane:ethyl acetate. Recrystallization from hot hexane afforded 0.35 g (9 %) of the title compound as an off-white granular solid.

3.2 Synthesis of tacrine derivatives via the Friedländer Condensation

General procedure: To a 50 mL round-bottomed flask, equipped with a stir bar, nitrogen inlet, and condenser, were added the appropriate aminobenzonitrile (1 equiv), cycloalkanone (1.1 equiv), and zinc chloride (1.7 g for 1.00 g of the benzonitrile). The reaction was stirred at 130 °C for 3 h, during which time the aminobenzonitrile and cycloalkanone codissolved. Over the course of the reaction, the reaction mixture thickened. Upon removal from heat, 2M sodium hydroxide solution was added. The resulting solid was filtered and washed with water and hexanes. The filtered solid was dissolved in methanol and converted to the hydrochloride salt by the addition of 1.1 equiv concentrated HCl. After removing the methanol solvent, the solid was purified by recrystallization from hot ethanol, filtering once before allowing the solid to crystallize.

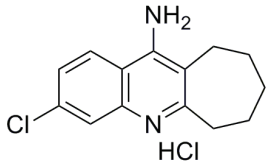

*3-chloro-7,8,9,10-tetrahydro-6H-cyclohepta[*b*]quinolin-11-amine hydrochloride* (**2b**): 2-Amino-4-chlorobenzonitrile (1.00 g, 6.55 mmol) was reacted with cycloheptanone (0.81 g, 7.21 mmol) as described above to yield 1.06 g (65 %) of a white granular solid. ^{1}H NMR (400 MHz, CD_3OD/DMSO-d_6) δ 8.42 (d, J = 9.0 Hz, 1H), 7.88 (d, J = 2.1 Hz, 1H), 7.67 (dd, J = 2.1 Hz, 9.0 Hz, 1H), 3.18 (t, J = 5.6 Hz, 2H), 2.96 (t, J = 5.4 Hz, 2H), 2.05 – 1.93 (m, 2H), 1.91 – 1.81 (m, 2H), 1.78 – 1.69 (m, 2H); ^{13}C NMR (100 MHz, DMSO-d_6) δ 161.28, 151.46, 141.06, 135.32, 125.31, 125.15, 121.69, 115.13, 114.85, 35.76, 31.12, 26.55, 25.69, 24.68; MS (FAB$^+$): Calc for $C_{14}H_{16}ClN_2^+$: 247.1002. Found: 247.1005 (+1.2 ppm, +0.3 mmu).

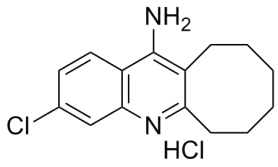

*3-chloro-6,7,8,9,10,11-hexahydrocycloocta[*b*]quinolin-12-amine hydrochloride* (**2c**): 2-Amino-4-chlorobenzonitrile (1.00 g, 6.55 mmol) was reacted with cyclooctanone (0.91 g, 7.21 mmol) as described above to yield 1.21 g (62 %) of a white granular solid. ^{1}H NMR (400 MHz,

CD_3OD/DMSO-d_6) δ 8.56 (d, *J* = 9.1 Hz, 1H), 8.00 (d, *J* = 2.0 Hz, 1H), 7.69 (dd, *J* = 2.0 Hz, 9.1 Hz, 1H), 3.20 (t, *J* = 6.2 Hz, 2H), 3.00 (t, *J* = 6.2 Hz, 2H), 2.02 – 1.89 (m, 2H), 1.86 – 1.74 (m, 2H), 1.64 – 1.54 (m, 2H), 1.49 – 1.40 (m, 2H); ^{13}C NMR (100 MHz, CD_3OD/DMSO-d_6) δ 157.44, 156.14, 139.40, 139.33, 127.64, 127.02, 119.54, 115.21, 113.87, 32.40, 31.65, 28.79, 27.06, 27.00, 24.41; MS (FAB$^+$): Calc for $C_{15}H_{18}ClN_2^+$: 261.1159. Found: 261.1160 (+0.6 ppm, +0.1 mmu).

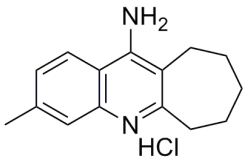

*3-methyl-7,8,9,10-tetrahydro-6H-cyclohepta[*b*]quinolin-11-amine hydrochloride* (**3b**): 2-Amino-4-methylbenzonitrile (1.00 g, 7.57 mmol) was reacted with cycloheptanone (0.93 g, 8.32 mmol) as described above to yield 0.97 g (56 %) of a white granular solid. ^{1}H NMR (400 MHz, CD_3OD) δ 8.19 (d, *J* = 8.8 Hz, 1H), 7.56 (s, 1H), 7.48 (dd, *J* = 1.5 Hz, 8.8 Hz, 1H), 3.13 (t, *J* = 5.6 Hz, 2H), 2.92 (t, *J* = 5.5 Hz, 2H), 2.56 (s, 3H), 2.01 – 1.92 (m, 2H), 1.87 – 1.79 (m, 2H), 1.75 – 1.67 (m, 2H); ^{13}C NMR (100 MHz, CD_3OD) δ 158.94, 156.32, 145.61, 138.40, 129.43, 124.08, 119.35, 115.68, 115.10, 34.96, 32.54, 27.46, 26.91, 25.89, 21.74; MS (FAB$^+$): Calc for $C_{15}H_{19}N_2^+$: 227.1548. Found: 227.1559 (+4.7 ppm, +1.1 mmu).

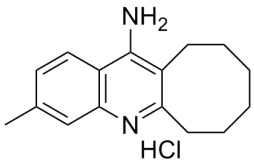

*3-methyl-6,7,8,9,10,11-hexahydrocycloocta[*b*]quinolin-12-amine hydrochloride* (**3c**): 2-Amino-4-methylbenzonitrile (1.00 g, 7.57 mmol) was reacted with cyclooctanone (1.05 g, 8.32 mmol) as described above to yield 1.20 g (65 %) of a white granular solid. ^{1}H NMR (400 MHz, CD_3OD) δ 8.18 (d, *J* = 8.7 Hz, 1H), 7.57 (s, 1H), 7.43 (d, *J* = 8.7 Hz, 1H), 3.09 (t, *J* = 6.2 Hz, 2H), 2.90 (t, *J* = 6.2 Hz, 2H), 2.54 (s, 3H), 1.94 – 1.84 (m, 2H), 1.80 – 1.70 (m, 2H), 1.57 – 1.47 (m, 2H), 1.43 – 1.33 (m, 2H); ^{13}C NMR (100 MHz, CD_3OD) δ 156.44, 156.43, 145.76, 139.08, 129.23, 123.97, 119.22, 114.69, 113.06, 32.47, 31.73, 28.71, 27.09 (2C), 24.46, 21.80; MS (FAB$^+$): Calc for $C_{16}H_{21}N_2^+$: 241.1705. Found: 241.1709 (+1.8 ppm, +0.4 mmu). Anal. Calc. for $C_{16}H_{20}N_2$·HCl: C, 69.43; H, 7.65; N, 10.12. Found: C, 69.20; H, 7.67; N, 10.02.

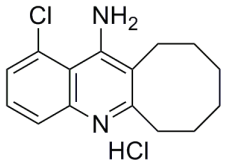

*1-chloro-6,7,8,9,10,11-hexahydrocycloocta[*b*]quinolin-12-amine hydrochloride* (**4c**): 2-Amino-6-chlorobenzonitrile (1.00 g, 6.55 mmol) was reacted with cyclooctanone (0.91 g, 7.21 mmol) as described above to yield 1.27 g (74 %) of a white granular solid. ^{1}H NMR (400 MHz, CD_3OD/DMSO-d_6) δ 7.99 (dd, *J* = 1.2 Hz, 8.5 Hz, 1H), 7.84 (dd, *J* = 7.7 Hz, 8.5 Hz, 1H), 7.71 (dd, *J* = 1.2 Hz, 7.7 Hz, 1H), 3.21 (t, *J* = 6.1 Hz, 2H), 3.00 (t, *J* = 6.2 Hz, 2H), 2.00 – 1.89 (m, 2H), 1.86 – 1.74 (m, 2H), 1.63 – 1.53 (m, 2H), 1.48 – 1.37 (m, 2H); ^{13}C NMR (100 MHz, CD_3OD/DMSO-d_6) δ 156.79, 155.83, 141.25, 133.98, 131.10, 130.33, 120.58, 115.09, 113.25, 32.27, 31.67, 28.34, 27.13, 26.98, 24.47; MS (FAB$^+$): Calc for $C_{15}H_{18}ClN_2^+$: 261.1159. Found: 261.1172 (+5.1 ppm, +1.3 mmu). Anal. Calc. for $C_{15}H_{17}ClN_2 \cdot HCl \cdot H_2O$: C, 57.15; H, 6.39; N, 8.89. Found: C, 57.55; H, 6.13; N, 8.88.

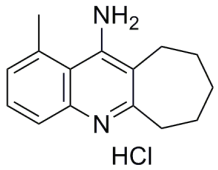

*1-methyl-7,8,9,10-tetrahydro-6H-cyclohepta[*b*]quinolin-11-amine hydrochloride* (**5b**): 2-Amino-6-methylbenzonitrile (1.00 g, 7.57 mmol) was reacted with cycloheptanone (0.93 g, 8.32 mmol) as described above to yield 1.77 g (89 %) of a white granular solid. ^{1}H NMR (400 MHz, CD_3OD/DMSO-d_6) δ 7.80 – 7.71 (m, 2H), 7.48 (d, *J* = 6.8 Hz, 1H), 3.20 (t, *J* = 5.6 Hz, 2H), 3.04 (s, 3H), 2.97 (t, *J* = 5.4 Hz, 2H), 2.06 – 1.95 (m, 2H), 1.92 – 1.82 (m, 2H), 1.80 – 1.70 (m, 2H); ^{13}C NMR (100 MHz, D_2O/DMSO-d_6) δ 157.77, 156.95, 138.90, 136.50, 133.58, 130.91, 118.45, 116.57, 116.00, 34.27, 31.93, 26.76, 26.52, 25.83, 24.54; MS (FAB$^+$): Calc for $C_{15}H_{19}N_2^+$: 227.1548. Found: 227.1548 (-0.1 ppm, 0.0 mmu).

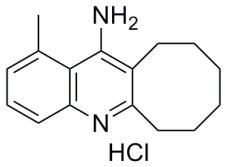

*1-methyl-6,7,8,9,10,11-hexahydrocycloocta[*b*]quinolin-12-amine hydrochloride* (**5c**): 2-Amino-6-methylbenzonitrile (1.00 g, 7.57 mmol) was reacted with cyclooctanone (1.05 g, 8.32 mmol) as described above to yield 1.63 g (78 %) of a white granular solid. ^{1}H NMR (400 MHz, CD_3OD/DMSO-d_6) δ 7.80 – 7.76 (m, 2H), 7.48 (d, J = 6.1 Hz, 1H), 3.18 (t, J = 6.2 Hz, 2H), 3.08 (s, 3H), 3.03 (t, J = 6.2 Hz, 2H), 2.01 – 1.91 (m, 2H), 1.88 – 1.78 (m, 2H), 1.67 – 1.57 (m, 2H), 1.51 – 1.41 (m, 2H); ^{13}C NMR (100 MHz, CD_3OD/D_2O) δ 157.09, 155.57, 139.90, 136.56, 133.59, 130.59, 118.32, 115.69, 113.83, 32.10, 31.33, 27.82, 26.66, 26.65, 24.31, 24.28; MS (FAB$^+$): Calc for $C_{16}H_{21}N_2^+$: 241.1705. Found: 241.1695 (-4.1 ppm, -1.0 mmu). Anal. Calc. for $C_{16}H_{20}N_2$·HCl: C, 69.42; H, 7.65; N, 10.12. Found: C, 69.33; H, 7.71; N, 7.72.

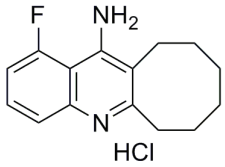

*1-fluoro-6,7,8,9,10,11-hexahydrocycloocta[*b*]quinolin-12-amine hydrochloride* (**6c**): 2-Amino-6-fluorobenzonitrile (1.00 g, 7.35 mmol) was reacted with cyclooctanone (1.02 g, 8.08 mmol) as described above to yield 1.71 g (83 %) of a white granular solid. ^{1}H NMR (400 MHz, CD_3OD/DMSO-d_6) δ 7.96 (apparent td, J = 5.6 Hz, 8.3 Hz, 1H), 7.78 (d, J = 8.5 Hz, 1H), 7.50 (ddd, J = 1.0 Hz, 8.0 Hz, 13.8 Hz, 1H), 3.20 (t, J = 6.2 Hz, 2H), 3.05 (t, J = 6.3 Hz, 2H), 2.06 – 1.91 (m, 2H), 1.90 – 1.76 (m, 2H), 1.70 – 1.56 (m, 2H), 1.54 – 1.41 (m, 2H); ^{13}C NMR (100 MHz, CD_3OD/DMSO-d_6) δ 160.75 (d, $^{1}J_{CF}$ = 253.0 Hz), 157.42, 155.01 (d, $^{4}J_{CF}$ = 2.5 Hz), 140.61 (d, $^{4}J_{CF}$ = 4.5 Hz), 135.00 (d, $^{3}J_{CF}$ = 11.3 Hz), 116.89 (d, $^{4}J_{CF}$ = 4.3 Hz), 114.39, 112.58 (d, $^{2}J_{CF}$ = 23.0 Hz), 107.33 (d, $^{3}J_{CF}$ = 12.1 Hz), 32.47, 31.67, 28.59, 27.11, 26.97, 24.01; MS (FAB$^+$): Calc for $C_{15}H_{18}FN_2^+$: 245.1454. Found: 245.1456 (+0.8 ppm, +0.2 mmu).

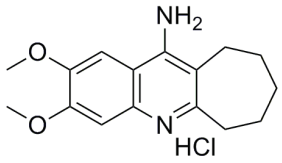

*2,3-dimethoxy-7,8,9,10-tetrahydro-6H-cyclohepta[*b*]quinolin-11-amine hydrochloride* (**7b**): 2-Amino-4,5-dimethoxybenzonitrile (1.00 g, 5.61 mmol) was reacted with cycloheptanone (0.69 g, 6.17 mmol) as described above to yield 1.10 g (72 %) of a white granular solid. ^{1}H NMR (400 MHz, CD_3OD) δ 7.62 (s, 1H), 7.12 (s, 1H), 4.00 (s, 3H), 3.99 (s, 3H), 3.10 (t, *J* = 5.6 Hz, 2H), 2.90 (t, *J* = 5.4 Hz, 2H), 2.01 – 1.91 (m, 2H), 1.86 – 1.76 (m, 2H), 1.75 – 1.65 (m, 2H); ^{13}C NMR (100 MHz, CD_3OD) δ 156.30, 156.24, 155.10, 151.02, 134.90, 115.33, 111.40, 103.11, 99.94, 56.98, 56.84, 34.92, 32.62, 27.55, 27.01, 25.94; MS (FAB^+): Calc for $C_{16}H_{21}N_2O_2^+$: 273.1603. Found: 273.1607 (+1.5 ppm, +0.4 mmu). Anal. Calc. for $C_{16}H_{20}N_2O_2 \cdot HCl$: C, 62.23; H, 6.85; N, 9.07. Found: C, 62.47; H, 6.69; 9.03.

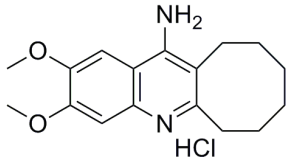

*2,3-dimethoxy-6,7,8,9,10,11-hexahydrocycloocta[*b*]quinolin-12-amine hydrochloride* (**7c**): 2-Amino-4,5-dimethoxybenzonitrile (1.00 g, 5.61 mmol) was reacted with cyclooctanone (0.78 g, 6.17 mmol) as described above to yield 0.34 g (21 %) of a white granular solid. ^{1}H NMR (400 MHz, CD_3OD) δ 7.61 (s, 1H), 7.12 (s, 1H), 4.00 (s, 3H), 3.99 (s, 3H), 3.07 (t, *J* = 6.0 Hz, 2H), 2.93 (t, *J* = 6.1 Hz, 2H), 1.94 – 183 (m, 2H), 1.82 – 1.72 (m, 2H), 1.61 – 1.50 (m, 2H), 1.45 – 1.36 (m, 2H); ^{13}C NMR (100 MHz, CD_3OD) δ 156.41, 155.22, 153.83, 150.90, 135.76, 112.62, 111.09, 102.89, 99.79, 57.00, 56.86, 32.43, 31.80, 28.79, 27.14, 27.07, 24.42; MS (FAB^+): Calc for $C_{17}H_{23}N_2O_2^+$: 287.1760. Found: 287.1740 (-6.8 ppm, -1.9 mmu).

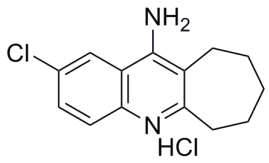

*2-chloro-7,8,9,10-tetrahydro-6H-cyclohepta[*b*]quinolin-11-amine hydrochloride* (**8b**): 2-Amino-5-chlorobenzonitrile (1.00 g, 6.55 mmol) was reacted with cycloheptanone (0.81 g, 7.21 mmol)

as described above to yield 1.60 g (87 %) of a white granular solid. ^{1}H NMR (400 MHz, CD_3OD/DMSO-d_6) δ 8.55 (s, 1H), 8.22 – 7.53 (m, 2H), 3.22 (t, *J* = 5.4 Hz, 2H), 2.96 (t, *J* = 5.3 Hz, 2H), 2.07 – 1.91 (m, 2H), 1.90 – 1.80 (m, 2H), 1.77 – 1.65 (m, 2H); ^{13}C NMR (100 MHz, CD_3OD/DMSO-d_6) δ 159.68, 155.24, 136.52, 134.33, 132.70, 123.93, 122.67, 117.91, 116.71, 34.87, 32.34, 27.29, 26.69, 25.95; MS (FAB$^+$): Calc for $C_{14}H_{16}ClN_2^+$: 247.1002. Found: 247.1005 (+1.2 ppm, +0.3 mmu).

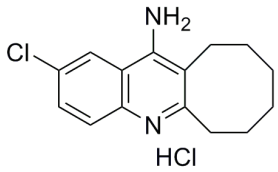

*2-chloro-6,7,8,9,10,11-hexahydrocycloocta[*b*]quinolin-12-amine hydrochloride* (**8c**): 2-Amino-5-chlorobenzonitrile (1.00 g, 6.55 mmol) was reacted with cyclooctanone (0.91 g, 7.21 mmol) as described above to yield 1.03 g (53 %) of a white granular solid. ^{1}H NMR (400 MHz, CD_3OD/DMSO-d_6) δ 8.68 (d, *J* = 2.1 Hz, 1H), 8.02 – 7.91 (m, 2H), 3.20 (t, *J* = 6.2 Hz, 2H), 3.01 (t, *J* = 6.2 Hz, 2H), 2.00 – 1.87 (m, 2H), 1.87 – 1.73 (m, 2H), 1.63 – 1.53 (m, 2H), 1.5 – 1.37 (m, 2H); ^{13}C NMR (100 MHz, CD_3OD/DMSO-d_6) δ 157.26, 155.44, 137.31, 134.48, 132.34, 124.00, 122.70, 117.54, 114.07, 32.36, 31.69, 28.73, 27.06, 27.00, 24.49; MS (FAB$^+$): Calc for $C_{15}H_{18}ClN_2^+$: 261.1159. Found: 261.1175 (+6.3 ppm, +1.6 mmu). Anal. Calc. for $C_{15}H_{17}ClN_2 \cdot HCl \cdot H_2O$: C, 57.15; H, 6.39; N, 8.89. Found: C, 57.04; H, 6.22; N, 8.72.

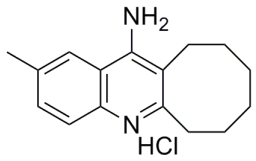

*2-methyl-6,7,8,9,10,11-hexahydrocycloocta[*b*]quinolin-12-amine hydrochloride* (**9c**): 2-Amino-5-methylbenzonitrile (0.10 g, 0.76 mmol) was reacted with cyclooctanone (0.11 g, 0.83 mmol) as described above to yield 0.04 g (23 %) of a white granular solid. ^{1}H NMR (400 MHz, CD_3OD) δ 8.15 (s, 1H), 7.77 – 7.67 (m, 2H), 3.12 (t, *J* = 6.2 Hz, 2H), 2.97 (t, *J* = 6.2 Hz, 2H), 2.57 (s, 3H), 1.97 – 1.86 (m, 2H), 1.85 – 1.74 (m, 2H), 1.62 – 1.52 (m, 2H), 1.48 – 1.37 (m, 2H); ^{13}C NMR (100 MHz, CD_3OD) δ 156.31 (2C), 138.07, 137.20, 136.06, 123.08, 120.05, 116.89, 113.42, 32.54, 31.78, 28.67, 27.11, 24.50, 21.53; MS (FAB$^+$): Calc for $C_{16}H_{21}N_2^+$: 241.1705. Found: 241.1713 (+3.4 ppm, +0.8 mmu).

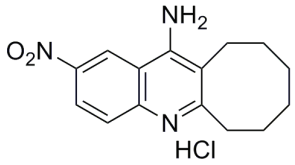

*2-nitro-6,7,8,9,10,11-hexahydrocycloocta[*b*]quinolin-12-amine hydrochloride* (**10c**): 2-Amino-5-nitrobenzonitrile (1.00 g, 6.13 mmol) was reacted with cyclooctanone (0.85 g, 6.74 mmol) as described above to yield 1.24 g (74 %) of a yellow granular solid. ^{1}H NMR (400 MHz, CD_3OD) δ 9.48 (d, J = 2.3 Hz, 1H), 8.63 (dd, J = 2.3 Hz, 9.3 Hz, 1H), 7.98 (d, J = 9.3 Hz, 1H), 3.18 (t, J = 6.3 Hz, 2H), 3.00 (t, J = 6.2 Hz, 2H), 2.02 – 1.89 (m, 2H), 1.86 – 1.74 (m, 2H), 1.64 – 1.52 (m, 2H), 1.52 – 1.38 (m, 2H); ^{13}C NMR (100 MHz, CD_3OD) δ 159.07, 157.92, 146.35, 141.82, 127.79, 122.11, 121.84, 116.18, 115.45, 32.71, 31.67, 28.56, 27.06 (2C), 24.64; MS (FAB^+): Calc for $C_{15}H_{18}N_3O_2^+$: 272.1399. Found: 272.1390 (-3.3 ppm, -0.9 mmu). Anal. Calc. for $C_{15}H_{17}N_3O_2 \cdot HCl \cdot H_2O$: C, 55.30; H, 6.19; N, 12.90. Found: C, 55.30; H, 6.21; N, 12.79.

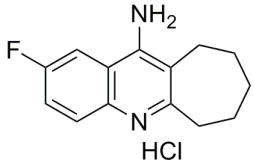

*2-fluoro-7,8,9,10-tetrahydro-6H-cyclohepta[*b*]quinolin-11-amine hydrochloride* (**11b**): 2-Amino-5-fluorobenzonitrile (1.00 g, 7.35 mmol) was reacted with cycloheptanone (0.91 g, 8.08 mmol) as described above to yield 1.64 g (97 %) of a white granular solid. ^{1}H NMR (400 MHz, CD_3OD/DMSO-d_6) δ 8.28 (dd, J = 2.6 Hz, 10.3 Hz, 1H), 8.00 (dd, J = 5.0 Hz, 9.3 Hz, 1H), 7.81 (ddd, J = 2.7 Hz, 8.0 Hz, 9.1 Hz, 1H), 3.23 (t, J = 5.5 Hz, 2H), 2.98 (t, J = 5.4 Hz, 2H), 2.06 – 1.92 (m, 2H), 1.91 – 1.81 (m, 2H), 1.79 – 1.66 (m, 2H); ^{13}C NMR (100 MHz, CD_3OD/DMSO-d_6) δ 161.25 (d, $^{1}J_{CF}$ = 245.7 Hz), 159.35, 155.56 (d, $^{4}J_{CF}$ = 3.8 Hz), 134.91, 123.45 (d, $^{2}J_{CF}$ = 26.9 Hz), 123.49, 118.07 (d, $^{3}J_{CF}$ = 9.1 Hz), 116.15, 109.23 (d, $^{2}J_{CF}$ = 24.7 Hz), 34.86, 32.37, 27.40, 26.76, 25.96; MS (FAB^+): Calc for $C_{14}H_{16}FN_2^+$: 231.1298. Found: 231.1291 (-2.8 ppm, -0.6 mmu). Anal. Calc. for $C_{14}H_{15}FN_2 \cdot 2HCl \cdot 3H_2O$: C, 47.07; H, 6.49; N, 7.84. Found: C, 47.37; H, 6.43; N, 7.72.

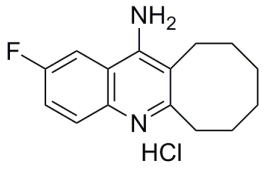

*2-fluoro-6,7,8,9,10,11-hexahydrocycloocta[*b*]quinolin-12-amine hydrochloride* (**11c**): 2-Amino-5-fluorobenzonitrile (1.00 g, 7.35 mmol) was reacted with cyclooctanone (1.02g, 8.08 mmol) as described above to yield 1.63 g (91 %) of a white granular solid. ^{1}H NMR (400 MHz, CD_3OD/DMSO-d_6) δ 8.45 (dd, J = 2.5 Hz, 10.4 Hz, 1H), 8.10 (dd, J = 5.0 Hz, 9.2 Hz, 1H), 7.88 (ddd, J = 2.6 Hz, 8.1 Hz, 9.3 Hz, 1H), 3.23 (t, J = 6.0 Hz, 2H), 3.03 (t, J = 6.0 Hz, 2H), 2.02 – 1.89 (m, 2H), 1.89 – 1.74 (m, 2H), 1.68 – 1.53 (m, 2H), 1.52 – 1.39 (m, 2H); ^{13}C NMR (100 MHz, CD_3OD/DMSO-d_6) δ 160.93 (d, $^{1}J_{CF}$ = 245.1 Hz), 156.87, 155.68 (d, $^{4}J_{CF}$ = 3.8 Hz), 135.69, 123.67 (d, $^{2}J_{CF}$ = 26.4 Hz), 123.62, 117.60 (d, $^{3}J_{CF}$ = 9.2 Hz), 113.41, 109.33 (d, $^{2}J_{CF}$ = 24.6 Hz), 32.29, 31.73, 28.78, 27.08, 27.01, 24.44; MS (FAB^{+}): Calc for $C_{15}H_{18}FN_2^{+}$: 245.1454 (-0.4 ppm, -0.1 mmu). Found: 245.1453.

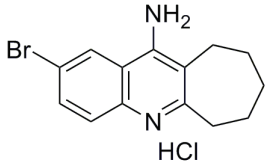

*2-bromo-7,8,9,10-tetrahydro-6H-cyclohepta[*b*]quinolin-11-amine hydrochloride* (**12b**): 2-Amino-5-bromobenzonitrile (1.00 g, 5.08 mmol) was reacted with cycloheptanone (0.63 g, 5.58 mmol) as described above to yield 1.39 g (94 %) of an off-white granular solid. ^{1}H NMR (400 MHz, CD_3OD/DMSO-d_6) δ 8.78 (d, J = 2.0 Hz, 1H), 8.06 (dd, J = 2.0 Hz, 9.0 Hz, 1H), 7.87 (d, J = 9.0 Hz, 1H), 3.23 (t, J = 5.4 Hz, 2H), 2.98 (t, J = 5.2 Hz, 2H), 2.08 – 1.94 (m, 2H), 1.93 – 1.80 (m, 2H), 1.79 – 1.66 (m, 2H); ^{13}C NMR (100 MHz, CD_3OD/DMSO-d_6) δ 159.67, 155.09, 136.96, 136.80, 127.22, 122.78, 120.43, 118.33, 116.73, 34.86, 32.34, 27.32, 26.65, 25.93; MS (FAB^{+}): Calc for $C_{14}H_{16}BrN_2^{+}$: 291.0497. Found: 291.0498 (+0.4 ppm, +0.1 mmu).

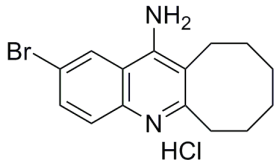

*2-bromo-6,7,8,9,10,11-hexahydrocycloocta[*b*]quinolin-12-amine hydrochloride* (**12c**): 2-Amino-5-bromobenzonitrile (1.00 g, 5.08 mmol) was reacted with cyclooctanone (0.70 g, 5.58 mmol) as described above to yield 1.49 g (97 %) of a white granular solid. ^{1}H NMR (400 MHz, CD_3OD/DMSO-d_6) δ 8.86 (d, *J* = 1.9 Hz, 1H), 8.07 (dd, *J* = 1.9 Hz, 9.0 Hz, 1H), 7.95 (d, *J* = 9.0 Hz, 1H), 3.21 (t, *J* = 6.0 Hz, 2H), 3.01 (t, *J* = 6.0 Hz, 2H), 2.03 – 1.89 (m, 2H), 1.87 – 1.73 (m, 2H), 1.66 – 1.53 (m, 2H), 1.49 – 1.38(m, 2H); ^{13}C NMR (100 MHz, CD_3OD/DMSO-d_6) δ 157.23, 155.25, 137.56, 137.04, 127.21, 122.74, 120.14, 117.93, 114.09, 32.33, 31.67, 28.77, 27.06, 27.01, 24.49; MS (FAB$^+$): Calc for $C_{15}H_{18}BrN_2^+$: 305.0653. Found: 305.0644 (-3.1 ppm, -0.9 mmu). Anal. Calc. for $C_{15}H_{17}BrN_2 \cdot HCl \cdot H_2O$: C, 50.09; H, 5.60; N, 7.79. Found: C, 50.19; H, 5.52; N, 7.67.

3.3 Synthesis of Bump-Hole optimized tacrine dimers

3.3.1 Synthesis of 2,12-dichloro-6,7,8,9,10,11-hexahydrocycloocta[*b*]quinoline

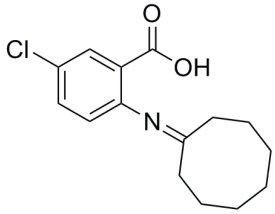

5-Chloro-2-cyclooctylideneaminobenzoic acid (**17**): The synthesis of this compound is analogous to that of spiro[2H-3,1-benzoxazine-2,10-cyclohexan]-4(1H)-one.[11] To a 100 mL round-bottomed flask, equipped with a stir bar, Dean-Stark trap, and N_2 inlet, were added 2-amino-5-chlorobenzoic acid (10.00 g, 58.3 mmol), cyclooctanone (8.83 g, 69.9 mmol), p-toluenesulfonic acid (0.11 g, 0.6 mmol), and 80 mL of toluene. This flask was lowered into a 130 °C oil bath. The reaction was allowed to stir under a nitrogen atmosphere for 12 h, at which time 1 equiv of water had collected in the Dean-Stark trap. Upon removal from heat, a white, highly insoluble solid precipitated from the reaction mixture. This solid was collected by filtration, washing with ethanol (25 mL) and hexanes (100 mL). The solid was dried *in vacuo*, yielding 11.21 g (78 %) of the title compound. ^{1}H NMR (500 MHz, DMSO-D_6) δ 11.57 (s, 1H), 7.98 (d, *J* = 2.5 Hz,

1H), 7.60 (dd, *J* = 2.5 Hz, 8.8 Hz, 1H), 7.52 (d, *J* = 8.8 Hz, 1H), 2.81 (t, *J* = 6.3 Hz, 2H), 2.68 (t, *J* = 6.1 Hz, 2H), 1.80 – 1.71 (m, 2H), 1.59 – 1.49 (m, 2H), 1.45 – 1.32 (m, 4H).

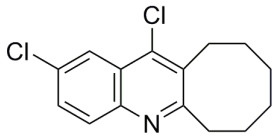

*2,12-Dichloro-6,7,8,9,10,11-hexahydrocycloocta[*b*]quinoline* (**18**): The synthesis of this compound is analogous to that of 9-Chloro-1,2,3,4-tetrahydroacridine.[11] To a 50 mL round-bottomed flask, equipped with a stir bar, condenser, and N_2 inlet, was added phosphorus oxychloride (7.88 g, 51.4 mmol). **17** (3.00 g, 12.2 mmol) was added to the $POCl_3$ in portions to restrict the exothermic reaction. Once all of the solid was added, the reaction flask was lowered into a 125 °C oil bath. The reaction was allowed to reflux for 2 h, after which time it was removed from the heat and allowed to cool slightly. The reaction mixture was added dropwise to an aqueous sodium hydroxide solution (21.37 g in 39.6 mL water) over 20 minutes. This mixture was allowed to stir for 1 h, at which time the product was extracted using ethyl acetate (3 x 200 mL). The combined organic layers were washed with water (2 x 100 mL) and brine (1 x 100 mL) and dried over sodium sulfate. The ethyl acetate was removed by rotary evaporation, and the resulting solid was recrystallized from hot acetone, yielding 2.60 g (76 %) of the title compound as a yellow granular solid. ^{1}H NMR (400 MHz, $CDCl_3$) δ 8.15 (d, *J* = 2.2 Hz, 1H), 7.94 (d, *J* = 8.9 Hz, 1H), 7.59 (dd, *J* = 2.2 Hz, 8.9 Hz, 1H), 3.22 – 3.13 (m, 4H), 1.93 – 1.77 (m, 4H), 1.52 – 1.44 (m, 2H), 1.38 – 1.29 (m, 2H); ^{13}C NMR (100 MHz, $CDCl_3$) δ 164.02, 145.52, 139.44, 133.07, 132.54, 130.62, 130.02, 126.37, 123.12, 36.92, 31.17, 28.87, 28.55, 26.42, 25.93; MS (FAB^+): Calc for $C_{15}H_{16}Cl_2N^+$: 280.0660. Found: 280.0667 (+2.6 ppm, +0.7 mmu).

3.3.2 Synthesis of the amino-terminated *N*-alkyltacrine derivatives

General procedure for the formation of amino-terminated N-*alkyltacrine derivatives* (**19c-l**, **21**): To a 25 mL round-bottomed flask, equipped with a stir bar, condenser and N_2 inlet, were added the appropriate 1,n-diaminoalkane, **18**, and 1-pentanol as described below. The reaction was lowered into a 160 °C oil bath and allowed to stir at reflux for 44 h. Once the reaction cooled to room temperature, 10 mL of a 2 M sodium hydroxide solution was added. The resulting mixture was extracted with methylene chloride (2 x 20 mL). The organic layers were combined, washed with water (1 x 10 mL) and dried over sodium sulfate. Chromatography with the appropriate

mixture of methanol, dichloromethane, and ammonium hydroxide, as described below, was performed to yield amino-terminated *N*-alkyltacrine derivatives.

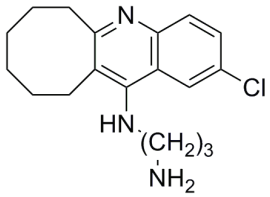

N^{1}*-(2-chloro-6,7,8,9,10,11-hexahydrocycloocta[*b*]quinolin-12-yl)propane-1,3-diamine* (**19c**): 1,3-diaminopropane (1166.0 mg, 15.7 mmol) was combined with **18** (440.8 mg, 1.6 mmol) in 3.0 mL 1-pentanol. The product mixture was chromatographed with 10 % methanol in methylene chloride with 10 mL concentrated NH_4OH per L of eluent, to afford 329.8 mg (66 %) of the title compound as a white solid. ^{1}H NMR (500 MHz, $CDCl_3$) δ 8.00 (d, *J* = 2.2 Hz, 1H), 7.87 (d, *J* = 8.9 Hz, 1H), 7.48 (dd, *J* = 2.2 Hz, 9.0 Hz, 1H), 4.79 (s, 1H), 3.50 (t, *J* = 6.6 Hz, 2H), 3.13 – 3.08 (t, *J* = 6.2 Hz, 2H), 2.98 – 2.91 (m, 4H), 1.88 – 1.79 (m, 4H), 1.75 – 1.66 (m, 2H), 1.51 – 1.44 (m, 2H), 1.39 – 1.29 (m, 3H); ^{13}C NMR (125 MHz, $CDCl_3$) δ 163.50, 149.99, 146.48, 130.80, 129.47, 128.93, 122.89, 122.25, 121.25, 49.55, 40.87, 37.05, 34.08, 31.16, 29.72, 26.65, 26.03, 25.35.

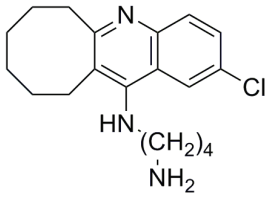

N^{1}*-(2-chloro-6,7,8,9,10,11-hexahydrocycloocta[*b*]quinolin-12-yl)butane-1,4-diamine* (**19d**): 1,4-diaminobutane (664.1 mg, 7.5 mmol) was combined with **18** (422.1 mg, 1.5 mmol) in 2.0 mL 1-pentanol. The product mixture was chromatographed with 15 % methanol in methylene chloride with 10 mL concentrated NH_4OH per L of eluent, to afford 438.6 mg (88 %) of the title compound as a brown oil. ^{1}H NMR (500 MHz, $CDCl_3$) δ 7.96 (s, 1H), 7.87 (d, *J* = 9.0 Hz, 1H), 7.48 (d, *J* = 9.0 Hz, 1H), 3.98 (s, 1H), 3.39 (t, *J* = 7.0 Hz, 2H), 3.11 (t, *J* = 5.6 Hz, 2H), 2.93 (t, *J* = 6.1 Hz, 2H), 2.76 (t, *J* = 6.8 Hz, 2H), 1.88 – 1.80 (m, 2H), 1.78 – 1.66 (m, 4H), 1.61 – 1.52 (m, 2H), 1.52 – 1.43 (m, 2H), 1.38 – 1.27 (m, 3H); ^{13}C NMR (125 MHz, $CDCl_3$) δ 163.48, 149.60,

146.47, 130.86, 129.55, 128.88, 122.68, 122.29, 121.35, 50.47, 41.88, 37.04, 31.07 (2C), 29.69, 29.05, 26.55, 25.96, 25.23.

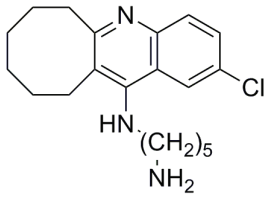

N[1]*-(2-chloro-6,7,8,9,10,11-hexahydrocycloocta[*b*]quinolin-12-yl)pentane-1,5-diamine* (**19e**): 1,5-diaminopentane (738.5 mg, 7.3 mmol) was combined with **18** (405.0 mg, 1.4 mmol) in 2.1 mL 1-pentanol. The product mixture was chromatographed with 15 % methanol in methylene chloride with 10 mL concentrated NH_4OH per L of eluent, to afford 392.1 mg (78 %) of the title compound as a brown oil. ^{1}H NMR (500 MHz, $CDCl_3$) δ 7.96 (d, *J* = 2.3 Hz, 1H), 7.87 (d, *J* = 9.0 Hz, 1H), 7.49 (dd, *J* = 2.3 Hz, 9.0 Hz, 1H), 3.85 (t, *J* = 6.2 Hz, 1H), 3.41 – 3.34 (m, 2H), 3.11 (t, *J* = 6.2 Hz, 2H), 2.93 (t, *J* = 6.4 Hz, 2H), 2.72 (t, *J* = 6.7 Hz, 2H), 1.89 – 1.80 (m, 2H), 1.76 – 1.66 (m, 4H), 1.51 – 1.31 (m, 10H); ^{13}C NMR (125 MHz, $CDCl_3$) δ 163.46, 149.61, 146.43, 130.82, 129.54, 128.91, 122.69, 122.25, 121.32, 50.52, 42.03, 37.06, 33.45, 31.51, 31.06, 29.63, 26.53, 25.92, 25.17, 24.30.

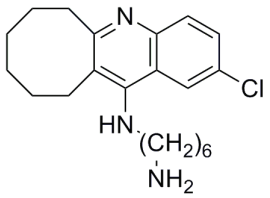

N[1]*-(2-chloro-6,7,8,9,10,11-hexahydrocycloocta[*b*]quinolin-12-yl)hexane-1,6-diamine* (**19f**): 1,6-diaminohexane (807.1 mg, 6.9 mmol) was combined with **18** (389.2 mg, 1.4 mmol) in 2.2 mL 1-pentanol. The product mixture was chromatographed with 15 % methanol in methylene chloride with 10 mL concentrated NH_4OH per L of eluent, to afford 410.3 mg (82 %) of the title compound as a brown oil. ^{1}H NMR (500 MHz, $CDCl_3$) δ 7.96 (d, *J* = 2.3 Hz, 1H), 7.87 (d, *J* = 9.0 Hz, 1H), 7.49 (dd, *J* = 2.3 Hz, 9.0 Hz, 1H), 3.84 (t, *J* = 6.3 Hz, 1H), 3.41 – 3.34 (m, 2H), 3.11 (t, *J* = 6.2 Hz, 2H), 2.94 (t, *J* = 6.4, Hz, 2H), 2.70 (t, *J* = 6.9, 2H), 1.89 – 1.81 (m, 2H), 1.75 – 1.65 (m, 4H), 1.52 – 1.30 (m, 12H); ^{13}C NMR (125 MHz, $CDCl_3$) δ 163.45, 149.66, 146.43, 130.81, 129.53, 128.92, 122.72, 122.24, 121.25, 50.53, 42.11, 37.08, 33.64, 31.63, 31.07, 29.60,

26.86, 26.69, 26.54, 25.92, 25.16. MS (ESI): Calc for $C_{21}H_{31}ClN_3^+$: 360.2207. Found: 360.2201 (-0.01 ppm, -0.6 mmu).

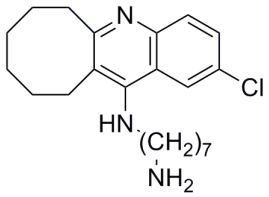

N[1]*-(2-chloro-6,7,8,9,10,11-hexahydrocycloocta[*b*]quinolin-12-yl)heptane-1,7-diamine* (**19g**): 1,7-diaminoheptane (870.6 mg, 6.7 mmol) was combined with **18** (374.6 mg, 1.3 mmol) in 2.3 mL 1-pentanol. The product mixture was chromatographed with 15 % methanol in methylene chloride with 10 mL concentrated NH_4OH per L of eluent, to afford 314.9 mg (63 %) of the title compound as a yellow oil. ^{1}H NMR (500 MHz, $CDCl_3$) δ 7.96 (d, *J* = 2.4 Hz, 1H), 7.87 (d, *J* = 9.0 Hz, 1H), 7.49 (dd, *J* = 2.4 Hz, 9.0 Hz, 1H), 3.84 (t, *J* = 6.3 Hz, 1H), 3.40 – 3.34 (m, 2H), 3.12 (t, *J* = 6.2 Hz, 2H), 2.94 (t, *J* = 6.4 Hz, 2H), 2.69 (t, *J* = 7.0 Hz, 2H), 1.89 – 1.81 (m, 2H), 1.75 – 1.65 (m, 4H), 1.52 – 1.30 (m, 14H); ^{13}C NMR (125 MHz, $CDCl_3$) δ 163.57, 149.81, 146.57, 130.94, 129.66, 129.05, 122.85, 122.38, 121.35, 50.69, 42.33, 37.19, 33.84, 31.73, 31.20, 29.73, 29.40, 27.09, 26.94, 26.68, 26.07, 25.31. MS (ESI): Calc for $C_{22}H_{33}ClN_3^+$: 374.2363. Found: 374.2364 (+1.73 ppm, +0.1 mmu).

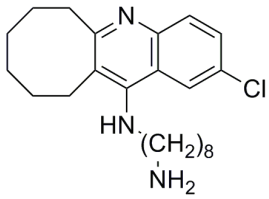

N[1]*-(2-chloro-6,7,8,9,10,11-hexahydrocycloocta[*b*]quinolin-12-yl)octane-1,8-diamine* (**19h**): 1,8-diaminooctane (929.5 mg, 6.4 mmol) was combined with **18** (361.1 mg, 1.3 mmol) in 2.4 mL 1-pentanol. The product mixture was chromatographed with 20 % methanol in methylene chloride with 10 mL concentrated NH_4OH per L of eluent, to afford 278.6 mg (56 %) of the title compound as a brown oil. ^{1}H NMR (500 MHz, $CDCl_3$) δ 7.96 (d, *J* = 2.3 Hz, 1H), 7.87 (d, *J* = 9.0 Hz, 1H), 7.49 (dd, *J* = 2.3 Hz, 9.0 Hz, 1H), 3.84 (t, *J* = 6.2 Hz, 1H), 3.41 – 3.33 (m, 2H), 3.11 (t, *J* = 6.2 Hz, 2H), 2.94 (t, *J* = 6.4 Hz, 2H), 2.68 (t, *J* = 7.0 Hz, 2H), 1.88 – 1.81 (m, 2H), 1.75 – 1.64 (m, 4H), 1.51 – 1.30 (m, 16H); ^{13}C NMR (125 MHz, $CDCl_3$) δ 163.43, 149.70, 146.42,

130.79, 129.50, 128.91, 122.75, 122.22, 121.16, 50.58, 42.24, 37.08, 33.80, 31.64, 31.07, 29.57, 29.39, 29.36, 26.92, 26.80, 26.54, 25.91, 25.15. MS (ESI): Calc for $C_{23}H_{35}ClN_3^+$: 388.2520. Found: 388.2510 (-1.04 ppm, -1.0 mmu).

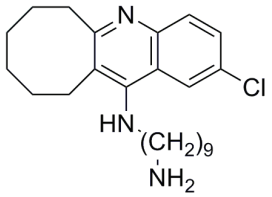

N*1*-*(2-chloro-6,7,8,9,10,11-hexahydrocycloocta[*b*]quinolin-12-yl)nonane-1,9-diamine* (**19i**): 1,9-diaminononane (984.3 mg, 6.2 mmol) was combined with **18** (348.5 mg, 1.2 mmol) in 2.5 mL 1-pentanol. The product mixture was chromatographed with 15 % methanol in methylene chloride with 10 mL concentrated NH_4OH per L of eluent, to afford 329.5 mg (66 %) of the title compound as a brown oil. ^{1}H NMR (500 MHz, $CDCl_3$) δ 7.96 (d, *J* = 2.3 Hz, 1H), 7.87 (d, *J* = 9.0 Hz, 1H), 7.49 (dd, *J* = 2.3 Hz, 9.0 Hz, 1H), 3.85 (t, *J* = 5.7 Hz, 1H), 3.41 – 3.33 (m, 2H), 3.11 (t, *J* = 6.2 Hz, 2H), 2.94 (t, *J* = 6.4 Hz, 2H), 2.68 (t, *J* = 7.0 Hz, 2H), 1.88 – 1.81 (m, 2H), 1.75 – 1.64 (m, 4H), 1.58 (s, 2H), 1.52 – 1.26 (m, 16H); ^{13}C NMR (125 MHz, $CDCl_3$) δ 163.41, 149.71, 146.41, 130.77, 129.50, 128.91, 122.75, 122.21, 121.14, 50.58, 42.17, 37.05, 33.69, 31.64, 31.06, 29.57, 29.49, 29.39, 29.33, 26.95, 26.85, 26.54, 25.92, 25.16. MS (ESI): Calc for $C_{24}H_{36}ClN_3^+$: 402.2676. Found: 402.2669 (-0.38 ppm, -0.7 mmu).

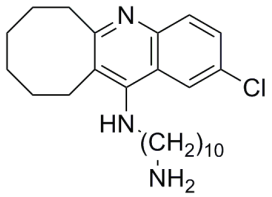

N*1*-*(2-chloro-6,7,8,9,10,11-hexahydrocycloocta[*b*]quinolin-12-yl)decane-1,10-diamine* (**19j**): 1,10-diaminodecane (1035.4 mg, 6.0 mmol) was combined with **18** (336.7 mg, 1.2 mmol) in 2.5 mL 1-pentanol. The product mixture was chromatographed with 20 % methanol in methylene chloride with 10 mL concentrated NH_4OH per L of eluent, to afford 265.9 mg (53 %) of the title compound as a brown oil. ^{1}H NMR (500 MHz, $CDCl_3$) δ 7.96 (d, *J* = 2.3 Hz, 1H), 7.87 (d, *J* = 8.8 Hz, 1H), 7.49 (dd, *J* = 2.3 Hz, 8.8 Hz, 1H), 3.84 (t, *J* = 6.2 Hz, 1H), 3.40 – 3.33 (m, 2H), 3.11

(t, *J* = 6.2 Hz, 2H), 2.94 (t, *J* = 6.3 Hz, 2H), 2.68 (t, *J* = 6.9 Hz, 2H), 1.89 – 1.81 (m, 2H), 1.76 – 1.64 (m, 4H), 1.53 – 1.25 (m, 20H).

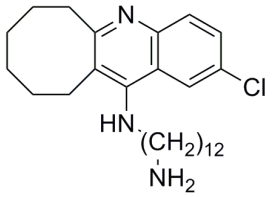

N[1]*-(2-chloro-6,7,8,9,10,11-hexahydrocycloocta[*b*]quinolin-12-yl)dodecane-1,12-diamine* (**19l**): 1,12-diaminododecane (1127.9 mg, 5.6 mmol) was combined with **18** (315.5 mg, 1.1 mmol) in 2.7 mL 1-pentanol. The product mixture was chromatographed with 20 % methanol in methylene chloride with 10 mL concentrated NH_4OH per L of eluent, to afford 185.6 mg (37 %) of the title compound as a brown oil. ^{1}H NMR (500 MHz, $CDCl_3$) δ 7.96 (d, *J* = 2.3 Hz, 1H), 7.87 (d, *J* = 9.0 Hz, 1H), 7.49 (dd, *J* = 2.3 Hz, 9.0 Hz, 1H), 3.84 (s, 1H), 3.40 – 3.33 (m, 2H), 3.12 (t, *J* = 6.2 Hz, 2H), 2.94 (t, *J* = 6.4 Hz, 2H), 2.68 (t, *J* = 7.0 Hz, 2H), 1.88 – 1.82 (m, 2H), 1.75 – 1.64 (m, 4H), 1.52 – 1.25 (m, 24H); ^{13}C NMR (126 MHz, $CDCl_3$) δ 163.41, 149.75, 146.43, 130.78, 129.53, 128.93, 122.77, 122.23, 121.14, 50.61, 42.24, 37.05, 33.78, 31.67, 31.07, 29.63, 29.59, 29.58, 29.55, 29.54, 29.51, 29.40, 26.98, 26.91, 26.56, 25.95, 25.19.

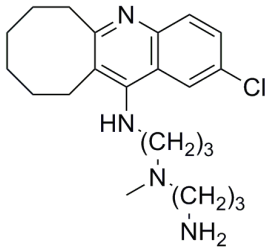

N[1]*-(3-aminopropyl)*-N[3]*-(2-chloro-6,7,8,9,10,11-hexahydrocycloocta[*b*]quinolin-12-yl)propane-1,3-diamine* (**21**): 3,3'-diamino-*N*-methyldipropylamine (1867.0 mg, 12.9 mmol) was combined with **18** (360.2 mg, 1.3 mmol) in 4.1 mL 1-pentanol. The product mixture was chromatographed with 30 % methanol in methylene chloride with 10 mL concentrated NH_4OH per L of eluent, to afford 428.1 mg (86 %) of the title compound as a brown oil. ^{1}H NMR (500 MHz, $CDCl_3$) δ 8.00 (d, *J* = 2.3 Hz, 1H), 7.86 (d, *J* = 9.0 Hz, 1H), 7.47 (dd, *J* = 2.3 Hz, 9.0 Hz, 1H), 3.48 (q, *J* = 6.1 Hz, 2H), 3.10 (t, *J* = 6.2 Hz, 2H), 2.95 (t, *J* = 6.3 Hz, 2H), 2.73 (t, *J* = 7.0 Hz, 2H), 2.55 (t, *J*

= 6.2 Hz, 2H), 2.46 (t, *J* = 7.5 Hz, 2H), 2.30 (s, 3H), 1.90 – 1.81 (m, 4H), 1.75 – 1.63 (m, 4H), 1.51 – 1.30 (m, 6H).

3.3.3 Synthesis of bump-hole optimized tacrine dimers

General procedure for the formation of dimers (**20c-l**, **22**): To a 5 mL round-bottomed flask, equipped with a stir bar, condenser and N_2 inlet, were added the appropriate dimer precursor free amine (0.2 mmol), **18** (0.5 mmol, 2.5 equiv), and 1-pentanol (380 μL). The reaction was lowered into a 160 °C oil bath and allowed to stir at reflux for 44 h. Once the reaction cooled slightly, it was poured into toluene (10 times the reaction volume). The resulting solid was collected by filtration. Subsequently, the solid was dissolved in methanol and 1.1 equiv concentrated HCl were added. Upon concentrating the product mixture, the solid was dissolved in hot methanol, and room temperature water was added dropwise until the solution became cloudy. Upon cooling the resulting mixture to 0 °C, the bump-hole optimized tacrine dimers obtained as off-white granular solids.

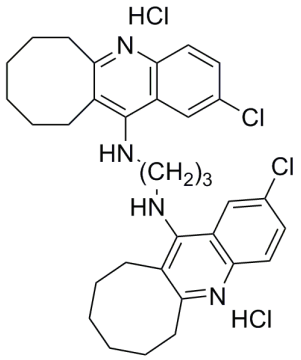

N[1],N[3]-*bis(2-chloro-6,7,8,9,10,11-hexahydrocycloocta[*b*]quinolin-12-yl)propane-1,3-diamine bishydrochloride* (**20c**): **19c** (56.6 mg) was combined with **18** (149.8 mg) in 1-pentanol. Workup and recrystallization yielded 67.8 mg (60 %) of the title compound. ^{1}H NMR (500 MHz, CD_3OD) δ 8.22 (d, *J* = 1.2 Hz, 2H), 7.87 – 7.79 (m, 4H), 4.02 (t, *J* = 6.2 Hz, 4H), 3.06 (t, *J* = 6.2 Hz, 4H), 2.91 (t, *J* = 6.3 Hz, 4H), 2.36 (quin., *J* = 6.2 Hz, 2H), 1.92 – 1.81 (m, 4H), 1.77 – 1.65 (m, 4H), 1.58 – 1.46 (m, 4H), 1.36 – 1.25 (m, 4H); ^{13}C NMR (125 MHz, CD_3OD) δ 156.88, 156.61, 138.36, 134.68, 132.25, 125.70, 122.47, 118.11, 117.00, 46.45, 32.97, 32.19, 31.63, 29.51, 27.23, 26.72, 24.60. Anal. Calc. for $C_{33}H_{38}Cl_2N_4 \cdot 2HCl \cdot 3H_2O$: C, 57.56; H, 6.73; N, 8.14. Found: C, 57.63; H, 6.64; N, 8.08.

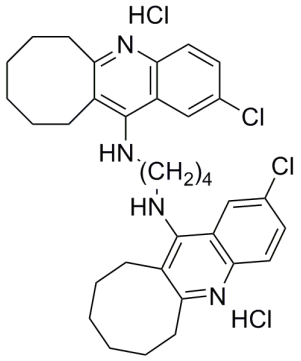

N[1],N[4]-*bis(2-chloro-6,7,8,9,10,11-hexahydrocycloocta[*b*]quinolin-12-yl)butane-1,4-diamine bis-hydrochloride* (**20d**): **19d** (57.7 mg) was combined with **18** (146.0 mg) in 1-pentanol. Workup and recrystallization yielded 55.9 mg (50 %) of the title compound. ^{1}H NMR (500 MHz, CD_3OD) δ 8.28 (d, *J* = 1.8 Hz, 2H), 7.86 – 7.77 (m, 4H), 3.12 (t, *J* = 6.2 Hz, 4H), 2.99 (t, *J* = 6.2 Hz, 4H), 2.01 – 1.84 (m, 8H), 1.80 – 1.68 (m, 4H), 1.63 – 1.50 (m, 4H), 1.40 – 1.30 (m, 4H); ^{13}C NMR (125 MHz, CD_3OD) δ 156.97, 156.04, 138.32, 134.56, 132.36, 125.34, 122.44, 118.45, 116.49, 48.22, 32.94, 31.73, 29.42, 28.40, 27.26, 26.74, 24.78. Anal. Calc. for $C_{34}H_{40}Cl_2N_4 \cdot 2HCl \cdot H_2O$: C, 61.27; H, 6.65; N, 8.41. Found: C, 61.04; H, 6.44; N, 8.25.

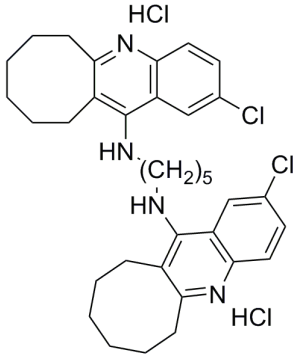

N[1],N[5]-*bis(2-chloro-6,7,8,9,10,11-hexahydrocycloocta[*b*]quinolin-12-yl)pentane-1,5-diamine bis-hydrochloride* (**20e**): **19e** (58.7 mg) was combined with **18** (142.6 mg) in 1-pentanol. Workup and recrystallization yielded 89.5 mg (80 %) of the title compound. ^{1}H NMR (500 MHz, CD_3OD) δ 8.34 (d, *J* = 1.9 Hz, 2H), 7.88 – 7.80 (m, 4H), 3.93 (t, *J* = 7.4 Hz, 4H), 3.13 (t, *J* = 6.2 Hz, 4H), 3.02 (t, *J* = 6.3 Hz, 4H), 1.97 – 1.87 (m, 8H), 1.82 – 1.74 (m, 4H), 1.62 – 1.52 (m, 6H), 1.44 – 1.34 (m, 4H); ^{13}C NMR (125 MHz, CD_3OD) δ 156.73, 156.37, 138.56, 134.50, 132.17, 125.64, 122.40, 118.36, 116.40, 49.14, 32.85, 31.71, 31.01, 29.43, 27.26, 26.82, 24.97, 24.76.

Anal. Calc. for $C_{35}H_{42}Cl_2N_4 \cdot 2HCl \cdot 1.5H_2O$: C, 60.96; H, 6.87; N, 8.12. Found: C, 61.28; H, 6.89; N, 8.05.

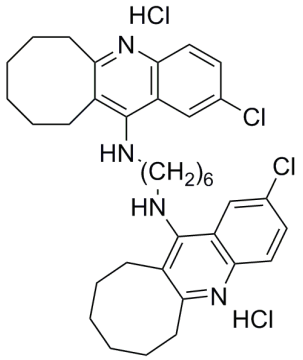

N[1],N[6]-*bis(2-chloro-6,7,8,9,10,11-hexahydrocycloocta[*b*]quinolin-12-yl)hexane-1,6-diamine bis-hydrochloride* (**20f**): **19f** (59.6 mg) was combined with **18** (139.2 mg) in 1-pentanol. Workup and recrystallization yielded 77.2 mg (69 %) of the title compound. ^{1}H NMR (500 MHz, CD_3OD) δ 8.34 (d, *J* = 1.1 Hz, 2H), 7.84 (m, 4H), 3.91 (t, *J* = 7.4 Hz, 4H), 3.14 (t, *J* = 6.2 Hz, 4H), 3.02 (t, *J* = 6.2 Hz, 4H), 1.98 – 1.83 (m, 8H), 1.83 – 1.74 (m, 4H), 1.62 – 1.47 (m, 8H), 1.45 – 1.35 (m, 4H); ^{13}C NMR (125 MHz, CD_3OD) δ 156.60, 156.43, 138.62, 134.47, 132.08, 125.72, 122.39, 118.30, 116.42, 49.10, 32.82, 31.72, 31.31, 29.36, 27.38, 27.27, 26.85, 24.73. Anal. Calc. for $C_{36}H_{44}Cl_2N_4 \cdot 2HCl \cdot 4H_2O$: C, 57.76; H, 7.27; N, 7.48. Found: C, 57.81; H, 7.07; N, 7.37.

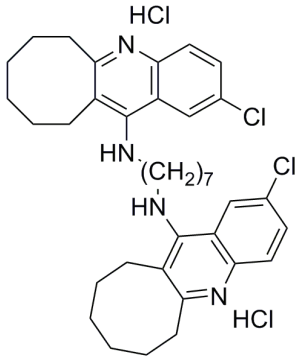

N[1],N[7]-*bis(2-chloro-6,7,8,9,10,11-hexahydrocycloocta[*b*]quinolin-12-yl)heptane-1,7-diamine bis-hydrochloride* (**20g**): **19g** (60.5 mg) was combined with **18** (136.1 mg) in 1-pentanol. Workup and recrystallization yielded 57.7 mg (52 %) of the title compound. ^{1}H NMR (500 MHz, CD_3OD) δ 8.34 (d, *J* = 1.2 Hz, 2H), 7.88 – 7.80 (m, 4H), 3.90 (t, *J* = 7.5 Hz, 4H), 3.14 (t, *J* = 6.2

Hz, 4H), 3.02 (t, *J* = 6.3 Hz, 4H), 1.98 – 1.74 (m, 12H), 1.64 – 1.52 (m, 4H), 1.51 – 1.35 (m, 10H); ^{13}C NMR (125 MHz, CD_3OD) δ 156.63, 156.44, 138.61, 134.44, 132.13, 125.69, 122.40, 118.31, 116.43, 49.15, 32.81, 31.71, 31.28, 29.80, 29.38, 27.58, 27.27, 26.89, 24.78. Anal. Calc. for $C_{37}H_{46}Cl_2N_4 \cdot 2HCl \cdot 1.5H_2O$: C, 61.93; H, 7.16; N, 7.81. Found: C, 61.73; H, 7.02; N, 7.68.

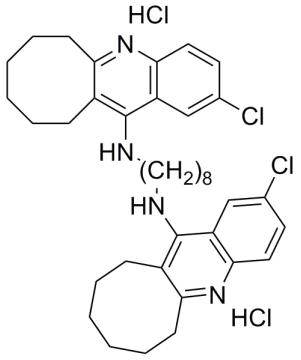

N^{1},N^{8}-*bis(2-chloro-6,7,8,9,10,11-hexahydrocycloocta[*b*]quinolin-12-yl)octane-1,8-diamine bis-hydrochloride* (**20h**): **19h** (61.4 mg) was combined with **18** (133.1 mg) in 1-pentanol. Workup and recrystallization yielded 40.0 mg (36 %) of the title compound. ^{1}H NMR (500 MHz, CD_3OD) δ 8.36 (d, *J* = 1.5 Hz, 2H), 7.87 – 7.79 (m, 4H), 3.90 (t, *J* = 7.5 Hz, 4H), 3.13 (t, *J* = 6.2 Hz, 4H), 3.02 (t, *J* = 6.3 Hz, 4H), 1.98 – 1.88 (m, 5H), 1.88 – 1.74 (m, 8H), 1.63 – 1.55 (m, 4H), 1.49 – 1.35 (m, 12H); ^{13}C NMR (125 MHz, CD_3OD) δ 156.53, 156.45, 138.64, 134.46, 132.06, 125.76, 122.37, 118.28, 116.35, 49.20, 32.80, 31.72, 31.36, 30.17, 29.34, 27.65, 27.26, 26.86, 24.72. Anal. Calc. for $C_{38}H_{48}Cl_2N_4 \cdot 2HCl \cdot 2.5H_2O$: C, 60.88; H, 7.39; N, 7.47. Found: C, 61.05; H, 7.20; N, 7.47.

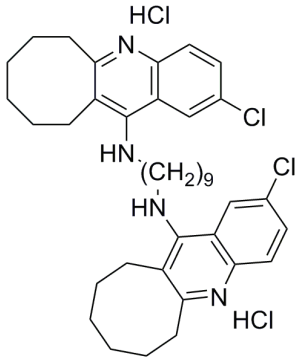

N^{1},N^{9}-*bis(2-chloro-6,7,8,9,10,11-hexahydrocycloocta[*b*]quinolin-12-yl)nonane-1,9-diamine bis-hydrochloride* (**20i**): **19i** (59.1 mg) was combined with **18** (123.6 mg) in 1-pentanol. Workup and recrystallization yielded 67.2 mg (71 %) of the title compound. ^{1}H NMR (500 MHz,

CD_3OD) δ 8.36 (d, *J* = 0.9 Hz, 2H), 7.90 – 7.80 (m, 4H), 3.89 (t, *J* = 7.4 Hz, 4H), 3.14 (t, *J* = 6.1 Hz, 4H), 3.02 (t, *J* = 6.1 Hz, 4H), 1.96 – 1.89 (m, 4H), 1.88 – 1.76 (m, 8H), 1.62 – 1.55 (m, 4H), 1.48 – 1.33 (m, 14H); ^{13}C NMR (125 MHz, CD_3OD) δ 156.49, 156.44, 138.65, 134.46, 132.04, 125.78, 122.36, 118.27, 116.32, 49.11, 32.80, 31.72, 31.39, 30.50, 30.16, 29.33, 27.70, 27.26, 26.86, 24.71. Anal. Calc. for $C_{39}H_{50}Cl_2N_4 \cdot 2HCl \cdot 2.5H_2O$: C, 61.34; H, 7.52; N, 7.34. Found: C, 61.23; H, 7.36; N, 7.30.

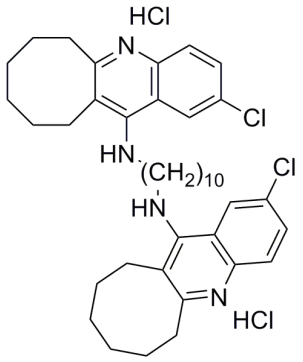

N^{1},N^{10}*-bis(2-chloro-6,7,8,9,10,11-hexahydrocycloocta[*b*]quinolin-12-yl)decane-1,10-diamine bishydrochloride* (**20j**): **19j** (63.1 mg) was combined with **18** (127.4 mg) in 1-pentanol. Workup and recrystallization yielded 53.6 mg (48 %) of the title compound. ^{1}H NMR (500 MHz, CD_3OD) δ 8.36 (d, *J* = 0.8 Hz, 2H), 7.89 – 7.79 (m, 4H), 3.89 (t, *J* = 7.5 Hz, 4H), 3.14 (t, *J* = 6.1 Hz, 4H), 3.02 (t, *J* = 6.2 Hz, 4H), 1.97 – 1.88 (m, 4H), 1.88 – 1.76 (m, 8H), 1.62 – 1.55 (m, 4H), 1.46 – 1.29 (m, 16H); ^{13}C NMR (125 MHz, CD_3OD) δ 156.54, 156.44, 138.69, 134.44, 132.05, 125.77, 122.40, 118.29, 116.36, 49.21, 32.81, 31.72, 31.40, 30.49, 30.23, 29.34, 27.72, 27.26, 26.87, 24.72. Anal. Calc. for $C_{40}H_{52}Cl_2N_4 \cdot 2HCl \cdot 2H_2O$: C, 62.50; H, 7.60; N, 7.29. Found: C, 62.90; H, 7.34; N, 7.15.

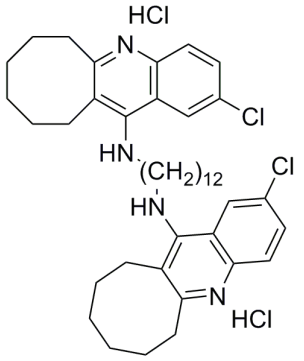

N[1],N[12]*-bis(2-chloro-6,7,8,9,10,11-hexahydrocycloocta[*b*]quinolin-12-yl)dodecane-1,12-diamine bishydrochloride* (**20l**): **19l** (64.6 mg) was combined with **18** (122.2 mg) in 1-pentanol. Workup and recrystallization yielded 34.8 mg (31 %) of the title compound. ^{1}H NMR (500 MHz, CD_3OD) δ 8.37 (apparent s, 2H), 7.89 – 7.81 (m, 4H), 3.90 (t, *J* = 7.3 Hz, 4H), 3.14 (t, *J* = 5.9 Hz, 4H), 3.03 (t, *J* = 6.0 Hz, 4H), 1.96 – 1.89 (m, 4H), 1.88 – 1.75 (m, 8H), 1.62 – 1.55 (m, 4H), 1.47 – 1.25 (m, 18H); ^{13}C NMR (125 MHz, CD_3OD) δ 156.50, 156.47, 138.66, 134.47, 132.06, 125.78, 122.36, 118.28, 116.33, 48.84, 32.79, 31.71, 31.39, 30.61, 30.58, 30.26, 29.34, 27.73, 27.26, 26.87, 24.72. Anal. Calc. for $C_{42}H_{56}Cl_2N_4 \cdot 2HCl \cdot 2.5H_2O$: C, 62.60; H, 7.88; N, 6.95. Found: C, 62.47; H, 7.39; N, 6.72.

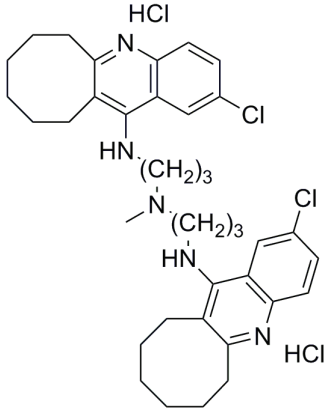

N[1]*-(2-chloro-6,7,8,9,10,11-hexahydrocycloocta[*b*]quinolin-12-yl)*-N[3]*-(3-(2-chloro-6,7,8,9,10,11-hexahydrocycloocta[*b*]quinolin-12-ylamino)propyl)*-N[3]*-methylpropane-1,3-diamine bishydrochloride* (**22**): **21** (61.5 mg) was combined with **18** (132.9 mg) in 1-pentanol. Workup and recrystallization yielded 23.6 mg (21 %) of the title compound. ^{1}H NMR (500 MHz, CD_3OD) δ 8.40 (apparent s, 2H), 7.86 (m, 4H), 4.05 (t, *J* = 7.2 Hz, 4H), 3.16 (t, *J* = 6.2 Hz, 4H), 3.09 (t, *J* = 6.2 Hz, 4H), 2.92 (s, 3H), 2.43 – 2.30 (m, 4H), 1.98 – 1.89 (m, 4H), 1.86 –

1.76 (m, 4H), 1.64 – 1.55 (m, 4H), 1.48 – 1.34 (m, 4H); ^{13}C NMR (125 MHz, CD_3OD) δ 157.41, 156.36, 138.44, 134.58, 132.58, 125.46, 122.47, 118.84, 117.03, 54.71, 46.19, 40.49, 32.97, 31.72, 29.75, 27.24, 26.78, 26.46, 24.97. Anal. Calc. for $C_{37}H_{47}Cl_2N_4 \cdot 3HCl \cdot 6H_2O$: C, 52.27; H, 7.35; N, 8.24. Found: C, 52.67; H, 6.95; N, 8.16.

3.4 Computational details

3.4.1 Conformational analysis calculation

Compound **8c** was constructed using Spartan 04. A conformer distribution calculation was performed using MMFF. Three minima were located (**A** – **C**). Cartesian coordinates follow below.

Conformation **A** (Relative energy = 0.0 kcal/mol)

C	-0.972	0.168	-0.593
C	-0.512	-0.676	0.443
N	-0.816	1.493	-0.473
C	-0.306	2.104	0.604
C	-0.250	3.508	0.640
C	0.154	1.328	1.692
H	0.982	1.489	3.707
C	0.114	-0.089	1.576
C	0.248	4.165	1.765
H	-0.596	4.113	-0.196
H	0.288	5.253	1.792
C	0.685	3.423	2.856
C	0.640	2.027	2.825
C	-1.565	-0.300	-1.774
H	-2.230	0.448	-2.224
C	-0.608	-2.079	0.324
H	-0.779	-2.561	1.298
H	-1.438	-2.421	-0.302
H	-2.180	-1.195	-1.624
C	-0.496	-0.645	-2.873
H	0.251	0.155	-2.942
H	-1.036	-0.652	-3.829
C	0.696	-2.720	-0.280
H	0.479	-3.780	-0.456
H	1.493	-2.684	0.473
C	1.197	-2.076	-1.573
H	1.608	-1.080	-1.371
H	2.044	-2.682	-1.921
C	0.160	-2.015	-2.696
H	-0.603	-2.791	-2.567

H	0.679	-2.242	-3.636
N	0.511	-0.897	2.665
H	1.238	-0.519	3.267
H	0.748	-1.857	2.417
Cl	1.286	4.227	4.249
H	-1.114	2.059	-1.263

Conformation **B** (Relative energy = 0.4 kcal/mol)

C	-0.949	0.102	-0.613
C	-0.505	-0.726	0.442
N	-0.870	1.432	-0.484
C	-0.442	2.063	0.617
C	-0.464	3.467	0.661
C	0.023	1.305	1.716
H	0.772	1.496	3.759
C	0.064	-0.112	1.590
C	-0.042	4.141	1.807
H	-0.812	4.057	-0.184
H	-0.064	5.230	1.842
C	0.398	3.417	2.908
C	0.431	2.021	2.868
C	-1.404	-0.395	-1.838
H	-2.175	0.245	-2.288
C	-0.576	-2.134	0.340
H	-0.666	-2.606	1.330
H	-1.453	-2.500	-0.206
H	-1.841	-1.397	-1.768
C	-0.241	-0.487	-2.891
H	0.048	0.529	-3.185
H	-0.654	-0.973	-3.784
C	0.700	-2.750	-0.343
H	0.702	-3.814	-0.072
H	1.610	-2.316	0.087
C	0.704	-2.655	-1.871
H	1.504	-3.318	-2.226
H	-0.231	-3.051	-2.282
C	0.995	-1.253	-2.416
H	1.662	-1.352	-3.282
H	1.552	-0.661	-1.680
N	0.490	-0.907	2.680
H	1.169	-0.484	3.308
H	0.816	-1.837	2.418
Cl	0.906	4.243	4.325
H	-1.156	1.981	-1.289

Conformation **C** (Relative energy = 9.1 kcal/mol)

C	-0.954	-0.004	-0.628
C	-0.457	-0.806	0.427
N	-0.964	1.327	-0.504
C	-0.584	1.988	0.596
C	-0.701	3.389	0.633
C	-0.077	1.265	1.699
H	0.643	1.523	3.748
C	0.060	-0.151	1.579
C	-0.333	4.096	1.777
H	-1.083	3.950	-0.217
H	-0.428	5.180	1.805
C	0.147	3.407	2.884
C	0.273	2.015	2.850
C	-1.350	-0.534	-1.858
H	-2.108	0.074	-2.368
C	-0.490	-2.217	0.340
H	-0.137	-2.733	1.239
H	-1.545	-2.534	0.269
H	-1.792	-1.531	-1.747
C	-0.130	-0.662	-2.861
H	-0.088	0.277	-3.429
H	-0.363	-1.458	-3.577
C	0.223	-2.905	-0.886
H	-0.504	-3.120	-1.676
H	0.534	-3.895	-0.523
C	1.450	-2.209	-1.452
H	2.177	-2.037	-0.649
H	1.929	-2.915	-2.143
C	1.240	-0.897	-2.219
H	1.998	-0.850	-3.011
H	1.485	-0.057	-1.558
N	0.527	-0.899	2.685
H	1.132	-0.410	3.339
H	0.960	-1.790	2.451
Cl	0.589	4.271	4.300
H	-1.280	1.854	-1.314

3.4.2 DFT optimization of MMFF generated conformations

Each of the conformations found in the MMFF conformer distribution was further optimized using B3LYP/6-31G* as implemented in Gaussian 03.[12] A frequency analysis was performed on the optimized structures to confirm that all were ground state conformations. The following Cartesian coordinates are for the optimized DFT structures. Table 3.1 summarizes the

electronic energies, zero point vibrational energies, and relative energies of the three conformations.

Conformation **A**

C	-0.957787	0.189448	-0.563839
C	-0.487936	-0.639031	0.453682
N	-0.870848	1.534962	-0.430630
C	-0.337567	2.174149	0.665227
C	-0.296490	3.580902	0.718169
C	0.164594	1.391332	1.729732
H	1.116992	1.516783	3.694039
C	0.092357	-0.049881	1.608932
C	0.241234	4.211044	1.819536
H	-0.688369	4.165948	-0.109278
H	0.278899	5.293468	1.872044
C	0.748166	3.441332	2.888584
C	0.713606	2.061454	2.848439
C	-1.558958	-0.296199	-1.860117
H	-2.167291	0.516656	-2.276190
C	-0.548377	-2.142565	0.294799
H	-0.789507	-2.615741	1.255764
H	-1.390013	-2.401920	-0.351776
H	-2.257327	-1.114417	-1.658330
C	-0.536097	-0.735436	-2.942370
H	0.207939	0.062027	-3.072873
H	-1.097150	-0.783795	-3.883027
C	0.739899	-2.770254	-0.288521
H	0.542501	-3.839282	-0.436435
H	1.554419	-2.708524	0.445405
C	1.229365	-2.151981	-1.609118
H	1.637190	-1.148788	-1.423301
H	2.081709	-2.753711	-1.944255
C	0.188218	-2.080907	-2.749885
H	-0.551124	-2.887308	-2.642770
H	0.700967	-2.283359	-3.697094
N	0.577236	-0.826674	2.593428
H	0.969116	-0.443348	3.439270
H	0.555455	-1.832612	2.525239
Cl	1.424660	4.252790	4.270754
H	-1.229683	2.112440	-1.183235

Conformation **B**

C	-0.946914	0.129575	-0.587849
C	-0.483456	-0.684900	0.444377
N	-0.929859	1.476583	-0.452614
C	-0.477834	2.136340	0.667322

C	-0.526072	3.542066	0.734157
C	0.038181	1.373330	1.739547
H	0.898580	1.536014	3.743541
C	0.058183	-0.069399	1.606209
C	-0.066341	4.192048	1.859112
H	-0.926379	4.110576	-0.100755
H	-0.098506	5.274018	1.923057
C	0.448683	3.442793	2.938562
C	0.502219	2.063940	2.884110
C	-1.400150	-0.391347	-1.922534
H	-2.158177	0.282443	-2.340897
C	-0.531230	-2.197286	0.320410
H	-0.658990	-2.631014	1.319784
H	-1.442389	-2.492301	-0.209464
H	-1.892465	-1.356419	-1.788666
C	-0.234591	-0.536110	-2.939288
H	0.077382	0.463534	-3.268270
H	-0.653238	-1.031657	-3.823312
C	0.687423	-2.859818	-0.368202
H	0.654954	-3.928605	-0.124086
H	1.615906	-2.471318	0.073333
C	0.766334	-2.726293	-1.900817
H	1.592171	-3.369038	-2.226138
H	-0.136110	-3.161817	-2.353553
C	1.008661	-1.304332	-2.458445
H	1.679094	-1.372220	-3.322687
H	1.554099	-0.706833	-1.715170
N	0.589625	-0.817620	2.589077
H	0.992286	-0.409032	3.417868
H	0.657284	-1.820391	2.507763
Cl	1.019663	4.278179	4.353828
H	-1.277026	2.037313	-1.223311

Conformation **C**

C	-0.711250	0.102317	-0.626319
C	-0.175937	-0.650285	0.422672
N	-0.937635	1.429673	-0.452090
C	-0.680116	2.133579	0.698645
C	-0.947946	3.514959	0.767784
C	-0.147208	1.437463	1.803879
H	0.537631	1.695538	3.866753
C	0.089677	0.017879	1.657622
C	-0.682255	4.205720	1.929786
H	-1.360669	4.031396	-0.094456
H	-0.881723	5.269408	1.997623
C	-0.143152	3.523176	3.042186

C	0.119746	2.168982	2.986075
C	-1.056187	-0.394374	-2.009896
H	-1.752643	0.318127	-2.469316
C	0.140817	-2.146704	0.401495
H	1.184394	-2.257012	0.737507
H	-0.476947	-2.609790	1.186728
H	-1.608324	-1.329109	-1.933725
C	0.168641	-0.560691	-2.948792
H	0.527366	0.436189	-3.234645
H	-0.196808	-1.032526	-3.868949
C	-0.008325	-3.025799	-0.855010
H	-1.027892	-2.974352	-1.244819
H	0.096521	-4.058847	-0.502472
C	1.042286	-2.810585	-1.963837
H	1.986989	-3.259988	-1.631070
H	0.731579	-3.386274	-2.845196
C	1.344072	-1.361672	-2.376867
H	2.132545	-1.382910	-3.138613
H	1.776794	-0.818216	-1.525857
N	0.572522	-0.673309	2.705584
H	0.749308	-0.237087	3.596904
H	0.735328	-1.666442	2.654934
Cl	0.191697	4.412458	4.499589
H	-1.333898	1.941107	-1.232841

Table 3.1. Electronic energy (E_h), ZPVE, and relative energy of three minima of **8c**

Conformation	Energy (E_h) [a]	Scaled [b] ZPVE (E_h)	Rel. Energy (kcal/mol)
A	-1151.965517	0.302905	0.0
B	-1151.964661	0.302832	0.5
C	-1151.959110	0.303264	4.2

[a] Calculated using B3LYP/6-31G*. [b] Frequencies were scaled by a factor of 0.9804.

References for Chapter 3

1. Kurosu, M.; Lin, M. H.; Kishi, Y. Fe/Cr- and Co/Cr-mediated catalytic asymmetric 2-haloallylations of aldehydes. *J. Am. Chem. Soc.* **2004,** 126, 12248-12249.

2. McKenna, M. T.; Proctor, G. R.; Young, L. C.; Harvey, A. L. Novel tacrine analogues for potential use against Alzheimer's disease: Potent and selective acetylcholinesterase inhibitors and 5-HT uptake inhibitors. *J. Med. Chem.* **1997,** 40, 3516-3523.

3. Recanatini, M.; Cavalli, A.; Belluti, F.; Piazzi, L.; Rampa, A.; Bisi, A.; Gobbi, S.; Valenti, P.; Andrisano, V.; Bartolini, M.; Cavrini, V. SAR of 9-Amino-1,2,3,4-

tetrahydroacridine-Based Acetylcholinesterase Inhibitors: Synthesis, Enzyme Inhibitory Activity, QSAR, and Structure-Based CoMFA of Tacrine Analogues. *J. Med. Chem.* **2000,** 43, 2007-2018.

4. Desai, M. C.; Thadeio, P. F.; Lipinski, C. A.; Liston, D. R.; Spencer, R. W.; Williams, I. H. Physical parameters for brain uptake: optimizing log P, log D and pKa of THA. *Bioorg. Med. Chem. Lett.* **1991,** 1, 411-414.

5. Doucet-Personeni, C.; Bentley, P. D.; Fletcher, R. J.; Kinkaid, A.; Kryger, G.; Pirard, B.; Taylor, A.; Taylor, R.; Taylor, J.; Viner, R.; Silman, I.; Sussman, J. L.; Greenblatt, H. M.; Lewis, T. A Structure-Based Design Approach to the Development of Novel, Reversible AChE Inhibitors. *J. Med. Chem.* **2001,** 44, 3203-3215.

6. Desai, M. C. Tricyclic 4-aminopyridine derivatives for treatment of Alzheimer's disease, and their pharmaceutical compositions, preparation, and intermediates. 88-309040 311303, September 29, 1989.

7. Sigal, M. V., Jr.; Brent, B. J.; Marchini, P. 7,8,9,10-Tetrahydro-6H-cyclohepta[b]quinolines and 1,2,3,4-tetrahydroacridines. US 3232945, February 1, 1966.

8. Li, J.-R.; Ma, S.-L.; Sun, Y.-J.; Wei, X.-J.; Zhou, Z.-M. Novel synthesis of 2H-3,1-benzoxazine derivatives. *J. Heterocycl. Chem.* **2006,** 43, 745-748.

9. Proctor, G. R.; Harvey, A. L.; McKenna, M. T.; Mullins, S. J. Polycyclic Compounds. US6130228, October 10, 2000.

10. Bielavsky, J. Analogs of 9-amino-1,2,3,4-tetrahydroacridine. *Collect. Czech. Chem. Commun.* **1977,** 42, 2802-8.

11. Carlier, P. R.; Han, Y. F.; Chow, E. S.-H.; Li, C. P.-L.; Wang, H.; Lieu, T. X.; Wong, H. S.; Pang, Y.-P. Evaluation of Short-tether Bis-THA AChE Inhibitors. A Further Test of the Dual Binding Site Hypothesis. *Bioorg. Med. Chem.* **1999,** 7, 351-357.

12. Frisch, M. J.; Trucks, G. W.; Schlegel, H. B.; Scuseria, G. E.; Robb, M. A.; Cheeseman, J. R.; J. A. Montgomery, J.; Vreven, T.; Kudin, K. N.; Burant, J. C.; Millam, J. M.; Iyengar, S. S.; Tomasi, J.; Barone, V.; Mennucci, B.; Cossi, M.; Scalmani, G.; Rega, N.; Petersson, G. A.; Nakatsuji, H.; Hada, M.; Ehara, M.; Toyota, K.; Fukuda, R.; Hasegawa, J.; Ishida, M.; Nakajima, T.; Honda, Y.; Kitao, O.; Nakai, H.; Klene, M.; Li, X.; Knox, J. E.; Hratchian, H. P.; Cross, J. B.; Adamo, C.; Jaramillo, J.; Gomperts, R.; Stratmann, R. E.; Yazyev, O.; Austin, A. J.; Cammi, R.; Pomelli, C.; Ochterski, J. W.; Ayala, P. Y.; Morokuma, K.; Voth, G. A.; Salvador, P.; Dannenberg, J. J.; Zakrzewski, V. G.; Dapprich, S.; Daniels, A. D.; Strain, M. C.; Farkas, O.;

Malick, D. K.; Rabuck, A. D.; Raghavachari, K.; Foresman, J. B.; Ortiz, J. V.; Cui, Q.; Baboul, A. G.; Clifford, S.; Cioslowski, J.; Stefanov, B. B.; Liu, G.; Liashenko, A.; Piskorz, P.; Komaromi, I.; Martin, R. L.; Fox, D. J.; Keith, T.; Al-Laham, M. A.; Peng, C. Y.; Nanayakkara, A.; Challacombe, M.; Gill, P. M. W.; Johnson, B.; Chen, W.; Wong, M. W.; Gonzalez, C.; Pople, J. A. *Gaussian 03*, Gaussian, Inc.: Pittsburgh, PA, 2003.

Chapter 4. Computational and Experimental Studies of Conformational Energies of Tacrine Analogs

4.1 Introduction and motivation

Tacrine (**1**, Figure 4.1) is well known as an inhibitor of acetylcholinesterase (AChE).[1,2] As discussed in Chapter 1, inhibition of human AChE is an effective means for treating memory loss in early stage Alzheimer's disease. Hetero- and homodimers containing the tacrine pharmacophore (Figure 4.2) have been described extensively in the literature and can be significantly more potent than the tacrine monomer for AChE inhibition.[3-13] Chapter 2 describes the synthesis and characterization of optimized tacrine-based homodimers which were found to be quite potent and selective for *Anopheles gambiae* AChE.

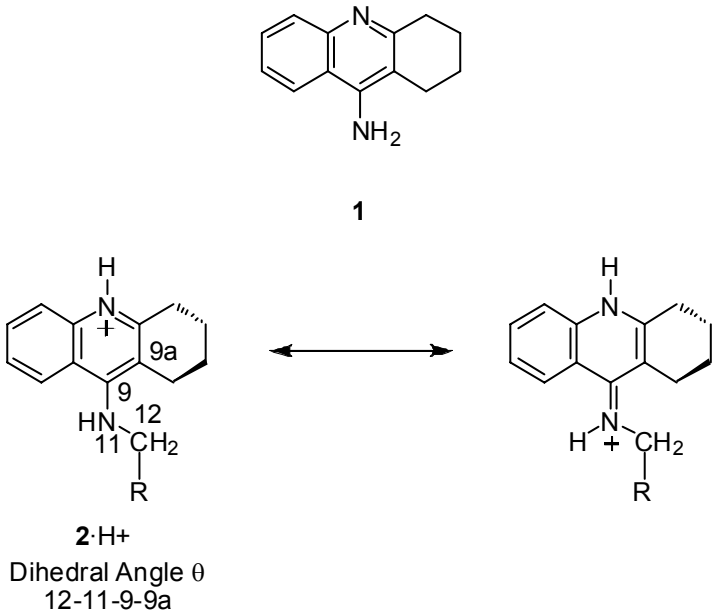

Figure 4.1. Structure of tacrine (**1**) and resonance in protonated *N*-alkyltacrines (**2**·H^+)

X-ray crystallography of the tacrine/*Torpedo californica* acetylcholinesterase (*Tc*AChE) complex (PDB ID 1ACJ) demonstrated that tacrine binds at the bottom of the active site gorge,[14] and this arrangement has been maintained in all of the structures of AChE-bound tacrine homo- and heterodimers.[15-18] Tacrine's mimicry of acetylcholine is due to its high basicity (pK_a of conjugate acid is 9.8[19]); thus tacrine and its derivatives likely bind in their protonated forms, both at physiological pH and in the acidic crystallization media. Furthermore, the approximately 3.0 Å distance between the endocyclic nitrogen of the *N*-alkyltacrine moiety and the carbonyl

oxygen of His440 (*Torpedo* numbering) seen in nearly all the structures is consistent with a hydrogen bond, further suggesting that the *N*-alkyltacrine units are protonated in the crystal structures (see Table 4.2). In order to achieve maximal resonance stabilization, a protonated *N*-alkyltacrine (**2**) is expected to adopt a conformation in which the dihedral angle θ formed by the *N*-alkyl substituent and the ring system is roughly coplanar (θ = 0° or 180°, Figure 4.1). This resonance stabilization is analogous to that found in amides. As such, one could reasonably conclude that the C-N bond of the *N*-alkyltacrines should possess a similar rotational potential surface to that of amide bond rotation, for which it is known that rotation involves two transition states (**B** – **C**, Figure 4.3) and 1 ground state (**A**).[20,21] Because of our interest and experience in bivalent tacrine-based AChE inhibitors (AChEI),[4-6,8,10,16,18,22,23] we were interested in fully characterizing the barriers of rotation in *N*-alkyltacrines.

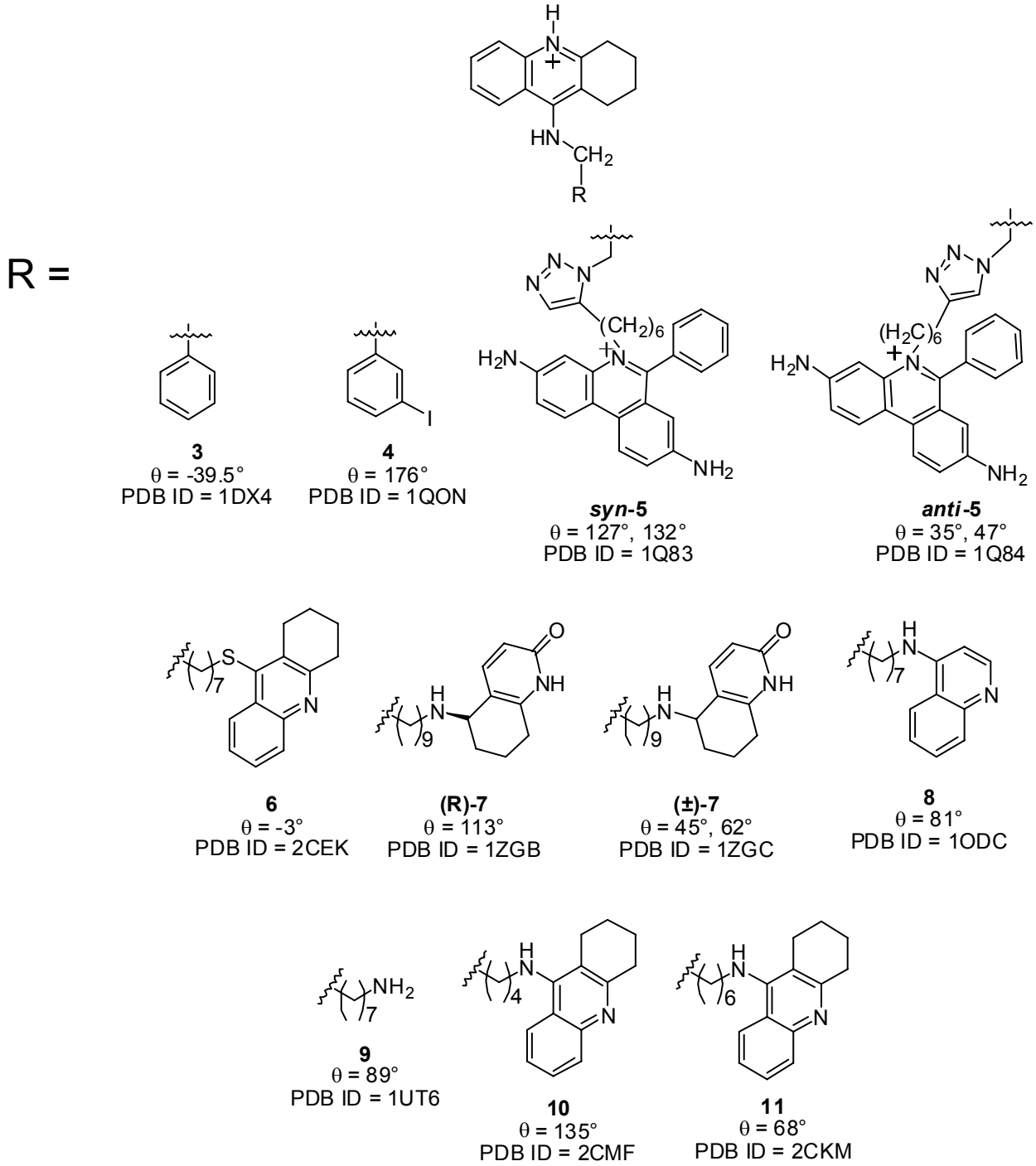

Figure 4.2. Substituents (R) of *N*-alkyltacrine based ligands **3** – **11** complexed to AChE found in the PDB (PDB ID given below each structure). Values for θ are defined as in Figure 4.1; where two θ values are given, two molecules are present in the asymmetric unit. In the case of **10** and **11**, only values for the catalytic site tacrine moieties are given.

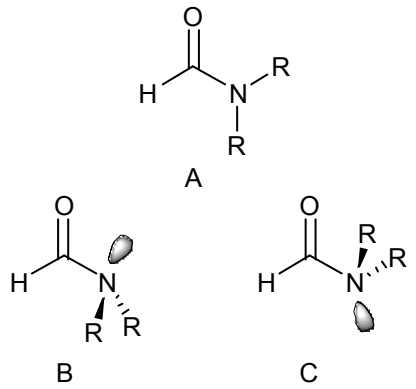

Figure 4.3. Ground state (**A**) and two pyramidalized C-N bond rotation transition structures (**B** – **C**) of a simple amide.[20,21]

4.2 Determination of Rotational Barriers

4.2.1 Experimentally determined rotational barriers

To begin, we sought to use ^{1}H NMR spectroscopy to determine the barrier to rotation of the exocyclic amino group in tacrines and related compounds. This approach was based on an observation of Ella Chow Clement, in our group, that **1**·HCl exhibited two distinguishable NH_2 proton signals in d_6-DMSO.[24] My efforts were successful for two tacrine derivatives (**1**·HCl and **13**·TFA, Figure 4.1, Figure 4.4) and two 4-aminoquinoline derivatives (**12**·HCl and **14**·HCl, Figure 4.4). In all cases except **13**, the HCl salt was used in the dynamic ^{1}H NMR experiments; the TFA salt was used for **13** because HCl caused opening of the azetidinyl ring. For reasons discussed below, our efforts were ultimately unsuccessful for salts of *N*,*N*-dimethyltacrine **15** and *N*-methyltacrine **16**.

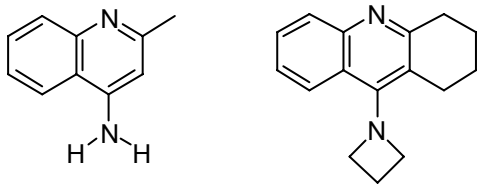

12

13

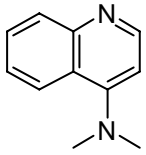

14

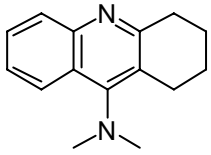

15

Figure 4.4. Free base structures of compounds studied by variable temperature ^{1}H NMR. Tacrine **1** is depicted in Figure 4.1.

Table 4.1. Experimental and computed C-N rotation barriers for salts of **1** and **12-15**

Tacrine derivative	Solvent	Estimated T_c (K)	Experimental $\Delta G^{\ddagger}$ (kcal/mol)[a]	Calculated $\Delta G^{\ddagger}$ (kcal/mol) at T_c (dihedral angle)[b]
12·HCl	d_6-DMSO	313 ± 2	15.6 ± 0.1	15.4 (57°) 15.7 (122°)
1·HCl	d_6-DMSO	311 ± 2	14.1 ± 0.1	14.1 (57°) 14.4 (121°)
13·TFA	CD_3OD	225 ± 1	11.3 ± 0.1	11.3 (120°) 11.6 (75°)
14·HCl	CD_3OD	205 ± 1	9.6 ± 0.1	8.4 (64°) 11.3 (110°)
15•HCl	CD_3OD	< 171[c]	< 7.9	nd

[a] The stated errors in $\Delta G^{\ddagger}$ are based on the indicated uncertainty in T_c. [b] Equilibrium geometries and rotation-inversion transition structures of the cationic fragments (anion not included) were determined using B3LYP/6-31G* with a PCM correction using the NMR solvent. Calculated free energy corrections to the electronic energies were based on B3LYP/6-31G* frequencies and the experimentally estimated coalescence temperature. See section 4.2.2 for details. Free energies of activation for C-N bond rotation calculated based on the given transition structure (corresponding dihedral angle given in parenthesis). [c] Coalescence was not observed down to the low temperature limit (171K).

For compounds **12**·HCl and **1**·HCl that bear an amino group, coalescence of the diastereotopic amino protons could be achieved at 313 K (Figure 4.5) and 311 K (Figure 4.6), respectively, in d_6-DMSO (Table 4.1). Compounds **13**·TFA and **14**·HCl feature dialkyl substitution of the exocyclic nitrogen, but the potentially diastereotopic alkyl protons are in fast exchange at room temperature in CD_3OD and d_6-DMSO; cooling in CD_3OD effected decoalescence at 225 K (Figure 4.7) and 205 K (Figure 4.8), respectively. The respective

barriers to rotation of the C-N bond ($\Delta G^{\ddagger}$) at the coalescence temperature (T_c) were calculated from the Eyring equation.[25] The range of values observed (9.6 – 15.6 kcal/mol) indicates significant penalties for the loss of resonance at the C-N bond rotation transition structures. Primary amine-bearing compounds **12**·HCl and **1**·HCl have the highest barriers to rotation (15.6 and 14.1 kcal/mol, respectively). Dialkylation of the exocyclic nitrogen reduces the barrier to C-N bond rotation (cf. **13**·TFA: 11.3 kcal/mol; **14**·HCl: 9.6 kcal/mol). This 2 – 6 kcal/mol reduction in the C-N bond rotation barrier is most likely due to destabilization of the ground state, which results from steric repulsion of the *N*-alkyl substituents with the ring system at near co-planarity (Figure 4.9). Further evidence for the destabilizing influence of this steric effect can be seen by comparing **13**·TFA and *N*,*N*-dimethyltacrine **15**·HCl. Whereas **13**·TFA can be decoalesced at 225 K, the methyl groups of **15**·HCl cannot be decoalesced down to 171 K, giving an estimated C-N barrier of less than 7.9 kcal/mol (assuming equivalent $\Delta\nu$ of the diastereotopic signals in **14**·HCl and **15**·HCl**)**. We propose that this > 3.4 kcal/mol lower rotational barrier in **15**•HCl relative to **13**•TFA results from the greater steric destabilization of the nearly planar ground state in **15**·HCl relative to that of **13**·TFA. Finally, all attempts to determine the rotation barrier in salts of *N*-methyltacrine **16** (Figure 4.10) were unsuccessful, presumably due to a significant preference for a single conformation about the C9-N11 bond, thus resulting in only one population of N-CH_3 protons. Computational studies (described below) support this hypothesis.

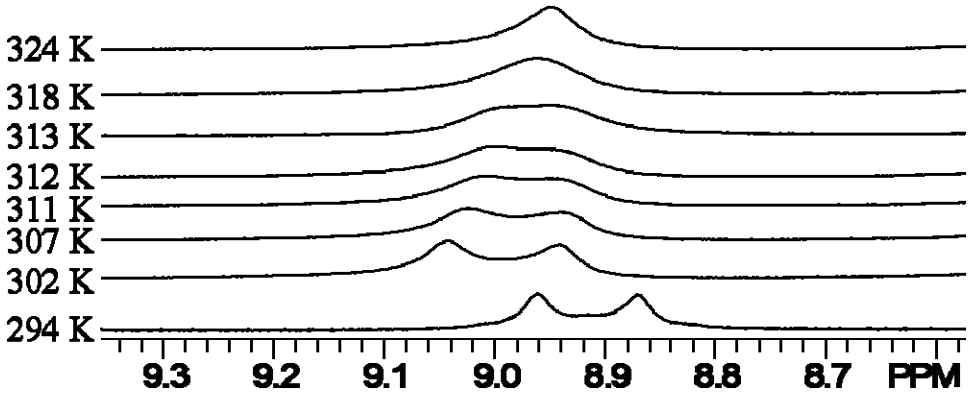

Figure 4.5. Variable temperature ^{1}H NMR of 4-aminoquinaldine HCl (**12**·HCl). Estimated T_c = 313 ± 2 K. Solvent = d_6-DMSO, spectra recorded at 400 MHz.

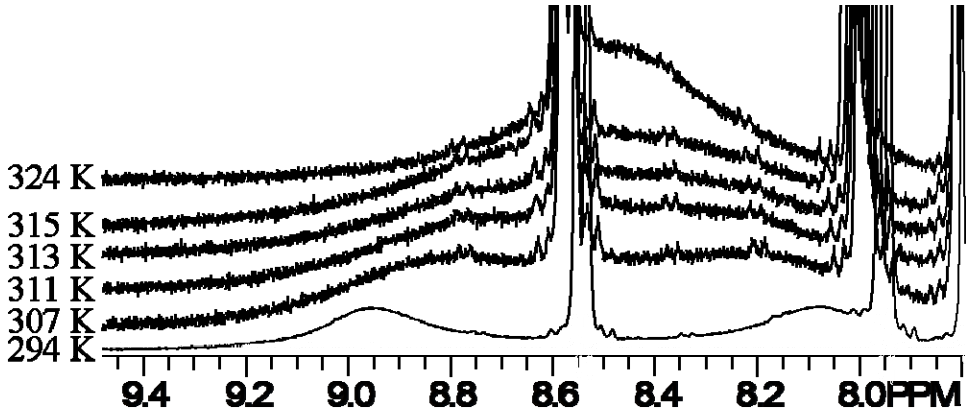

Figure 4.6. Variable temperature ^{1}H NMR of tacrine HCl (**1**·HCl). Estimated T_c = 311 ± 2 K. Solvent = d_6-DMSO, spectra recorded at 400 MHz.

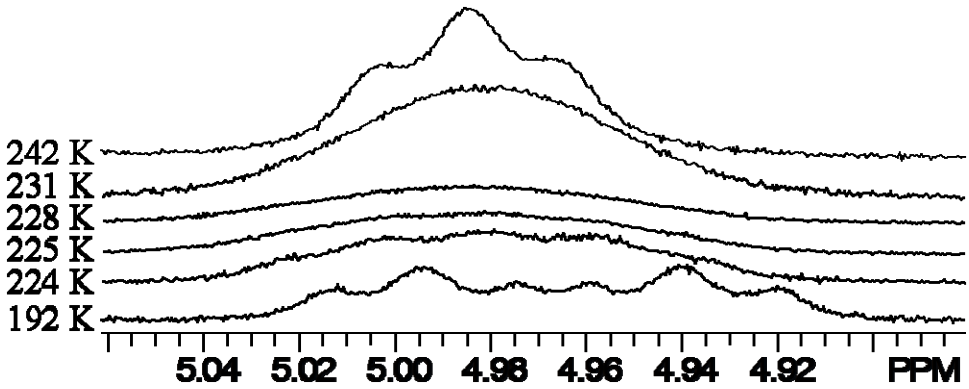

Figure 4.7. Variable temperature ^{1}H NMR of 9-azetidinyl-1,2,3,4-tetrahydroacridine TFA (**13**·TFA). Estimated T_c = 225 ± 1 K. Solvent = CD_3OD, spectra recorded at 400 MHz.

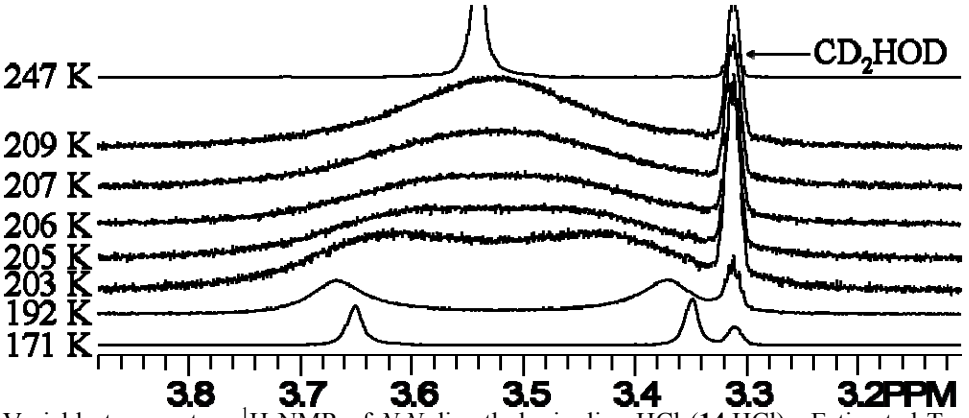

Figure 4.8. Variable temperature ^{1}H NMR of *N*,*N*-dimethylquinoline HCl (**14**·HCl). Estimated T_c = 205 ± 1 K. Solvent = CD_3OD, spectra recorded at 400 MHz.

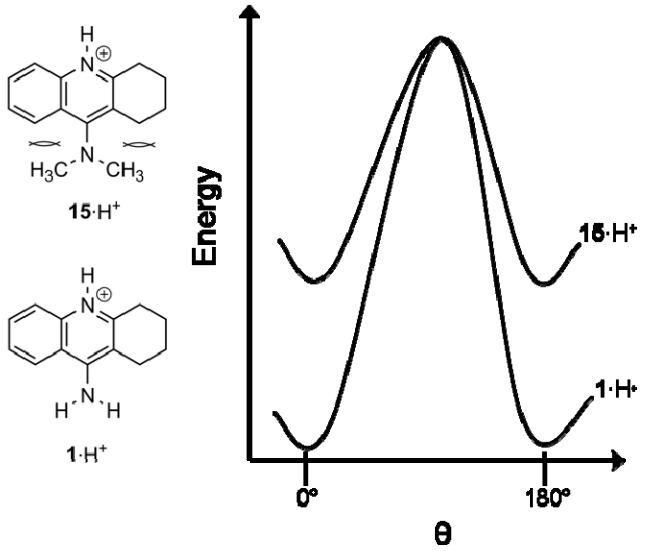

Figure 4.9. Highly simplified schematic of ground state destabilization of **15**·H^+ relative to **1**·H^+. Calculated (B3LYP/6-31G*) potential energy plots are displayed in Figure 4.22 and Figure 4.19

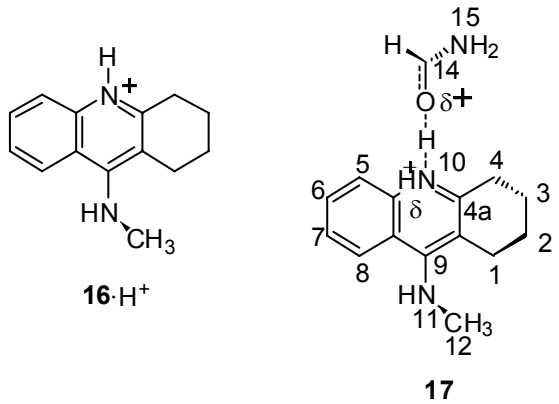

Figure 4.10. Protonated *N*-methyltacrine (**16**·H^+) and protonated *N*-methyltacrine/formamide complex (**17**), Φ (15-14-10-4a) = 90°.

4.2.2 Calculated rotational barriers

While Wiberg's[20,21] treatment of amide bond rotation used the *ab initio* MP2 method, Lopez and coworkers[26] used density functional theory (DFT) to model the amide bond rotation ground state and transition state structures. Furthermore, independent work at DuPont[27] and in the Karplus[28] lab have shown that DFT is adequate to model amide bond hydrolysis reaction enthalpies. Also, our group has demonstrated that calculations at the B3LYP/6-31G* level can reproduce dynamic ^{1}H NMR-derived, experimental conformational inversion barriers of benzodiazepines to within 2 kcal/mol (Scheme 4.1 and Table 4.2),[29] and we used this method to estimate conformational energies of protonated *N*-methyltacrine **16**·H^+ and its formamide complex **17** (Figure 4.10).[18]

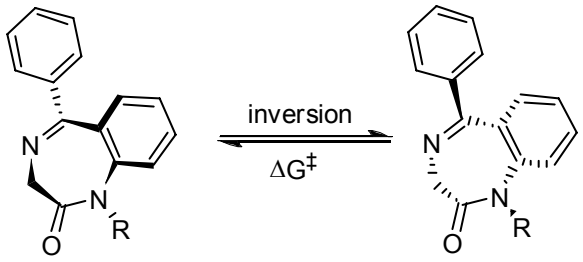

18-21

Scheme 4.1. Inversion of benzodiazepines as investigated by Lam and Carlier.[29]

Table 4.2. Substituents, coalescence temperatures (T_c), and inversion barriers of benzodiazepines as reported by Lam and Carlier.[29]

Compound	R	T_c (K)	Calculated $\Delta G^{\ddagger}$ (kcal/mol)[a]	Experimental $\Delta G^{\ddagger}$ (kcal/mol)[b]
18	Me	391	16.9	18.0 ± 0.2
19	Bn	422	17.8	19.5 ± 0.2
20	*i*-Pr	>458	21.6	21.3 – 21.7[c]
21	$CHPh_2$	458	20.8	21.5 ± 0.2

[a] Calculated from B3LYP/6-31+G(d)//B3LYP/6-31G(d) in DMSO using Tomasi's polarized continuum model (PCM), including the Gibbs free energy correction at *T*c. [b] The stated errors in the inversion barrier are based on an estimated error in T_c of 3 K. [c] The coalescence temperature is above 458 K which gives a lower bound value for the inversion barrier of 21.3 kcal/mol, and an upper bound value of 21.7 kcal/mol is estimated by comparing the dynamic ^{1}H NMR spectra of **14** with similar compounds; the corresponding T_c is estimated to be 463 – 468 K.

To determine whether the experimental barriers to C-N rotation in protonated species **1**·HCl, **12**·HCl, **13**•TFA, and **14**·HCl could be matched by computation, the equilibrium geometries and C-N bond rotation transition structures for the corresponding cationic fragments were located using B3LYP/6-31G*. PCM implicit solvation (with the relevant dielectric constant for the deuterated solvent employed in the dynamic NMR experiments) was applied during the equilibrium and transition state geometry optimizations and frequency calculations. Equilibrium geometries of **1**·H^+ and **12**·H^+ – **14**·H^+ featured near zero dihedral angles (θ = -14.6° – 22.7°), as expected (i.e. **D**, **G**, **J**, and **M** in Figure 4.11, Figure 4.12, Figure 4.13, and Figure 4.14, respectively). Interestingly, in the rotation transition structures, the exocyclic nitrogen is pyramidalized; inspection of the atomic displacements associated with the sole imaginary frequency revealed that pyramidal inversion accompanies rotation of the C-N axis. Thus we termed these saddle points "rotation-inversion" transition structures. This general feature is discernable in previous calculation of amide bond rotation[20,21,28] but did not elicit commentary. Two different C-N bond rotation-inversion transition structures were located for each of **1**·H^+ and **12**·H^+ – **14**·H^+, in which the lone pair of the pyramidalized exocyclic amine is aligned roughly parallel (**E**, **H**, **K**, and **N**) or antiparallel (**F**, **I**, **L**, and **O**) to the aryl ring system. Free

energy corrections at the observed coalescence temperatures were then applied to each structure, using scaled frequencies. Barriers to C-N bond rotation were calculated as the free energy difference between each transition structure and the equilibrium geometry, as shown in Table 4.1. As can be seen, the lowest calculated barrier for **14**·H^+ matches the experimental C-N bond rotation barrier to within 1.2 kcal/mol; the match for **1**·H^+, **12**·H^+, and **13**·H^+ (< 0.2 kcal/mol) is even closer. Thus calculations at the B3LYP/6-31G* level provide acceptable accuracy for determining potential barrier heights for rotation of the exocyclic amine in tacrine and its derivatives.

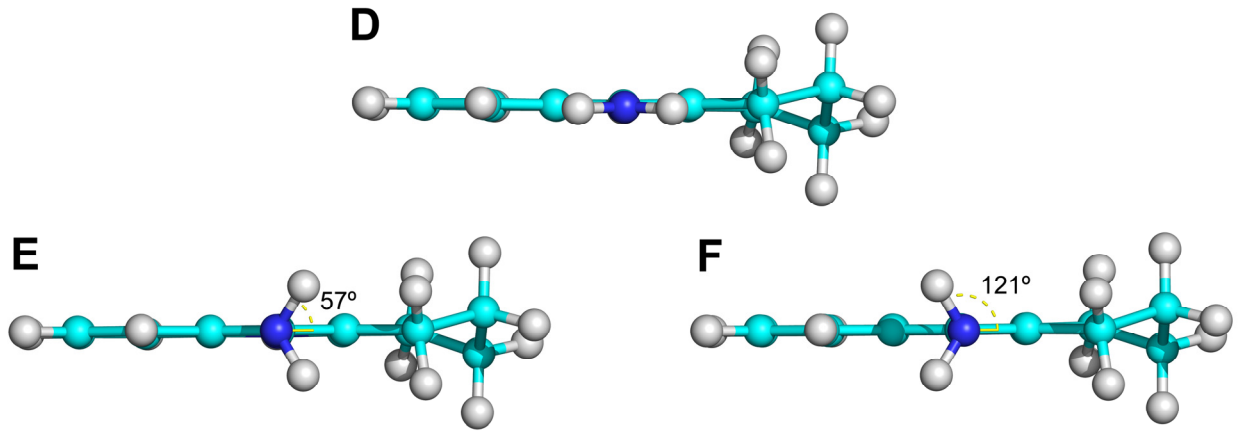

Figure 4.11. Calculated (B3LYP/6-31G*) structures for protonated tacrine **1**·H^+, viewed along the N11-C9 axis: **D** (θ = 358.2°) is the equilibrium geometry, and **E** and **F** are rotation-inversion transition structures (dihedral angles θ are noted).

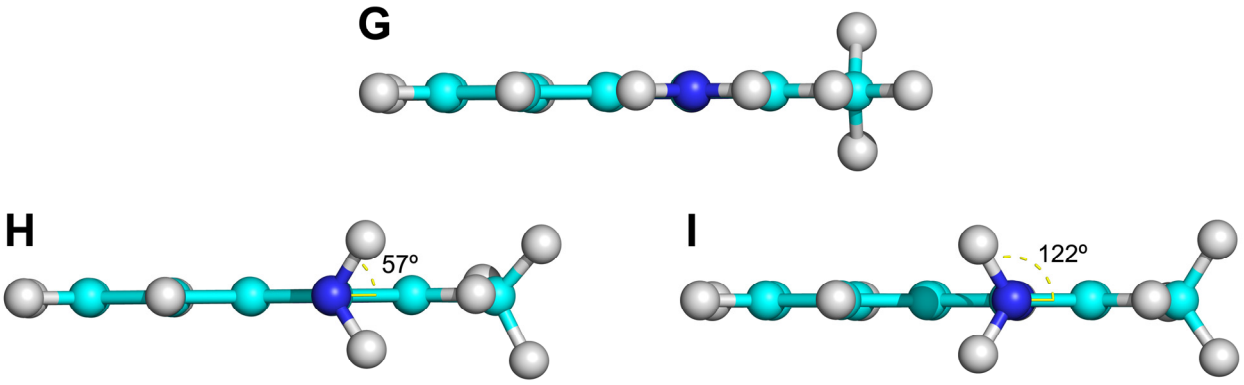

Figure 4.12. Calculated (B3LYP/6-31G*) structures for protonated 4-aminoquinaldine **12**·H^+, viewed along the N9-C4 axis: **G** (θ = 359.8°) is the equilibrium geometry, and **H** and **I** are rotation-inversion transition structures (dihedral angles θ are noted).

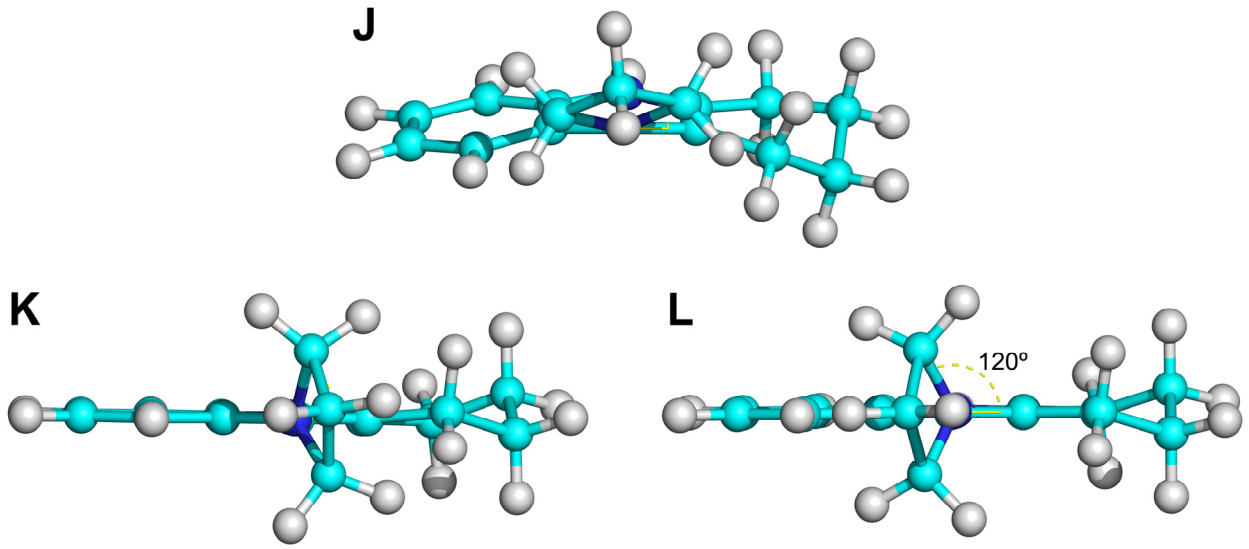

Figure 4.13. Calculated (B3LYP/6-31G*) structures for protonated 9-azetidinyl-1,2,3,4-tetrahydroacridine **13**·H^+, viewed along the N11-C9 axis: **J** (θ = 22.7°) is the equilibrium geometry, and **K** (θ = 74.5°) and **L** (dihedral angle θ noted) are rotation-inversion transition structures.

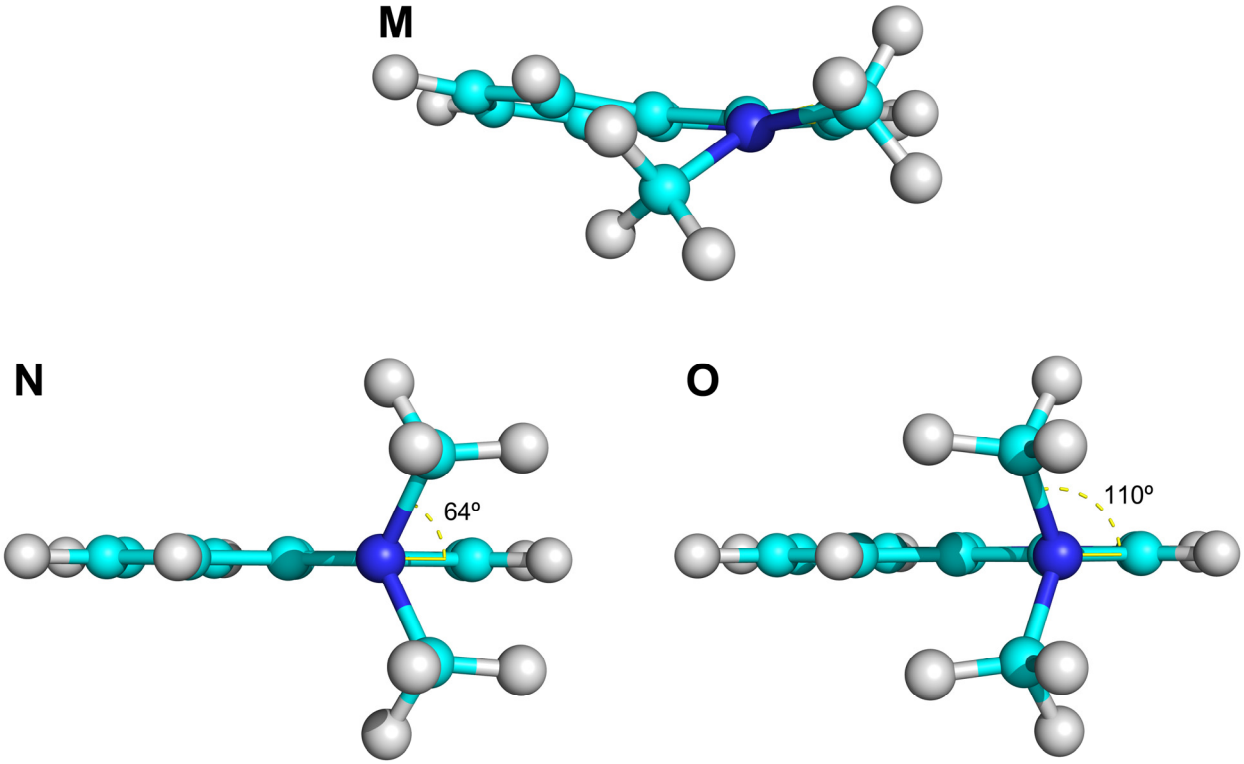

Figure 4.14. Calculated (B3LYP/6-31G*) structures for protonated *N*,*N*-dimethylquinoline **14**·H^+, viewed along the N9-C4 axis: **M** (θ = 14.6°) is the equilibrium geometry, and **N** and **O** are rotation-inversion transition structures (dihedral angles θ are noted).

Because the B3LYP/6-31G* computational method employed reproduced the experimental rotational barriers of **1**·H^+ and **12**·H^+ – **14**·H^+ to within 1.2 kcal/mol, we turned our attention to protonated *N*-methyltacrine **16**·H^+. This molecule was selected as a model

compound capable of exhibiting both the amide bond mimicking effects of protonated *N*-alkyltacrines and the steric effects of the *N*-alkyl moiety interacting with the ring system. Two equilibrium geometries were found; **P** features a nearly coplanar orientation of the methyl group with the saturated ring, and **Q** features a nearly coplanar orientation of the methyl group with the aromatic ring (Figure 4.15). Structure **Q** is the global minimum, presumably due to reduced steric hindrance relative to **P**. Due to the significant energetic preference for the 194° conformation **Q**, at equilibrium there would be only one detectable population of *N*-methyl protons. Thus ^{1}H NMR spectroscopy in the slow exchange domain would reveal only one *N*-methyl signal. Experimentally, that is exactly what we observed: down to -98 °C (the freezing point of CD_3OD), only one *N*-methyl signal was observed in the ^{1}H NMR spectrum of *N*-methyltacrine HCl (**16**·HCl).

Whereas protonated tacrine **1**·H^+ possesses two rotation-inversion transition structures (Figure 4.11), four transition structures, **R** – **U**, were located for protonated *N*-methyltacrine **16**·H^+ (Figure 4.15). These transition structures differ in the orientation of the exocyclic amine lone pair to the fused saturated ring (parallel or antiparallel) and the position of the methyl group (above or below the plane of the ring). The dihedral angles observed (63.8°, 117.9°, 241.0°, 298.2°) reflect the roughly 60° out of plane dihedral angles seen in the rotation-inversion transition structures of related molecules **1**·H^+ and **12**·H^+ – **14**·H^+. With this in mind, it should also be noted that many of the crystallographic dihedral angles reported in Figure 4.2 resemble those of the calculated transition structures in Figure 4.15.

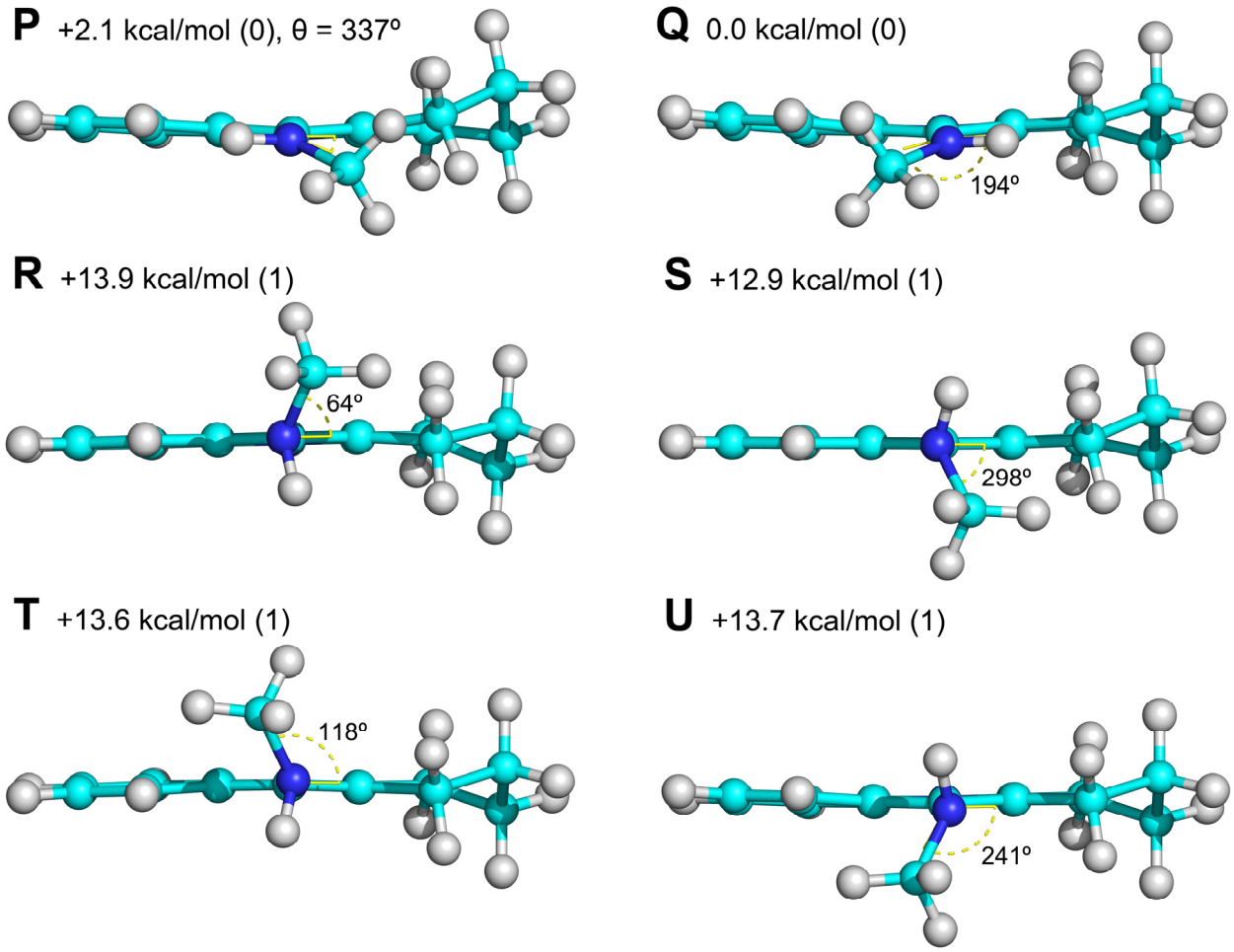

Figure 4.15. Calculated (B3LYP/6-31G*) structures for protonated *N*-methyltacrine **16**·H$^+$, viewed along the N11-C9 axis. Structures **P** and **Q** are equilibrium geometries; structures **R** – **U** are rotation-inversion transition structures. Structure **Q** is the global minimum; indicated energies are relative to it and are ZPVE-corrected. The ZPVE values were scaled by an empirical value of 0.9804. Values in parentheses represent the number of imaginary frequencies.

4.3 Calculation of the rotational potential energy surface of *N*-methyltacrine

As stated previously, the X-ray crystal structures of many tacrine-containing hetero- and homodimers complexed to AChE have been described in the literature. Silman, Sussman, and co-workers[30] published the first X-ray crystal structures of *N*-alkyltacrine ligands complexed to AChE (**3** and **4**, Figure 4.2); the species of enzyme in this case was from *Drosophila melanogaster* (fruit fly). The first crystal structures of bivalent tacrine heterodimers were those of *syn*-**5** and *anti*-**5** complexed to mouse AChE;[15] the syn-ligand was first identified by *Electrophorus electricus* AChE-mediated assembly of azide- and acetylene-bearing building blocks ("in situ click chemistry").[8] Structures of AChE-complexed **6**,[17] **7**,[16] and **8** – **11**[18] were reported shortly thereafter (Figure 4.2). Interestingly, among these structures the dihedral angles θ range from nearly coplanar (357°, **6**) to completely orthogonal (89°, **9**).

To better assess the conformational energies of protonated *N*-alkyltacrines **3** – **11** bound to the catalytic site of AChE, we mapped the entire rotational potential energy surface of protonated *N*-methyltacrine (**16**·H^+) in a clockwise fashion by constraining the dihedral angle θ in 10° increments from 360° to 0° while allowing the remainder of the molecule to optimize. This constrained optimization approach was first presented in our publication of the X-ray crystal structure of **10** and **11** bound to *Tc*AChE;[18] however, we now will discuss our findings in greater detail. Figure 4.16 shows the potential energy curve generated by plotting the relative energy obtained at each step of the calculation versus θ. On the clockwise curve, we found two maxima (θ = 240° and 70°) corresponding to two of the C-N bond rotation transition states (**U** and **R**, Figure 4.15). As expected, we found minima at θ = 190° and 340°. The lack of symmetry in the curve around 180° is notable; we attribute this behavior to the non-planar half-chair conformation of the saturated moiety of the fused ring system. A similar lack of symmetry can also be seen around θ = 0° (e.g. 320° – 40°).

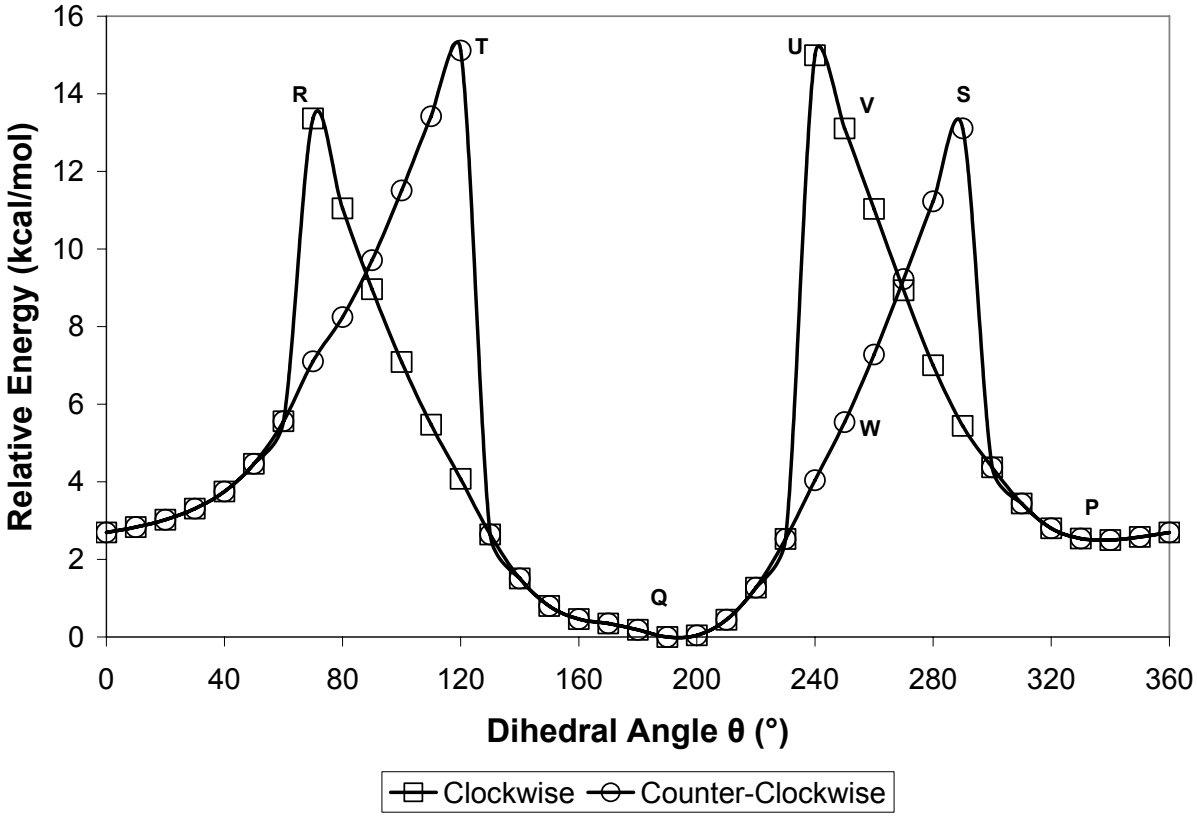

Figure 4.16. Results of the dynamically constrained optimization of protonated *N*-methyltacrine **16**·H^+ (Cl^- anion not included). Counterclockwise rotation generates data from 0° to 360°; clockwise rotation generates data from 360° to 0° (or 0° to -360°). Labels **P** – **W** correspond to labels from Figure 4.15 and Figure 4.17.

To locate the remaining two transition structures **S** and **T** on the potential surface, we performed the constrained optimization in the counterclockwise direction. In this way, two new energetic maxima (θ = 120° and 290°) were found, corresponding to C-N bond rotation-inversion transition states **S** and **T** (Figure 4.15). The potential energy curves generated by clockwise and counterclockwise rotation were identical except in two regions (θ = 70° – 120° and 240° – 290°). These regions feature pyramidalized exocyclic nitrogen, and careful inspection reveals that the two curves represent two different pyramidalizations at the same θ. As shown in Figure 4.17 for θ = 250°, the only difference between the "clockwise" and "counterclockwise" structures (**V** and **W**, respectively) is the placement of the proton of the *N*-methylamino group. Improved resonance interaction in structure **W** relative to that in structure **V** is thus responsible for the difference in energy between these structures. Scheme 4.2 illustrates how the different pyramidalizations at the exocyclic N are generated, and how clockwise rotation from **P** leads to rotation transition structures **U** and **R**. Rotation transition structures **S** and **T** then result only from counterclockwise rotation. Interestingly, when a similar analysis was applied to **1**·H^+ and **12**·H^+ – **14**·H^+, the same effect due to clockwise and counterclockwise rotation was observed (Figure 4.18 – Figure 4.22).

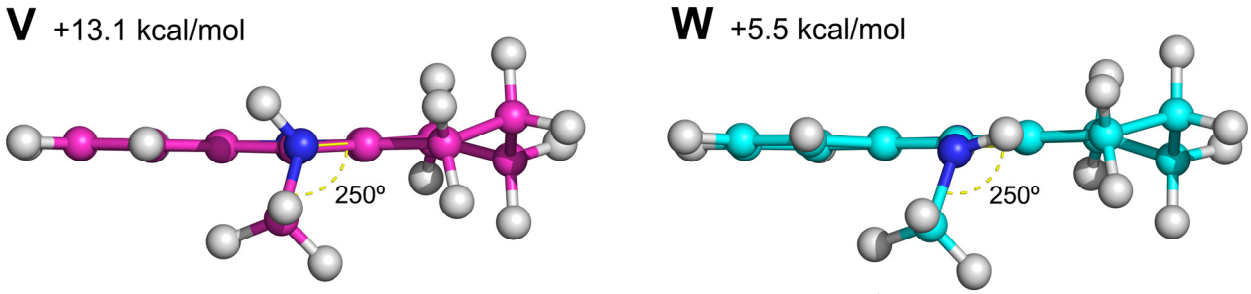

Figure 4.17. Calculated (B3LYP/6-31G*) structures of *N*-methyltacrine **16**·H^+, viewed along the N11-C9 axis. Clockwise (**V**) and counterclockwise (**W**) structures at θ = 250° are depicted; energies given are relative to the global minimum E (Figure 4.16).

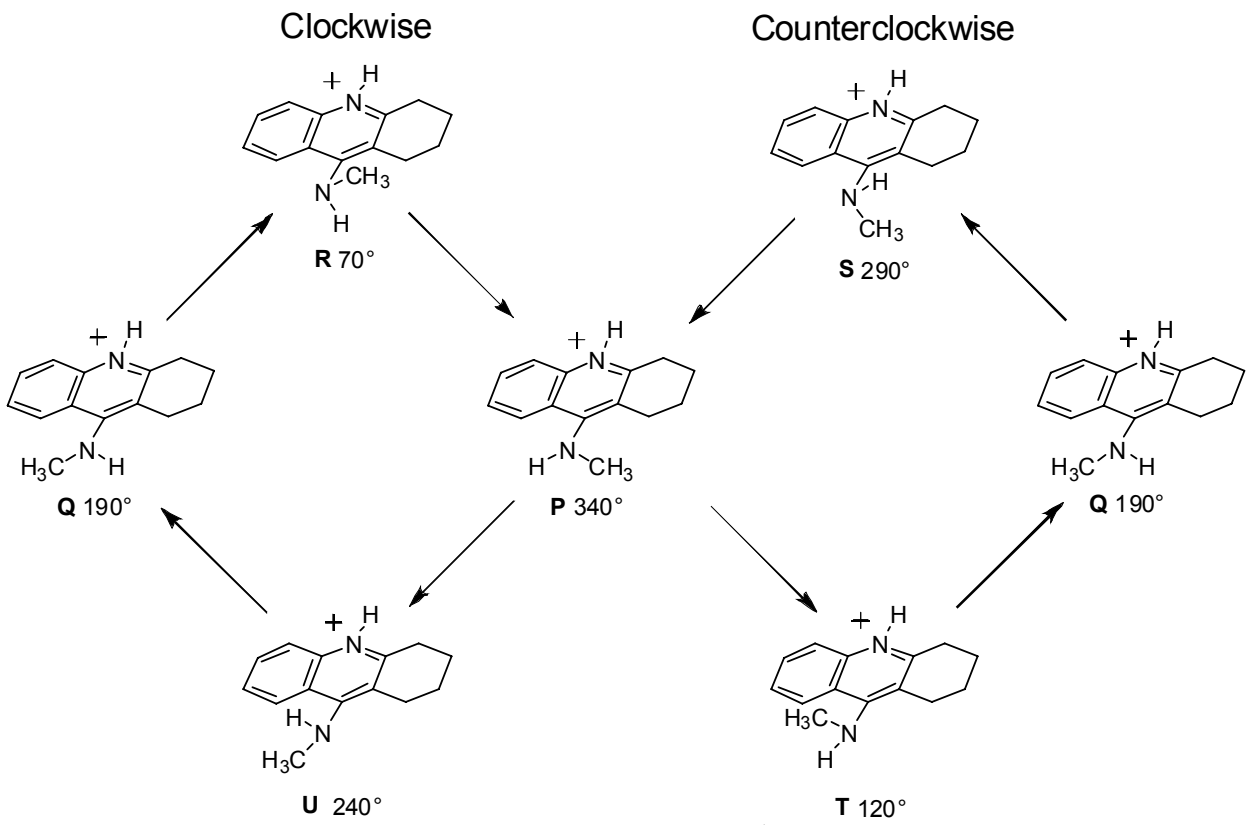

Scheme 4.2. Schematic of constrained optimization results for **16**·H^+. Corresponding θ values from Figure 4.16 given below each structure.

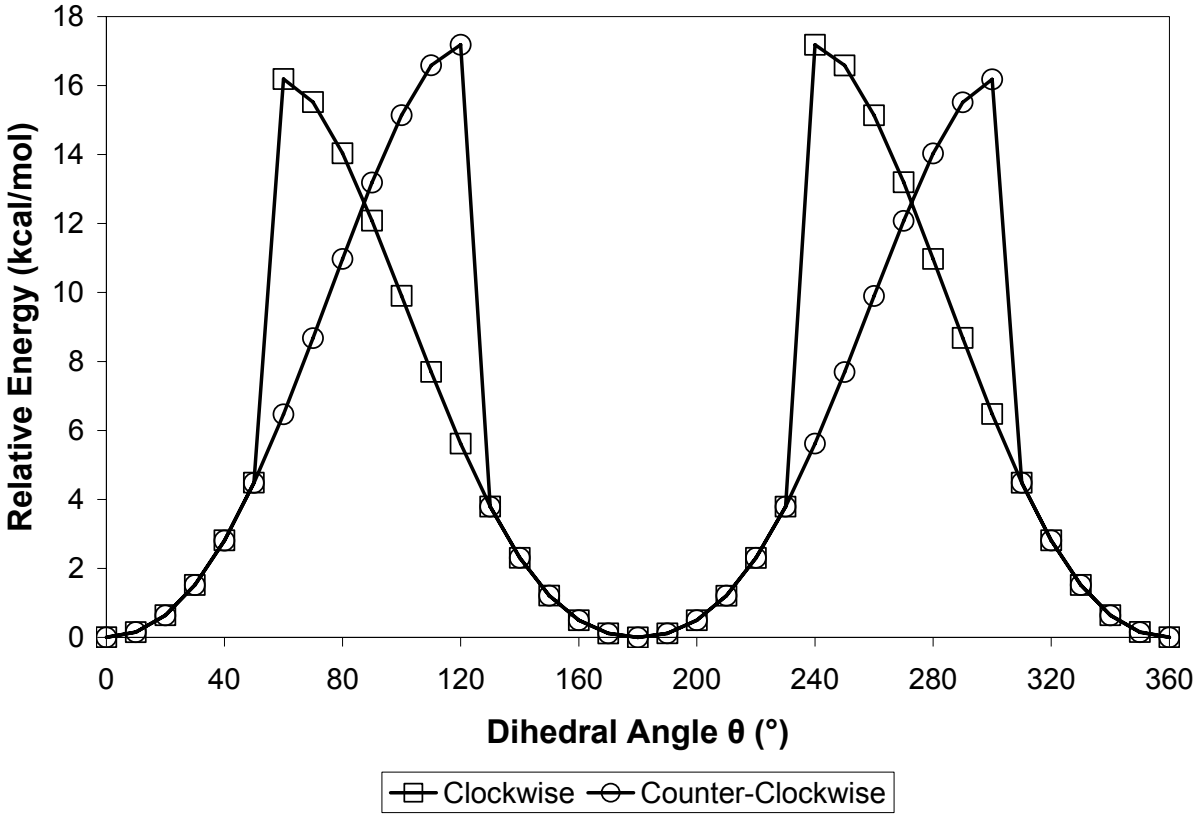

Figure 4.18. Results of the dynamically constrained optimization of protonated 4-aminoquinaldine **12**·H^+ (Cl^- anion not included). Counterclockwise rotation generates data from 0° to 360°; clockwise rotation generates data from 360° to 0° (or 0° to -360°).

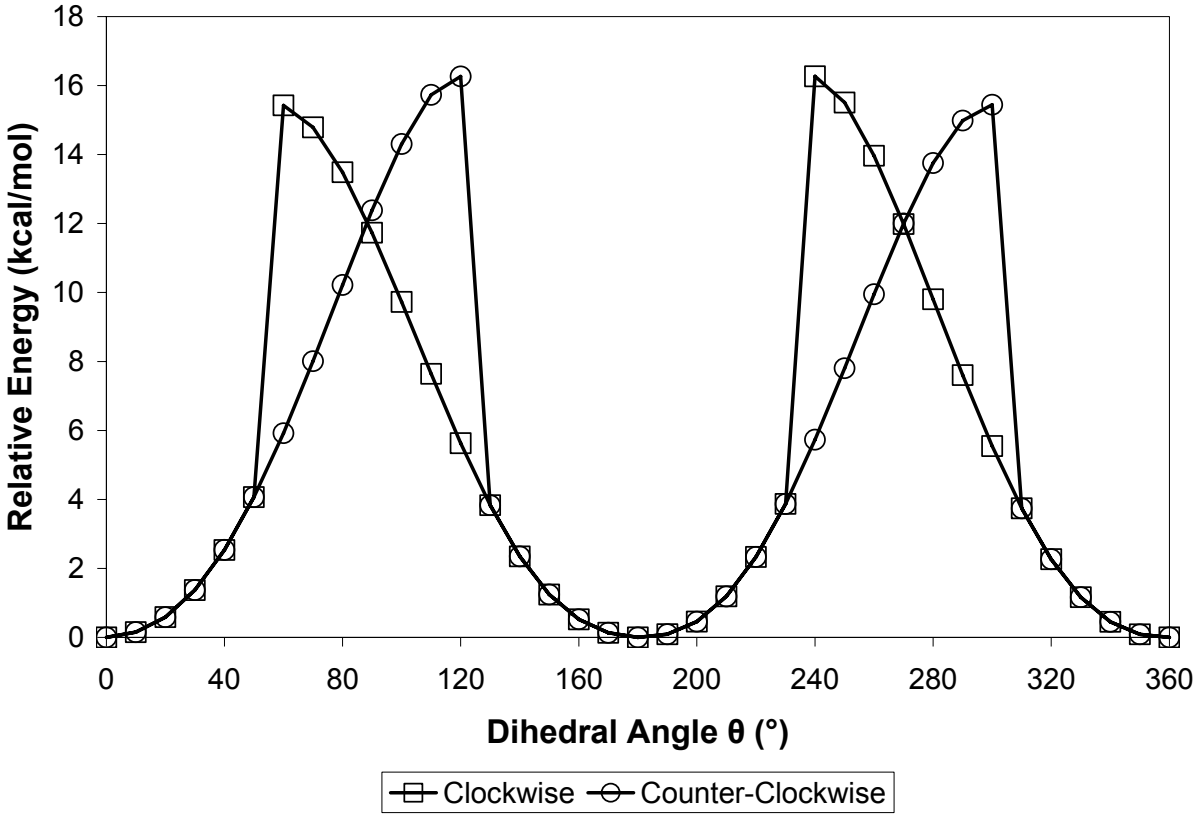

Figure 4.19. Results of the dynamically constrained optimization of protonated tacrine **1**·H^+ (Cl^- anion not included). Counterclockwise rotation generates data from 0° to 360°; clockwise rotation generates data from 360° to 0° (or 0° to -360°).

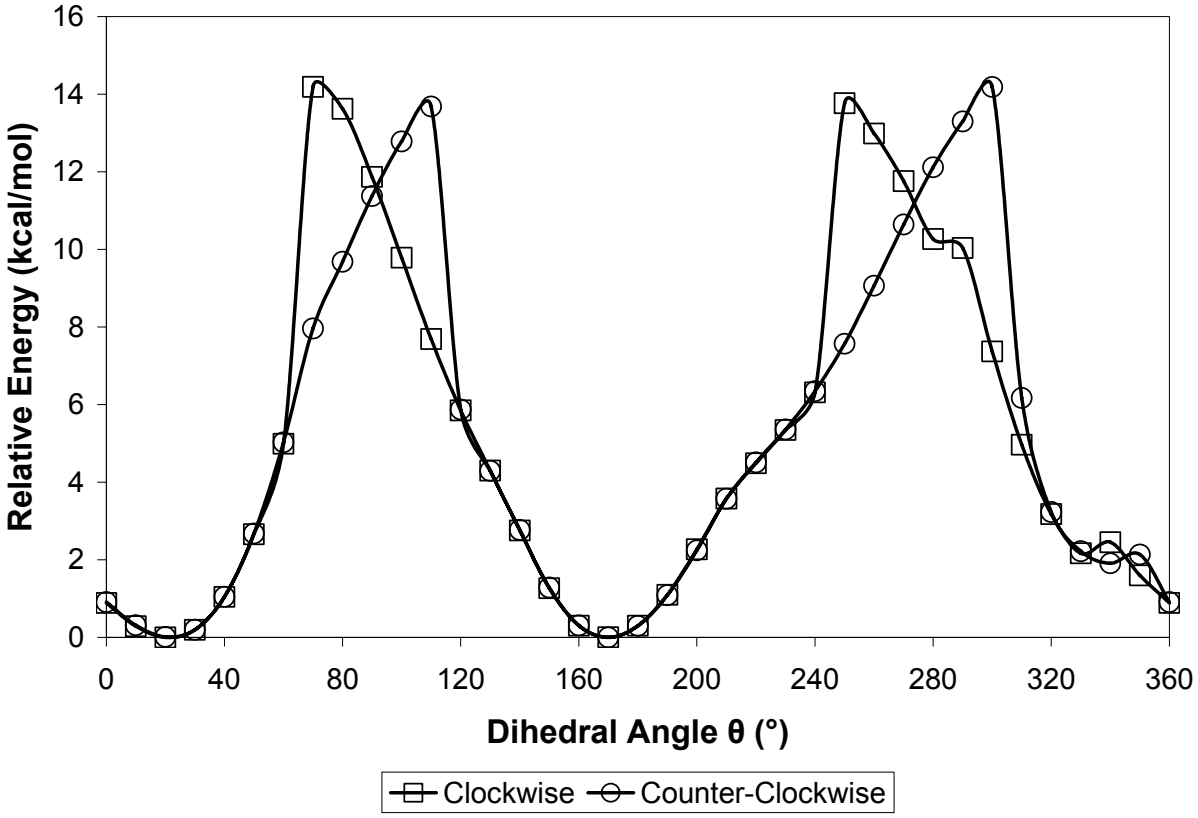

Figure 4.20. Results of the dynamically constrained optimization of protonated 9-azetidinyl-1,2,3,4-tetrahydroacridine **13**·H^+ (TFA^- anion not included). Counterclockwise rotation generates data from 0° to 360°; clockwise rotation generates data from 360° to 0° (or 0° to -360°).

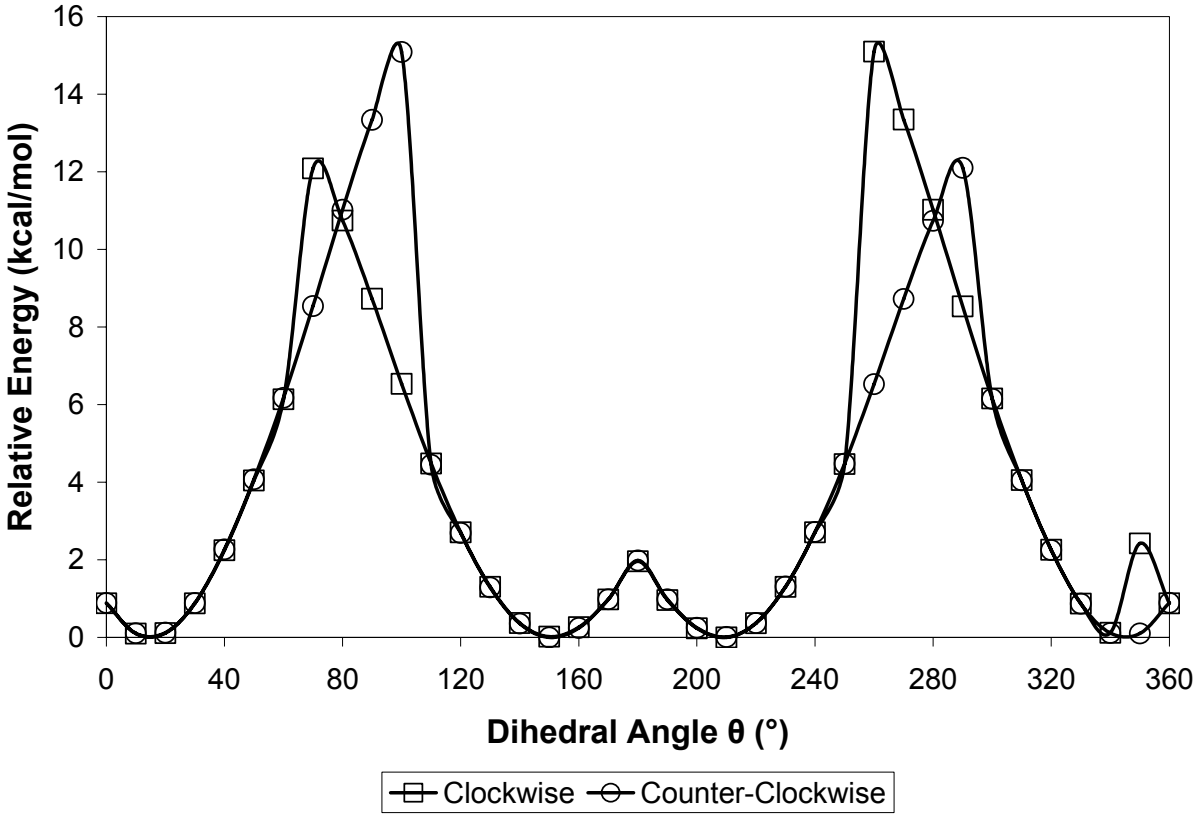

Figure 4.21. Results of the dynamically constrained optimization of protonated *N*,*N*-dimethylquinoline **14**·H^+ (Cl^- anion not included). Counterclockwise rotation generates data from 0° to 360°; clockwise rotation generates data from 360° to 0° (or 0° to -360°).

Applying the constrained optimization approach to *N*,*N*-dimethyltacrine **15**·H^+ (Figure 4.22) allows us to rationalize our inability to experimentally determine the barrier of rotation of **15**·HCl. Because the steric interactions are so great in the nearly co-planar conformations (near 0° and 180°), the equilibrium geometries are destabilized (cf. Figure 4.9). The barrier of rotation for **15**·HCl is quite low; from Figure 4.22, the barrier is approximately 7 kcal/mol. Therefore, it was impossible to achieve exchange between the two conformational populations above the freezing point of CD_3OD to experimentally determine the barrier of rotation for this compound. We estimate a coalescence temperature of approximately -120 ºC, based on $\Delta\nu$ = 121 Hz observed for *N*,*N*-dimethylquinoline HCl (**14**·HCl).

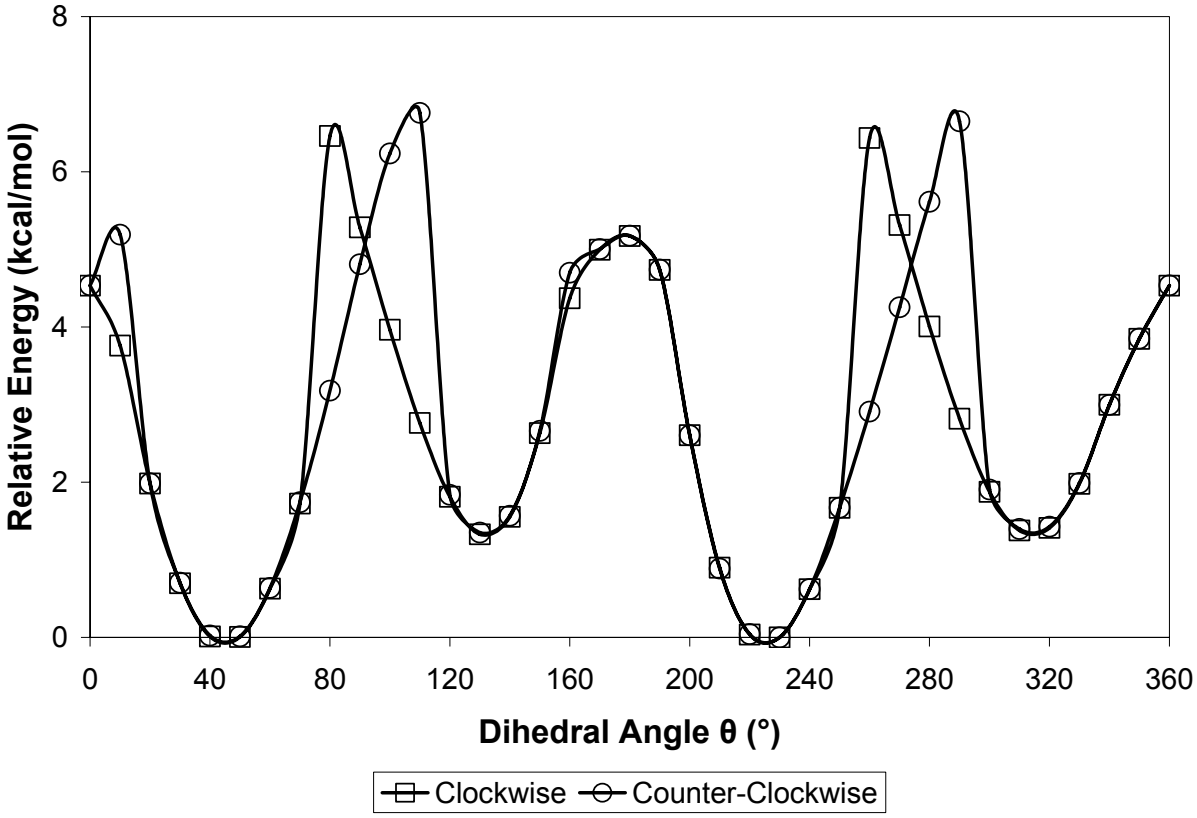

Figure 4.22. Results of the dynamically constrained optimization of protonated *N*,*N*-dimethyltacrine **15**·H^+ (Cl^- anion not included). Counterclockwise rotation generates data from 0° to 360°; clockwise rotation generates data from 360° to 0° (or 0° to -360°).

Because ultimately we were only interested in the penalty of adopting a specific conformation for *N*-alkyltacrines and not the pathway by which the molecule adopts that conformation, we created a curve (Figure 4.23) that indicated the lowest energy possible at a given θ for **16**·H^+. This composite curve could then be used to determine the energetic penalty associated with the crystallographically observed dihedral angles θ seen for *N*-alkyltacrines depicted in Figure 4.2 (Table 4.3).

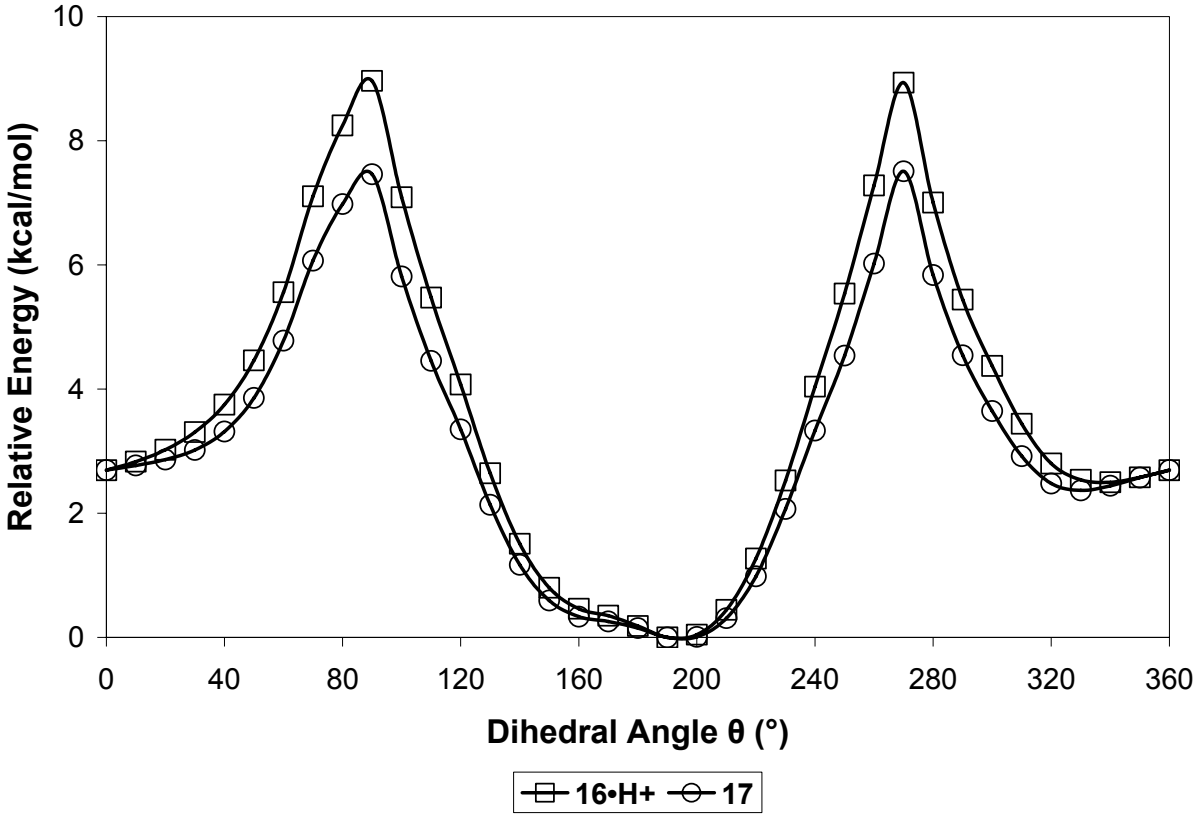

Figure 4.23. Overlay of the composite curves of protonated *N*-methyltacrine **16·H**$^+$ and formamide complex **17**. Note that formamide complexation preferentially stabilizes the pyramidalized structures (θ ca. 90°, 270°) relative to the planar structures (θ ca. 190°, 340°).

Table 4.3. Comparison of observed dihedral angles θ (defined in Figure 4.1) of *N*-alkyltacrines (Figure 4.2) complexed to the bottom of the active site gorge of AChE, and the calculated energetic penalty for *N*-methyltacrine **16**·H^+ and formamide complex **17** to adopt those conformations.

N-alkyltacrine ligand (AChE Species[a])	Crystallographic resolution (Å)	Distance to His440 Carbonyl (Å)[b]	Observed θ (°)	Compare to calculated θ (°)	Energetic penalty[c] associated with **16**·H^+ (kcal/mol)	Energetic penalty[c] associated with **17** (kcal/mol)
3 (*Dm*)	2.70	3.7	320	320	2.8	2.5
4 (*Dm*)	2.72	3.7	176	180	0.2	0.2
syn-**5** (*Mm*)	2.65	2.9	127	130	2.6	2.1
		2.9	132	130	2.6	2.1
anti-**5** (*Mm*)	2.45	2.9	35	40	3.7	3.3
		2.9	47	50	4.5	3.9
6 (*Tc*)	2.20	3.0	357	0	2.7	2.7
(*R*)-**7** (*Tc*)	2.30	3.0	113	110	5.5	4.5
(±)-**7** (*Tc*)	2.10	2.9	45	50	4.5	3.9
		2.9	62	60	5.6	4.8
8 (*Tc*)	2.20	2.9	81	80	**8.2**	**7.0**
9 (*Tc*)	2.40	2.9	89	90	**9.0**	**7.5**
10 (*Tc*)	2.50	2.9	135	140	1.5	1.2
11 (*Tc*)	2.15	3.0	68	70	**7.1**	**6.1**

[a] Abbreviations: *Dm*, *Drosophila melanogaster, Mm, Mus musculus; Tc, Torpedo californica.* [b] Distance from endocyclic nitrogen of the *N*-alkyltacrine ligand; His440 reflects *Torpedo* numbering. The corresponding residues are His447 (*Mm)* and His480 (*Dm*). [c] Energetic penalties taken from the composite curve of the appropriate dynamically constrained optimization energy profile (Figure 4.23). [d] Harel *et al*., 2000.[30] [e] Bourne *et al*., 2004.[15] [f] The crystal form has two molecules in the asymmetric unit; the values are given for each. [g] Wiek *et al*., 2006.[17] [h] Haviv *et al*., 2005.[16] [i] Wong, D. M., Brumshtein, B., Greenblatt, H. M., Carlier, P. R., Han, Y.-F., Pang, Y.-P., Silman, I., Sussman, J. L. Unpublished results. [j] Rydberg *et al*., 2006.[18]

As can be seen, compounds **8**, **9**, and **11** adopt conformations with quite large energetic penalties (7.1 – 9.0 kcal/mol). Since the crystal structures of the *N*-alkyltacrines **5** – **11** bound to AChE evidenced a hydrogen-bonding interaction between the protonated tacrine endocyclic nitrogen with the carbonyl oxygen of a proximal histidine residue (2.9 – 3.0 Å, Table 4.3), additional calculations were performed. Compound **17**, the formamide complex of **16**·H^+, was used to model the effect of this potentially stabilizing hydrogen-bonding interaction. We applied the constrained optimization approach with compound **17** as described above, yielding counterclockwise and clockwise rotation curves which were subsequently combined into a composite curve (Figure 4.23). It is important to note that in the optimized structures, the distance between the carbonyl oxygen of the formamide moiety and the endocyclic nitrogen atom of the tacrine unit was allowed to vary and ranged from 2.7 – 2.8 Å, similar to the 2.9 – 3.0 Å distance described above. Because hydrogen-bonding in the formamide complex provided more stabilization for the nearly orthogonal conformations than for the nearly co-planar conformations, a small reduction in conformational energies was seen for formamide complex **17**. Therefore, even including hydrogen-bond stabilization, we estimate that ligands **8**, **9**, and **11** bind with conformational penalties of 6.1 – 7.5 kcal/mol. In addition, *anti*-**5** and **7**, bind with conformational penalties near 4 kcal/mol.

4.4 Relationship to virtual ligand screening and conclusion

Virtual screening of drug-like molecules for binding to protein targets remains a popular strategy at the outset of drug discovery efforts.[31-34] However, a number of studies have shown that neglect of the conformational energy of the ligand makes it difficult to translate scoring functions into even approximate association constants. For example, Vieth, Hirst, and Brooks[35] examined 10 protein-ligand complexes from the Brookhaven Protein Data Bank (PDB) and found that the ligand often existed in conformations up to 10 kcal/mol above the global minimum, as estimated by a modified CHARMM force field. Perola and Charifson[36] followed up on this study by examining 100 protein-ligand complexes from the PDB using molecular mechanics methods. Within this group of complexes the average conformational energy of the bound ligands was 4.0 and 5.1 kcal/mol above that of the global minimum structure, when calculated with the MMFF and OPLS-AA force fields, respectively. Furthermore, 10% of the ligands bound with a conformational energy exceeding 9.0 kcal/mol above the global minimum.

Since the difference in free energy of binding between a 50 nM ligand and a 100 μM ligand is only 4.5 kcal/mol, the typical neglect of conformational energy in scoring functions is inevitably problematic.[37] In this chapter, we provided additional confirmation that virtual screening efforts cannot prudently exclude highly energetic ligand conformations by showing that homo- and heterodimeric inhibitors of tacrine bound to AChE exhibit quite large conformational energies.

References for Chapter 4

1. Shaw, F. H.; Bentley, G. A. The pharmacology of some new anticholinesterases. *Aust. J. Exp. Biol. Med. Sci.* **1953,** 31, 573-576.

2. Relman, A. S. Tacrine as a treatment for Alzheimer's dementia. *New England Journal of Medicine* **1991,** 324, 349-352.

3. Pang, Y.-P.; Quiram, P.; Jelacic, T.; Hong, F.; Brimijoin, S. Highly Potent, Selective, and Low Cost Bis-tetrahydroaminacrine Inhibitors of Acetylcholinesterase. *J. Biol. Chem.* **1996,** 271, 23646-23649.

4. Carlier, P. R.; Du, D.-M.; Han, Y.; Liu, J.; Pang, Y.-P. Potent, Easily Synthesized Huperzine A-Tacrine Hybrid Acetylcholinesterase Inhibitors. *Bioorg. Med. Chem. Lett.* **1999,** 9, 2335-2338.

5. Carlier, P. R.; Han, Y. F.; Chow, E. S.-H.; Li, C. P.-L.; Wang, H.; Lieu, T. X.; Wong, H. S.; Pang, Y.-P. Evaluation of Short-tether Bis-THA AChE Inhibitors. A Further Test of the Dual Binding Site Hypothesis. *Bioorg. Med. Chem.* **1999,** 7, 351-357.

6. Carlier, P. R.; Chow, E. S.-H.; Han, Y.; Liu, J.; Yazal, J. E.; Pang, Y.-P. Heterodimeric Tacrine-Based Acetylcholinesterase Inhibitors: Investigating Ligand-Peripheral Site Interactions. *J. Med. Chem.* **1999,** 42, 4225-4231.

7. Hu, M.-K.; Wu, L.-J.; Hsiao, G.; Yen, M.-H. Homodimeric Tacrine Congeners as Acetylcholinesterase Inhibitors. *J. Med. Chem.* **2002,** 45, 2277-2282.

8. Lewis, W. G.; Green, L. G.; Grynszpan, F.; Radic, Z.; Carlier, P. R.; Taylor, P.; Finn, M. G.; Sharpless, K. B. Click Chemistry In Situ: Acetylcholinesterase as a Reaction Vessel for the Selective Assembly of a Femtomolar Inhibitor from an Array of Building Blocks. *Angew. Chem., Int. Ed.* **2002,** 41, 1053-1057.

9. Savini, L.; Gaeta, A.; Fattorusso, C.; Catalanotti, B.; Campiani, G.; Chiasserini, L.; Pellerano, C.; Novellino, E.; McKissic, D.; Saxena, A. Specific Targeting of

Acetylcholinesterase and Butyrylcholinesterase Recognition Sites. Rational Design of Novel, Selective, and Highly Potent Cholinesterase Inhibitors. *J. Med. Chem.* **2003,** 46, 1-4.

10. Du, D.-M.; Carlier, P. R. Development of Bivalent Acetylcholinesterase Inhibitors as Potential Therapeutic Drugs for Alzheimer's Disease. *Curr. Pharm. Des.* **2004,** 10, 3141-3156.

11. Bolognesi, M. L.; Andrisano, V.; Bartolini, M.; Banzi, R.; Melchiorre, C. Propidium-Based Polyamine Ligands as Potent Inhibitors of Acetylcholinesterase and Acetylcholinesterase-Induced Amyloid-β Aggregation. *J. Med. Chem.* **2005,** 48, 24-27.

12. Rosini, M.; Andrisano, V.; Bartolini, M.; Bolognesi, M. L.; Hrelia, P.; Minarini, A.; Tarozzi, A.; Melchiorre, C. Rational approach to discover multipotent anti-Alzheimer drugs. *J. Med. Chem.* **2005,** 48, 360-363.

13. Bolognesi, M. L.; Cavalli, A.; Valgimigli, L.; Bartolini, M.; Rosini, M.; Andrisano, V.; Recanatini, M.; Melchiorre, C. Multi-target-directed drug design strategy: From a dual binding site acetylcholinesterase inhibitor to a trifunctional compound against Alzheimer's disease. *Journal of Medicinal Chemistry* **2007,** 50, 6446-6449.

14. Harel, M.; Schalk, I.; Ehret-Sabatier, L.; Bouet, F.; Goeldner, M.; Hirth, C.; Axelsen, P. H.; Silman, I.; Sussman, J. L. Quaternary Ligand Binding to Aromatic Residues in the Active-Site Gorge of Acetylcholinesterase. *Proc. Natl. Acad. Sci. U. S. A.* **1993,** 90, 9031-9035.

15. Bourne, Y.; Kolb, H. C.; Radic, Z.; Sharpless, K. B.; Taylor, P.; Marchot, P. Freeze-Frame Inhibitor Captures Acetylcholinesterase in a Unique Conformation. *Proc. Natl. Acad. Sci. U. S. A.* **2004,** 101, 1449-1454.

16. Haviv, H.; Wong, D. M.; Greenblatt, H. M.; Carlier, P. R.; Pang, Y.-P.; Silman, I.; Sussman, J. L. Crystal Packing Mediates Enantioselective Ligand Recognition at the Peripheral Site of Acetylcholinesterase. *J. Am. Chem. Soc.* **2005,** 127, 11029-11036.

17. Colletier, J. P.; Sanson, B.; Nachon, F.; Gabellieri, E.; Fattorusso, C.; Campiani, G.; Weik, M. Conformational Flexibility in the Peripheral Site of Torpedo californica Acetylcholinesterase Revealed by the Complex Structure with a Bifunctional Inhibitor. *J. Am. Chem. Soc.* **2006,** 128, 4526-4527.

18. Rydberg, E. H.; Brumshtein, B.; Greenblatt, H. M.; Wong, D. M.; Shaya, D.; Williams, L. D.; Carlier, P. R.; Pang, Y. P.; Silman, I.; Sussman, J. L. Complexes of alkylene-linked tacrine dimers with *Torpedo californica* acetylcholinesterase: Binding of bis(5)-tacrine produces a dramatic rearrangement in the active-site gorge. *J. Med. Chem.* **2006,** 49, 5491-5500.

19. Desai, M. C.; Thadeio, P. F.; Lipinski, C. A.; Liston, D. R.; Spencer, R. W.; Williams, I. H. Physical parameters for brain uptake: optimizing log P, log D and pKa of THA. *Bioorg. Med. Chem. Lett.* **1991,** 1, 411-414.

20. Wiberg, K. B.; Rablen, P. R.; Rush, D. J.; Keith, T. A. Amides. 3. Experimental and Theoretical Studies of the Effect of the Medium on the Rotational Barriers for N,N-Dimethylformamide and N,N-Dimethylacetamide. *J. Am. Chem. Soc.* **1995,** 117, 4261-4270.

21. Wiberg, K. B.; Breneman, C. M. Resonance interactions in acyclic systems. 3. Formamide internal rotation revisited. Charge and energy redistribution along the C-N bond rotational pathway. *J. Am. Chem. Soc.* **1992,** 114, 831-840.

22. Han, Y. F.; Li, C. P.; Chow, E.; Wang, H.; Pang, Y. P.; Carlier, P. R. Dual-Site Binding of Bivalent 4-Aminopyridine- and 4-Aminoquinoline-Based AChE Inhibitors: Contribution of the Hydrophobic Alkylene Tether to Monomer and Dimer Affinities. *Bioorg. Med. Chem.* **1999,** 7, 2569-2575.

23. Wong, D. M.; Greenblatt, H. M.; Dvir, H.; Carlier, P. R.; Han, Y.-F.; Pang, Y.-P.; Silman, I.; Sussman, J. L. Acetylcholinesterase Complexed with Bivalent Ligands Related to Huperzine A: Experimental Evidence for Species-Dependent Protein-Ligand Complementarity. *J. Am. Chem. Soc.* **2003,** 125, 363-373.

24. Chow, E. S.-H. Synthesis and Evaluation of Homodimeric and Heterodimeric Acetylcholinesterase Inhibitors. M. Phil., Hong Kong University of Science and Technology, Hong Kong, 1999.

25. Free energy of activation $\Delta G^{\ddagger} = 4.58T_c[10.32+\log(T_c/k_c)]$, where T_c is the coalescence temperature, $\Delta\nu$ is the frequency difference between the decoalesced exchanging signals, and $k_c = \pi(\Delta\nu/1.414)$.

26. Mujika, J. I.; Matxain, J. M.; Eriksson, L. A.; Lopez, X. Resonance Structures of the Amide Bond: The Advantages of Planarity. *Chem.–Eur. J.* **2006,** 12, 7215-7224.

27. Dobbs, K. D.; Dixon, D. A. Reliable Reaction Enthalpies for Neutral Amide Hydrolysis and the Heat of Formation for Formamide. *J. Phys. Chem.* **1996,** 100, 3965-3973.

28. Lopez, X.; Mujika, J. I.; Blackburn, G. M.; Karplus, M. Alkaline Hydrolysis of Amide Bonds: Effect of Bond Twist and Nitrogen Pyramidalization. *J. Phys. Chem. A* **2003,** 107, 2304-2315.

29. Lam, P. C. H.; Carlier, P. R. Experimental and Computational Studies of Ring Inversion of 1,4-Benzodiazepin-2-ones: Implications for Memory of Chirality Transformations. *J. Org. Chem.* **2005,** 70, 1530-1538.

30. Harel, M.; Kryger, G.; Rosenberry, T. L.; Mallender, W. D.; Lewis, T.; Fletcher, R. J.; Guss, J. M.; Silman, I.; Sussman, J. L. Three-dimensional structures of Drosophila melanogaster acetylcholinesterase and of its complexes with two potent inhibitors. *Protein Sci.* **2000,** 9, 1063-1072.

31. Sousa, S. F.; Fernandes, P. A.; Ramos, M. J. Protein-ligand docking: Current status and future challenges. *Proteins: Struct., Funct., Bioinf.* **2006,** 65, 15-26.

32. Branson, K. M.; Smith, B. J. The role of virtual screening in computer aided structure-based drug design. *Aust. J. Chem.* **2004,** 57, 1029-1037.

33. Hattotuwagama, C. K.; Davies, M. N.; Flower, D. R. Receptor-ligand binding sites and virtual screening. *Curr. Med. Chem.* **2006,** 13, 1283-1304.

34. Pozzan, A. Molecular descriptors and methods for ligand based virtual high throughput screening in drug discovery. *Curr. Pharm. Des.* **2006,** 12, 2099-2110.

35. Vieth, M.; Hirst, J. D.; Brooks III, C. L. Do active site conformations of small ligands correspond to low free-energy solution structures? *J. Comp.-Aided Mol. Des.* **1998,** 12, 563-572.

36. Perola, E.; Charifson, P. S. Conformational analysis of drug-like molecules bound to proteins: An extensive study of ligand reorganization upon binding. *J. Med. Chem.* **2004,** 47, 2499-2510.

37. Leach, A. R.; Shoichet, B. K.; Peishoff, C. E. Prediction of protein -ligand interaction. Docking and scoring: Successes and gaps. *J. Med. Chem.* **2006,** 49, 5851-5855.

Chapter 5. Experimental and Computational Procedures for Tacrine Derivative Rotational Barriers

5.1 Experimental Details

5.1.1 Synthetic details

Tacrine hydrochloride (**1**·HCl) was purchased from Acros Organics, Morris Plains, NJ 07950 and used as received. 4-aminoquinaldine (**12**) was purchased from Aldrich Chemical Company, Milwaukee, WI 53201 and subsequently converted to the hydrochloride salt. The synthesis of 9-azetadinyl-1,2,3,4-tetrahydroacridine (**13**) has been previously described,[1] and all analytical data were identical. Attempts to convert **13** to the HCl salt were unsuccessful as the Cl^- nucleophile caused ring opening of the azetidinyl moiety; TFA was used to protonate **13** for the variable temperature ^{1}H NMR experiments. *N*,*N*-dimethylquinoline (**14**) was synthesized according to a published procedure,[2] and all analytical data were identical. ^{1}H and ^{13}C NMR spectra were recorded at 400 MHz and 100 MHz, respectively. All NMR coalescence experiments were performed using a Varian Unity 400 MHz spectrometer with a calibrated temperature control unit.

***N*-Methyltacrine** (**16**): synthesized as previously described.[3] ^{1}H NMR (CD_3OD) δ 1.88 (5-let, *J* = 3.3 Hz, 4H), 2.69 (t, *J* = 5.1 Hz, 2H), 2.94 (t, *J* = 5.1 Hz, 2H), 3.26 (s, 3H), 7.32 (t, *J* = 8.5 Hz, 1H), 7.53 (t, *J* = 7.8 Hz, 1H), 7.73 (d, *J* = 7.8 Hz, 1H), 8.17 (d, J = 8.5 Hz, 1H); ^{13}C NMR (CD_3OD) δ 23.58, 24.05, 25.86, 33.84, 35.97, 114.94, 120.22, 124.30, 124.71, 127.38, 129.85, 147.62, 154.34, 158.28.

5.1.2 Calibration for variable temperature ^{1}H NMR

The temperature of the NMR spectrometer was calibrated through the use of an ethylene glycol standard. The instrument was set at five distinct temperatures, and the Varian software used the chemical shift differences between the two ethylene glycol signals to compute an actual temperature. Plotting the computed actual temperature versus the set temperature produced the line shown in Figure 5.1. Finally, the equation of the line was used to obtain the calibrated temperature for each variable temperature ^{1}H NMR experiment (Table 5.1).

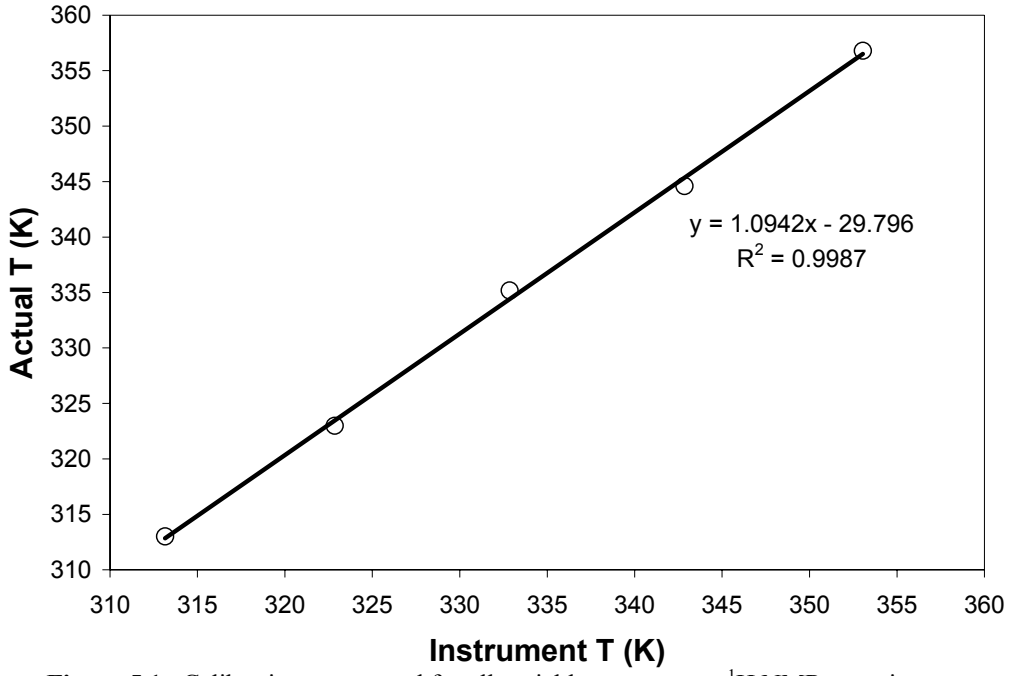

Figure 5.1. Calibration curve used for all variable temperature ^{1}H NMR experiments

Table 5.1. Temperature calibrations from the variable temperature ^{1}H NMR experiments.

Compound	Instrument T (ºC)	Instrument T (K)	Actual T (K)
12·HCl	50	323.15	324
	45	318.15	318
	40	313.15	313
	39	312.15	312
	38	311.15	311
	35	308.15	307
	30	303.15	302
	23	296.15	294
1·HCl	50	323.15	324
	42	315.15	315
	40	313.15	313
	38	311.15	311
	35	308.15	307
	23	296.15	294
13·TFA	-25	248.15	242
	-35	238.15	231
	-38	235.15	228
	-40	233.15	225
	-41	232.15	224
	-70	203.15	192
14·HCl	-20	253.15	247
	-55	218.15	209
	-57	216.15	207
	-58	215.15	206
	-59	214.15	205
	-60	213.15	203
	-70	203.15	192
	-90	183.15	171

5.2 Computational details

5.2.1 Conformational energy calculations

All calculations were performed using B3LYP/6-31G* as implemented in Gaussian 03.[4] Conformational profiles were obtained by performing a series of constrained optimization calculations in which the dihedral angle θ was varied from 0° to 360° and 0° to -360° in 10° increments. The θ = 0° conformation was defined as the conformation in which the *N*-alkyl moiety was co-planar with the cyclohexene unit of the tacrine derivative. For all of the systems studied, the profiles were generated for the protonated *N*-alkyltacrine derivative. Furthermore, in order to model the hydrogen-bonding interaction of the *N*-alkyltacrine ligand with the carbonyl

of a proximal histidine residue in the X-ray crystal structures, a formamide molecule was complexed to protonated *N*-methyltacrine **16**·H^+ with an N-O bond distance of 2.8 Å initially and the 15-14-10-4a dihedral (defined in Chapter 4) constrained to +90°; the constrained optimization conformational profile was obtained as described above for this complex. The N-O bond distance remained within a range of 2.7 – 2.8 Å throughout the constrained optimization.

5.2.1.1 Cartesian coordinates for constrained optimization calculations of 16·H^+

Rotation in the counterclockwise direction:

Point 1 θ = 0°

C	-1.025991	-0.017977	-0.775190
C	-1.091260	0.047937	0.653714
N	1.354770	0.149803	-0.647005
C	0.153518	0.004358	1.419268
C	0.223214	0.061926	-1.384209
C	1.382518	0.088194	0.726485
C	0.219035	-0.110935	2.831376
H	3.539318	0.178481	0.838741
H	2.239704	0.225823	-1.136680
C	1.427848	-0.108126	3.498116
H	-0.679382	-0.240170	3.426785
H	1.446947	-0.206349	4.578390
C	2.635005	0.012100	2.782125
H	3.582472	0.018913	3.311279
C	2.615300	0.103907	1.405831
C	0.449027	0.041976	-2.879430
H	1.198425	0.802895	-3.135158
H	0.898374	-0.930176	-3.131635
C	-2.262142	-0.163837	-1.660615
H	-2.794034	0.794860	-1.713287
H	-2.950466	-0.882910	-1.210928
C	-1.945021	-0.617604	-3.092010
H	-1.640252	-1.672711	-3.091381
H	-2.857093	-0.551753	-3.693598
C	-0.832600	0.240251	-3.691736
H	-1.126213	1.297613	-3.677962
H	-0.643744	-0.024997	-4.736257
N	-2.225856	0.162362	1.369931
H	-2.084280	0.233440	2.365564
C	-3.640651	0.250732	0.992633
H	-3.802797	0.984530	0.204197
H	-4.184556	0.582668	1.878707
H	-4.045137	-0.718224	0.687938

Point 2 θ = 10°

C	-1.022106	-0.028647	-0.779401
C	-1.088574	0.061098	0.647618
N	1.362109	0.092559	-0.649123
C	0.154389	0.026471	1.416227
C	0.230459	0.014053	-1.386568
C	1.386418	0.072766	0.725404
C	0.214990	-0.054068	2.831121
H	3.544057	0.137164	0.840965
H	2.248868	0.141845	-1.138906
C	1.421978	-0.046455	3.501095
H	-0.686675	-0.161980	3.425675
H	1.437146	-0.117144	4.583590
C	2.632482	0.039600	2.785760
H	3.578514	0.049907	3.317422
C	2.617710	0.091082	1.407286
C	0.456368	-0.025309	-2.881155
H	1.262131	0.674982	-3.137748
H	0.827290	-1.029804	-3.134168
C	-2.262431	-0.110047	-1.667075
H	-2.757992	0.869925	-1.682243
H	-2.976532	-0.817289	-1.240953
C	-1.970332	-0.531831	-3.113988
H	-1.730605	-1.603024	-3.148379
H	-2.876988	-0.392238	-3.711213
C	-0.807146	0.272424	-3.690677
H	-1.034330	1.345370	-3.650343
H	-0.632411	0.021528	-4.741195
N	-2.222019	0.207747	1.362266
H	-2.072383	0.344688	2.349841
C	-3.645163	0.131919	1.013552
H	-3.908511	0.824068	0.214550
H	-4.203857	0.419567	1.905717
H	-3.942854	-0.883927	0.739046

Point 3 θ = 20°

C	-1.019889	-0.037160	-0.783255
C	-1.086807	0.075013	0.640997
N	1.365998	0.035074	-0.650153
C	0.152977	0.049327	1.412552
C	0.234835	-0.031140	-1.388919
C	1.387625	0.054917	0.724345
C	0.208242	0.006400	2.829399
H	3.545954	0.086343	0.844653
H	2.254432	0.057345	-1.138986

C	1.413448	0.015101	3.502376
H	-0.697484	-0.073284	3.422002
H	1.424989	-0.025796	4.586461
C	2.627173	0.061096	2.788466
H	3.571763	0.071571	3.322690
C	2.617355	0.071895	1.408970
C	0.458648	-0.084284	-2.883118
H	1.309472	0.560306	-3.139557
H	0.758994	-1.111048	-3.140270
C	-2.262356	-0.061285	-1.670290
H	-2.727633	0.933937	-1.648341
H	-2.997377	-0.758672	-1.265134
C	-1.990734	-0.450912	-3.130577
H	-1.810612	-1.532125	-3.197998
H	-2.888144	-0.244269	-3.722277
C	-0.784510	0.301568	-3.687507
H	-0.950840	1.384472	-3.623312
H	-0.621987	0.064104	-4.743107
N	-2.223576	0.255166	1.346829
H	-2.072657	0.452797	2.324060
C	-3.637739	0.018990	1.031763
H	-3.997572	0.668687	0.234037
H	-4.204363	0.249833	1.935290
H	-3.823626	-1.026965	0.771910

Point 4 $\theta = 30°$

C	-1.018891	-0.041608	-0.787895
C	-1.086056	0.091104	0.632721
N	1.366807	-0.021848	-0.650164
C	0.149077	0.073874	1.407594
C	0.237125	-0.073553	-1.391705
C	1.386000	0.036109	0.723388
C	0.198393	0.070683	2.825370
H	3.544471	0.028585	0.851068
H	2.256878	-0.027996	-1.136718
C	1.401486	0.077264	3.501793
H	-0.711917	0.024678	3.414280
H	1.409453	0.067862	4.586655
C	2.618227	0.078412	2.790956
H	3.561044	0.086242	3.328362
C	2.613710	0.048388	1.411636
C	0.457478	-0.139587	-2.885415
H	1.346696	0.450226	-3.142781
H	0.690023	-1.182677	-3.147015
C	-2.262040	-0.013842	-1.671968
H	-2.700997	0.992407	-1.613781

H	-3.015047	-0.702079	-1.285184
C	-2.007588	-0.371906	-3.143947
H	-1.884805	-1.458651	-3.242877
H	-2.892014	-0.101681	-3.729461
C	-0.762549	0.327993	-3.683243
H	-0.870385	1.416778	-3.597224
H	-0.610943	0.103129	-4.743239
N	-2.230487	0.303811	1.322967
H	-2.083055	0.557364	2.288090
C	-3.618884	-0.092069	1.050839
H	-4.078455	0.513725	0.268679
H	-4.179898	0.067365	1.973177
H	-3.688853	-1.151503	0.789044

Point 5 $\theta = 40°$

C	-1.018907	-0.041553	-0.793674
C	-1.086928	0.106108	0.623032
N	1.364453	-0.077523	-0.649058
C	0.142358	0.096411	1.401568
C	0.237436	-0.113184	-1.394894
C	1.381169	0.016430	0.722678
C	0.185669	0.133857	2.819125
H	3.539031	-0.028864	0.860075
H	2.256071	-0.112446	-1.131899
C	1.386340	0.138570	3.499347
H	-0.729166	0.123378	3.402513
H	1.391172	0.161716	4.584034
C	2.605578	0.094844	2.793260
H	3.546305	0.100592	3.334361
C	2.606412	0.024294	1.415364
C	0.453212	-0.193497	-2.887731
H	1.376149	0.340292	-3.147876
H	0.617979	-1.248625	-3.152311
C	-2.261351	0.034510	-1.673410
H	-2.675154	1.049256	-1.580872
H	-3.031336	-0.643319	-1.301788
C	-2.021550	-0.293233	-3.155609
H	-1.956643	-1.381727	-3.285105
H	-2.889071	0.039169	-3.734330
C	-0.739941	0.351566	-3.678565
H	-0.790193	1.442764	-3.572639
H	-0.597979	0.138218	-4.742289
N	-2.243088	0.350359	1.291122
H	-2.102527	0.652334	2.243818
C	-3.589494	-0.201427	1.072551
H	-4.147023	0.351306	0.314026

H	-4.128622	-0.113747	2.017483
H	-3.546362	-1.259832	0.801697

Point 6 θ = 50°

C	-1.018632	-0.033467	-0.802356
C	-1.089043	0.123983	0.610159
N	1.360466	-0.120235	-0.648264
C	0.132734	0.116043	1.393590
C	0.237541	-0.140407	-1.400150
C	1.373737	-0.000357	0.721694
C	0.168438	0.184882	2.810258
H	3.530176	-0.082152	0.872678
H	2.253774	-0.180215	-1.125970
C	1.365707	0.183313	3.495868
H	-0.751557	0.206026	3.385053
H	1.366705	0.231457	4.579758
C	2.587622	0.100561	2.796811
H	3.525408	0.101078	3.343049
C	2.595358	-0.000501	1.420760
C	0.449222	-0.232572	-2.891904
H	1.394755	0.258081	-3.155323
H	0.563028	-1.294104	-3.157524
C	-2.260088	0.076322	-1.676880
H	-2.655167	1.096254	-1.560037
H	-3.042301	-0.591853	-1.311886
C	-2.030092	-0.231659	-3.165457
H	-2.010041	-1.319148	-3.316217
H	-2.881615	0.146808	-3.739589
C	-0.721650	0.368232	-3.677335
H	-0.728147	1.459216	-3.558579
H	-0.586521	0.161748	-4.743299
N	-2.259464	0.402297	1.250690
H	-2.124664	0.750927	2.189059
C	-3.551325	-0.293394	1.103130
H	-4.200902	0.191681	0.370799
H	-4.052131	-0.260092	2.072603
H	-3.407332	-1.341753	0.828811

Point 7 θ = 60°

C	-1.017260	-0.014301	-0.815199
C	-1.092596	0.144537	0.593535
N	1.356224	-0.145683	-0.648919
C	0.119960	0.130788	1.383582
C	0.238926	-0.149332	-1.408868
C	1.364041	-0.013799	0.720053
C	0.145840	0.217964	2.799617

H	3.518247	-0.130320	0.888403
H	2.251713	-0.224540	-1.120362
C	1.338294	0.204161	3.492723
H	-0.780082	0.265006	3.363149
H	1.334050	0.266697	4.575884
C	2.563594	0.090658	2.802575
H	3.497277	0.081569	3.355754
C	2.580573	-0.026962	1.427874
C	0.449595	-0.248597	-2.899582
H	1.404784	0.221812	-3.165076
H	0.540504	-1.312768	-3.163578
C	-2.257642	0.114777	-1.685459
H	-2.635308	1.140708	-1.563329
H	-3.050568	-0.538822	-1.314779
C	-2.033189	-0.196606	-3.174186
H	-2.036796	-1.284029	-3.326785
H	-2.874658	0.201307	-3.749917
C	-0.710734	0.375492	-3.684244
H	-0.694653	1.466347	-3.565417
H	-0.579501	0.166506	-4.750187
N	-2.278560	0.457431	1.203785
H	-2.145317	0.855424	2.123779
C	-3.507656	-0.363404	1.148851
H	-4.239703	0.043004	0.446152
H	-3.955846	-0.360161	2.144536
H	-3.279551	-1.397866	0.879635

Point 8 $\theta = 70°$

C	-1.017732	0.014900	-0.831491
C	-1.101000	0.167265	0.574388
N	1.348291	-0.170418	-0.646190
C	0.100430	0.148888	1.373401
C	0.239192	-0.152841	-1.417615
C	1.348334	-0.024774	0.721437
C	0.113217	0.257217	2.788305
H	3.499122	-0.177646	0.912946
H	2.246287	-0.274356	-1.108582
C	1.298853	0.230887	3.491809
H	-0.819497	0.334789	3.337003
H	1.287462	0.310312	4.573830
C	2.528432	0.083972	2.813962
H	3.456340	0.065136	3.376567
C	2.557795	-0.051462	1.441073
C	0.454438	-0.268383	-2.906059
H	1.416550	0.186586	-3.173674
H	0.532586	-1.336618	-3.157853

C	-2.251066	0.179006	-1.705099
H	-2.579231	1.224108	-1.605217
H	-3.076971	-0.423633	-1.319280
C	-2.031892	-0.172879	-3.184752
H	-2.058632	-1.263207	-3.313086
H	-2.862122	0.230641	-3.772751
C	-0.695705	0.361568	-3.702435
H	-0.658973	1.454012	-3.604654
H	-0.566836	0.130259	-4.764043
N	-2.307211	0.498090	1.152013
H	-2.185374	0.967432	2.041277
C	-3.453063	-0.439980	1.211594
H	-4.347150	-0.002246	0.758583
H	-3.669083	-0.675757	2.257475
H	-3.211793	-1.373869	0.701116

Point 9 $\theta = 80°$

C	-1.025029	0.025955	-0.861353
C	-1.121859	0.196445	0.538483
N	1.337010	-0.182458	-0.643068
C	0.065594	0.170446	1.353387
C	0.240811	-0.159612	-1.430316
C	1.321929	-0.025870	0.722578
C	0.058770	0.295952	2.767838
H	3.468114	-0.205300	0.947022
H	2.240077	-0.301997	-1.092477
C	1.233585	0.258790	3.488158
H	-0.880953	0.399575	3.299650
H	1.208188	0.351512	4.568903
C	2.471486	0.086325	2.830405
H	3.390164	0.060279	3.407678
C	2.520625	-0.062088	1.459566
C	0.475387	-0.292129	-2.914092
H	1.448723	0.144284	-3.171883
H	0.538693	-1.363719	-3.155735
C	-2.242553	0.189996	-1.756074
H	-2.571241	1.234844	-1.662691
H	-3.075752	-0.408740	-1.380670
C	-2.003450	-0.168655	-3.231219
H	-2.040009	-1.258920	-3.357518
H	-2.820423	0.242019	-3.832594
C	-0.654063	0.349150	-3.730732
H	-0.605479	1.441434	-3.636521
H	-0.511388	0.111923	-4.789249
N	-2.345885	0.539432	1.101006
H	-2.211752	1.070037	1.956534

C	-3.387670	-0.484598	1.336337
H	-4.303913	0.023285	1.644127
H	-3.087341	-1.197425	2.114877
H	-3.596396	-1.043174	0.423642

Point 10 $\theta = 90°$

C	-1.023901	0.075494	-0.885687
C	-1.132277	0.224384	0.510773
N	1.328995	-0.178986	-0.647316
C	0.040562	0.174627	1.338448
C	0.244231	-0.129901	-1.447601
C	1.302002	-0.036726	0.719769
C	0.017885	0.299179	2.753127
H	3.442984	-0.251942	0.969534
H	2.235380	-0.312578	-1.086996
C	1.183441	0.237667	3.485915
H	-0.927542	0.427254	3.269039
H	1.148663	0.330293	4.566432
C	2.426264	0.043956	2.841554
H	3.336992	-0.000733	3.430186
C	2.491213	-0.097188	1.470675
C	0.485528	-0.268369	-2.929414
H	1.450986	0.184775	-3.188665
H	0.572191	-1.341102	-3.159267
C	-2.239489	0.235777	-1.782029
H	-2.548365	1.288880	-1.725336
H	-3.081108	-0.332696	-1.377597
C	-2.000298	-0.174368	-3.242796
H	-2.027399	-1.268740	-3.331137
H	-2.819314	0.208901	-3.859170
C	-0.654292	0.340309	-3.757633
H	-0.615974	1.435113	-3.692041
H	-0.510756	0.077964	-4.810068
N	-2.378812	0.573477	1.047881
H	-2.247241	1.169567	1.861769
C	-3.305383	-0.520028	1.426159
H	-4.240338	-0.071295	1.767700
H	-2.896306	-1.159705	2.219280
H	-3.524520	-1.146258	0.558511

Point 11 $\theta = 100°$

C	-1.026600	0.111132	-0.913451
C	-1.148085	0.237566	0.479991
N	1.318470	-0.180174	-0.653671
C	0.011554	0.169384	1.320255
C	0.246381	-0.106134	-1.466793

C	1.278333	-0.053029	0.714656
C	-0.025743	0.299041	2.734479
H	3.413963	-0.297900	0.988563
H	2.228426	-0.324326	-1.083507
C	1.130560	0.219181	3.479419
H	-0.975323	0.452769	3.234842
H	1.086426	0.316781	4.559190
C	2.377904	0.004130	2.849074
H	3.280550	-0.055506	3.448722
C	2.458157	-0.133156	1.478743
C	0.498395	-0.243672	-2.946666
H	1.458769	0.222837	-3.201574
H	0.603309	-1.315950	-3.171507
C	-2.237198	0.266280	-1.816635
H	-2.538072	1.322430	-1.784840
H	-3.082498	-0.285305	-1.396243
C	-1.990075	-0.173429	-3.266947
H	-2.007475	-1.269642	-3.333000
H	-2.808820	0.190523	-3.895192
C	-0.645468	0.343810	-3.785128
H	-0.616547	1.439718	-3.734721
H	-0.496121	0.068617	-4.833435
N	-2.416667	0.576700	1.000330
H	-2.294523	1.259128	1.747243
C	-3.220988	-0.545101	1.544581
H	-4.162862	-0.136745	1.916705
H	-2.713276	-1.086689	2.354155
H	-3.450856	-1.256267	0.746362

Point 12 $\theta = 110°$

C	-1.032813	0.138222	-0.938064
C	-1.169585	0.229264	0.454249
N	1.303946	-0.194018	-0.658787
C	-0.018880	0.153239	1.304983
C	0.245472	-0.089192	-1.483199
C	1.252057	-0.078731	0.710238
C	-0.062125	0.305745	2.717241
H	3.383054	-0.348639	1.000116
H	2.216402	-0.351545	-1.079440
C	1.088497	0.218955	3.469782
H	-1.010448	0.494882	3.206335
H	1.039913	0.337602	4.547292
C	2.336933	-0.025291	2.851383
H	3.234001	-0.093171	3.458456
C	2.425639	-0.171413	1.482803
C	0.510259	-0.224750	-2.961096

H	1.470691	0.246257	-3.207845
H	0.623554	-1.296893	-3.182911
C	-2.232071	0.305436	-1.854125
H	-2.512194	1.367764	-1.843110
H	-3.089391	-0.220453	-1.426819
C	-1.977314	-0.156155	-3.295762
H	-1.995477	-1.253264	-3.346273
H	-2.791496	0.199691	-3.934486
C	-0.628904	0.354190	-3.811823
H	-0.600105	1.450554	-3.772773
H	-0.472668	0.068258	-4.856229
N	-2.463035	0.530101	0.962278
H	-2.381800	1.312712	1.611756
C	-3.143145	-0.581098	1.671837
H	-4.094678	-0.203408	2.052137
H	-2.561935	-1.002076	2.503089
H	-3.358352	-1.385774	0.962767

Point 13 $\theta = 120°$

C	-1.036108	0.170509	-0.955261
C	-1.187901	0.218036	0.438093
N	1.291601	-0.211607	-0.663899
C	-0.041156	0.129333	1.294563
C	0.245705	-0.065378	-1.495135
C	1.231226	-0.113297	0.706052
C	-0.080638	0.315015	2.703336
H	3.357018	-0.416234	1.002629
H	2.203696	-0.387467	-1.078694
C	1.067239	0.221344	3.458765
H	-1.022028	0.553831	3.181461
H	1.020700	0.371596	4.532460
C	2.311729	-0.062799	2.848891
H	3.205513	-0.140786	3.459560
C	2.401326	-0.221956	1.482246
C	0.520690	-0.201010	-2.971897
H	1.480546	0.275279	-3.211207
H	0.643686	-1.272993	-3.189383
C	-2.221498	0.357317	-1.884475
H	-2.470826	1.427895	-1.899023
H	-3.093270	-0.133945	-1.446433
C	-1.965794	-0.130179	-3.316793
H	-1.989071	-1.227934	-3.348791
H	-2.776184	0.218805	-3.964097
C	-0.613675	0.367778	-3.835386
H	-0.582857	1.464516	-3.812371
H	-0.453297	0.066360	-4.874804

N	-2.506112	0.429471	0.934094
H	-2.574340	1.342165	1.382379
C	-3.076110	-0.619568	1.804620
H	-4.081614	-0.301098	2.089078
H	-2.503927	-0.840851	2.714301
H	-3.170271	-1.545146	1.229119

Point 14 $\theta = 130°$

C	-1.029213	0.185338	-0.964161
C	-1.179842	0.237319	0.450873
N	1.294139	-0.232930	-0.682479
C	-0.021182	0.087810	1.299816
C	0.235157	-0.037979	-1.500916
C	1.232127	-0.177868	0.691888
C	-0.041148	0.260740	2.708247
H	3.343374	-0.562024	0.967685
H	2.199555	-0.406759	-1.106927
C	1.107321	0.109729	3.457406
H	-0.962291	0.547880	3.198436
H	1.073635	0.253795	4.532299
C	2.330042	-0.213513	2.832509
H	3.227222	-0.337876	3.430549
C	2.399309	-0.344760	1.460198
C	0.510402	-0.138335	-2.982110
H	1.468947	0.349223	-3.202746
H	0.637823	-1.201280	-3.235583
C	-2.229342	0.356774	-1.880647
H	-2.549334	1.409789	-1.859233
H	-3.072103	-0.230141	-1.491910
C	-1.967897	-0.062465	-3.335990
H	-1.981783	-1.157654	-3.410711
H	-2.782020	0.306947	-3.966970
C	-0.617821	0.463243	-3.827598
H	-0.591044	1.558205	-3.759277
H	-0.457543	0.205167	-4.878716
N	-2.416354	0.410920	0.994778
H	-3.110809	0.705324	0.320648
C	-3.008540	-0.413983	2.065485
H	-3.925832	-0.872525	1.686075
H	-3.259955	0.187366	2.944637
H	-2.321001	-1.208477	2.358445

Point 15 $\theta = 140°$

C	-1.031251	0.154127	-0.976056
C	-1.193593	0.183267	0.442155
N	1.294564	-0.236761	-0.686964

C	-0.032644	0.055070	1.295762
C	0.236095	-0.045713	-1.508152
C	1.225453	-0.190219	0.686949
C	-0.048025	0.227956	2.704828
H	3.341075	-0.546224	0.958196
H	2.204400	-0.392309	-1.108404
C	1.104108	0.094469	3.452072
H	-0.967369	0.501966	3.203340
H	1.069018	0.238887	4.526847
C	2.329276	-0.213108	2.826156
H	3.229416	-0.326175	3.421971
C	2.395536	-0.342807	1.453836
C	0.522737	-0.115526	-2.988981
H	1.477936	0.385539	-3.193065
H	0.661961	-1.171927	-3.262610
C	-2.229461	0.318973	-1.896621
H	-2.575676	1.362982	-1.851431
H	-3.060565	-0.299052	-1.530396
C	-1.951965	-0.060472	-3.360177
H	-1.951510	-1.153578	-3.461264
H	-2.766643	0.313771	-3.987591
C	-0.605180	0.492396	-3.829844
H	-0.591457	1.585773	-3.736637
H	-0.434595	0.259893	-4.885325
N	-2.440251	0.329806	0.955965
H	-3.139474	0.572188	0.267694
C	-3.013531	-0.350217	2.128059
H	-3.989442	-0.751213	1.843494
H	-3.158236	0.334695	2.969680
H	-2.376708	-1.179457	2.440513

Point 16 $\theta = 150°$

C	-1.032106	0.120505	-0.984002
C	-1.203354	0.129972	0.436931
N	1.297559	-0.232424	-0.690904
C	-0.039894	0.022325	1.294270
C	0.238026	-0.050776	-1.513508
C	1.222911	-0.197370	0.682670
C	-0.049980	0.184133	2.705378
H	3.343716	-0.520659	0.945267
H	2.211872	-0.364529	-1.110140
C	1.106498	0.065677	3.448905
H	-0.967643	0.437200	3.215267
H	1.069842	0.201248	4.524764
C	2.334620	-0.216970	2.819193
H	3.238381	-0.319727	3.411358

C	2.396968	-0.336208	1.446037
C	0.533221	-0.089152	-2.993743
H	1.482034	0.429415	-3.183237
H	0.688733	-1.137949	-3.286965
C	-2.230328	0.273195	-1.907128
H	-2.606125	1.305859	-1.839484
H	-3.045818	-0.377285	-1.561538
C	-1.938484	-0.066368	-3.377999
H	-1.919056	-1.156606	-3.504567
H	-2.756647	0.308509	-4.000487
C	-0.599062	0.519013	-3.828033
H	-0.603427	1.610185	-3.710972
H	-0.419422	0.312237	-4.887378
N	-2.459275	0.248718	0.923568
H	-3.158168	0.449136	0.222663
C	-3.027210	-0.272316	2.172100
H	-4.042865	-0.612822	1.958507
H	-3.083672	0.494053	2.952035
H	-2.447844	-1.123221	2.535174

Point 17 $\theta = 160°$

C	-1.031116	0.084242	-0.988011
C	-1.207723	0.081558	0.435175
N	1.304921	-0.208076	-0.694508
C	-0.042054	-0.011160	1.294998
C	0.241910	-0.048391	-1.517187
C	1.226060	-0.192126	0.678792
C	-0.048813	0.115483	2.710374
H	3.353818	-0.469016	0.929499
H	2.223589	-0.308793	-1.112588
C	1.112175	0.009403	3.449053
H	-0.967565	0.327048	3.234199
H	1.072529	0.116466	4.528006
C	2.345560	-0.226369	2.812233
H	3.253409	-0.318866	3.399793
C	2.405001	-0.316478	1.437082
C	0.542224	-0.056242	-2.996793
H	1.478782	0.487938	-3.174870
H	0.723395	-1.096107	-3.306521
C	-2.231339	0.215406	-1.912459
H	-2.640269	1.234305	-1.827261
H	-3.026717	-0.467882	-1.582806
C	-1.926910	-0.088580	-3.388764
H	-1.879772	-1.175401	-3.535625
H	-2.753167	0.276892	-4.006166
C	-0.601913	0.538352	-3.824288

H	-0.633834	1.626839	-3.687956
H	-0.414473	0.354803	-4.886561
N	-2.471700	0.178004	0.898425
H	-3.165293	0.342058	0.183735
C	-3.048529	-0.169800	2.198370
H	-4.098937	-0.418124	2.033898
H	-3.005801	0.663965	2.906943
H	-2.553447	-1.044354	2.625791

Point 18 $\theta = 170°$

C	-1.028948	0.045689	-0.988888
C	-1.208114	0.043733	0.436042
N	1.315936	-0.142145	-0.696347
C	-0.041348	-0.047924	1.297509
C	0.247250	-0.029095	-1.518821
C	1.233416	-0.161637	0.676318
C	-0.049098	-0.005449	2.718533
H	3.370429	-0.361468	0.914361
H	2.238857	-0.195617	-1.113574
C	1.116027	-0.102301	3.452118
H	-0.973524	0.118860	3.257362
H	1.070581	-0.064180	4.535461
C	2.358382	-0.244526	2.806432
H	3.270455	-0.325676	3.389095
C	2.417710	-0.268120	1.428937
C	0.549723	-0.009816	-2.997918
H	1.461993	0.576190	-3.169064
H	0.776453	-1.038081	-3.316242
C	-2.232382	0.137697	-1.914250
H	-2.679701	1.140190	-1.823869
H	-3.001827	-0.577874	-1.590978
C	-1.915041	-0.143792	-3.392308
H	-1.822832	-1.226697	-3.546389
H	-2.755892	0.191011	-4.007433
C	-0.617771	0.541420	-3.822614
H	-0.696042	1.626615	-3.678854
H	-0.422180	0.373263	-4.885959
N	-2.477819	0.136949	0.881060
H	-3.163321	0.262933	0.151528
C	-3.068601	-0.020625	2.209615
H	-4.148497	-0.102226	2.075054
H	-2.872983	0.843810	2.852030
H	-2.717288	-0.934109	2.696054

Point 19 $\theta = 180°$

C	-1.029278	0.004027	-0.989639

C	-1.209626	0.026218	0.434924
N	1.322020	0.011167	-0.690707
C	-0.045162	-0.093800	1.296380
C	0.249638	0.027184	-1.516681
C	1.236647	-0.078126	0.679266
C	-0.064065	-0.238628	2.710350
H	3.381476	-0.132712	0.923388
H	2.247309	0.042329	-1.104749
C	1.101608	-0.330040	3.444023
H	-0.999196	-0.301443	3.241521
H	1.047709	-0.445724	4.521452
C	2.354514	-0.278330	2.805468
H	3.267550	-0.344117	3.388564
C	2.422030	-0.157248	1.433323
C	0.553840	0.067316	-2.995171
H	1.412055	0.730012	-3.166723
H	0.872354	-0.939133	-3.304781
C	-2.234144	0.022774	-1.916678
H	-2.727582	1.005607	-1.849628
H	-2.970486	-0.720801	-1.579483
C	-1.894617	-0.269044	-3.386912
H	-1.719163	-1.344846	-3.516169
H	-2.756918	-0.012992	-4.010105
C	-0.653890	0.507005	-3.829919
H	-0.819117	1.584985	-3.706855
H	-0.443527	0.335213	-4.889833
N	-2.476311	0.161012	0.874829
H	-3.164515	0.228902	0.139870
C	-3.052011	0.224787	2.217034
H	-4.110004	0.466128	2.102821
H	-2.587689	1.013269	2.814971
H	-2.977449	-0.733952	2.739848

Point 20 $\theta = 190°$

C	-1.032974	-0.030405	-0.992370
C	-1.215031	-0.011002	0.430486
N	1.316555	0.071937	-0.684520
C	-0.051558	-0.126119	1.291860
C	0.246366	0.044900	-1.514267
C	1.231133	-0.047972	0.683551
C	-0.078266	-0.347265	2.695224
H	3.375128	-0.030104	0.945009
H	2.240747	0.145300	-1.095629
C	1.084806	-0.428835	3.434204
H	-1.016863	-0.489819	3.206998
H	1.029250	-0.607312	4.502946

C	2.338872	-0.290380	2.810070
H	3.249386	-0.344479	3.398310
C	2.413126	-0.109209	1.444451
C	0.551561	0.108493	-2.991663
H	1.384033	0.804739	-3.157042
H	0.908961	-0.882853	-3.307570
C	-2.236617	-0.043967	-1.920380
H	-2.759525	0.923197	-1.849028
H	-2.950596	-0.810942	-1.587416
C	-1.883494	-0.316652	-3.390977
H	-1.668508	-1.384655	-3.524926
H	-2.752722	-0.088923	-4.015527
C	-0.670859	0.507088	-3.826249
H	-0.876470	1.577414	-3.697350
H	-0.452125	0.349469	-4.886649
N	-2.479286	0.111871	0.879481
H	-3.180048	0.138522	0.153232
C	-3.013423	0.356163	2.218670
H	-4.024116	0.750622	2.098912
H	-2.417114	1.100669	2.750890
H	-3.076330	-0.562489	2.811269

Point 21 $\theta = 200°$

C	-1.036361	-0.063485	-0.993092
C	-1.218225	-0.058344	0.427712
N	1.311050	0.096019	-0.679460
C	-0.054939	-0.156098	1.288655
C	0.242901	0.047471	-1.511337
C	1.227085	-0.040238	0.687468
C	-0.087916	-0.410483	2.685621
H	3.369130	0.023695	0.963406
H	2.233365	0.197667	-1.088906
C	1.072344	-0.479498	3.430087
H	-1.029214	-0.592471	3.182114
H	1.016390	-0.685569	4.493835
C	2.326199	-0.294962	2.816137
H	3.234061	-0.338261	3.409370
C	2.405830	-0.086306	1.454396
C	0.546716	0.137556	-2.987486
H	1.364807	0.852602	-3.144033
H	0.923601	-0.842177	-3.316747
C	-2.239338	-0.093268	-1.921336
H	-2.785356	0.859548	-1.834232
H	-2.934346	-0.882251	-1.599979
C	-1.878834	-0.334828	-3.395686
H	-1.640103	-1.395533	-3.546308

H	-2.752162	-0.116530	-4.017865
C	-0.684216	0.522213	-3.816447
H	-0.913300	1.585599	-3.670748
H	-0.461562	0.386269	-4.879008
N	-2.480728	0.034179	0.892341
H	-3.192302	0.024120	0.175697
C	-2.978052	0.447009	2.206444
H	-3.946399	0.928580	2.055662
H	-2.302158	1.169295	2.668500
H	-3.123968	-0.404521	2.879225

Point 22 $\theta = 210°$

C	-1.038703	-0.094232	-0.990785
C	-1.217491	-0.111361	0.427538
N	1.307420	0.101708	-0.675243
C	-0.054164	-0.186583	1.287151
C	0.240241	0.043233	-1.507536
C	1.226426	-0.044394	0.691104
C	-0.092840	-0.453081	2.681125
H	3.366590	0.054004	0.978310
H	2.227481	0.224359	-1.084332
C	1.064782	-0.506989	3.430571
H	-1.037116	-0.656364	3.165963
H	1.008969	-0.723323	4.492295
C	2.318273	-0.295538	2.822853
H	3.223746	-0.327738	3.420450
C	2.402508	-0.075796	1.462848
C	0.540017	0.160704	-2.982441
H	1.349684	0.887131	-3.129925
H	0.926417	-0.809595	-3.328281
C	-2.242373	-0.131048	-1.917913
H	-2.806553	0.808628	-1.809891
H	-2.921131	-0.939549	-1.610992
C	-1.879606	-0.337625	-3.397139
H	-1.625787	-1.391536	-3.569283
H	-2.756473	-0.119596	-4.014393
C	-0.697659	0.544320	-3.802079
H	-0.941080	1.601411	-3.635351
H	-0.474603	0.432203	-4.867312
N	-2.477392	-0.056132	0.912916
H	-3.196814	-0.105300	0.205092
C	-2.949856	0.517763	2.178509
H	-3.880492	1.052628	1.975869
H	-2.221733	1.227219	2.575828
H	-3.156689	-0.252533	2.928472

Point 23 θ = 220°

C	-1.040152	-0.123733	-0.985036
C	-1.212687	-0.167837	0.430290
N	1.305610	0.097929	-0.671446
C	-0.049084	-0.218805	1.287324
C	0.238183	0.035673	-1.502466
C	1.229351	-0.055453	0.694647
C	-0.092937	-0.485830	2.680493
H	3.367862	0.072650	0.990188
H	2.223007	0.237897	-1.081417
C	1.062395	-0.522338	3.434041
H	-1.040458	-0.701483	3.155945
H	1.007396	-0.739565	4.495643
C	2.315404	-0.293592	2.829569
H	3.218800	-0.314032	3.430838
C	2.403471	-0.071708	1.469911
C	0.531360	0.181353	-2.976071
H	1.335438	0.915628	-3.114761
H	0.922177	-0.780370	-3.340500
C	-2.245935	-0.162135	-1.909523
H	-2.824822	0.765140	-1.778119
H	-2.910398	-0.987850	-1.618202
C	-1.884761	-0.332293	-3.393869
H	-1.620233	-1.379411	-3.589790
H	-2.765480	-0.110316	-4.004168
C	-0.713079	0.570163	-3.783281
H	-0.966091	1.621071	-3.593356
H	-0.492373	0.482854	-4.851298
N	-2.468158	-0.149585	0.941063
H	-3.193053	-0.246768	0.242897
C	-2.929542	0.578128	2.134314
H	-3.813876	1.157880	1.858456
H	-2.158741	1.266004	2.485231
H	-3.204595	-0.102264	2.946452

Point 24 θ = 230°

C	-1.040928	-0.151637	-0.974829
C	-1.204173	-0.223377	0.436973
N	1.304946	0.091407	-0.667392
C	-0.039735	-0.251875	1.289970
C	0.236244	0.027793	-1.495439
C	1.235656	-0.068925	0.698548
C	-0.086513	-0.515495	2.683257
H	3.372771	0.087649	0.998296
H	2.219020	0.247937	-1.079400

C	1.067576	-0.533207	3.438943
H	-1.036414	-0.741577	3.151319
H	1.014833	-0.748076	4.501164
C	2.319240	-0.290231	2.835143
H	3.221365	-0.298395	3.438626
C	2.409017	-0.069578	1.475192
C	0.520270	0.201155	-2.967697
H	1.319555	0.941983	-3.098875
H	0.913413	-0.752183	-3.351254
C	-2.250209	-0.189127	-1.895204
H	-2.841028	0.726503	-1.740583
H	-2.901940	-1.029535	-1.618625
C	-1.893644	-0.324272	-3.384293
H	-1.620335	-1.364483	-3.603687
H	-2.778939	-0.097716	-3.986209
C	-0.731760	0.596463	-3.760269
H	-0.992276	1.641075	-3.547132
H	-0.515556	0.533379	-4.830888
N	-2.453916	-0.239325	0.976457
H	-3.180983	-0.393235	0.289490
C	-2.919046	0.633434	2.072267
H	-3.724719	1.269996	1.695958
H	-2.106213	1.271868	2.419877
H	-3.301576	0.048607	2.914296

Point 25 $\theta = 240°$

C	-1.041842	-0.173000	-0.954241
C	-1.191142	-0.260765	0.454404
N	1.302567	0.107336	-0.662067
C	-0.021968	-0.278281	1.298054
C	0.231503	0.032182	-1.483683
C	1.246675	-0.066304	0.703081
C	-0.060422	-0.558284	2.688170
H	3.382688	0.128272	0.995988
H	2.210674	0.287106	-1.078593
C	1.096634	-0.558782	3.439007
H	-1.006792	-0.813709	3.149659
H	1.053665	-0.787028	4.498920
C	2.341656	-0.284358	2.832764
H	3.245642	-0.280670	3.433491
C	2.423614	-0.051133	1.474456
C	0.501297	0.225264	-2.956005
H	1.288982	0.978581	-3.086287
H	0.904607	-0.718717	-3.352072
C	-2.256203	-0.221598	-1.868351
H	-2.861368	0.681654	-1.700031

H	-2.891906	-1.075344	-1.596827
C	-1.906580	-0.335065	-3.360791
H	-1.616876	-1.368057	-3.593106
H	-2.799440	-0.117609	-3.954802
C	-0.763009	0.609223	-3.734796
H	-1.038808	1.647033	-3.508084
H	-0.553407	0.561691	-4.807499
N	-2.436630	-0.311163	1.023117
H	-3.159649	-0.521523	0.344209
C	-2.927588	0.698215	1.986039
H	-3.395691	1.534132	1.453688
H	-2.104156	1.086829	2.583538
H	-3.662725	0.240870	2.652652

Point 26 $\theta = 250°$

C	-1.042136	-0.191082	-0.933306
C	-1.175619	-0.310388	0.470654
N	1.303399	0.098142	-0.657325
C	-0.004788	-0.309207	1.306552
C	0.228742	0.028447	-1.472139
C	1.259380	-0.082170	0.707298
C	-0.039877	-0.577969	2.698818
H	3.395258	0.134366	0.993241
H	2.207801	0.287160	-1.078805
C	1.118918	-0.560584	3.445882
H	-0.986568	-0.835436	3.158873
H	1.081733	-0.778937	4.508133
C	2.360961	-0.280779	2.833649
H	3.266016	-0.266203	3.432614
C	2.439026	-0.053316	1.474165
C	0.484993	0.242092	-2.943815
H	1.270134	0.998424	-3.071802
H	0.885901	-0.696087	-3.355935
C	-2.262903	-0.233822	-1.839924
H	-2.871769	0.662672	-1.652657
H	-2.891956	-1.094417	-1.576635
C	-1.923991	-0.322559	-3.336446
H	-1.631186	-1.350414	-3.587145
H	-2.822473	-0.100462	-3.920148
C	-0.787832	0.632679	-3.705666
H	-1.065759	1.665827	-3.461017
H	-0.586821	0.602286	-4.780611
N	-2.416882	-0.388733	1.069601
H	-3.131032	-0.660141	0.401136
C	-2.930666	0.735529	1.886778
H	-3.185007	1.600137	1.261298

H	-2.187370	1.044167	2.622053
H	-3.823628	0.397778	2.416630

Point 27 θ = 260°

C	-1.041522	-0.201783	-0.910963
C	-1.159211	-0.357337	0.487482
N	1.306887	0.080464	-0.651111
C	0.012584	-0.341835	1.316266
C	0.227633	0.025219	-1.458825
C	1.273784	-0.106540	0.712627
C	-0.021748	-0.591743	2.712161
H	3.410258	0.121084	0.992311
H	2.208614	0.273479	-1.077456
C	1.138444	-0.560032	3.455820
H	-0.971398	-0.838676	3.172185
H	1.104811	-0.761592	4.521529
C	2.379409	-0.285940	2.836858
H	3.285381	-0.263527	3.434240
C	2.455634	-0.068828	1.475492
C	0.471839	0.258496	-2.929386
H	1.256647	1.015643	-3.054605
H	0.868053	-0.674770	-3.357038
C	-2.269004	-0.230371	-1.809565
H	-2.873549	0.665059	-1.606129
H	-2.899252	-1.091030	-1.551508
C	-1.941041	-0.300543	-3.309320
H	-1.650321	-1.325188	-3.575404
H	-2.843620	-0.070927	-3.883702
C	-0.807473	0.659333	-3.675259
H	-1.082914	1.689285	-3.414817
H	-0.614868	0.643255	-4.752032
N	-2.395984	-0.453855	1.116425
H	-3.097198	-0.804270	0.469522
C	-2.942306	0.759297	1.773825
H	-3.140996	1.563436	1.053927
H	-2.241306	1.127255	2.525107
H	-3.872269	0.484484	2.275343

Point 28 θ = 270°

C	-1.040262	-0.197655	-0.883830
C	-1.141876	-0.386119	0.509060
N	1.311758	0.070084	-0.642999
C	0.032471	-0.367873	1.328910
C	0.226960	0.031904	-1.442262
C	1.290790	-0.127132	0.719061
C	0.002192	-0.607237	2.727132

H	3.429091	0.102676	0.988343
H	2.211132	0.263188	-1.075182
C	1.165868	-0.570318	3.464350
H	-0.949763	-0.842459	3.188392
H	1.137577	-0.761191	4.532204
C	2.405071	-0.302352	2.837494
H	3.313478	-0.278262	3.431156
C	2.476657	-0.088403	1.475326
C	0.460084	0.276795	-2.912673
H	1.242221	1.036669	-3.038394
H	0.855932	-0.652734	-3.348873
C	-2.274165	-0.211844	-1.774191
H	-2.866678	0.690121	-1.566337
H	-2.913184	-1.063542	-1.510267
C	-1.956226	-0.282491	-3.275712
H	-1.667358	-1.307062	-3.544449
H	-2.862293	-0.052218	-3.844309
C	-0.825260	0.678402	-3.647915
H	-1.099436	1.707631	-3.383350
H	-0.640079	0.665046	-4.726010
N	-2.375685	-0.495038	1.165689
H	-3.055020	-0.938064	0.550815
C	-2.973428	0.775913	1.649108
H	-3.151771	1.495189	0.839320
H	-2.313780	1.237100	2.387887
H	-3.921020	0.538275	2.136506

Point 29 $\theta = 280°$

C	-1.039795	-0.164573	-0.852907
C	-1.126108	-0.384309	0.534545
N	1.317778	0.072139	-0.633937
C	0.053540	-0.379790	1.342974
C	0.226497	0.057736	-1.423132
C	1.309628	-0.140082	0.725256
C	0.031325	-0.620494	2.741770
H	3.452048	0.073603	0.978431
H	2.215823	0.256937	-1.073372
C	1.201350	-0.595176	3.468642
H	-0.922345	-0.839355	3.206953
H	1.180204	-0.784778	4.536909
C	2.438613	-0.336985	2.832515
H	3.351555	-0.323058	3.419558
C	2.502159	-0.114974	1.471303
C	0.453052	0.300863	-2.895128
H	1.225523	1.069995	-3.025132
H	0.861573	-0.625767	-3.325972

C	-2.276997	-0.163539	-1.738680
H	-2.840766	0.761010	-1.554749
H	-2.941490	-0.985713	-1.447795
C	-1.963588	-0.275423	-3.237985
H	-1.673255	-1.305977	-3.481561
H	-2.871220	-0.060603	-3.810148
C	-0.836712	0.680959	-3.634055
H	-1.115248	1.714083	-3.390192
H	-0.653983	0.646630	-4.712082
N	-2.356517	-0.506345	1.218473
H	-3.000081	-1.061851	0.656324
C	-3.034913	0.777784	1.528513
H	-3.242644	1.389435	0.641092
H	-2.415136	1.359293	2.216106
H	-3.975872	0.545327	2.031464

Point 30 $\theta = 290°$

C	-1.037654	-0.097917	-0.820283
C	-1.112091	-0.343254	0.562369
N	1.327405	0.084145	-0.625953
C	0.075718	-0.371921	1.356753
C	0.229331	0.103395	-1.403306
C	1.330890	-0.145581	0.729586
C	0.064060	-0.622339	2.754678
H	3.479943	0.024963	0.960661
H	2.225481	0.248381	-1.074235
C	1.242657	-0.629921	3.467357
H	-0.891510	-0.813298	3.227349
H	1.229172	-0.825086	4.534768
C	2.478778	-0.392000	2.820199
H	3.397952	-0.403125	3.397531
C	2.532215	-0.152724	1.461689
C	0.453990	0.328155	-2.879256
H	1.210595	1.111477	-3.018989
H	0.886969	-0.596854	-3.289319
C	-2.273887	-0.075239	-1.705619
H	-2.783272	0.888742	-1.576896
H	-2.982850	-0.838775	-1.366050
C	-1.962930	-0.273263	-3.195646
H	-1.673369	-1.315562	-3.384502
H	-2.869941	-0.086742	-3.778679
C	-0.837386	0.665435	-3.636134
H	-1.122066	1.707251	-3.441809
H	-0.652160	0.581869	-4.711014
N	-2.337628	-0.486693	1.270879
H	-2.917370	-1.184297	0.803973

C	-3.138067	0.752048	1.418522
H	-3.437787	1.215104	0.470453
H	-2.565275	1.481339	1.997915
H	-4.035912	0.499289	1.987007

Point 31 $\theta = 300°$

C	-1.025555	0.050783	-0.813981
C	-1.116990	-0.172161	0.586209
N	1.349641	0.051255	-0.638890
C	0.093246	-0.317567	1.368164
C	0.237223	0.171697	-1.396222
C	1.345182	-0.206095	0.712038
C	0.115480	-0.527714	2.771786
H	3.502114	-0.251493	0.875983
H	2.250624	0.137459	-1.099049
C	1.306201	-0.658049	3.455474
H	-0.808588	-0.565451	3.338859
H	1.297428	-0.816750	4.528732
C	2.536324	-0.569210	2.770581
H	3.468590	-0.672973	3.316419
C	2.560055	-0.335201	1.411231
C	0.473831	0.363691	-2.876037
H	1.234601	1.143210	-3.017627
H	0.911297	-0.567917	-3.264998
C	-2.258000	0.061024	-1.701014
H	-2.761180	1.034680	-1.623280
H	-2.962938	-0.686822	-1.320127
C	-1.946230	-0.205758	-3.179918
H	-1.672109	-1.259632	-3.321434
H	-2.849167	-0.031373	-3.773177
C	-0.804945	0.695560	-3.653528
H	-1.073178	1.748430	-3.499246
H	-0.616522	0.568817	-4.723753
N	-2.329209	-0.377014	1.191966
H	-2.237764	-0.804896	2.104845
C	-3.448679	0.583864	1.188769
H	-3.806096	0.784466	0.180607
H	-3.162332	1.531539	1.660656
H	-4.268351	0.136603	1.753958

Point 32 $\theta = 310°$

C	-1.019676	0.049798	-0.793543
C	-1.107870	-0.165737	0.609709
N	1.355116	0.067604	-0.620868
C	0.104958	-0.331350	1.386585
C	0.239490	0.186327	-1.375452

C	1.353183	-0.211924	0.726325
C	0.131991	-0.568978	2.784933
H	3.510270	-0.261850	0.881884
H	2.254690	0.167808	-1.080332
C	1.324995	-0.714747	3.461922
H	-0.789117	-0.621532	3.355945
H	1.319707	-0.896492	4.531526
C	2.552148	-0.612783	2.774295
H	3.486618	-0.727305	3.314178
C	2.570244	-0.354101	1.419288
C	0.469973	0.404775	-2.852206
H	1.226229	1.190682	-2.982239
H	0.909366	-0.516817	-3.262094
C	-2.257725	0.032679	-1.676772
H	-2.811024	0.974303	-1.568584
H	-2.923370	-0.760364	-1.317557
C	-1.942069	-0.184140	-3.163366
H	-1.650069	-1.228642	-3.335526
H	-2.848704	-0.008843	-3.750706
C	-0.815147	0.746400	-3.614232
H	-1.094592	1.790870	-3.426149
H	-0.630754	0.654546	-4.688717
N	-2.314197	-0.322981	1.221678
H	-2.252083	-0.707933	2.153465
C	-3.479219	0.569254	1.063678
H	-4.205854	0.178711	0.347505
H	-3.164892	1.568645	0.753243
H	-3.968615	0.651114	2.036185

Point 33 $\theta = 320°$

C	-1.022295	0.067413	-0.781162
C	-1.106379	-0.138295	0.626873
N	1.355001	0.075379	-0.616314
C	0.112853	-0.326378	1.395579
C	0.235626	0.195997	-1.365630
C	1.357098	-0.212886	0.729060
C	0.148585	-0.582532	2.790255
H	3.514205	-0.278715	0.869100
H	2.252582	0.175519	-1.079115
C	1.344826	-0.744234	3.458491
H	-0.766558	-0.645207	3.369917
H	1.343931	-0.941688	4.525303
C	2.568017	-0.640757	2.765277
H	3.505349	-0.766705	3.297570
C	2.577639	-0.369356	1.412793
C	0.467536	0.417696	-2.842134

H	1.216023	1.211664	-2.968356
H	0.918534	-0.498905	-3.250457
C	-2.258417	0.038340	-1.670636
H	-2.818446	0.976855	-1.576767
H	-2.921116	-0.757221	-1.312998
C	-1.935959	-0.191054	-3.153868
H	-1.633379	-1.234390	-3.314716
H	-2.843130	-0.030478	-3.744655
C	-0.817063	0.745801	-3.609686
H	-1.105535	1.789057	-3.428674
H	-0.629772	0.648652	-4.683200
N	-2.296496	-0.233890	1.268930
H	-2.234725	-0.570258	2.218369
C	-3.512719	0.558681	1.024405
H	-4.200182	0.067859	0.332184
H	-3.259569	1.551516	0.645814
H	-4.022067	0.679521	1.982447

Point 34 $\theta = 330°$

C	-1.024421	0.079755	-0.772668
C	-1.105600	-0.105914	0.641082
N	1.354726	0.093390	-0.610763
C	0.118117	-0.320520	1.401990
C	0.232595	0.204506	-1.358112
C	1.359527	-0.203605	0.732680
C	0.159431	-0.610997	2.789623
H	3.516614	-0.272015	0.863394
H	2.250715	0.198673	-1.074998
C	1.357900	-0.785326	3.451216
H	-0.751991	-0.707105	3.370890
H	1.359458	-1.011881	4.512210
C	2.578669	-0.662900	2.757799
H	3.517996	-0.797315	3.284448
C	2.582423	-0.369871	1.409918
C	0.466490	0.423944	-2.835030
H	1.209260	1.223354	-2.960733
H	0.926328	-0.490346	-3.238557
C	-2.258626	0.042012	-1.667830
H	-2.820465	0.980244	-1.587847
H	-2.922238	-0.752343	-1.310794
C	-1.929999	-0.201130	-3.147446
H	-1.619457	-1.243896	-3.296575
H	-2.837138	-0.053272	-3.741670
C	-0.816937	0.739171	-3.608909
H	-1.112595	1.781914	-3.436719
H	-0.626422	0.634799	-4.681175

N	-2.278570	-0.132838	1.310752
H	-2.207155	-0.400808	2.280393
C	-3.540624	0.552780	0.999252
H	-4.186856	-0.034469	0.343872
H	-3.352222	1.530236	0.550425
H	-4.064932	0.708771	1.943884

Point 35 θ = 340°

C	-1.025431	0.085355	-0.768964
C	-1.103751	-0.071991	0.650393
N	1.355463	0.117597	-0.605631
C	0.121849	-0.315085	1.403676
C	0.231365	0.208652	-1.353942
C	1.362069	-0.185873	0.736365
C	0.162359	-0.652348	2.780468
H	3.519177	-0.241773	0.869010
H	2.250001	0.231993	-1.070079
C	1.361145	-0.833229	3.440293
H	-0.750022	-0.803084	3.349006
H	1.362287	-1.099225	4.492079
C	2.581814	-0.675348	2.754462
H	3.521494	-0.812984	3.279646
C	2.585052	-0.355186	1.412617
C	0.467199	0.419418	-2.832086
H	1.209295	1.218812	-2.961584
H	0.929148	-0.497107	-3.228073
C	-2.258588	0.046813	-1.667848
H	-2.814606	0.989166	-1.598507
H	-2.928747	-0.741307	-1.310894
C	-1.926748	-0.209956	-3.144372
H	-1.614926	-1.253779	-3.283161
H	-2.833301	-0.068499	-3.741108
C	-0.814121	0.727368	-3.611816
H	-1.111295	1.771217	-3.449138
H	-0.621171	0.614045	-4.682743
N	-2.257141	-0.026209	1.346286
H	-2.160307	-0.195946	2.335514
C	-3.561654	0.546208	0.991140
H	-4.161448	-0.127729	0.376663
H	-3.443994	1.504528	0.481489
H	-4.098465	0.722485	1.924842

Point 36 θ = 350°

C	-1.022119	0.103600	-0.769513
C	-1.100734	-0.044232	0.652249
N	1.361273	0.098443	-0.610309

C	0.126295	-0.295644	1.404462
C	0.236278	0.198350	-1.356328
C	1.366736	-0.186827	0.735273
C	0.165720	-0.630054	2.782080
H	3.523136	-0.264683	0.864721
H	2.255899	0.192778	-1.078838
C	1.363395	-0.817599	3.442365
H	-0.746837	-0.778504	3.350980
H	1.362494	-1.081222	4.494745
C	2.584748	-0.673483	2.755245
H	3.523719	-0.816542	3.280238
C	2.588923	-0.363832	1.410959
C	0.477679	0.388687	-2.836914
H	1.246177	1.161331	-2.973892
H	0.909308	-0.546774	-3.222947
C	-2.254630	0.122269	-1.671349
H	-2.753724	1.097157	-1.610232
H	-2.971339	-0.622396	-1.315300
C	-1.935669	-0.160825	-3.145529
H	-1.663057	-1.216822	-3.274722
H	-2.837706	0.008992	-3.741800
C	-0.790749	0.731084	-3.622598
H	-1.052059	1.786435	-3.473138
H	-0.600379	0.598218	-4.691762
N	-2.240632	0.029835	1.365032
H	-2.125202	-0.105254	2.357433
C	-3.599945	0.445489	1.002194
H	-4.157712	-0.350644	0.503130
H	-3.588633	1.337873	0.376544
H	-4.116654	0.691799	1.931521

Rotation in the clockwise direction:

Point 1 $\theta = 0°$

C	-1.025991	-0.017977	-0.775190
C	-1.091260	0.047937	0.653714
N	1.354770	0.149803	-0.647005
C	0.153518	0.004358	1.419268
C	0.223214	0.061926	-1.384209
C	1.382518	0.088194	0.726485
C	0.219035	-0.110935	2.831376
H	3.539318	0.178481	0.838741
H	2.239704	0.225823	-1.136680
C	1.427848	-0.108126	3.498116
H	-0.679382	-0.240170	3.426785
H	1.446947	-0.206349	4.578390
C	2.635005	0.012100	2.782125

H	3.582472	0.018913	3.311279
C	2.615300	0.103907	1.405831
C	0.449027	0.041976	-2.879430
H	1.198425	0.802895	-3.135158
H	0.898374	-0.930176	-3.131635
C	-2.262142	-0.163837	-1.660615
H	-2.794034	0.794860	-1.713287
H	-2.950466	-0.882910	-1.210928
C	-1.945021	-0.617604	-3.092010
H	-1.640252	-1.672711	-3.091381
H	-2.857093	-0.551753	-3.693598
C	-0.832600	0.240251	-3.691736
H	-1.126213	1.297613	-3.677962
H	-0.643744	-0.024997	-4.736257
N	-2.225856	0.162362	1.369931
H	-2.084280	0.233440	2.365564
C	-3.640651	0.250732	0.992633
H	-3.802797	0.984530	0.204197
H	-4.184556	0.582668	1.878707
H	-4.045137	-0.718224	0.687938

Point 2 $\theta = 350°$

C	-1.029728	-0.018731	-0.771359
C	-1.093508	0.027279	0.658072
N	1.346581	0.188294	-0.644365
C	0.151274	-0.017066	1.421794
C	0.215773	0.093244	-1.382155
C	1.377587	0.095490	0.727648
C	0.220316	-0.150379	2.832005
H	3.533470	0.208620	0.838053
H	2.229787	0.287221	-1.133172
C	1.430506	-0.147375	3.496078
H	-0.676095	-0.289142	3.428361
H	1.452917	-0.259661	4.574916
C	2.634916	-0.004458	2.779436
H	3.583391	0.002788	3.306779
C	2.611411	0.112910	1.405157
C	0.438235	0.093894	-2.877886
H	1.141428	0.898801	-3.130830
H	0.943474	-0.848744	-3.135897
C	-2.261371	-0.224475	-1.650810
H	-2.837550	0.706454	-1.719091
H	-2.914851	-0.967017	-1.185453
C	-1.923348	-0.684101	-3.075427
H	-1.566479	-1.722638	-3.060216
H	-2.837276	-0.671690	-3.677610

C	-0.855178	0.220973	-3.686807
H	-1.200665	1.262605	-3.682059
H	-0.656716	-0.044240	-4.729533
N	-2.234421	0.108110	1.368495
H	-2.106828	0.120860	2.368483
C	-3.623786	0.358429	0.969579
H	-3.686374	1.152326	0.225477
H	-4.156844	0.690356	1.862325
H	-4.116046	-0.541935	0.594013

Point 3 $\theta = 340°$

C	-1.031581	-0.036871	-0.768200
C	-1.094300	-0.000552	0.660173
N	1.339065	0.209083	-0.642129
C	0.148356	-0.037194	1.423774
C	0.209946	0.104309	-1.381036
C	1.372742	0.096987	0.728787
C	0.218660	-0.175061	2.833387
H	3.527483	0.233594	0.839600
H	2.220506	0.329069	-1.129632
C	1.429376	-0.165418	3.496134
H	-0.677381	-0.318005	3.429266
H	1.454064	-0.281393	4.574535
C	2.631915	-0.007033	2.779088
H	3.580621	0.005761	3.305923
C	2.606670	0.122327	1.405890
C	0.425184	0.125296	-2.877107
H	1.099211	0.956114	-3.125967
H	0.959850	-0.797159	-3.148095
C	-2.259073	-0.299759	-1.636730
H	-2.890120	0.595081	-1.691689
H	-2.861942	-1.081830	-1.164915
C	-1.909926	-0.732446	-3.067468
H	-1.514098	-1.756835	-3.063979
H	-2.826003	-0.749216	-3.666184
C	-0.878371	0.217140	-3.675132
H	-1.259538	1.246077	-3.655113
H	-0.678735	-0.028535	-4.722388
N	-2.246357	0.049207	1.357967
H	-2.134450	0.027126	2.359834
C	-3.593623	0.460125	0.943706
H	-3.554886	1.343897	0.303846
H	-4.141206	0.722088	1.850658
H	-4.138059	-0.338975	0.437195

Point 4 $\theta = 330°$

C	-1.030032	-0.043004	-0.771169
C	-1.093414	-0.035730	0.655595
N	1.340357	0.184509	-0.643718
C	0.145001	-0.043111	1.422925
C	0.211653	0.099719	-1.384585
C	1.371621	0.078975	0.727767
C	0.212177	-0.133240	2.836776
H	3.527331	0.203303	0.838643
H	2.223992	0.295957	-1.129684
C	1.421980	-0.116666	3.500500
H	-0.687425	-0.220575	3.437508
H	1.443800	-0.192397	4.582548
C	2.627532	0.005886	2.780980
H	3.575571	0.022211	3.308919
C	2.605135	0.107647	1.405547
C	0.424381	0.129319	-2.880579
H	1.099338	0.960546	-3.125648
H	0.956490	-0.792296	-3.159328
C	-2.258583	-0.304210	-1.636305
H	-2.894805	0.587780	-1.679981
H	-2.854717	-1.091811	-1.163907
C	-1.913746	-0.723916	-3.072031
H	-1.519544	-1.748900	-3.079085
H	-2.830927	-0.733741	-3.669148
C	-0.881774	0.229379	-3.673932
H	-1.261113	1.258745	-3.644217
H	-0.685208	-0.007697	-4.723741
N	-2.259152	-0.063403	1.337754
H	-2.164510	-0.186964	2.334189
C	-3.573427	0.468235	0.950598
H	-3.466150	1.385531	0.368000
H	-4.107065	0.711681	1.871210
H	-4.170768	-0.254761	0.391598

Point 5 $\theta = 320°$

C	-1.026904	-0.056169	-0.777931
C	-1.091695	-0.069868	0.645990
N	1.342039	0.166578	-0.646579
C	0.140082	-0.050154	1.417490
C	0.215377	0.090876	-1.390831
C	1.369819	0.069523	0.725638
C	0.198843	-0.106183	2.833614
H	3.525315	0.198120	0.845503
H	2.227697	0.273659	-1.130320
C	1.405370	-0.076309	3.502266
H	-0.707203	-0.161360	3.428143

H	1.422317	-0.122967	4.586061
C	2.614907	0.028156	2.785639
H	3.560240	0.053497	3.318080
C	2.600161	0.108697	1.408590
C	0.426082	0.122588	-2.886694
H	1.107073	0.948930	-3.131560
H	0.949761	-0.802617	-3.169611
C	-2.257921	-0.308376	-1.638742
H	-2.892394	0.585939	-1.668852
H	-2.853059	-1.097035	-1.165627
C	-1.920134	-0.715534	-3.079804
H	-1.533576	-1.743261	-3.098184
H	-2.838314	-0.712620	-3.675382
C	-0.882220	0.235828	-3.675677
H	-1.254655	1.267426	-3.637469
H	-0.689330	0.005430	-4.727652
N	-2.268970	-0.170764	1.310499
H	-2.178318	-0.365423	2.296551
C	-3.546222	0.479359	0.974185
H	-3.375559	1.426589	0.457713
H	-4.061928	0.691608	1.912739
H	-4.192680	-0.157162	0.366216

Point 6 $\theta = 310°$

C	-1.022778	-0.075325	-0.787844
C	-1.090961	-0.099659	0.632760
N	1.342863	0.158100	-0.649869
C	0.132504	-0.056914	1.409428
C	0.220132	0.080082	-1.399215
C	1.365798	0.069718	0.722976
C	0.180968	-0.094393	2.826764
H	3.519984	0.216223	0.856185
H	2.230548	0.265596	-1.130328
C	1.382903	-0.047643	3.502018
H	-0.731911	-0.140975	3.411346
H	1.394100	-0.078381	4.586473
C	2.596595	0.056206	2.791158
H	3.538100	0.093827	3.329651
C	2.591455	0.124177	1.413254
C	0.429763	0.108705	-2.894841
H	1.119149	0.927246	-3.142255
H	0.942277	-0.822521	-3.178665
C	-2.256599	-0.315251	-1.644147
H	-2.885039	0.584366	-1.660193
H	-2.854439	-1.101918	-1.170036
C	-1.926550	-0.710448	-3.090345

H	-1.550417	-1.741729	-3.119964
H	-2.845372	-0.692305	-3.684584
C	-0.880129	0.236231	-3.680217
H	-1.243672	1.270722	-3.634989
H	-0.690534	0.011016	-4.733918
N	-2.279478	-0.266981	1.276109
H	-2.184707	-0.512062	2.251414
C	-3.513787	0.497515	1.010890
H	-3.282646	1.466846	0.562582
H	-4.007751	0.672468	1.968677
H	-4.206372	-0.045537	0.363724

Point 7 $\theta = 300°$

C	-1.028973	-0.077677	-0.807967
C	-1.099073	-0.111024	0.610677
N	1.338346	0.141267	-0.666182
C	0.120446	-0.046918	1.389078
C	0.218399	0.064124	-1.418047
C	1.357674	0.074361	0.707280
C	0.162547	-0.057548	2.807854
H	3.511249	0.228604	0.847256
H	2.228286	0.235825	-1.145779
C	1.361209	0.006054	3.487119
H	-0.754199	-0.091424	3.386929
H	1.367537	-0.002222	4.572032
C	2.578515	0.099119	2.780249
H	3.517158	0.148669	3.322762
C	2.580328	0.143294	1.401405
C	0.435642	0.067758	-2.913207
H	1.128943	0.879724	-3.171095
H	0.948108	-0.869838	-3.175604
C	-2.259601	-0.291462	-1.671506
H	-2.841629	0.639076	-1.722260
H	-2.899420	-1.034458	-1.181727
C	-1.929447	-0.734365	-3.103421
H	-1.569199	-1.771690	-3.101705
H	-2.844795	-0.718412	-3.703042
C	-0.867621	0.182853	-3.712058
H	-1.221885	1.221439	-3.701102
H	-0.671276	-0.075285	-4.756931
N	-2.288982	-0.328546	1.255051
H	-2.160557	-0.616788	2.216931
C	-3.484427	0.527454	1.134290
H	-3.277236	1.551518	1.467679
H	-4.263200	0.096669	1.766179
H	-3.858866	0.556851	0.112863

Point 8 θ = 290°

C	-1.028034	-0.094052	-0.823651
C	-1.102300	-0.131511	0.591520
N	1.334994	0.145294	-0.672588
C	0.107227	-0.050056	1.375744
C	0.220934	0.056030	-1.431201
C	1.348121	0.087488	0.701277
C	0.136722	-0.057833	2.795113
H	3.498878	0.272539	0.858397
H	2.227163	0.244353	-1.147769
C	1.329132	0.026636	3.482339
H	-0.787183	-0.105726	3.361587
H	1.328719	0.021728	4.567310
C	2.550605	0.136204	2.783518
H	3.483954	0.201212	3.333518
C	2.564298	0.176062	1.404487
C	0.439831	0.046282	-2.925714
H	1.138488	0.851134	-3.191215
H	0.946088	-0.897113	-3.179578
C	-2.260807	-0.293914	-1.684582
H	-2.827097	0.646629	-1.736601
H	-2.913359	-1.020369	-1.186909
C	-1.934515	-0.743570	-3.115085
H	-1.584320	-1.784317	-3.110420
H	-2.848455	-0.720244	-3.716554
C	-0.863455	0.162549	-3.726054
H	-1.210868	1.203503	-3.722659
H	-0.666748	-0.103366	-4.768931
N	-2.304668	-0.398831	1.212208
H	-2.170139	-0.760095	2.150200
C	-3.432046	0.555694	1.207602
H	-3.182565	1.475700	1.750457
H	-4.284817	0.072813	1.688711
H	-3.719777	0.816146	0.189525

Point 9 θ = 280°

C	-1.026685	-0.127035	-0.843455
C	-1.109300	-0.157590	0.567419
N	1.329731	0.147391	-0.678030
C	0.087954	-0.056120	1.360680
C	0.224918	0.038340	-1.446010
C	1.333419	0.099883	0.696291
C	0.102612	-0.063540	2.780585
H	3.479874	0.321955	0.874192
H	2.224726	0.256337	-1.146448

C	1.286849	0.044728	3.477778
H	-0.827977	-0.132941	3.333647
H	1.277741	0.040384	4.562738
C	2.513153	0.176082	2.789573
H	3.439518	0.259187	3.348882
C	2.541227	0.211778	1.410631
C	0.447349	0.023287	-2.939352
H	1.157792	0.817237	-3.206076
H	0.939348	-0.928110	-3.191770
C	-2.259708	-0.318761	-1.703740
H	-2.825884	0.623055	-1.736270
H	-2.911076	-1.048116	-1.209306
C	-1.935386	-0.747668	-3.140934
H	-1.594248	-1.791396	-3.152255
H	-2.847826	-0.707611	-3.743740
C	-0.855301	0.157134	-3.739325
H	-1.194037	1.200868	-3.725320
H	-0.658976	-0.099230	-4.784677
N	-2.327994	-0.454937	1.165070
H	-2.186247	-0.885209	2.074258
C	-3.366315	0.592224	1.292411
H	-3.030930	1.428577	1.918445
H	-4.253118	0.137868	1.738536
H	-3.641207	0.978950	0.309573

Point 10 $\theta = 270°$

C	-1.028669	-0.162147	-0.867643
C	-1.121350	-0.181556	0.538664
N	1.320959	0.148912	-0.684850
C	0.062975	-0.059871	1.342323
C	0.227323	0.017988	-1.463198
C	1.313479	0.112972	0.689826
C	0.061499	-0.067553	2.762569
H	3.454766	0.371195	0.890135
H	2.218986	0.268833	-1.145542
C	1.236411	0.064126	3.470826
H	-0.875150	-0.160067	3.301608
H	1.217427	0.059517	4.555689
C	2.467827	0.217298	2.794757
H	3.386163	0.318400	3.364256
C	2.511806	0.248137	1.416119
C	0.457019	-0.000034	-2.954819
H	1.179466	0.783588	-3.219477
H	0.935710	-0.958646	-3.205911
C	-2.258781	-0.349755	-1.732288
H	-2.828422	0.590764	-1.745724

H	-2.907955	-1.085592	-1.245977
C	-1.930768	-0.755015	-3.175449
H	-1.596066	-1.800586	-3.203378
H	-2.840379	-0.699907	-3.781290
C	-0.842577	0.151332	-3.757578
H	-1.174446	1.197055	-3.731852
H	-0.643489	-0.093293	-4.805222
N	-2.358475	-0.488927	1.118909
H	-2.212554	-1.003120	1.984733
C	-3.287461	0.630924	1.402312
H	-2.860857	1.363506	2.099864
H	-4.202397	0.214016	1.827894
H	-3.548023	1.144506	0.473711

Point 11 $\theta = 260°$

C	-1.035150	-0.193066	-0.893478
C	-1.139731	-0.194763	0.508379
N	1.307001	0.158777	-0.691926
C	0.032704	-0.058048	1.322869
C	0.226241	0.002290	-1.480770
C	1.287868	0.131464	0.682820
C	0.017594	-0.076787	2.743189
H	3.423505	0.423375	0.904180
H	2.207647	0.292599	-1.144432
C	1.183750	0.071566	3.462077
H	-0.922731	-0.198603	3.269232
H	1.156187	0.056807	4.546699
C	2.418974	0.251557	2.798250
H	3.329564	0.366526	3.377468
C	2.477123	0.285604	1.420310
C	0.467161	-0.016256	-2.970160
H	1.194818	0.764011	-3.230162
H	0.942767	-0.977265	-3.218283
C	-2.257765	-0.386959	-1.768070
H	-2.835385	0.548790	-1.771560
H	-2.904277	-1.130258	-1.291574
C	-1.917317	-0.774771	-3.213052
H	-1.579492	-1.819144	-3.250511
H	-2.822844	-0.716180	-3.824636
C	-0.827700	0.139546	-3.780157
H	-1.161565	1.184440	-3.747567
H	-0.620848	-0.095670	-4.828441
N	-2.398825	-0.487538	1.075448
H	-2.263376	-1.098321	1.879986
C	-3.197991	0.677767	1.528346
H	-2.677761	1.291691	2.275917

H	-4.131961	0.303518	1.952532
H	-3.444182	1.310300	0.671076

Point 12 θ = 250°

C	-1.043449	-0.212524	-0.917173
C	-1.162094	-0.186919	0.480604
N	1.290491	0.180646	-0.698480
C	0.001745	-0.046127	1.305320
C	0.223476	-0.005945	-1.496515
C	1.260348	0.159946	0.676110
C	-0.019337	-0.094128	2.725367
H	3.390310	0.483277	0.912977
H	2.193014	0.329278	-1.143272
C	1.140716	0.061793	3.452064
H	-0.958061	-0.256868	3.241891
H	1.109133	0.021246	4.535958
C	2.376221	0.278285	2.798707
H	3.280832	0.402185	3.385383
C	2.442783	0.327531	1.421889
C	0.477951	-0.029713	-2.983227
H	1.206159	0.750840	-3.240662
H	0.957617	-0.991035	-3.222537
C	-2.255840	-0.420326	-1.804334
H	-2.841227	0.510224	-1.810600
H	-2.902318	-1.167007	-1.335149
C	-1.897861	-0.805084	-3.245831
H	-1.551139	-1.846739	-3.280969
H	-2.798404	-0.754169	-3.865406
C	-0.810842	0.117492	-3.804420
H	-1.152222	1.160017	-3.774546
H	-0.593114	-0.116256	-4.850804
N	-2.446360	-0.442046	1.032994
H	-2.351882	-1.163051	1.748916
C	-3.114326	0.726499	1.657574
H	-2.518528	1.211469	2.442323
H	-4.060489	0.384275	2.082163
H	-3.339303	1.469934	0.887685

Point 13 θ = 240°

C	-1.045672	-0.236338	-0.932767
C	-1.178828	-0.170257	0.461315
N	1.278873	0.202451	-0.704588
C	-0.020246	-0.023235	1.292797
C	0.224455	-0.021905	-1.507511
C	1.240121	0.194581	0.669692
C	-0.038855	-0.106630	2.711638

H	3.364871	0.547565	0.913484
H	2.181069	0.367344	-1.144678
C	1.118233	0.053330	3.441655
H	-0.971221	-0.317287	3.220256
H	1.088357	-0.019858	4.523918
C	2.350122	0.309072	2.794915
H	3.251236	0.440428	3.385329
C	2.418582	0.374801	1.419254
C	0.487917	-0.049533	-2.992160
H	1.219741	0.727982	-3.248138
H	0.965121	-1.013318	-3.226727
C	-2.249949	-0.463979	-1.828290
H	-2.852766	0.454694	-1.826572
H	-2.887617	-1.225500	-1.372536
C	-1.880036	-0.835082	-3.270671
H	-1.525191	-1.873836	-3.312284
H	-2.778259	-0.786888	-3.893849
C	-0.797089	0.097991	-3.818858
H	-1.143737	1.138585	-3.783041
H	-0.573467	-0.127619	-4.865746
N	-2.490178	-0.351678	0.990357
H	-2.516203	-1.204409	1.549928
C	-3.047646	0.770139	1.777975
H	-2.446123	1.079300	2.642049
H	-4.038664	0.469043	2.125021
H	-3.172951	1.637045	1.122830

Point 14 $\theta = 230°$

C	-1.029456	-0.314308	-0.932311
C	-1.170186	-0.202064	0.479271
N	1.280621	0.210196	-0.719836
C	-0.000836	0.010438	1.298881
C	0.216420	-0.079632	-1.504257
C	1.242194	0.238338	0.656395
C	-0.005705	-0.056906	2.716065
H	3.353752	0.655047	0.878448
H	2.168928	0.400309	-1.172107
C	1.151258	0.151409	3.438068
H	-0.921773	-0.311157	3.234408
H	1.132064	0.084648	4.520861
C	2.364270	0.434202	2.775527
H	3.268158	0.604423	3.351807
C	2.416758	0.468396	1.396308
C	0.465957	-0.087881	-2.992851
H	1.181167	0.705434	-3.245877
H	0.953818	-1.040167	-3.249130

C	-2.237097	-0.606036	-1.808325
H	-2.919600	0.256499	-1.768682
H	-2.793847	-1.461415	-1.401044
C	-1.882966	-0.913152	-3.272237
H	-1.503499	-1.940143	-3.350754
H	-2.793130	-0.866649	-3.877888
C	-0.828593	0.059994	-3.801733
H	-1.195861	1.091749	-3.730271
H	-0.617526	-0.131335	-4.858043
N	-2.405874	-0.270243	1.046420
H	-3.119431	-0.593655	0.405724
C	-2.949511	0.696163	2.020786
H	-3.259028	0.200311	2.945813
H	-3.822054	1.186030	1.579634
H	-2.205392	1.458158	2.254926

Point 15 $\theta = 220°$

C	-1.031866	-0.288104	-0.946291
C	-1.184465	-0.149307	0.465185
N	1.280621	0.215408	-0.725051
C	-0.013401	0.041640	1.291782
C	0.217338	-0.073053	-1.512474
C	1.234680	0.250014	0.650546
C	-0.014927	-0.028263	2.709262
H	3.350673	0.637945	0.872147
H	2.174029	0.389451	-1.173175
C	1.145336	0.161410	3.431622
H	-0.929682	-0.270533	3.233547
H	1.124172	0.092384	4.514210
C	2.361148	0.429762	2.770191
H	3.267674	0.587768	3.345791
C	2.411701	0.464607	1.391094
C	0.478688	-0.107955	-2.998794
H	1.199576	0.678036	-3.258570
H	0.964878	-1.066246	-3.234925
C	-2.236201	-0.580419	-1.826165
H	-2.907895	0.291814	-1.811292
H	-2.807276	-1.420354	-1.405984
C	-1.874117	-0.920971	-3.280685
H	-1.502945	-1.952523	-3.334878
H	-2.779411	-0.879223	-3.893968
C	-0.807812	0.032781	-3.821291
H	-1.168010	1.068396	-3.773846
H	-0.589882	-0.181688	-4.871769
N	-2.429619	-0.188429	0.999454
H	-3.147213	-0.457332	0.339841

C	-2.953077	0.649152	2.090620
H	-3.146139	0.065644	2.996407
H	-3.896653	1.089440	1.758850
H	-2.255925	1.455748	2.322607

Point 16 $\theta = 210°$

C	-1.033603	-0.259898	-0.956018
C	-1.195123	-0.094466	0.454825
N	1.281826	0.219483	-0.729593
C	-0.021654	0.072945	1.287224
C	0.218343	-0.065882	-1.518647
C	1.230647	0.260515	0.645368
C	-0.017825	0.003776	2.705264
H	3.351333	0.618340	0.862547
H	2.179649	0.376841	-1.174630
C	1.146630	0.175843	3.425766
H	-0.930435	-0.224881	3.237161
H	1.124778	0.107268	4.508352
C	2.364564	0.427104	2.763384
H	3.274463	0.573082	3.336808
C	2.411289	0.459815	1.384337
C	0.488990	-0.128107	-3.002532
H	1.215991	0.649590	-3.270221
H	0.971970	-1.092610	-3.218968
C	-2.236070	-0.551383	-1.838517
H	-2.895197	0.330909	-1.848650
H	-2.822525	-1.373951	-1.404863
C	-1.868691	-0.926604	-3.283038
H	-1.506872	-1.962455	-3.312705
H	-2.769924	-0.889537	-3.902586
C	-0.790575	0.006193	-3.836511
H	-1.142429	1.045491	-3.812947
H	-0.567857	-0.231898	-4.880904
N	-2.448806	-0.100965	0.958937
H	-3.166200	-0.323892	0.283163
C	-2.966301	0.594480	2.143265
H	-3.083958	-0.079135	2.998224
H	-3.949837	0.997294	1.890930
H	-2.312592	1.423694	2.419775

Point 17 $\theta = 200°$

C	-1.034644	-0.229724	-0.962607
C	-1.201385	-0.042392	0.447665
N	1.285913	0.213671	-0.733307
C	-0.025472	0.103220	1.284374
C	0.220352	-0.061980	-1.523184

C	1.230875	0.264343	0.640925
C	-0.017060	0.047098	2.703559
H	3.356934	0.587139	0.851470
H	2.188093	0.350808	-1.175924
C	1.151601	0.204065	3.421045
H	-0.928753	-0.158813	3.243999
H	1.128689	0.145922	4.504211
C	2.372568	0.428106	2.756079
H	3.286003	0.562959	3.326577
C	2.415719	0.449032	1.376980
C	0.497707	-0.150923	-3.004594
H	1.234046	0.615258	-3.279995
H	0.972547	-1.123271	-3.203089
C	-2.237274	-0.514425	-1.847102
H	-2.879867	0.379752	-1.880325
H	-2.841781	-1.317316	-1.401299
C	-1.868507	-0.923847	-3.281803
H	-1.520696	-1.964882	-3.288665
H	-2.766359	-0.887025	-3.906280
C	-0.775447	-0.016478	-3.847997
H	-1.114014	1.027493	-3.846593
H	-0.550634	-0.277785	-4.886394
N	-2.461736	-0.015648	0.926331
H	-3.175550	-0.200296	0.236124
C	-2.986227	0.525500	2.181987
H	-3.034501	-0.232719	2.970540
H	-4.001519	0.878467	1.989799
H	-2.385621	1.371690	2.521492

Point 18 $\theta = 190°$

C	-1.034899	-0.196949	-0.966463
C	-1.203128	0.004795	0.443833
N	1.293705	0.190146	-0.735395
C	-0.025062	0.133577	1.283188
C	0.223796	-0.064486	-1.525925
C	1.235735	0.256965	0.637723
C	-0.013553	0.111674	2.703878
H	3.368391	0.533109	0.839833
H	2.200559	0.299925	-1.175958
C	1.159278	0.256138	3.417392
H	-0.926358	-0.053338	3.254108
H	1.134054	0.225882	4.501640
C	2.385055	0.433746	2.748571
H	3.302269	0.557810	3.315417
C	2.425447	0.426519	1.369599
C	0.505134	-0.179514	-3.004926

H	1.257431	0.568578	-3.286943
H	0.962224	-1.163294	-3.188098
C	-2.239947	-0.465992	-1.852902
H	-2.861398	0.442340	-1.904333
H	-2.865319	-1.247639	-1.398160
C	-1.875186	-0.906321	-3.279333
H	-1.549655	-1.954507	-3.268001
H	-2.770079	-0.860537	-3.907471
C	-0.761231	-0.031643	-3.855930
H	-1.077720	1.019092	-3.872729
H	-0.538062	-0.314380	-4.889077
N	-2.468530	0.059023	0.903154
H	-3.175706	-0.089989	0.198240
C	-3.011442	0.434062	2.208220
H	-2.970699	-0.392924	2.924778
H	-4.059364	0.701166	2.060051
H	-2.491742	1.303966	2.616020

Point 19 $\theta = 180°$

C	-1.034974	-0.162133	-0.968589
C	-1.201533	0.042818	0.442982
N	1.305297	0.130786	-0.733601
C	-0.021830	0.166885	1.282899
C	0.228604	-0.081548	-1.526131
C	1.244450	0.227815	0.637174
C	-0.010195	0.222145	2.703250
H	3.385448	0.430780	0.831808
H	2.217644	0.198571	-1.171316
C	1.166358	0.356556	3.412563
H	-0.927649	0.138504	3.261676
H	1.136492	0.389302	4.496620
C	2.399821	0.447018	2.741339
H	3.320843	0.559248	3.304444
C	2.439489	0.379314	1.364428
C	0.511138	-0.220083	-3.002961
H	1.292129	0.497066	-3.287360
H	0.931623	-1.221702	-3.176742
C	-2.244785	-0.399858	-1.858136
H	-2.838858	0.526180	-1.916979
H	-2.894564	-1.160155	-1.401520
C	-1.891738	-0.860723	-3.281191
H	-1.604356	-1.919926	-3.262874
H	-2.782929	-0.786554	-3.911888
C	-0.745276	-0.031002	-3.859993
H	-1.022785	1.030531	-3.884954
H	-0.529025	-0.328758	-4.890412

N	-2.470624	0.106848	0.891902
H	-3.169918	-0.000553	0.172287
C	-3.035351	0.300217	2.226374
H	-2.853903	-0.561833	2.875990
H	-4.114149	0.412008	2.106710
H	-2.650895	1.209234	2.696202

Point 20 θ = 170°

C	-1.039310	-0.121245	-0.973426
C	-1.201560	0.060079	0.441994
N	1.315350	-0.022534	-0.718176
C	-0.022243	0.212667	1.277362
C	0.231689	-0.138073	-1.520500
C	1.250475	0.144377	0.645390
C	-0.018775	0.455132	2.678203
H	3.399107	0.202115	0.853697
H	2.234069	-0.038696	-1.147602
C	1.158064	0.584151	3.387749
H	-0.945164	0.558454	3.218083
H	1.120754	0.770587	4.455925
C	2.401292	0.480903	2.736386
H	3.323195	0.577788	3.300891
C	2.447595	0.268550	1.374645
C	0.514096	-0.297220	-2.995113
H	1.357317	0.349614	-3.269927
H	0.844789	-1.331252	-3.172566
C	-2.255874	-0.285796	-1.871159
H	-2.805767	0.667808	-1.909859
H	-2.941668	-1.024061	-1.431512
C	-1.926883	-0.739266	-3.303159
H	-1.722349	-1.817725	-3.306931
H	-2.805142	-0.583411	-3.937092
C	-0.714180	0.008353	-3.858214
H	-0.905195	1.089056	-3.865264
H	-0.513624	-0.287407	-4.892397
N	-2.468989	0.083453	0.902213
H	-3.171953	0.032324	0.180277
C	-3.025006	0.055312	2.254493
H	-2.573098	-0.738470	2.854652
H	-4.091468	-0.156325	2.160618
H	-2.915545	1.017759	2.764319

Point 21 θ = 160°

C	-1.045673	-0.083012	-0.977752
C	-1.204981	0.097347	0.436018
N	1.311325	-0.088198	-0.707357

C	-0.026405	0.247929	1.269711
C	0.228194	-0.157107	-1.516268
C	1.246704	0.113462	0.651905
C	-0.030587	0.571963	2.653309
H	3.394506	0.095895	0.883255
H	2.230714	-0.152016	-1.131077
C	1.143364	0.691703	3.369079
H	-0.960610	0.759538	3.166275
H	1.104781	0.945505	4.423247
C	2.387503	0.496827	2.739410
H	3.306626	0.582426	3.310251
C	2.440643	0.219876	1.389156
C	0.510924	-0.343171	-2.987654
H	1.382555	0.264052	-3.264285
H	0.797616	-1.392096	-3.153881
C	-2.263420	-0.208618	-1.879798
H	-2.776982	0.764364	-1.926918
H	-2.978134	-0.916849	-1.437333
C	-1.945221	-0.685238	-3.306745
H	-1.785019	-1.771180	-3.301825
H	-2.812412	-0.497926	-3.947326
C	-0.698991	0.007098	-3.859868
H	-0.844375	1.094760	-3.875907
H	-0.505186	-0.304533	-4.890685
N	-2.466758	0.127853	0.913912
H	-3.181744	0.117068	0.201563
C	-2.989161	-0.090135	2.264080
H	-2.399294	-0.839274	2.796513
H	-4.008982	-0.466795	2.163110
H	-3.027523	0.835481	2.847886

Point 22 $\theta = 150°$

C	-1.050618	-0.046488	-0.978814
C	-1.205671	0.145988	0.430933
N	1.306480	-0.112669	-0.700489
C	-0.027635	0.280805	1.264198
C	0.224367	-0.159157	-1.512365
C	1.244245	0.108102	0.656324
C	-0.038564	0.638232	2.638841
H	3.390182	0.045109	0.905723
H	2.224799	-0.207652	-1.121022
C	1.132398	0.745562	3.361090
H	-0.971897	0.864968	3.132435
H	1.093922	1.027109	4.408205
C	2.376208	0.504780	2.744938
H	3.292476	0.580173	3.321800

C	2.435058	0.199985	1.400573
C	0.505039	-0.375861	-2.980000
H	1.391388	0.205806	-3.264806
H	0.767360	-1.433886	-3.128007
C	-2.268720	-0.150085	-1.882537
H	-2.750527	0.837612	-1.949965
H	-3.007021	-0.825410	-1.428210
C	-1.959474	-0.662614	-3.298722
H	-1.826372	-1.751928	-3.272313
H	-2.819755	-0.465986	-3.945777
C	-0.694694	-0.012000	-3.861057
H	-0.813052	1.078429	-3.897508
H	-0.506299	-0.347152	-4.885472
N	-2.461435	0.202684	0.928988
H	-3.185565	0.229409	0.225571
C	-2.957016	-0.192253	2.252334
H	-2.287259	-0.919446	2.715077
H	-3.933580	-0.661895	2.114884
H	-3.084770	0.666732	2.919150

Point 23 $\theta = 140°$

C	-1.053290	-0.012035	-0.975665
C	-1.201483	0.200182	0.428473
N	1.303936	-0.116950	-0.696111
C	-0.023725	0.313701	1.260960
C	0.221823	-0.153553	-1.507850
C	1.246121	0.115602	0.659343
C	-0.040760	0.681109	2.632194
H	3.390479	0.020714	0.921609
H	2.220279	-0.235180	-1.115569
C	1.127667	0.773435	3.360167
H	-0.977892	0.926800	3.112036
H	1.089894	1.063516	4.404992
C	2.371074	0.508274	2.751126
H	3.285002	0.573404	3.332951
C	2.434612	0.193823	1.408879
C	0.497043	-0.401939	-2.971511
H	1.391351	0.161155	-3.268630
H	0.744220	-1.466320	-3.098866
C	-2.272814	-0.103518	-1.878275
H	-2.726922	0.895135	-1.970149
H	-3.029491	-0.745771	-1.407414
C	-1.973757	-0.655590	-3.281385
H	-1.858881	-1.746086	-3.229124
H	-2.830676	-0.459815	-3.933132
C	-0.698591	-0.038760	-3.858862

H	-0.799581	1.052327	-3.919534
H	-0.516551	-0.399466	-4.875698
N	-2.450472	0.289510	0.949426
H	-3.179342	0.360520	0.252964
C	-2.935470	-0.273314	2.219305
H	-2.211423	-0.980316	2.627530
H	-3.866734	-0.808877	2.019052
H	-3.141650	0.505284	2.960768

Point 24 $\theta = 130°$

C	-1.054570	0.020534	-0.968151
C	-1.193307	0.256200	0.429336
N	1.303087	-0.112331	-0.692511
C	-0.015489	0.347815	1.259997
C	0.219932	-0.145064	-1.501809
C	1.251670	0.129443	0.662012
C	-0.037031	0.714415	2.630785
H	3.394782	0.007403	0.932509
H	2.216797	-0.250161	-1.112366
C	1.129703	0.789540	3.363010
H	-0.977471	0.971222	3.100724
H	1.093532	1.079301	4.408007
C	2.372319	0.509162	2.756984
H	3.284578	0.563398	3.342551
C	2.438910	0.193604	1.414865
C	0.486856	-0.424892	-2.961326
H	1.385868	0.122640	-3.273068
H	0.722905	-1.494168	-3.067489
C	-2.276742	-0.063640	-1.867517
H	-2.705743	0.943301	-1.984721
H	-3.048265	-0.673168	-1.378591
C	-1.989564	-0.655315	-3.256624
H	-1.888607	-1.745626	-3.177556
H	-2.845499	-0.464604	-3.911150
C	-0.708431	-0.068286	-3.852262
H	-0.796648	1.022216	-3.938011
H	-0.534098	-0.454535	-4.861009
N	-2.434744	0.376957	0.976215
H	-3.164250	0.500137	0.286270
C	-2.924002	-0.344844	2.166679
H	-2.154049	-1.017097	2.547541
H	-3.793841	-0.942041	1.879761
H	-3.224591	0.345484	2.960914

Point 25 $\theta = 120°$

C	-1.054977	0.048860	-0.951807

C	-1.180376	0.297968	0.440513
N	1.302259	-0.122219	-0.686787
C	0.000649	0.375969	1.264407
C	0.216703	-0.144037	-1.491206
C	1.262301	0.132071	0.666158
C	-0.016794	0.753787	2.631899
H	3.404531	-0.022634	0.935899
H	2.211345	-0.283789	-1.108999
C	1.151509	0.812426	3.362652
H	-0.956375	1.033795	3.092216
H	1.122636	1.111525	4.405281
C	2.389438	0.506498	2.757115
H	3.302568	0.550148	3.342213
C	2.451734	0.181965	1.416847
C	0.470291	-0.448907	-2.948012
H	1.375856	0.079582	-3.273368
H	0.689167	-1.523289	-3.038947
C	-2.281868	-0.019589	-1.846298
H	-2.682349	0.996661	-1.981789
H	-3.068471	-0.596182	-1.342806
C	-2.012741	-0.642784	-3.224956
H	-1.930259	-1.733098	-3.126213
H	-2.868449	-0.449258	-3.878928
C	-0.725015	-0.088090	-3.837621
H	-0.795758	1.002067	-3.941824
H	-0.562752	-0.494399	-4.840452
N	-2.414998	0.450456	1.014447
H	-3.139343	0.636215	0.330531
C	-2.932005	-0.422454	2.090017
H	-2.107473	-0.895083	2.622863
H	-3.562571	-1.209660	1.662332
H	-3.524412	0.162479	2.798621

Point 26 $\theta = 110°$

C	-1.055157	0.074939	-0.930350
C	-1.164561	0.343421	0.455429
N	1.301903	-0.122064	-0.681218
C	0.018953	0.406236	1.271646
C	0.212981	-0.141117	-1.478423
C	1.275175	0.142841	0.669993
C	0.007481	0.782762	2.639385
H	3.417266	-0.037867	0.933227
H	2.206249	-0.301557	-1.107358
C	1.178459	0.824918	3.366121
H	-0.930926	1.073540	3.095956
H	1.157459	1.122416	4.409435

C	2.411874	0.505230	2.756055
H	3.326752	0.538631	3.339108
C	2.468173	0.179381	1.415901
C	0.451182	-0.470747	-2.932275
H	1.360751	0.040739	-3.273237
H	0.655842	-1.549234	-3.007272
C	-2.287837	0.016841	-1.818073
H	-2.663870	1.039764	-1.971422
H	-3.085642	-0.529457	-1.299845
C	-2.037512	-0.636546	-3.186087
H	-1.969418	-1.725946	-3.067588
H	-2.895146	-0.443389	-3.837608
C	-0.747166	-0.110270	-3.818340
H	-0.804555	0.978662	-3.941645
H	-0.597841	-0.536448	-4.814877
N	-2.395099	0.521207	1.056026
H	-3.108326	0.762813	0.375492
C	-2.938142	-0.489943	1.992034
H	-2.175966	-0.790759	2.710902
H	-3.283408	-1.383195	1.456780
H	-3.775931	-0.048801	2.536128

Point 27 $\theta = 100°$

C	-1.053701	0.094820	-0.908322
C	-1.147462	0.392705	0.468711
N	1.304959	-0.104761	-0.676318
C	0.036675	0.440498	1.278911
C	0.211667	-0.134775	-1.465070
C	1.289742	0.168721	0.673206
C	0.025691	0.798273	2.651638
H	3.432533	-0.022471	0.930923
H	2.205859	-0.292833	-1.106968
C	1.198173	0.826400	3.375871
H	-0.915980	1.078401	3.108590
H	1.180987	1.107268	4.423880
C	2.430435	0.512545	2.758389
H	3.346288	0.538521	3.340336
C	2.484963	0.196765	1.415618
C	0.435705	-0.490635	-2.914795
H	1.344622	0.009870	-3.273339
H	0.634692	-1.571374	-2.971280
C	-2.292255	0.037595	-1.787877
H	-2.649948	1.063739	-1.961775
H	-3.096867	-0.480966	-1.253145
C	-2.057684	-0.647173	-3.143065
H	-1.995945	-1.734351	-3.002259

H	-2.919106	-0.461972	-3.791870
C	-0.769418	-0.141893	-3.796928
H	-0.821940	0.944566	-3.942222
H	-0.630954	-0.589189	-4.785712
N	-2.374053	0.583972	1.097035
H	-3.072028	0.897581	0.428133
C	-2.946855	-0.538679	1.879438
H	-2.240360	-0.859639	2.646869
H	-3.190272	-1.400875	1.245262
H	-3.854162	-0.183656	2.372135

Point 28 $\theta = 90°$

C	-1.051579	0.104682	-0.881485
C	-1.129966	0.425917	0.488113
N	1.309277	-0.091117	-0.668874
C	0.056185	0.468384	1.290090
C	0.210797	-0.134403	-1.447864
C	1.306552	0.193500	0.678092
C	0.048090	0.812346	2.666608
H	3.451403	0.003569	0.925231
H	2.206802	-0.284440	-1.105065
C	1.224011	0.836027	3.384771
H	-0.896721	1.077782	3.125975
H	1.211738	1.104236	4.436182
C	2.454978	0.532023	2.758159
H	3.373241	0.557426	3.336376
C	2.505582	0.221482	1.413868
C	0.421092	-0.512330	-2.893912
H	1.329709	-0.022834	-3.268043
H	0.613701	-1.595002	-2.934637
C	-2.295103	0.053790	-1.754633
H	-2.631600	1.084074	-1.945254
H	-3.108339	-0.437091	-1.208521
C	-2.076556	-0.656872	-3.098907
H	-2.022325	-1.741992	-2.939870
H	-2.941386	-0.476029	-3.744395
C	-0.789999	-0.172038	-3.771700
H	-0.836999	0.911958	-3.936034
H	-0.662040	-0.637592	-4.753427
N	-2.354036	0.620049	1.144038
H	-3.029534	1.024143	0.498782
C	-2.971280	-0.585221	1.752702
H	-2.310301	-0.989587	2.522937
H	-3.174549	-1.374874	1.017244
H	-3.906845	-0.282965	2.227452

Point 29 θ = 80°

C	-1.050701	0.100216	-0.851404
C	-1.115672	0.437393	0.513085
N	1.313180	-0.085453	-0.659301
C	0.075315	0.487951	1.303439
C	0.208980	-0.144001	-1.427479
C	1.323491	0.215297	0.683349
C	0.073800	0.826430	2.681941
H	3.471716	0.038598	0.914397
H	2.207330	-0.281884	-1.101711
C	1.255266	0.858133	3.389949
H	-0.873197	1.074115	3.146314
H	1.249427	1.120623	4.442878
C	2.484501	0.566211	2.752916
H	3.406682	0.598933	3.324548
C	2.528228	0.253098	1.408986
C	0.407582	-0.540455	-2.870205
H	1.320064	-0.066872	-3.255134
H	0.586939	-1.625875	-2.897787
C	-2.294895	0.071738	-1.725255
H	-2.597130	1.110444	-1.927259
H	-3.124650	-0.384843	-1.177117
C	-2.093771	-0.657420	-3.061912
H	-2.055302	-1.741515	-2.891337
H	-2.958802	-0.470382	-3.705400
C	-0.804181	-0.198149	-3.746744
H	-0.838915	0.883961	-3.925990
H	-0.685978	-0.678618	-4.722474
N	-2.337085	0.618154	1.200251
H	-2.986431	1.125420	0.600120
C	-3.009979	-0.635039	1.627040
H	-2.390843	-1.144568	2.370128
H	-3.205209	-1.331856	0.801189
H	-3.955759	-0.362784	2.099978

Point 30 θ = 70°

C	-1.050895	0.085911	-0.820598
C	-1.105613	0.423505	0.543323
N	1.317140	-0.082849	-0.649993
C	0.093459	0.495062	1.318570
C	0.207010	-0.159686	-1.405896
C	1.340230	0.237023	0.687292
C	0.101366	0.830134	2.698574
H	3.493648	0.094460	0.894499
H	2.208179	-0.279447	-1.099115

C	1.290512	0.886492	3.391579
H	-0.847443	1.048546	3.173176
H	1.291841	1.146274	4.445215
C	2.518173	0.617531	2.740839
H	3.445888	0.668259	3.302152
C	2.552553	0.297861	1.398245
C	0.395996	-0.575744	-2.844635
H	1.316546	-0.124780	-3.237227
H	0.555280	-1.664671	-2.856694
C	-2.288957	0.098329	-1.704921
H	-2.536618	1.149119	-1.918964
H	-3.146354	-0.308210	-1.164109
C	-2.108068	-0.649665	-3.033392
H	-2.095168	-1.732659	-2.851950
H	-2.969654	-0.448385	-3.677310
C	-0.810445	-0.226025	-3.725795
H	-0.825684	0.853442	-3.922712
H	-0.701091	-0.724344	-4.693585
N	-2.321650	0.573978	1.266590
H	-2.938057	1.203311	0.751357
C	-3.066694	-0.686206	1.509736
H	-2.494144	-1.313092	2.199125
H	-3.277531	-1.271898	0.606299
H	-4.009754	-0.424578	1.994325

Point 31 $\theta = 60°$

C	-1.018805	-0.151633	-0.794665
C	-1.096290	0.225118	0.571866
N	1.358820	-0.074916	-0.655694
C	0.119201	0.430212	1.330261
C	0.239858	-0.284974	-1.383476
C	1.366023	0.275441	0.674267
C	0.148176	0.745389	2.713467
H	3.523903	0.350820	0.817118
H	2.254391	-0.160671	-1.125775
C	1.342946	0.933387	3.376562
H	-0.774621	0.812063	3.280145
H	1.341519	1.168574	4.435737
C	2.568473	0.803558	2.689678
H	3.503890	0.954175	3.218982
C	2.584867	0.468251	1.351314
C	0.447023	-0.606248	-2.843029
H	1.360943	-0.113922	-3.198734
H	0.618328	-1.689078	-2.935511
C	-2.271594	-0.257646	-1.650173
H	-2.726468	0.743300	-1.686071

H	-3.009062	-0.900857	-1.164673
C	-2.034249	-0.786325	-3.074187
H	-1.954721	-1.881278	-3.051167
H	-2.908069	-0.550560	-3.689600
C	-0.763727	-0.205632	-3.694591
H	-0.831394	0.888207	-3.751836
H	-0.624201	-0.572724	-4.715823
N	-2.298678	0.541263	1.147300
H	-2.190251	1.090787	1.989229
C	-3.460514	-0.368396	1.247860
H	-3.154659	-1.412191	1.140420
H	-4.227875	-0.135278	0.505121
H	-3.899185	-0.241213	2.239675

Point 32 $\theta = 50°$

C	-1.018496	-0.168366	-0.779088
C	-1.091203	0.208242	0.591239
N	1.361158	-0.049022	-0.658961
C	0.132829	0.418641	1.342209
C	0.238047	-0.274673	-1.376198
C	1.374494	0.290085	0.673760
C	0.172722	0.716573	2.728784
H	3.531743	0.397071	0.794394
H	2.253113	-0.117245	-1.138087
C	1.371139	0.915765	3.382717
H	-0.742241	0.759961	3.310325
H	1.375810	1.137268	4.444814
C	2.590979	0.814576	2.682453
H	3.529591	0.973818	3.203479
C	2.597169	0.494698	1.340275
C	0.446065	-0.589238	-2.837848
H	1.348507	-0.076833	-3.194505
H	0.640764	-1.667894	-2.932468
C	-2.270671	-0.294783	-1.635894
H	-2.742623	0.697993	-1.676618
H	-2.996406	-0.952206	-1.153558
C	-2.027578	-0.820673	-3.059934
H	-1.923687	-1.913532	-3.034640
H	-2.909973	-0.605647	-3.670752
C	-0.773522	-0.213566	-3.686556
H	-0.864359	0.878608	-3.743967
H	-0.630011	-0.578284	-4.708103
N	-2.275231	0.496531	1.201627
H	-2.161431	1.000783	2.069403
C	-3.510092	-0.309507	1.192078
H	-3.286941	-1.374372	1.085743

H	-4.200565	0.001195	0.404509
H	-4.005101	-0.158966	2.153370

Point 33 θ = 40°

C	-1.017965	-0.175457	-0.769154
C	-1.087826	0.192882	0.606662
N	1.361903	-0.007487	-0.666125
C	0.143677	0.402023	1.353067
C	0.236135	-0.247924	-1.374971
C	1.380408	0.307452	0.672266
C	0.193401	0.670948	2.745157
H	3.536142	0.448112	0.773926
H	2.250319	-0.052470	-1.154009
C	1.394604	0.876068	3.392781
H	-0.713906	0.685803	3.340088
H	1.404823	1.074286	4.459415
C	2.608815	0.811182	2.679724
H	3.549860	0.975197	3.194824
C	2.605929	0.519515	1.331198
C	0.447474	-0.551278	-2.839513
H	1.324652	0.001447	-3.199323
H	0.691451	-1.619850	-2.934799
C	-2.268414	-0.336106	-1.625855
H	-2.759186	0.646074	-1.688837
H	-2.980884	-1.001596	-1.136004
C	-2.013854	-0.878950	-3.040916
H	-1.865764	-1.966079	-2.995982
H	-2.908353	-0.710244	-3.648706
C	-0.789523	-0.231999	-3.684522
H	-0.923386	0.855100	-3.753510
H	-0.638551	-0.602393	-4.702952
N	-2.255033	0.453082	1.248997
H	-2.132070	0.914046	2.138346
C	-3.555657	-0.227349	1.147276
H	-3.431808	-1.309161	1.048179
H	-4.159766	0.152280	0.321060
H	-4.093648	-0.030154	2.076214

Point 34 θ = 30°

C	-1.017820	-0.174487	-0.763568
C	-1.085873	0.180067	0.618464
N	1.359967	0.047850	-0.676007
C	0.151911	0.381565	1.362515
C	0.232907	-0.208162	-1.378126
C	1.383533	0.327801	0.669878
C	0.210549	0.610742	2.761294

H	3.536831	0.504494	0.756204
H	2.244620	0.030810	-1.172087
C	1.413851	0.817416	3.405008
H	-0.689568	0.591421	3.367105
H	1.429583	0.983668	4.477010
C	2.622159	0.796122	2.680236
H	3.564989	0.961899	3.191471
C	2.611017	0.543857	1.323889
C	0.448066	-0.497489	-2.845812
H	1.286738	0.109027	-3.211317
H	0.759829	-1.548347	-2.940984
C	-2.265068	-0.384101	-1.616933
H	-2.780466	0.582193	-1.712982
H	-2.959824	-1.055696	-1.110392
C	-1.993003	-0.955152	-3.016772
H	-1.786447	-2.031082	-2.942021
H	-2.899592	-0.851145	-3.621202
C	-0.809892	-0.259139	-3.685067
H	-1.001818	0.817848	-3.773088
H	-0.648066	-0.640219	-4.697852
N	-2.238823	0.414080	1.287249
H	-2.105193	0.830152	2.196380
C	-3.594000	-0.124366	1.108436
H	-3.583141	-1.214398	1.021514
H	-4.104186	0.310629	0.247953
H	-4.159770	0.139143	2.003603

Point 35 $\theta = 20°$

C	-1.019029	-0.169836	-0.759640
C	-1.085403	0.165652	0.629097
N	1.354831	0.103254	-0.684790
C	0.157510	0.358999	1.371271
C	0.227554	-0.166819	-1.381913
C	1.383594	0.346613	0.668003
C	0.224943	0.550126	2.775289
H	3.533684	0.560232	0.741068
H	2.235710	0.113428	-1.187501
C	1.430087	0.758668	3.415321
H	-0.668064	0.499184	3.389946
H	1.451660	0.894671	4.491464
C	2.632012	0.780223	2.680596
H	3.576316	0.948360	3.188314
C	2.612616	0.567025	1.317736
C	0.445316	-0.443560	-2.852142
H	1.241874	0.213607	-3.224682
H	0.822848	-1.472689	-2.946705

C	-2.261453	-0.430964	-1.607750
H	-2.802614	0.516600	-1.737053
H	-2.937405	-1.107441	-1.082161
C	-1.969659	-1.029604	-2.991408
H	-1.706454	-2.090736	-2.887774
H	-2.884171	-0.989778	-3.591602
C	-0.829149	-0.287843	-3.684519
H	-1.078714	0.775483	-3.791866
H	-0.655398	-0.679691	-4.691174
N	-2.228249	0.370774	1.318093
H	-2.086939	0.734197	2.248020
C	-3.621705	-0.019785	1.071749
H	-3.727238	-1.105058	0.987125
H	-4.036002	0.463033	0.186775
H	-4.198909	0.310678	1.936816

Point 36 $\theta = 10°$

C	-1.021789	-0.161096	-0.757203
C	-1.086123	0.152988	0.637819
N	1.346551	0.159744	-0.692773
C	0.160544	0.337416	1.378579
C	0.219831	-0.122414	-1.386692
C	1.380908	0.364432	0.666356
C	0.236064	0.491715	2.786612
H	3.527698	0.609698	0.729634
H	2.223715	0.196140	-1.200627
C	1.442981	0.698921	3.423927
H	-0.650744	0.413610	3.407586
H	1.470351	0.805706	4.503218
C	2.638651	0.759390	2.681536
H	3.584331	0.927102	3.186817
C	2.611299	0.585905	1.313249
C	0.438756	-0.385601	-2.859507
H	1.185912	0.323090	-3.240317
H	0.885192	-1.386712	-2.954783
C	-2.257556	-0.478765	-1.596826
H	-2.828032	0.445410	-1.759972
H	-2.911706	-1.159917	-1.049255
C	-1.942586	-1.105550	-2.962375
H	-1.620431	-2.146915	-2.828669
H	-2.861082	-1.133481	-3.557165
C	-0.849154	-0.319295	-3.682519
H	-1.158901	0.725707	-3.810886
H	-0.662013	-0.722758	-4.682150
N	-2.223061	0.326993	1.340663
H	-2.078417	0.632555	2.290486

C	-3.638141	0.088151	1.035360
H	-3.857632	-0.978330	0.933583
H	-3.959446	0.619816	0.140429
H	-4.211971	0.473343	1.879866

5.2.1.2 Cartesian coordinates for constrained optimization calculations of 17

Rotation in the counterclockwise direction:

Point 1 $\theta = 0°$

C	-0.197952	0.021377	-0.037011
C	-0.279207	-0.071798	1.385136
N	2.154295	0.435346	0.137799
C	0.955468	-0.030269	2.163976
C	1.044485	0.297535	-0.613292
C	2.167847	0.263142	1.498298
C	1.027895	-0.255681	3.563179
H	4.286686	0.629749	1.646014
H	3.046306	0.667194	-0.328712
C	2.223241	-0.158286	4.245931
H	0.150130	-0.543498	4.133540
H	2.248655	-0.343636	5.314780
C	3.409589	0.175153	3.561492
H	4.344136	0.260774	4.106943
C	3.386525	0.379618	2.198615
C	-1.408569	-0.146654	-0.953169
H	-2.035099	0.753693	-0.903642
H	-2.024110	-0.977785	-0.602330
C	1.274866	0.452385	-2.101009
H	1.801228	-0.449911	-2.446388
H	1.967340	1.286659	-2.263581
C	-0.016344	0.625950	-2.902077
H	-0.409343	1.642295	-2.768359
H	0.197514	0.505376	-3.968754
C	-1.044652	-0.396565	-2.422823
H	-1.957235	-0.349532	-3.025974
H	-0.638536	-1.410458	-2.539776
N	-1.424421	-0.184792	2.093428
H	-1.294841	-0.194781	3.092388
C	-2.835878	-0.245803	1.705916
H	-3.100058	0.545113	1.004487
H	-3.421248	-0.096464	2.615215
H	-3.107095	-1.218401	1.285509
C	5.563783	0.814329	-1.602495
H	5.740480	-0.269999	-1.697510
O	4.563852	1.278010	-1.049587
N	6.536561	1.562333	-2.144225

H	6.473285	2.572473	-2.106539
H	7.344898	1.143812	-2.582808

Point 2 $\theta = 10°$

C	-0.196141	0.016962	-0.042057
C	-0.279100	-0.061419	1.380335
N	2.159319	0.416747	0.130577
C	0.952668	0.000477	2.161879
C	1.049799	0.276388	-0.619991
C	2.167972	0.277999	1.494851
C	1.020271	-0.198325	3.565458
H	4.286239	0.648517	1.642710
H	3.053406	0.636707	-0.337796
C	2.212449	-0.083247	4.250949
H	0.141197	-0.481300	4.136031
H	2.234181	-0.247543	5.323324
C	3.401076	0.237731	3.564429
H	4.333112	0.337059	4.111852
C	3.383908	0.410388	2.197030
C	-1.417460	-0.095303	-0.952159
H	-2.021611	0.816822	-0.852456
H	-2.049000	-0.925347	-0.630311
C	1.278333	0.422772	-2.108501
H	1.736173	-0.511701	-2.466015
H	2.023689	1.209173	-2.273881
C	-0.007991	0.689159	-2.891544
H	-0.346082	1.719534	-2.720444
H	0.190539	0.592516	-3.963643
C	-1.081838	-0.296564	-2.436681
H	-1.998377	-0.178891	-3.023989
H	-0.729778	-1.323788	-2.602555
N	-1.425727	-0.164151	2.090323
H	-1.298242	-0.112049	3.088278
C	-2.819163	-0.411060	1.710878
H	-3.190677	0.326699	0.999844
H	-3.413995	-0.327319	2.622280
H	-2.960897	-1.417743	1.306747
C	5.578350	0.763460	-1.597654
H	5.753164	-0.322441	-1.676461
O	4.575383	1.236894	-1.058450
N	6.556807	1.501898	-2.142112
H	6.495359	2.512608	-2.119039
H	7.367160	1.075687	-2.569453

Point 3 $\theta = 20°$

C	-0.195276	0.017556	-0.046450

C	-0.279651	-0.051242	1.375171
N	2.161585	0.407749	0.125830
C	0.946717	0.034880	2.160316
C	1.053217	0.265289	-0.625492
C	2.165121	0.298812	1.492890
C	1.007871	-0.136011	3.567908
H	4.282770	0.673555	1.642698
H	3.058074	0.616915	-0.343355
C	2.196442	-0.003334	4.256303
H	0.125999	-0.410953	4.137850
H	2.213832	-0.145466	5.331930
C	3.388007	0.304506	3.568508
H	4.317203	0.416966	4.118223
C	3.377838	0.446635	2.197463
C	-1.425130	-0.049589	-0.948564
H	-2.017153	0.863884	-0.796192
H	-2.063742	-0.884594	-0.656243
C	1.277629	0.409783	-2.114238
H	1.674675	-0.546577	-2.486553
H	2.064664	1.153611	-2.281683
C	-0.001706	0.758664	-2.876379
H	-0.291464	1.796800	-2.667669
H	0.183433	0.688862	-3.952971
C	-1.113323	-0.195263	-2.445573
H	-2.030635	-0.013168	-3.014956
H	-0.809112	-1.228512	-2.661088
N	-1.432905	-0.150099	2.079035
H	-1.316734	-0.044156	3.074289
C	-2.783357	-0.583127	1.709097
H	-3.262001	0.099475	1.005992
H	-3.375298	-0.589752	2.626140
H	-2.785681	-1.597264	1.298635
C	5.585982	0.702539	-1.592792
H	5.748540	-0.386441	-1.652554
O	4.586167	1.196449	-1.065963
N	6.575028	1.420510	-2.145139
H	6.524867	2.432107	-2.139590
H	7.381983	0.978006	-2.562249

Point 4 $\theta = 30°$

C	-0.195137	0.023454	-0.050838
C	-0.281665	-0.037484	1.369214
N	2.162239	0.403602	0.123162
C	0.937683	0.068639	2.158586
C	1.055757	0.261120	-0.630365
C	2.160204	0.318371	1.492077

C	0.990450	-0.077492	3.569297
H	4.278363	0.690400	1.646355
H	3.061642	0.602667	-0.345586
C	2.175584	0.066605	4.261025
H	0.103680	-0.341281	4.136707
H	2.187808	-0.055912	5.339144
C	3.371555	0.359033	3.573526
H	4.298020	0.479497	4.126166
C	3.369769	0.475568	2.199949
C	-1.431287	-0.012756	-0.944322
H	-2.019774	0.894574	-0.745475
H	-2.069890	-0.855977	-0.677124
C	1.275406	0.407614	-2.118949
H	1.623269	-0.561939	-2.506079
H	2.092650	1.117369	-2.288160
C	0.002842	0.822477	-2.860300
H	-0.248484	1.863497	-2.618778
H	0.177339	0.777692	-3.939999
C	-1.137278	-0.106594	-2.449895
H	-2.053280	0.127335	-3.002130
H	-0.870335	-1.140181	-2.708397
N	-1.446890	-0.128041	2.060202
H	-1.346767	0.023159	3.051775
C	-2.733451	-0.737445	1.706687
H	-3.309160	-0.125301	1.010324
H	-3.308337	-0.825675	2.630456
H	-2.602558	-1.741656	1.292785
C	5.587886	0.644545	-1.590376
H	5.734588	-0.447327	-1.636246
O	4.595022	1.159539	-1.070264
N	6.587222	1.341124	-2.151235
H	6.551722	2.353352	-2.158375
H	7.388068	0.881831	-2.561957

Point 5 $\theta = 40°$

C	-0.197134	0.033632	-0.057437
C	-0.285438	-0.020020	1.360331
N	2.161428	0.395217	0.117661
C	0.926865	0.097038	2.153249
C	1.056466	0.256726	-0.638331
C	2.154358	0.329204	1.487858
C	0.970591	-0.028080	3.566289
H	4.274645	0.689289	1.647850
H	3.064019	0.584414	-0.349963
C	2.153219	0.119483	4.261114
H	0.077151	-0.277022	4.129785

H	2.160232	0.013570	5.341051
C	3.354684	0.393004	3.574547
H	4.279128	0.515563	4.130116
C	3.361533	0.488477	2.199255
C	-1.439078	0.020915	-0.940938
H	-2.023166	0.923043	-0.706685
H	-2.078817	-0.826515	-0.689091
C	1.270764	0.402520	-2.126979
H	1.576882	-0.576703	-2.524737
H	2.111273	1.083221	-2.300637
C	0.004472	0.869451	-2.849845
H	-0.213796	1.912178	-2.584809
H	0.169808	0.841864	-3.931558
C	-1.159718	-0.035455	-2.451807
H	-2.072796	0.240538	-2.989191
H	-0.925348	-1.068289	-2.742507
N	-1.466707	-0.092176	2.034210
H	-1.381671	0.100844	3.020580
C	-2.676359	-0.861540	1.713945
H	-3.339619	-0.331064	1.027328
H	-3.216786	-1.016615	2.649828
H	-2.428264	-1.842932	1.299308
C	5.592300	0.600139	-1.584761
H	5.731049	-0.493033	-1.622496
O	4.601106	1.126041	-1.072104
N	6.598758	1.285549	-2.146310
H	6.570707	2.297940	-2.160666
H	7.397736	0.817589	-2.550868

Point 6 $\theta = 50°$

C	-0.199821	0.050417	-0.065715
C	-0.290887	-0.000411	1.349026
N	2.159670	0.388796	0.112598
C	0.913857	0.120272	2.146193
C	1.056764	0.258008	-0.647257
C	2.147159	0.335026	1.483491
C	0.947361	0.011168	3.560888
H	4.270177	0.677916	1.652086
H	3.065951	0.568147	-0.352845
C	2.127572	0.156195	4.259764
H	0.045987	-0.221686	4.118505
H	2.128796	0.063115	5.340919
C	3.335506	0.410411	3.576002
H	4.257850	0.530635	4.135575
C	3.351935	0.490718	2.199742
C	-1.446054	0.052627	-0.940109

H	-2.025904	0.951258	-0.682139
H	-2.087243	-0.796243	-0.694159
C	1.266978	0.403460	-2.135757
H	1.544613	-0.581309	-2.540591
H	2.122250	1.064382	-2.313334
C	0.005063	0.904820	-2.845143
H	-0.189779	1.948377	-2.565606
H	0.164020	0.887659	-3.928020
C	-1.176519	0.018695	-2.453826
H	-2.086015	0.323872	-2.981323
H	-0.966107	-1.013322	-2.764878
N	-1.491858	-0.048917	2.001176
H	-1.420175	0.184497	2.980800
C	-2.613901	-0.963294	1.732108
H	-3.349740	-0.528813	1.050942
H	-3.112363	-1.160066	2.683555
H	-2.262836	-1.917453	1.328596
C	5.594686	0.564291	-1.580912
H	5.726275	-0.529764	-1.617409
O	4.605625	1.097177	-1.071035
N	6.606751	1.242731	-2.140522
H	6.585224	2.255286	-2.155840
H	7.403606	0.769329	-2.542963

Point 7 $\theta = 60°$

C	-0.203264	0.077405	-0.076465
C	-0.298166	0.020817	1.334511
N	2.156521	0.390908	0.107900
C	0.898669	0.138122	2.136915
C	1.056455	0.271551	-0.657401
C	2.138138	0.339635	1.478901
C	0.921248	0.036707	3.552541
H	4.263717	0.663993	1.659574
H	3.066971	0.561846	-0.353992
C	2.098772	0.174014	4.256788
H	0.011359	-0.181972	4.101937
H	2.093827	0.087452	5.338490
C	3.313517	0.412664	3.578118
H	4.233435	0.526757	4.142961
C	3.340162	0.486921	2.201647
C	-1.451965	0.085371	-0.944093
H	-2.027604	0.984202	-0.677577
H	-2.095415	-0.761336	-0.693056
C	1.265132	0.418141	-2.145353
H	1.533230	-0.568133	-2.553022
H	2.124929	1.072719	-2.324747

C	0.003631	0.930766	-2.849252
H	-0.181547	1.975192	-2.566467
H	0.159760	0.915354	-3.932549
C	-1.186203	0.054158	-2.458522
H	-2.092894	0.370542	-2.984142
H	-0.986337	-0.978557	-2.774211
N	-1.520823	-0.004427	1.962418
H	-1.459732	0.272527	2.932606
C	-2.547433	-1.047587	1.766437
H	-3.342739	-0.718962	1.091980
H	-2.997586	-1.262535	2.738025
H	-2.106806	-1.972109	1.382572
C	5.593058	0.534773	-1.577569
H	5.713632	-0.560438	-1.616074
O	4.608680	1.076638	-1.067747
N	6.612357	1.204202	-2.134492
H	6.600907	2.216966	-2.147887
H	7.404887	0.723718	-2.537116

Point 8 $\theta = 70°$

C	-0.208594	0.079650	-0.101136
C	-0.309224	0.030800	1.307363
N	2.150951	0.390651	0.092178
C	0.883386	0.138145	2.113549
C	1.054947	0.276523	-0.677873
C	2.128665	0.331686	1.462365
C	0.898181	0.034591	3.529877
H	4.256256	0.639394	1.653486
H	3.064085	0.562054	-0.365904
C	2.073964	0.158990	4.238903
H	-0.017520	-0.174506	4.073027
H	2.063753	0.070258	5.320410
C	3.294456	0.388463	3.566422
H	4.212390	0.493105	4.136289
C	3.328830	0.467217	2.190472
C	-1.452233	0.067778	-0.972941
H	-2.073555	0.920341	-0.663181
H	-2.048805	-0.823559	-0.759167
C	1.262629	0.442158	-2.163217
H	1.506686	-0.541563	-2.591477
H	2.134285	1.082689	-2.335353
C	0.005677	0.993371	-2.846791
H	-0.169027	2.028084	-2.524598
H	0.160844	1.016760	-3.930067
C	-1.190120	0.110894	-2.489486
H	-2.096279	0.458870	-2.995530

H	-0.999897	-0.906267	-2.856806
N	-1.545787	0.032018	1.931373
H	-1.467513	0.363112	2.885506
C	-2.486153	-1.106068	1.881757
H	-3.000159	-1.166127	0.921829
H	-3.243631	-0.936340	2.649286
H	-1.987551	-2.062530	2.080014
C	5.589743	0.522757	-1.577610
H	5.702910	-0.573120	-1.617938
O	4.607427	1.070356	-1.069393
N	6.614833	1.186474	-2.130163
H	6.610251	2.199344	-2.141462
H	7.405378	0.701552	-2.531429

Point 9 $\theta = 80°$

C	-0.230431	0.148350	-0.107770
C	-0.325374	0.060297	1.295447
N	2.132998	0.411091	0.086681
C	0.860701	0.155807	2.104527
C	1.036937	0.327445	-0.686697
C	2.109671	0.344028	1.456390
C	0.867388	0.047934	3.520763
H	4.240394	0.629993	1.656668
H	3.051089	0.565521	-0.369505
C	2.042332	0.157250	4.232760
H	-0.056536	-0.144110	4.056057
H	2.028900	0.067778	5.314192
C	3.267956	0.375671	3.563954
H	4.184746	0.468088	4.137791
C	3.309191	0.462895	2.188692
C	-1.478135	0.199549	-0.973864
H	-2.015998	1.121055	-0.709177
H	-2.159381	-0.614120	-0.713634
C	1.250771	0.483435	-2.172390
H	1.510694	-0.503304	-2.584550
H	2.117310	1.130619	-2.346536
C	-0.005108	1.010329	-2.877358
H	-0.176564	2.057795	-2.597155
H	0.152748	0.990995	-3.960297
C	-1.209378	0.152285	-2.486442
H	-2.108668	0.480818	-3.017202
H	-1.024954	-0.885226	-2.796240
N	-1.583043	0.016861	1.897414
H	-1.546082	0.408980	2.833234
C	-2.343529	-1.249209	1.940404
H	-2.473603	-1.657384	0.937480

H	-3.332820	-1.040788	2.353603
H	-1.846134	-2.008752	2.558221
C	5.571658	0.480030	-1.576520
H	5.660902	-0.617725	-1.623694
O	4.600339	1.045738	-1.066532
N	6.611840	1.124848	-2.122685
H	6.629248	2.137653	-2.127610
H	7.392406	0.625487	-2.525832

Point 10 $\theta = 90°$

C	-0.240508	0.199936	-0.125610
C	-0.340789	0.088694	1.270829
N	2.123588	0.424296	0.079952
C	0.837170	0.158310	2.087607
C	1.032193	0.366463	-0.701010
C	2.093342	0.337639	1.448489
C	0.829882	0.041608	3.503348
H	4.227092	0.592148	1.667141
H	3.047108	0.570619	-0.370004
C	2.001674	0.126181	4.223126
H	-0.104510	-0.132030	4.026456
H	1.980298	0.031098	5.303978
C	3.235921	0.330214	3.563859
H	4.149569	0.403269	4.145451
C	3.289558	0.431733	2.190052
C	-1.486268	0.241753	-0.993339
H	-2.013570	1.177676	-0.761535
H	-2.175744	-0.554758	-0.700811
C	1.252191	0.522838	-2.185505
H	1.541753	-0.459408	-2.588854
H	2.104227	1.190160	-2.356685
C	-0.010578	1.012932	-2.905533
H	-0.199771	2.063549	-2.649538
H	0.152928	0.972917	-3.987028
C	-1.206245	0.147410	-2.500898
H	-2.104388	0.446963	-3.050300
H	-1.004208	-0.896669	-2.776106
N	-1.621241	0.046824	1.850249
H	-1.603437	0.511838	2.754725
C	-2.246996	-1.282763	2.026723
H	-2.360067	-1.777508	1.059158
H	-3.242566	-1.138375	2.452123
H	-1.663476	-1.941795	2.684139
C	5.563142	0.468639	-1.573717
H	5.638554	-0.629240	-1.637727
O	4.598085	1.038719	-1.056309

N	6.611921	1.108782	-2.108292
H	6.641878	2.121276	-2.097712
H	7.386766	0.606067	-2.518308

Point 11 θ = 100°

C	-0.251728	0.236798	-0.148382
C	-0.358007	0.098590	1.241484
N	2.112784	0.429689	0.069476
C	0.812505	0.150534	2.066363
C	1.026819	0.397954	-0.718327
C	2.075130	0.323717	1.436647
C	0.792381	0.036012	3.482368
H	4.210801	0.552501	1.671044
H	3.041438	0.569651	-0.373858
C	1.960557	0.103502	4.209389
H	-0.150635	-0.113686	3.996621
H	1.930607	0.011862	5.290367
C	3.202830	0.289776	3.558795
H	4.113128	0.348157	4.147246
C	3.267858	0.398621	2.186124
C	-1.492899	0.272558	-1.022150
H	-2.017616	1.214588	-0.811425
H	-2.185235	-0.515139	-0.712375
C	1.254658	0.562528	-2.200603
H	1.566511	-0.413687	-2.602142
H	2.096193	1.245223	-2.364011
C	-0.010802	1.029631	-2.931602
H	-0.214387	2.080290	-2.687013
H	0.160020	0.981735	-4.011606
C	-1.199898	0.154924	-2.525124
H	-2.096025	0.435541	-3.087595
H	-0.983333	-0.891061	-2.781778
N	-1.656943	0.040834	1.802987
H	-1.673631	0.599432	2.654825
C	-2.151956	-1.314151	2.139373
H	-2.239106	-1.911092	1.227033
H	-3.148709	-1.214416	2.574904
H	-1.501309	-1.853273	2.841980
C	5.555773	0.456239	-1.569791
H	5.619178	-0.641242	-1.650585
O	4.594994	1.029076	-1.047120
N	6.613528	1.092932	-2.090129
H	6.654677	2.104759	-2.063630
H	7.384323	0.588099	-2.505194

Point 12 θ = 110°

C	-0.263169	0.261070	-0.169940
C	-0.374289	0.083585	1.213051
N	2.102306	0.422537	0.057629
C	0.790808	0.128418	2.045142
C	1.020997	0.420444	-0.734532
C	2.058261	0.299210	1.423195
C	0.761971	0.032650	3.462734
H	4.194886	0.511877	1.666913
H	3.035183	0.556753	-0.380095
C	1.926918	0.096102	4.194948
H	-0.186918	-0.086554	3.972653
H	1.889342	0.022411	5.277095
C	3.175631	0.260235	3.550050
H	4.083149	0.312522	4.143321
C	3.248591	0.364419	2.177705
C	-1.497804	0.307603	-1.052425
H	-2.010275	1.259901	-0.857904
H	-2.201838	-0.464952	-0.732970
C	1.258108	0.596623	-2.214186
H	1.585226	-0.374171	-2.616823
H	2.094036	1.288850	-2.366809
C	-0.005289	1.052499	-2.955644
H	-0.216293	2.103437	-2.718637
H	0.173541	0.999758	-4.034123
C	-1.193268	0.174851	-2.551344
H	-2.085935	0.446075	-3.123814
H	-0.970134	-0.872756	-2.795863
N	-1.687375	-0.010272	1.758005
H	-1.765200	0.650784	2.530903
C	-2.070017	-1.349705	2.261126
H	-2.115683	-2.050828	1.422379
H	-3.071265	-1.274969	2.691700
H	-1.383760	-1.761321	3.013816
C	5.550818	0.443719	-1.568455
H	5.606433	-0.652393	-1.669995
O	4.591321	1.013734	-1.039999
N	6.615969	1.082458	-2.070454
H	6.664246	2.093287	-2.024422
H	7.385250	0.580113	-2.491347

Point 13 $\theta = 120°$

C	-0.274690	0.288415	-0.184775
C	-0.388593	0.061222	1.190927
N	2.092077	0.422912	0.047274
C	0.774428	0.106504	2.027911
C	1.013174	0.454470	-0.744831

C	2.044491	0.279368	1.410848
C	0.742132	0.040366	3.447459
H	4.182281	0.478490	1.656342
H	3.027981	0.549930	-0.387124
C	1.905498	0.105989	4.181740
H	-0.210418	-0.040073	3.955922
H	1.862567	0.060106	5.265267
C	3.158632	0.243221	3.539051
H	4.065119	0.292067	4.134159
C	3.234621	0.337841	2.166509
C	-1.501979	0.352733	-1.075550
H	-1.995678	1.318808	-0.897737
H	-2.221123	-0.400169	-0.745024
C	1.258035	0.643698	-2.222203
H	1.602836	-0.320233	-2.626544
H	2.086663	1.347282	-2.363310
C	-0.003298	1.086751	-2.974348
H	-0.222368	2.137938	-2.745890
H	0.183332	1.028350	-4.051237
C	-1.189429	0.206034	-2.570907
H	-2.079681	0.468750	-3.151077
H	-0.960910	-0.843007	-2.804240
N	-1.706267	-0.120059	1.710461
H	-1.940810	0.652334	2.333010
C	-1.985097	-1.407275	2.378843
H	-1.913301	-2.212888	1.641831
H	-3.016016	-1.377746	2.739801
H	-1.322632	-1.655689	3.217980
C	5.544588	0.418042	-1.566754
H	5.585158	-0.677263	-1.682754
O	4.589717	0.994722	-1.036974
N	6.622109	1.048116	-2.052856
H	6.684477	2.057447	-1.992906
H	7.386852	0.540501	-2.475707

Point 14 $\theta = 130°$

C	-0.272060	0.308012	-0.184814
C	-0.390940	0.078418	1.211076
N	2.096687	0.416124	0.042292
C	0.793055	0.073756	2.035383
C	0.998844	0.488188	-0.733943
C	2.053075	0.228207	1.402073
C	0.775447	-0.001657	3.452847
H	4.195350	0.354908	1.625567
H	3.024551	0.545925	-0.396790
C	1.948981	0.012669	4.176936

H	-0.171882	-0.035738	3.975209
H	1.914979	-0.037105	5.260491
C	3.193846	0.113492	3.518993
H	4.111438	0.122079	4.099070
C	3.250758	0.233092	2.146220
C	-1.504559	0.349068	-1.072515
H	-2.065852	1.273315	-0.865076
H	-2.173225	-0.481746	-0.809443
C	1.242026	0.717043	-2.207497
H	1.594504	-0.228574	-2.645700
H	2.065202	1.431452	-2.323684
C	-0.019005	1.184478	-2.941357
H	-0.246064	2.223300	-2.668626
H	0.162840	1.171519	-4.020619
C	-1.195420	0.276900	-2.576475
H	-2.091823	0.552829	-3.140671
H	-0.954394	-0.758281	-2.852133
N	-1.621163	-0.140563	1.764967
H	-2.384408	0.084312	1.141044
C	-1.959773	-1.256714	2.666376
H	-1.092204	-1.900540	2.817966
H	-2.754689	-1.852331	2.208377
H	-2.313550	-0.898207	3.638403
C	5.555748	0.409456	-1.612000
H	5.584978	-0.683959	-1.751070
O	4.609519	0.984440	-1.068335
N	6.640388	1.037137	-2.089170
H	6.714847	2.043959	-2.007410
H	7.398422	0.529343	-2.523375

Point 15 $\theta = 140°$

C	-0.266952	0.276059	-0.202497
C	-0.392167	0.028000	1.193545
N	2.098822	0.395384	0.033790
C	0.790190	0.035264	2.024539
C	1.001991	0.468517	-0.745002
C	2.050484	0.200657	1.392033
C	0.778707	-0.037658	3.442820
H	4.190971	0.342157	1.612956
H	3.026706	0.536972	-0.400219
C	1.952620	-0.012824	4.166399
H	-0.162711	-0.078620	3.972890
H	1.918149	-0.061623	5.249960
C	3.195808	0.094998	3.508424
H	4.114261	0.110009	4.086993
C	3.248443	0.213290	2.135664

C	-1.497016	0.316009	-1.093888
H	-2.075966	1.224798	-0.866746
H	-2.151724	-0.533570	-0.854800
C	1.248770	0.722273	-2.213886
H	1.603236	-0.214996	-2.668049
H	2.071017	1.439893	-2.315650
C	-0.011293	1.201168	-2.941478
H	-0.242685	2.233182	-2.647398
H	0.172946	1.211350	-4.020380
C	-1.184368	0.281216	-2.598768
H	-2.081350	0.565609	-3.157832
H	-0.938101	-0.746193	-2.897667
N	-1.628447	-0.201549	1.714441
H	-2.382662	-0.021709	1.067102
C	-1.989932	-1.183520	2.746362
H	-1.174412	-1.890859	2.907754
H	-2.864107	-1.739747	2.398157
H	-2.247619	-0.705993	3.697520
C	5.563689	0.433461	-1.613787
H	5.599215	-0.657830	-1.767565
O	4.613861	0.995722	-1.063418
N	6.645385	1.073484	-2.081577
H	6.714157	2.079507	-1.986341
H	7.406559	0.575717	-2.521816

Point 16 $\theta = 150°$

C	-0.260351	0.241803	-0.216020
C	-0.390187	-0.021392	1.180335
N	2.102042	0.378465	0.027176
C	0.791345	-0.003540	2.016649
C	1.005874	0.448622	-0.753600
C	2.050913	0.175850	1.383751
C	0.788662	-0.083289	3.435399
H	4.189646	0.334853	1.599197
H	3.029316	0.532934	-0.402624
C	1.964195	-0.050557	4.156375
H	-0.145719	-0.137279	3.974202
H	1.931337	-0.105884	5.239658
C	3.204405	0.071304	3.497100
H	4.124516	0.091677	4.072848
C	3.250328	0.195376	2.124962
C	-1.488765	0.278475	-1.110232
H	-2.084624	1.171852	-0.865541
H	-2.129081	-0.588148	-0.892806
C	1.254142	0.725385	-2.218057
H	1.612117	-0.203401	-2.686606

H	2.073796	1.447533	-2.307527
C	-0.006792	1.211352	-2.938974
H	-0.244393	2.236322	-2.625839
H	0.178733	1.242618	-4.017265
C	-1.174249	0.277881	-2.615427
H	-2.072941	0.567576	-3.169012
H	-0.921098	-0.741479	-2.935222
N	-1.631699	-0.262880	1.671346
H	-2.375912	-0.114169	1.005994
C	-2.030957	-1.095227	2.809418
H	-1.271621	-1.849750	3.024583
H	-2.957229	-1.608230	2.540024
H	-2.222772	-0.502963	3.710537
C	5.570469	0.462072	-1.615076
H	5.613620	-0.627412	-1.779544
O	4.616594	1.012302	-1.059771
N	6.648077	1.114037	-2.076111
H	6.709873	2.119517	-1.971014
H	7.412868	0.625797	-2.520701

Point 17 $\theta = 160°$

C	-0.251169	0.202148	-0.225780
C	-0.385594	-0.063017	1.172678
N	2.106974	0.365071	0.023587
C	0.796746	-0.046537	2.011629
C	1.011968	0.424364	-0.759871
C	2.054688	0.150663	1.377892
C	0.806028	-0.156070	3.429112
H	4.191751	0.327513	1.586163
H	3.032959	0.535124	-0.402244
C	1.984578	-0.124675	4.145470
H	-0.119896	-0.238171	3.976237
H	1.956060	-0.205306	5.227277
C	3.220065	0.025104	3.484748
H	4.142716	0.045520	4.056399
C	3.256700	0.171584	2.114920
C	-1.477926	0.231061	-1.123027
H	-2.088340	1.112090	-0.868711
H	-2.105376	-0.648670	-0.919949
C	1.260807	0.717299	-2.221055
H	1.626288	-0.204121	-2.698256
H	2.075012	1.446533	-2.301876
C	-0.002618	1.200821	-2.938845
H	-0.249806	2.219961	-2.614273
H	0.184133	1.245986	-4.016434
C	-1.161511	0.252921	-2.627840

H	-2.062616	0.540735	-3.178499
H	-0.898480	-0.759911	-2.960032
N	-1.634037	-0.301493	1.639838
H	-2.364869	-0.173886	0.956428
C	-2.088905	-0.962107	2.862434
H	-1.419437	-1.778900	3.141642
H	-3.075313	-1.384752	2.659832
H	-2.187972	-0.264289	3.700918
C	5.576900	0.512250	-1.617049
H	5.635613	-0.574845	-1.792258
O	4.615797	1.043145	-1.055555
N	6.644576	1.184180	-2.072746
H	6.692069	2.189341	-1.957700
H	7.415916	0.711345	-2.522619

Point 18 $\theta = 170°$

C	-0.242052	0.156991	-0.233673
C	-0.380823	-0.093448	1.169076
N	2.109672	0.368291	0.022506
C	0.805252	-0.098141	2.005986
C	1.016934	0.400446	-0.765315
C	2.059193	0.132551	1.372983
C	0.831526	-0.281200	3.416270
H	4.193044	0.341921	1.575083
H	3.033022	0.560588	-0.399066
C	2.014522	-0.260006	4.125877
H	-0.082517	-0.428534	3.967207
H	1.994876	-0.401623	5.201593
C	3.241287	-0.047753	3.467443
H	4.167167	-0.030782	4.033943
C	3.264608	0.152127	2.104441
C	-1.466928	0.171038	-1.134156
H	-2.087809	1.046079	-0.883501
H	-2.085317	-0.715616	-0.932471
C	1.265382	0.699073	-2.225396
H	1.648154	-0.216055	-2.701230
H	2.067337	1.442047	-2.303093
C	-0.003352	1.160715	-2.947922
H	-0.268390	2.176192	-2.625918
H	0.185711	1.206978	-4.025052
C	-1.147125	0.194405	-2.638131
H	-2.051621	0.466099	-3.191443
H	-0.866808	-0.814783	-2.967209
N	-1.638189	-0.300891	1.623710
H	-2.354271	-0.194338	0.921942
C	-2.150942	-0.762577	2.910948

H	-1.635564	-1.666290	3.246983
H	-3.205260	-1.007752	2.770218
H	-2.085947	0.010415	3.683661
C	5.581640	0.591021	-1.607082
H	5.663823	-0.494825	-1.780699
O	4.608209	1.102101	-1.048528
N	6.635905	1.284840	-2.061373
H	6.661937	2.290896	-1.947380
H	7.418192	0.827805	-2.508647

Point 19 $\theta = 180°$

C	-0.235950	0.104063	-0.243276
C	-0.378941	-0.112510	1.164998
N	2.106419	0.387440	0.025077
C	0.811646	-0.160662	1.994595
C	1.018912	0.374088	-0.770807
C	2.059480	0.120939	1.369887
C	0.852940	-0.466009	3.383137
H	4.186909	0.378951	1.580851
H	3.025576	0.609575	-0.390765
C	2.038608	-0.464349	4.088682
H	-0.048096	-0.721775	3.915315
H	2.031144	-0.706595	5.146443
C	3.253064	-0.151088	3.448025
H	4.179827	-0.141323	4.013245
C	3.265390	0.136299	2.100665
C	-1.458593	0.097981	-1.146583
H	-2.084044	0.974650	-0.912790
H	-2.073693	-0.788198	-0.932464
C	1.267878	0.666018	-2.232056
H	1.676789	-0.244264	-2.695396
H	2.051186	1.428306	-2.312831
C	-0.007352	1.087182	-2.968046
H	-0.296912	2.101333	-2.663343
H	0.186528	1.121120	-4.044771
C	-1.131896	0.101298	-2.648903
H	-2.038776	0.345133	-3.211269
H	-0.829227	-0.907368	-2.959240
N	-1.642401	-0.254549	1.625575
H	-2.352107	-0.185509	0.912645
C	-2.182566	-0.483836	2.962556
H	-1.906577	-1.468340	3.353522
H	-3.270339	-0.447344	2.881415
H	-1.870654	0.294653	3.664497
C	5.580526	0.702300	-1.581470
H	5.695146	-0.382617	-1.742205

O	4.589491	1.191162	-1.034137
N	6.616932	1.421182	-2.037897
H	6.613413	2.428761	-1.934946
H	7.414798	0.981910	-2.475352

Point 20 $\theta = 190°$

C	-0.235553	0.057413	-0.253115
C	-0.379679	-0.139085	1.156441
N	2.101828	0.381301	0.025087
C	0.811422	-0.212638	1.981358
C	1.018289	0.342099	-0.776382
C	2.056680	0.096156	1.366479
C	0.852958	-0.594133	3.350334
H	4.180238	0.374974	1.595031
H	3.017905	0.623182	-0.386353
C	2.037552	-0.610227	4.057610
H	-0.045302	-0.909932	3.856779
H	2.034903	-0.914401	5.099275
C	3.246677	-0.239845	3.436689
H	4.171565	-0.239350	4.005076
C	3.259664	0.103214	2.101992
C	-1.457457	0.042646	-1.156592
H	-2.084240	0.920050	-0.929229
H	-2.071486	-0.842811	-0.936463
C	1.267198	0.632927	-2.237717
H	1.689133	-0.273985	-2.696043
H	2.040648	1.405101	-2.319626
C	-0.011481	1.034036	-2.979629
H	-0.313571	2.046697	-2.682166
H	0.185162	1.063583	-4.055975
C	-1.126598	0.037944	-2.657753
H	-2.033958	0.268793	-3.224824
H	-0.812639	-0.969704	-2.960074
N	-1.640543	-0.247260	1.631860
H	-2.357761	-0.211389	0.923472
C	-2.163319	-0.258870	2.995638
H	-2.072482	-1.243667	3.466507
H	-3.224802	-0.009664	2.939993
H	-1.669458	0.492844	3.616101
C	5.579000	0.789356	-1.561965
H	5.727460	-0.290842	-1.726751
O	4.570409	1.245465	-1.018534
N	6.595855	1.541442	-2.008875
H	6.561048	2.547960	-1.901525
H	7.409212	1.128624	-2.443543

Point 21 θ = 200°

C	-0.236196	0.020832	-0.259576
C	-0.377630	-0.178709	1.147669
N	2.098706	0.369392	0.024064
C	0.812542	-0.252003	1.971004
C	1.016853	0.319353	-0.779550
C	2.055845	0.073739	1.363534
C	0.849474	-0.665481	3.330172
H	4.176586	0.367274	1.606542
H	3.012320	0.624882	-0.384985
C	2.031529	-0.685735	4.041382
H	-0.050631	-1.006417	3.819281
H	2.030025	-1.015679	5.075177
C	3.238864	-0.288079	3.432532
H	4.161236	-0.289604	4.005017
C	3.255678	0.079868	2.104163
C	-1.458560	0.001672	-1.162063
H	-2.091988	0.872109	-0.927244
H	-2.065254	-0.890202	-0.947812
C	1.262637	0.622310	-2.238855
H	1.691091	-0.278449	-2.703264
H	2.029784	1.401159	-2.316562
C	-0.020006	1.017750	-2.977471
H	-0.330382	2.025763	-2.672746
H	0.176299	1.056769	-4.053570
C	-1.127290	0.010344	-2.663124
H	-2.036104	0.238208	-3.229062
H	-0.805251	-0.992527	-2.972737
N	-1.633015	-0.295199	1.638874
H	-2.358263	-0.287218	0.937224
C	-2.133707	-0.116464	3.001553
H	-2.149583	-1.055719	3.564832
H	-3.159732	0.251216	2.931122
H	-1.540277	0.623790	3.542519
C	5.574970	0.835045	-1.548391
H	5.741200	-0.241844	-1.717710
O	4.556890	1.272533	-1.007272
N	6.581771	1.605266	-1.986991
H	6.530615	2.610585	-1.875015
H	7.403431	1.207474	-2.420076

Point 22 θ = 210°

C	-0.235644	-0.013761	-0.262010
C	-0.371923	-0.225470	1.141136
N	2.098393	0.350386	0.023618

C	0.816681	-0.288930	1.963754
C	1.016953	0.296850	-0.780177
C	2.058416	0.048201	1.362026
C	0.846568	-0.714502	3.318644
H	4.177132	0.352678	1.617257
H	3.009708	0.617195	-0.384115
C	2.025482	-0.733008	4.034755
H	-0.057836	-1.065838	3.794838
H	2.023359	-1.072773	5.065371
C	3.232925	-0.321954	3.433307
H	4.152612	-0.322591	4.010114
C	3.255141	0.056435	2.107608
C	-1.459531	-0.032733	-1.162369
H	-2.099731	0.828484	-0.913497
H	-2.057961	-0.932510	-0.958901
C	1.257438	0.617302	-2.236527
H	1.687311	-0.276870	-2.712277
H	2.021379	1.399820	-2.308306
C	-0.029393	1.015681	-2.966699
H	-0.344167	2.017989	-2.647926
H	0.164358	1.070087	-4.042578
C	-1.130895	-0.001690	-2.663753
H	-2.041803	0.229048	-3.225122
H	-0.804071	-0.998425	-2.987838
N	-1.620617	-0.363487	1.651304
H	-2.351136	-0.388900	0.954781
C	-2.107133	-0.003067	2.986475
H	-2.204224	-0.875441	3.641419
H	-3.096583	0.446411	2.873470
H	-1.446785	0.729550	3.454595
C	5.569499	0.866472	-1.541621
H	5.748713	-0.206803	-1.720167
O	4.545452	1.287085	-0.998195
N	6.567616	1.652508	-1.971688
H	6.504241	2.656121	-1.850947
H	7.394534	1.268454	-2.407173

Point 23 $\theta = 220°$

C	-0.233822	-0.045099	-0.260238
C	-0.362153	-0.278037	1.136978
N	2.099811	0.332417	0.024753
C	0.824629	-0.324744	1.959253
C	1.018012	0.278913	-0.777786
C	2.064008	0.024720	1.362344
C	0.847570	-0.750906	3.313459
H	4.180198	0.344811	1.627924

H	3.008705	0.609733	-0.382580
C	2.023076	-0.759915	4.034918
H	-0.061002	-1.107967	3.779768
H	2.020417	-1.100078	5.065419
C	3.230500	-0.339610	3.437887
H	4.147344	-0.334511	4.019198
C	3.257781	0.040573	2.112512
C	-1.460173	-0.061481	-1.157564
H	-2.107430	0.788492	-0.890461
H	-2.049370	-0.970150	-0.968318
C	1.251081	0.621140	-2.230261
H	1.680407	-0.265250	-2.720900
H	2.012589	1.406579	-2.294951
C	-0.040809	1.025914	-2.948311
H	-0.358958	2.021152	-2.611200
H	0.148722	1.099801	-4.023765
C	-1.136356	-0.001984	-2.659224
H	-2.050146	0.234016	-3.213650
H	-0.805578	-0.991068	-3.002222
N	-1.602827	-0.446124	1.668998
H	-2.335056	-0.514497	0.976144
C	-2.088361	0.084699	2.951295
H	-2.257130	-0.708792	3.686665
H	-3.039855	0.592702	2.774047
H	-1.380847	0.808236	3.360027
C	5.561739	0.884141	-1.538733
H	5.746683	-0.186877	-1.724569
O	4.535522	1.295519	-0.992037
N	6.555207	1.678536	-1.963729
H	6.486333	2.680967	-1.836266
H	7.384014	1.302034	-2.402236

Point 24 $\theta = 230°$

C	-0.231030	-0.074242	-0.253115
C	-0.348775	-0.329553	1.137515
N	2.102994	0.313712	0.027014
C	0.837131	-0.360742	1.957722
C	1.019794	0.261739	-0.772526
C	2.073380	0.000762	1.363889
C	0.854477	-0.783899	3.312374
H	4.187203	0.337278	1.636843
H	3.009024	0.601140	-0.381168
C	2.027128	-0.780709	4.038122
H	-0.057976	-1.145855	3.769669
H	2.024933	-1.118258	5.069508
C	3.233940	-0.352728	3.443242

H	4.148441	-0.340328	4.028138
C	3.265005	0.025813	2.117206
C	-1.461146	-0.086480	-1.145829
H	-2.113256	0.753307	-0.860626
H	-2.042781	-1.002165	-0.969101
C	1.243546	0.624523	-2.221340
H	1.670628	-0.254684	-2.726717
H	2.003387	1.411945	-2.280579
C	-0.054033	1.036178	-2.925530
H	-0.373749	2.024755	-2.570725
H	0.129623	1.128200	-4.000588
C	-1.144322	-0.000479	-2.647720
H	-2.061534	0.241032	-3.194047
H	-0.811285	-0.982306	-3.009001
N	-1.580418	-0.526067	1.695248
H	-2.310837	-0.650960	1.006792
C	-2.080711	0.166127	2.897412
H	-2.381435	-0.544890	3.673400
H	-2.951182	0.769457	2.623615
H	-1.314611	0.829322	3.300885
C	5.553230	0.900443	-1.539247
H	5.743725	-0.168159	-1.732930
O	4.525418	1.302304	-0.988106
N	6.541547	1.703347	-1.959719
H	6.467270	2.704475	-1.825126
H	7.371735	1.334651	-2.402268

Point 25 $\theta = 240°$

C	-0.227213	-0.100547	-0.233821
C	-0.332614	-0.363307	1.152512
N	2.105179	0.309572	0.035210
C	0.856635	-0.390675	1.964933
C	1.020706	0.250485	-0.759613
C	2.086769	-0.012234	1.370492
C	0.880045	-0.827940	3.314722
H	4.198632	0.344670	1.640555
H	3.006791	0.609297	-0.376012
C	2.054205	-0.816041	4.037523
H	-0.029396	-1.210842	3.762399
H	2.059970	-1.165049	5.065120
C	3.255190	-0.367859	3.443695
H	4.170499	-0.350371	4.027173
C	3.280587	0.020328	2.120330
C	-1.461350	-0.118369	-1.122037
H	-2.120036	0.712405	-0.827559
H	-2.033480	-1.040323	-0.949132

C	1.232484	0.624602	-2.207151
H	1.661757	-0.248718	-2.720902
H	1.986734	1.417341	-2.266545
C	-0.072951	1.030761	-2.900177
H	-0.399197	2.013592	-2.535480
H	0.103899	1.133232	-3.975401
C	-1.152098	-0.018152	-2.624631
H	-2.074140	0.218828	-3.164737
H	-0.811682	-0.993971	-2.995291
N	-1.558025	-0.587306	1.735417
H	-2.280253	-0.768244	1.047794
C	-2.093270	0.263758	2.817639
H	-2.783337	-0.318698	3.433415
H	-2.625950	1.128048	2.402937
H	-1.284469	0.629760	3.448449
C	5.538494	0.927759	-1.541430
H	5.735507	-0.139620	-1.734999
O	4.509399	1.323100	-0.987448
N	6.519890	1.737093	-1.964991
H	6.439227	2.737786	-1.830633
H	7.351340	1.373855	-2.409740

Point 26 $\theta = 250°$

C	-0.223972	-0.123224	-0.215185
C	-0.312530	-0.415001	1.162594
N	2.109094	0.294377	0.039883
C	0.876588	-0.425253	1.969950
C	1.021081	0.240917	-0.748046
C	2.101702	-0.033511	1.373741
C	0.900809	-0.850435	3.323314
H	4.211455	0.343436	1.640932
H	3.007485	0.601756	-0.375093
C	2.074580	-0.821290	4.045372
H	-0.009906	-1.233277	3.768739
H	2.084013	-1.159149	5.076695
C	3.272950	-0.369334	3.446886
H	4.187885	-0.341193	4.030549
C	3.296404	0.012022	2.121507
C	-1.464455	-0.134819	-1.095548
H	-2.124373	0.688274	-0.784118
H	-2.031616	-1.060799	-0.930864
C	1.219376	0.633704	-2.192325
H	1.644930	-0.232667	-2.720794
H	1.971846	1.428287	-2.249127
C	-0.093629	1.045131	-2.868106
H	-0.420103	2.021528	-2.486718

H	0.074034	1.163675	-3.943124
C	-1.166548	-0.011870	-2.598747
H	-2.093521	0.229086	-3.128518
H	-0.825191	-0.980873	-2.986179
N	-1.531790	-0.663783	1.772389
H	-2.241962	-0.902140	1.087805
C	-2.095578	0.321308	2.722396
H	-2.964128	-0.127029	3.209640
H	-2.402546	1.245045	2.215125
H	-1.362373	0.574235	3.488465
C	5.528347	0.934095	-1.544781
H	5.727724	-0.131909	-1.743016
O	4.498568	1.324568	-0.988032
N	6.507017	1.747755	-1.965488
H	6.423861	2.747686	-1.826821
H	7.338950	1.388676	-2.412768

Point 27 $\theta = 260°$

C	-0.217436	-0.135014	-0.193768
C	-0.288462	-0.463550	1.173367
N	2.116302	0.287896	0.048598
C	0.898868	-0.453351	1.977713
C	1.024124	0.244159	-0.732171
C	2.119408	-0.047733	1.380401
C	0.921462	-0.860249	3.336671
H	4.226776	0.348038	1.646020
H	3.012230	0.600533	-0.370147
C	2.094026	-0.812243	4.058990
H	0.007432	-1.235952	3.781631
H	2.105092	-1.133297	5.095679
C	3.290977	-0.361099	3.455176
H	4.205083	-0.321917	4.039539
C	3.314110	0.010750	2.126985
C	-1.464398	-0.138023	-1.065446
H	-2.124981	0.676149	-0.733998
H	-2.027083	-1.067933	-0.910884
C	1.208739	0.659516	-2.171758
H	1.630040	-0.198089	-2.717686
H	1.959530	1.455958	-2.223949
C	-0.111912	1.078432	-2.828211
H	-0.437976	2.046814	-2.426586
H	0.046050	1.216810	-3.902302
C	-1.178954	0.012888	-2.568455
H	-2.110974	0.260034	-3.086360
H	-0.837470	-0.947692	-2.976363
N	-1.500831	-0.741856	1.806838

H	-2.186717	-1.066877	1.131314
C	-2.120062	0.339764	2.608864
H	-3.025471	-0.056383	3.073488
H	-2.379508	1.215505	1.999328
H	-1.438623	0.657260	3.400443
C	5.519360	0.919657	-1.552508
H	5.707413	-0.147936	-1.752899
O	4.496275	1.319309	-0.989417
N	6.502977	1.724513	-1.977797
H	6.430081	2.725052	-1.837556
H	7.328979	1.358160	-2.430198

Point 28 $\theta = 270°$

C	-0.214705	-0.133959	-0.165727
C	-0.269136	-0.493392	1.191769
N	2.123331	0.275309	0.058231
C	0.920016	-0.481113	1.988602
C	1.025096	0.248063	-0.712960
C	2.137829	-0.070884	1.386872
C	0.944433	-0.877494	3.350949
H	4.246802	0.325398	1.643694
H	3.017438	0.588637	-0.365683
C	2.119584	-0.825375	4.068156
H	0.026514	-1.239895	3.798763
H	2.133840	-1.135655	5.108108
C	3.316120	-0.381397	3.456740
H	4.232147	-0.341404	4.038080
C	3.335963	-0.012468	2.127647
C	-1.467536	-0.125066	-1.029134
H	-2.116769	0.696710	-0.695590
H	-2.039811	-1.047096	-0.866685
C	1.199688	0.674950	-2.150442
H	1.623130	-0.176967	-2.703638
H	1.946349	1.475423	-2.201244
C	-0.126135	1.090548	-2.798687
H	-0.452767	2.057680	-2.394538
H	0.025735	1.230493	-3.873437
C	-1.189312	0.022273	-2.533442
H	-2.123979	0.266756	-3.047835
H	-0.847475	-0.938326	-2.941223
N	-1.477993	-0.781360	1.850535
H	-2.134785	-1.198988	1.195118
C	-2.153956	0.375196	2.487616
H	-3.074667	0.015441	2.951894
H	-2.396675	1.175384	1.775485
H	-1.514542	0.789186	3.271033

C	5.513355	0.920514	-1.561321
H	5.701046	-0.144340	-1.775806
O	4.492544	1.312489	-0.988397
N	6.494237	1.731340	-1.980919
H	6.421262	2.730034	-1.827988
H	7.318258	1.371359	-2.442012

Point 29 $\theta = 280°$

C	-0.215030	-0.095992	-0.129252
C	-0.252057	-0.490175	1.217497
N	2.128821	0.293557	0.073230
C	0.942692	-0.487674	2.002687
C	1.023385	0.286527	-0.686202
C	2.156969	-0.070645	1.396155
C	0.975794	-0.891286	3.363316
H	4.269462	0.318125	1.638607
H	3.022020	0.602397	-0.357743
C	2.157163	-0.847883	4.070172
H	0.056133	-1.243897	3.814692
H	2.178596	-1.161335	5.109074
C	3.351211	-0.405306	3.451714
H	4.271941	-0.373606	4.026136
C	3.361929	-0.023078	2.126363
C	-1.470064	-0.073888	-0.989071
H	-2.090456	0.780286	-0.685043
H	-2.072847	-0.968388	-0.791614
C	1.193320	0.714342	-2.124516
H	1.641990	-0.129792	-2.669787
H	1.922026	1.531493	-2.174410
C	-0.135868	1.095162	-2.786667
H	-0.477002	2.067873	-2.408783
H	0.018468	1.210070	-3.864008
C	-1.188084	0.022297	-2.495805
H	-2.122584	0.241685	-3.021713
H	-0.834818	-0.947680	-2.870621
N	-1.454158	-0.804061	1.898787
H	-2.059943	-1.343344	1.282043
C	-2.228384	0.368226	2.372252
H	-3.134496	-0.001176	2.857748
H	-2.509520	1.065133	1.571587
H	-1.641790	0.913539	3.116623
C	5.507868	0.908345	-1.570613
H	5.680293	-0.157902	-1.790749
O	4.495852	1.311049	-0.989251
N	6.496126	1.708236	-1.993306
H	6.437113	2.707127	-1.835601

H	7.312409	1.339644	-2.461342
Point 30	θ = 290°		
C	-0.215096	-0.032666	-0.087348
C	-0.240298	-0.455326	1.249911
N	2.137866	0.314844	0.090158
C	0.963162	-0.479293	2.020316
C	1.024947	0.336109	-0.655960
C	2.176961	-0.067393	1.407051
C	1.005843	-0.894445	3.377788
H	4.297111	0.291704	1.629467
H	3.032002	0.610297	-0.349479
C	2.195978	-0.875972	4.070383
H	0.082721	-1.226739	3.836678
H	2.223884	-1.195851	5.107197
C	3.390046	-0.445025	3.443043
H	4.317326	-0.432570	4.007607
C	3.391038	-0.044858	2.123127
C	-1.469454	0.009987	-0.945615
H	-2.041833	0.912009	-0.690976
H	-2.117378	-0.837605	-0.694915
C	1.195385	0.748936	-2.099380
H	1.671870	-0.092665	-2.624540
H	1.906030	1.581783	-2.154772
C	-0.132761	1.087364	-2.786475
H	-0.484997	2.072950	-2.455320
H	0.029241	1.155715	-3.866632
C	-1.181420	0.022978	-2.453176
H	-2.113168	0.213801	-2.994906
H	-0.823121	-0.963884	-2.775861
N	-1.435497	-0.796829	1.948233
H	-1.960282	-1.481684	1.404515
C	-2.336210	0.334832	2.260301
H	-3.193991	-0.063639	2.807497
H	-2.701580	0.883847	1.383216
H	-1.813802	1.036574	2.916607
C	5.506820	0.897756	-1.589998
H	5.666217	-0.167109	-1.825904
O	4.504852	1.302797	-0.992970
N	6.498570	1.693414	-2.012161
H	6.451132	2.690664	-1.840643
H	7.306363	1.323195	-2.493477
Point 31	θ = 300°		
C	-0.216926	0.108178	-0.060655
C	-0.260536	-0.315665	1.289775
N	2.150469	0.358199	0.102911

C	0.968629	-0.416326	2.045457
C	1.020252	0.451151	-0.620323
C	2.185877	-0.067408	1.406585
C	1.039244	-0.804926	3.409286
H	4.326223	0.154846	1.561100
H	3.048545	0.617950	-0.342462
C	2.247859	-0.872520	4.069391
H	0.136231	-1.032046	3.966349
H	2.276228	-1.169549	5.112724
C	3.446438	-0.538156	3.402698
H	4.391682	-0.589209	3.933896
C	3.420009	-0.129680	2.086457
C	-1.459126	0.107551	-0.933432
H	-2.071124	0.991505	-0.705822
H	-2.065889	-0.766745	-0.670017
C	1.202506	0.874085	-2.060247
H	1.712400	0.051339	-2.582996
H	1.892775	1.725748	-2.093830
C	-0.119332	1.188358	-2.767811
H	-0.492556	2.169495	-2.446526
H	0.055175	1.253154	-3.846375
C	-1.151145	0.108228	-2.436968
H	-2.079543	0.272365	-2.993216
H	-0.768428	-0.875133	-2.741650
N	-1.436403	-0.737278	1.866108
H	-1.280340	-1.264252	2.715651
C	-2.645682	0.095646	1.994241
H	-3.381623	-0.478835	2.560038
H	-3.080452	0.330180	1.023852
H	-2.438556	1.032228	2.526793
C	5.526595	0.815360	-1.643008
H	5.611983	-0.242544	-1.941655
O	4.576845	1.244134	-0.982569
N	6.547327	1.573865	-2.067586
H	6.567420	2.561184	-1.842277
H	7.311426	1.183530	-2.601300

Point 32 $\theta = 310°$

C	-0.210957	0.104297	-0.040876
C	-0.253386	-0.307208	1.315273
N	2.156488	0.355498	0.118075
C	0.981326	-0.428760	2.062594
C	1.022956	0.450771	-0.601116
C	2.195664	-0.083792	1.417582
C	1.059370	-0.834464	3.420365
H	4.338068	0.122684	1.559608

H	3.052156	0.620517	-0.327627
C	2.272219	-0.919447	4.071099
H	0.160824	-1.067076	3.982651
H	2.305787	-1.231439	5.109883
C	3.467721	-0.584484	3.400077
H	4.416598	-0.647676	3.923434
C	3.433812	-0.161390	2.088613
C	-1.455398	0.081272	-0.914029
H	-2.104387	0.931102	-0.665687
H	-2.026323	-0.823332	-0.674697
C	1.198520	0.891950	-2.036140
H	1.704951	0.077258	-2.574552
H	1.888420	1.744207	-2.061089
C	-0.128167	1.216658	-2.728958
H	-0.505013	2.187761	-2.382239
H	0.039191	1.307692	-3.806768
C	-1.149803	0.121424	-2.417915
H	-2.081251	0.287697	-2.968411
H	-0.757493	-0.850705	-2.745636
N	-1.428109	-0.674703	1.910330
H	-1.302221	-1.156346	2.788683
C	-2.678603	0.105174	1.880490
H	-3.213211	-0.093002	2.811511
H	-3.328248	-0.181553	1.050978
H	-2.473924	1.178599	1.823722
C	5.523859	0.829392	-1.645097
H	5.606809	-0.226106	-1.953013
O	4.579573	1.252834	-0.973816
N	6.541538	1.591167	-2.071786
H	6.563703	2.576568	-1.838510
H	7.301418	1.204967	-2.614422

Point 33 $\theta = 320°$

C	-0.214172	0.122150	-0.024865
C	-0.254331	-0.280736	1.337148
N	2.157185	0.359460	0.124933
C	0.988538	-0.423312	2.073899
C	1.019878	0.458556	-0.588648
C	2.200311	-0.086770	1.421945
C	1.075631	-0.843975	3.426334
H	4.344868	0.101096	1.547564
H	3.051080	0.622543	-0.323971
C	2.292930	-0.945547	4.066915
H	0.183136	-1.082666	3.995815
H	2.331569	-1.270655	5.101474
C	3.485249	-0.612805	3.390352

H	4.437947	-0.687957	3.905100
C	3.443025	-0.179346	2.082593
C	-1.456292	0.091331	-0.905315
H	-2.110667	0.940088	-0.670952
H	-2.025776	-0.814117	-0.668160
C	1.197251	0.902095	-2.023166
H	1.711777	0.091410	-2.559794
H	1.881883	1.758772	-2.043879
C	-0.127410	1.218931	-2.722166
H	-0.510217	2.189657	-2.380994
H	0.042859	1.305759	-3.799862
C	-1.143232	0.119970	-2.407942
H	-2.073605	0.275303	-2.963510
H	-0.742899	-0.852266	-2.725595
N	-1.418867	-0.594359	1.966982
H	-1.300326	-1.038929	2.864504
C	-2.714843	0.087468	1.835944
H	-3.233140	-0.007061	2.792343
H	-3.346721	-0.355002	1.062732
H	-2.578178	1.151838	1.627457
C	5.524724	0.831785	-1.649487
H	5.607238	-0.222727	-1.961047
O	4.582000	1.252814	-0.974842
N	6.541540	1.595040	-2.076136
H	6.564261	2.579620	-1.839569
H	7.300274	1.210550	-2.621548

Point 34 $\theta = 330°$

C	-0.216260	0.134014	-0.014526
C	-0.256868	-0.250757	1.355565
N	2.158074	0.362050	0.130262
C	0.992682	-0.416235	2.082721
C	1.018837	0.458521	-0.581237
C	2.202884	-0.086247	1.426376
C	1.087073	-0.857858	3.427915
H	4.348622	0.088854	1.540689
H	3.050744	0.623639	-0.320692
C	2.307416	-0.973017	4.060889
H	0.200620	-1.115637	3.998774
H	2.349857	-1.316604	5.089290
C	3.497041	-0.635066	3.383193
H	4.452327	-0.719718	3.891612
C	3.448666	-0.190291	2.079574
C	-1.456878	0.105098	-0.900689
H	-2.107021	0.959716	-0.678046
H	-2.033396	-0.795378	-0.664602

C	1.200059	0.897369	-2.017156
H	1.714709	0.083836	-2.549300
H	1.886721	1.752398	-2.038176
C	-0.120757	1.214595	-2.722005
H	-0.502171	2.188253	-2.387701
H	0.052406	1.294247	-3.799795
C	-1.138729	0.119914	-2.402397
H	-2.067736	0.271553	-2.961343
H	-0.738728	-0.855555	-2.710508
N	-1.411343	-0.503233	2.020359
H	-1.290637	-0.890460	2.943000
C	-2.746018	0.069949	1.809995
H	-3.275111	0.016969	2.763601
H	-3.329581	-0.478860	1.067830
H	-2.680312	1.120764	1.518271
C	5.525784	0.837406	-1.653159
H	5.610774	-0.216440	-1.966450
O	4.583599	1.254566	-0.975629
N	6.539347	1.604314	-2.081454
H	6.559839	2.588562	-1.843368
H	7.297943	1.222774	-2.629100

Point 35 $\theta = 340°$

C	-0.217554	0.142018	-0.009227
C	-0.259323	-0.216649	1.370153
N	2.159095	0.366244	0.133832
C	0.995049	-0.409370	2.087130
C	1.019189	0.452904	-0.578728
C	2.204349	-0.080778	1.430210
C	1.093310	-0.883487	3.420869
H	4.350237	0.090287	1.541752
H	3.050802	0.627298	-0.318326
C	2.314925	-1.009283	4.049823
H	0.211216	-1.178198	3.980892
H	2.359853	-1.380869	5.068321
C	3.502384	-0.653677	3.378033
H	4.458695	-0.745169	3.883325
C	3.451173	-0.192668	2.080161
C	-1.458931	0.127670	-0.897290
H	-2.090925	0.998549	-0.686072
H	-2.055164	-0.757970	-0.657620
C	1.205324	0.877583	-2.018683
H	1.712465	0.053696	-2.542113
H	1.900688	1.725267	-2.046561
C	-0.110287	1.201249	-2.729501
H	-0.482205	2.182425	-2.406660

H	0.065288	1.266975	-3.807848
C	-1.139371	0.120950	-2.398612
H	-2.066778	0.275698	-2.959451
H	-0.749477	-0.862310	-2.694761
N	-1.402738	-0.404194	2.068261
H	-1.270220	-0.709076	3.019381
C	-2.770530	0.051300	1.800528
H	-3.304610	0.039472	2.752600
H	-3.303584	-0.601131	1.105747
H	-2.779648	1.075460	1.422423
C	5.528947	0.849220	-1.652035
H	5.620685	-0.204860	-1.962728
O	4.584405	1.261944	-0.975278
N	6.537484	1.621564	-2.082781
H	6.551852	2.606469	-1.847021
H	7.298407	1.243452	-2.629555

Point 36 $\theta = 350°$

C	-0.218527	0.161218	-0.006213
C	-0.260857	-0.188990	1.376721
N	2.161787	0.368120	0.132108
C	0.996476	-0.388521	2.090539
C	1.020882	0.454725	-0.579155
C	2.206154	-0.066633	1.432372
C	1.095720	-0.870471	3.421458
H	4.352224	0.100590	1.542068
H	3.053936	0.620604	-0.323386
C	2.317313	-0.997451	4.050551
H	0.215256	-1.178565	3.976920
H	2.362233	-1.375863	5.066528
C	3.504503	-0.638909	3.380325
H	4.460883	-0.730971	3.885379
C	3.453099	-0.179457	2.081895
C	-1.463365	0.196397	-0.890203
H	-2.048756	1.100843	-0.682033
H	-2.103678	-0.655508	-0.647305
C	1.213057	0.863622	-2.023420
H	1.697467	0.021731	-2.539891
H	1.930208	1.692414	-2.060347
C	-0.093813	1.214994	-2.736548
H	-0.438678	2.209378	-2.424242
H	0.082200	1.264129	-3.815731
C	-1.151544	0.167455	-2.392568
H	-2.076971	0.344944	-2.950052
H	-0.792311	-0.829515	-2.681718
N	-1.393692	-0.352883	2.094776

H	-1.245930	-0.614656	3.056293
C	-2.797467	-0.059267	1.794903
H	-3.324712	-0.010896	2.749728
H	-3.266886	-0.837959	1.188063
H	-2.907355	0.906976	1.302524
C	5.537092	0.830614	-1.655669
H	5.628024	-0.225104	-1.961018
O	4.591994	1.247806	-0.982507
N	6.547330	1.599592	-2.088613
H	6.562511	2.585624	-1.857680
H	7.308670	1.217850	-2.632266

Rotation in the clockwise direction:

Point 1 $\theta = 0°$

H	-2.772392	1.204231	-1.653893
C	-2.827277	0.594054	-0.757847
C	-2.897168	-0.989354	1.547708
C	-1.629011	0.134297	-0.172944
C	-4.035373	0.260800	-0.184257
C	-4.068856	-0.525783	0.985015
C	-1.633218	-0.688717	0.976708
H	-4.961614	0.612673	-0.627529
H	-5.019966	-0.766257	1.448697
H	-2.979020	-1.567530	2.462920
C	0.851671	-0.687583	0.914280
C	-0.357815	-1.180020	1.491247
C	1.958642	0.708900	-0.939996
H	2.010736	1.779443	-0.691529
H	1.769561	0.658251	-2.018713
C	3.279701	0.034930	-0.566273
H	4.114149	0.631944	-0.947585
H	3.348261	-0.950881	-1.044585
C	3.354101	-0.116735	0.951593
H	3.269463	0.870535	1.425754
H	4.319446	-0.532636	1.258137
C	2.235484	-1.037088	1.458381
H	2.223086	-0.998897	2.549675
H	2.488411	-2.069108	1.181362
N	-0.430408	-2.090749	2.487061
H	-1.369172	-2.349619	2.744830
C	0.586030	-2.820101	3.249172
H	1.078712	-2.186131	3.992052
H	1.333270	-3.274378	2.599420
H	0.070057	-3.622899	3.779378
C	0.762742	0.135135	-0.211235

N	-0.428049	0.494274	-0.728655
H	-0.445979	1.081066	-1.578551
C	-0.535302	3.059378	-3.592769
H	-0.536629	3.939233	-2.928065
O	-0.540086	1.903413	-3.163491
N	-0.527474	3.375764	-4.896260
H	-0.530469	4.336712	-5.208506
H	-0.530247	2.639432	-5.591706

Point 2 $\theta = 350°$

H	-2.770912	1.216677	-1.640829
C	-2.826220	0.611844	-0.741190
C	-2.898236	-0.965452	1.568752
C	-1.628842	0.143224	-0.161440
C	-4.033935	0.293509	-0.158526
C	-4.068541	-0.492438	1.011211
C	-1.634268	-0.671204	0.994740
H	-4.959336	0.652924	-0.597478
H	-5.019812	-0.728536	1.476803
H	-2.982782	-1.553443	2.477450
C	0.849907	-0.690130	0.916573
C	-0.359774	-1.167072	1.505227
C	1.959110	0.681208	-0.955149
H	1.983882	1.763336	-0.759067
H	1.788603	0.574857	-2.033180
C	3.288392	0.054991	-0.529814
H	4.115213	0.663874	-0.908906
H	3.396265	-0.941831	-0.977024
C	3.330400	-0.052925	0.993492
H	3.199648	0.942634	1.438951
H	4.301125	-0.427474	1.334318
C	2.230143	-0.998716	1.493008
H	2.188006	-0.944363	2.583629
H	2.522960	-2.025488	1.239119
N	-0.423123	-2.059872	2.517626
H	-1.356374	-2.269659	2.833581
C	0.593010	-2.905834	3.148487
H	1.181211	-2.365556	3.895319
H	1.257948	-3.351329	2.408799
H	0.064865	-3.716090	3.655194
C	0.762654	0.118729	-0.218649
N	-0.428543	0.481910	-0.732399
H	-0.447124	1.061898	-1.587008
C	-0.529992	3.032097	-3.610436
H	-0.520941	3.916275	-2.951510
O	-0.542679	1.879085	-3.173639

N	-0.525066	3.340040	-4.915990
H	-0.521559	4.298965	-5.234384
H	-0.537283	2.599334	-5.606664

Point 3 $\theta = 340°$

H	-2.772500	1.214475	-1.636769
C	-2.826341	0.617546	-0.731777
C	-2.897251	-0.944744	1.589889
C	-1.628628	0.149011	-0.152647
C	-4.032921	0.308987	-0.141390
C	-4.067220	-0.470550	1.032971
C	-1.634321	-0.654427	1.011949
H	-4.958462	0.669038	-0.579537
H	-5.018437	-0.702654	1.500689
H	-2.979504	-1.533330	2.498396
C	0.848041	-0.675408	0.930432
C	-0.360812	-1.147679	1.521174
C	1.962338	0.658517	-0.962691
H	1.980051	1.747066	-0.806179
H	1.803476	0.511750	-2.037928
C	3.289496	0.053862	-0.500083
H	4.117978	0.652094	-0.892193
H	3.406399	-0.958271	-0.908945
C	3.314642	0.003208	1.027021
H	3.166519	1.013549	1.431785
H	4.285594	-0.345495	1.393450
C	2.218990	-0.936053	1.549281
H	2.143350	-0.824256	2.634977
H	2.535230	-1.969119	1.360663
N	-0.406991	-2.029362	2.546090
H	-1.333137	-2.227159	2.890038
C	0.597469	-2.980926	3.031284
H	1.330944	-2.517919	3.694656
H	1.111262	-3.470923	2.201655
H	0.065720	-3.747752	3.597842
C	0.762984	0.114127	-0.218436
N	-0.428801	0.471554	-0.734767
H	-0.448113	1.040379	-1.597194
C	-0.526209	3.005047	-3.619422
H	-0.511344	3.887921	-2.958835
O	-0.546647	1.851272	-3.184823
N	-0.518906	3.315457	-4.924329
H	-0.509662	4.274967	-5.240851
H	-0.536278	2.576199	-5.616448

Point 4 $\theta = 330°$

H	-2.771724	1.225449	-1.625872
C	-2.824605	0.622761	-0.724658
C	-2.895338	-0.966853	1.579802
C	-1.626102	0.158757	-0.143489
C	-4.031304	0.298887	-0.142857
C	-4.065981	-0.499288	1.019306
C	-1.631063	-0.647588	1.020097
H	-4.957665	0.654672	-0.582764
H	-5.018822	-0.755627	1.470810
H	-2.977357	-1.588828	2.465573
C	0.849920	-0.664960	0.936468
C	-0.356680	-1.118911	1.540824
C	1.967174	0.649669	-0.967143
H	1.990150	1.739631	-0.821839
H	1.808673	0.492609	-2.041037
C	3.290649	0.042393	-0.496315
H	4.122710	0.630901	-0.895461
H	3.401390	-0.975182	-0.893183
C	3.316215	0.009801	1.031711
H	3.173420	1.025846	1.423852
H	4.285926	-0.338656	1.401515
C	2.215857	-0.917257	1.566128
H	2.129426	-0.785924	2.649674
H	2.529847	-1.955042	1.400879
N	-0.381220	-1.954735	2.608146
H	-1.293952	-2.097075	3.011232
C	0.581947	-2.994140	2.990446
H	1.399214	-2.608074	3.603160
H	0.990942	-3.493041	2.108623
H	0.039878	-3.737684	3.578108
C	0.765959	0.116871	-0.218341
N	-0.426628	0.481650	-0.726496
H	-0.447436	1.050587	-1.589321
C	-0.524191	3.006420	-3.617676
H	-0.503361	3.892605	-2.961767
O	-0.545041	1.854878	-3.176945
N	-0.523553	3.309845	-4.924134
H	-0.513017	4.267641	-5.245801
H	-0.546259	2.566994	-5.612255

Point 5 $\theta = 320°$

H	-2.772149	1.224883	-1.621899
C	-2.821409	0.619504	-0.722309
C	-2.885769	-0.985151	1.574175
C	-1.620604	0.165633	-0.138001
C	-4.026620	0.279623	-0.146289

C	-4.058512	-0.529360	1.009017
C	-1.622713	-0.640598	1.026742
H	-4.955002	0.626806	-0.588826
H	-5.011323	-0.806129	1.448398
H	-2.960569	-1.628440	2.445005
C	0.855571	-0.649538	0.943355
C	-0.348117	-1.089828	1.557176
C	1.975351	0.655184	-0.964158
H	2.004356	1.744805	-0.817213
H	1.816942	0.500443	-2.038413
C	3.295156	0.039125	-0.492729
H	4.130727	0.621101	-0.894112
H	3.397918	-0.979666	-0.888624
C	3.324653	0.008016	1.035799
H	3.192620	1.025883	1.426914
H	4.292706	-0.348300	1.402327
C	2.217151	-0.907704	1.575198
H	2.126142	-0.773047	2.658654
H	2.520943	-1.949840	1.416034
N	-0.350076	-1.877332	2.666625
H	-1.251404	-1.971122	3.109453
C	0.547721	-3.004278	2.959128
H	1.430103	-2.702345	3.527626
H	0.862451	-3.502882	2.038689
H	-0.013114	-3.723221	3.559864
C	0.772268	0.126631	-0.216186
N	-0.421459	0.493617	-0.719104
H	-0.444267	1.062912	-1.582211
C	-0.528675	3.006610	-3.618934
H	-0.505784	3.896824	-2.968655
O	-0.545947	1.857698	-3.170898
N	-0.534837	3.301650	-4.927165
H	-0.526729	4.257401	-5.254966
H	-0.559702	2.554432	-5.610486

Point 6 $\theta = 310°$

H	-2.772259	1.204787	-1.630172
C	-2.816469	0.602255	-0.728431
C	-2.870182	-0.998530	1.573712
C	-1.612390	0.165506	-0.137832
C	-4.019004	0.247645	-0.155509
C	-4.045781	-0.560989	1.000864
C	-1.609754	-0.634539	1.032427
H	-4.950182	0.580771	-0.602967
H	-4.997364	-0.852981	1.433038
H	-2.935010	-1.648185	2.440435

C	0.864895	-0.627499	0.951809
C	-0.334814	-1.060084	1.571683
C	1.986004	0.670086	-0.958179
H	2.021897	1.758185	-0.801195
H	1.827036	0.525890	-2.033775
C	3.302049	0.040939	-0.491579
H	4.141155	0.616890	-0.894273
H	3.394157	-0.977230	-0.891687
C	3.339227	0.003944	1.037214
H	3.223326	1.022171	1.432421
H	4.305110	-0.365757	1.396012
C	2.222611	-0.898022	1.581073
H	2.131117	-0.765118	2.665265
H	2.509982	-1.945401	1.421507
N	-0.313228	-1.800808	2.720399
H	-1.207962	-1.852663	3.185277
C	0.494714	-3.014838	2.934464
H	1.451498	-2.798649	3.414811
H	0.675117	-3.539169	1.991474
H	-0.071370	-3.677727	3.591862
C	0.781445	0.141149	-0.213790
N	-0.414055	0.501986	-0.715800
H	-0.439720	1.069598	-1.580671
C	-0.537458	3.005784	-3.617230
H	-0.518721	3.896343	-2.967384
O	-0.547643	1.856837	-3.168557
N	-0.547236	3.299871	-4.925468
H	-0.544386	4.255451	-5.253908
H	-0.568355	2.552102	-5.608342

Point 7 $\theta = 300°$

H	-2.764591	1.176558	-1.644232
C	-2.804450	0.573698	-0.742508
C	-2.846655	-1.027726	1.561255
C	-1.597662	0.153789	-0.145437
C	-4.004249	0.201203	-0.175262
C	-4.025037	-0.609027	0.980559
C	-1.588279	-0.643669	1.027409
H	-4.938061	0.520261	-0.627460
H	-4.974697	-0.917643	1.405384
H	-2.903701	-1.682369	2.424526
C	0.883565	-0.625493	0.946937
C	-0.312748	-1.047853	1.576871
C	1.997010	0.699238	-0.952405
H	2.012988	1.786752	-0.787984
H	1.845485	0.560059	-2.029725

C	3.323062	0.091125	-0.485064
H	4.151773	0.693508	-0.870248
H	3.441831	-0.916743	-0.903710
C	3.350642	0.022925	1.042991
H	3.214622	1.029179	1.461673
H	4.320076	-0.339531	1.399584
C	2.245601	-0.911120	1.554214
H	2.160424	-0.838684	2.644708
H	2.539698	-1.946560	1.332189
N	-0.285903	-1.743404	2.763390
H	-1.180451	-1.732658	3.236218
C	0.377269	-3.045833	2.950759
H	1.454384	-2.973858	2.810302
H	-0.020065	-3.805439	2.265841
H	0.193949	-3.364214	3.978841
C	0.796263	0.149131	-0.216513
N	-0.400740	0.505069	-0.716218
H	-0.428969	1.078068	-1.578147
C	-0.532281	3.016079	-3.608923
H	-0.518064	3.905851	-2.957986
O	-0.537482	1.866405	-3.161547
N	-0.542298	3.311371	-4.916702
H	-0.544374	4.267309	-5.244170
H	-0.559886	2.564245	-5.600412

Point 8 $\theta = 290°$

H	-2.764404	1.139717	-1.656775
C	-2.796358	0.544779	-0.749501
C	-2.821551	-1.033341	1.574313
C	-1.585006	0.145138	-0.147704
C	-3.991142	0.162574	-0.177899
C	-4.003670	-0.635291	0.987542
C	-1.568278	-0.640921	1.034068
H	-4.928749	0.465312	-0.633486
H	-4.950602	-0.949529	1.414385
H	-2.864678	-1.677433	2.446239
C	0.899305	-0.606129	0.952322
C	-0.292460	-1.026752	1.584934
C	2.010144	0.727432	-0.940859
H	2.021494	1.813008	-0.763070
H	1.863748	0.600817	-2.020398
C	3.337337	0.118331	-0.475199
H	4.164515	0.728015	-0.852145
H	3.460236	-0.883939	-0.905942
C	3.365741	0.030491	1.052617
H	3.232490	1.031298	1.485045

H	4.335449	-0.338091	1.402041
C	2.259214	-0.907773	1.552189
H	2.172258	-0.862881	2.644000
H	2.545948	-1.940625	1.307769
N	-0.238400	-1.690112	2.798870
H	-1.113440	-1.613223	3.304971
C	0.282153	-3.065538	2.916516
H	1.315809	-3.122600	2.575870
H	-0.318157	-3.781086	2.340087
H	0.258548	-3.345761	3.971694
C	0.809719	0.164754	-0.214815
N	-0.390176	0.506987	-0.716176
H	-0.422774	1.078687	-1.579687
C	-0.540987	3.006630	-3.612492
H	-0.536842	3.897962	-2.963651
O	-0.535634	1.857855	-3.162272
N	-0.551766	3.298381	-4.920849
H	-0.561308	4.253442	-5.250796
H	-0.559732	2.549414	-5.602756

Point 9 $\theta = 280°$

H	-2.762925	1.099256	-1.666027
C	-2.785788	0.512221	-0.753351
C	-2.790645	-1.041646	1.590602
C	-1.569363	0.135989	-0.146653
C	-3.974575	0.117376	-0.177677
C	-3.977072	-0.667105	0.997808
C	-1.543375	-0.639200	1.043366
H	-4.916383	0.401391	-0.636652
H	-4.920479	-0.987825	1.427685
H	-2.819618	-1.672259	2.472907
C	0.919520	-0.574262	0.965198
C	-0.265994	-1.002914	1.595558
C	2.024854	0.759927	-0.929243
H	2.041942	1.842372	-0.732889
H	1.875907	0.651909	-2.010349
C	3.350228	0.136399	-0.475299
H	4.179644	0.741494	-0.854741
H	3.460896	-0.863866	-0.913990
C	3.391447	0.038136	1.052246
H	3.276385	1.038263	1.491535
H	4.360255	-0.344305	1.388930
C	2.277885	-0.887489	1.559557
H	2.192297	-0.846161	2.651312
H	2.547451	-1.925195	1.314967
N	-0.184806	-1.650011	2.828176

H	-1.034383	-1.503697	3.365057
C	0.168911	-3.084285	2.875641
H	1.152195	-3.248710	2.431100
H	-0.562644	-3.710786	2.348771
H	0.216289	-3.388645	3.923390
C	0.825674	0.189402	-0.208454
N	-0.377605	0.511939	-0.712706
H	-0.416336	1.079295	-1.579819
C	-0.553477	2.994595	-3.614686
H	-0.562030	3.886909	-2.967348
O	-0.534937	1.846523	-3.162372
N	-0.564630	3.283642	-4.923396
H	-0.585211	4.237919	-5.255172
H	-0.561506	2.533404	-5.603981

Point 10 $\theta = 270°$

H	-2.759582	1.060809	-1.667509
C	-2.772566	0.479726	-0.750839
C	-2.754168	-1.053945	1.609799
C	-1.550738	0.125979	-0.141310
C	-3.954432	0.071071	-0.170575
C	-3.945355	-0.701365	1.013698
C	-1.513576	-0.641640	1.054214
H	-4.900821	0.337149	-0.630875
H	-4.884637	-1.027901	1.448282
H	-2.768968	-1.669924	2.502649
C	0.944612	-0.539026	0.981568
C	-0.233467	-0.983796	1.605874
C	2.039098	0.798160	-0.917135
H	2.063744	1.876727	-0.700422
H	1.883036	0.710662	-1.998959
C	3.363469	0.158863	-0.480936
H	4.194333	0.757344	-0.867636
H	3.458157	-0.840241	-0.926021
C	3.422875	0.053855	1.045928
H	3.328677	1.054542	1.489081
H	4.391271	-0.342152	1.367732
C	2.304406	-0.856739	1.569324
H	2.224886	-0.810061	2.660685
H	2.557022	-1.900699	1.332272
N	-0.129091	-1.635907	2.846187
H	-0.939663	-1.412172	3.418756
C	0.030848	-3.107396	2.828500
H	0.955008	-3.375171	2.310199
H	-0.806374	-3.619270	2.335074
H	0.109098	-3.454730	3.861006

C	0.843688	0.219255	-0.197999
N	-0.363188	0.518776	-0.704967
H	-0.409142	1.080995	-1.576091
C	-0.565053	2.978936	-3.618039
H	-0.586450	3.874113	-2.975086
O	-0.533609	1.833171	-3.159924
N	-0.576108	3.261081	-4.927995
H	-0.607483	4.213372	-5.264679
H	-0.561757	2.507549	-5.604829

Point 11 $\theta = 260°$

H	-2.752950	1.028594	-1.660942
C	-2.756545	0.451603	-0.741605
C	-2.715158	-1.064605	1.632637
C	-1.529633	0.114101	-0.132959
C	-3.931768	0.034240	-0.154229
C	-3.911138	-0.726032	1.038415
C	-1.480589	-0.650392	1.064674
H	-4.882546	0.287654	-0.612607
H	-4.846449	-1.051681	1.482209
H	-2.717681	-1.663392	2.536865
C	0.973105	-0.510361	0.996429
C	-0.196768	-0.978461	1.611159
C	2.052197	0.840270	-0.903787
H	2.077985	1.915200	-0.669180
H	1.889558	0.770056	-1.985779
C	3.379223	0.194898	-0.484055
H	4.207642	0.793410	-0.875900
H	3.466457	-0.801947	-0.935695
C	3.453296	0.082547	1.041770
H	3.369004	1.082336	1.489158
H	4.423563	-0.318352	1.351626
C	2.337533	-0.824831	1.576345
H	2.266038	-0.778327	2.667387
H	2.582678	-1.871003	1.341220
N	-0.071959	-1.659579	2.845714
H	-0.818547	-1.352563	3.467510
C	-0.125662	-3.138503	2.773409
H	0.724887	-3.508356	2.193900
H	-1.048980	-3.517272	2.313637
H	-0.039737	-3.532281	3.788613
C	0.863102	0.248415	-0.185662
N	-0.346950	0.523985	-0.694927
H	-0.400639	1.082324	-1.568984
C	-0.575901	2.957665	-3.626211
H	-0.611515	3.859053	-2.992744

O	-0.530178	1.817100	-3.155904
N	-0.586931	3.225566	-4.938930
H	-0.629979	4.173738	-5.285861
H	-0.560068	2.465184	-5.607716

Point 12 $\theta = 250°$

H	-2.740033	0.995644	-1.660238
C	-2.737872	0.424458	-0.737284
C	-2.680913	-1.065864	1.654200
C	-1.507547	0.094281	-0.131230
C	-3.908981	0.011906	-0.138880
C	-3.880239	-0.729396	1.065883
C	-1.449198	-0.668590	1.067493
H	-4.862869	0.260355	-0.593469
H	-4.813143	-1.039136	1.525915
H	-2.676329	-1.638795	2.574263
C	1.000559	-0.494699	1.004847
C	-0.161341	-0.994408	1.604230
C	2.064193	0.878304	-0.891905
H	2.081637	1.950674	-0.644614
H	1.899673	0.819003	-1.974176
C	3.397384	0.240144	-0.480794
H	4.219887	0.846692	-0.872703
H	3.489911	-0.753796	-0.937717
C	3.476675	0.121590	1.044208
H	3.386818	1.119264	1.495450
H	4.451015	-0.272947	1.349418
C	2.370789	-0.796943	1.580283
H	2.305192	-0.756500	2.671007
H	2.621337	-1.840783	1.341933
N	-0.015145	-1.721075	2.820632
H	-0.659568	-1.330880	3.508714
C	-0.281006	-3.175603	2.725177
H	0.473112	-3.639703	2.082934
H	-1.273267	-3.423918	2.324447
H	-0.180348	-3.603217	3.725367
C	0.882490	0.268709	-0.177013
N	-0.329225	0.518514	-0.691754
H	-0.389463	1.073811	-1.567984
C	-0.590257	2.933481	-3.635373
H	-0.646588	3.838578	-3.008803
O	-0.524806	1.797372	-3.156302
N	-0.599902	3.191204	-4.949973
H	-0.659616	4.135753	-5.304295
H	-0.555018	2.426516	-5.612894

Point 13 θ = 240°

H	-2.726842	0.964637	-1.667367
C	-2.722569	0.399224	-0.740871
C	-2.657824	-1.062384	1.668188
C	-1.490645	0.073236	-0.135229
C	-3.891846	-0.003726	-0.133252
C	-3.858580	-0.722623	1.085178
C	-1.426430	-0.691448	1.062728
H	-4.847360	0.242885	-0.585405
H	-4.790242	-1.008293	1.563036
H	-2.649796	-1.602769	2.606701
C	1.018884	-0.477528	1.014279
C	-0.134921	-1.018497	1.591212
C	2.070683	0.918571	-0.875196
H	2.084368	1.987422	-0.612478
H	1.903310	0.873249	-1.957592
C	3.407396	0.281187	-0.474957
H	4.226662	0.891068	-0.868378
H	3.499185	-0.710681	-0.936506
C	3.493218	0.158055	1.049028
H	3.403250	1.154842	1.502416
H	4.469946	-0.234341	1.349397
C	2.393515	-0.765345	1.590043
H	2.335967	-0.719638	2.680416
H	2.646784	-1.809621	1.359169
N	0.039700	-1.811466	2.766846
H	-0.421988	-1.352746	3.552535
C	-0.418792	-3.214566	2.687444
H	0.194115	-3.748216	1.955009
H	-1.472393	-3.347781	2.410384
H	-0.248024	-3.675468	3.663288
C	0.895119	0.293266	-0.164505
N	-0.316247	0.514497	-0.690308
H	-0.380649	1.065318	-1.569347
C	-0.602279	2.910446	-3.647846
H	-0.683910	3.817885	-3.027512
O	-0.516749	1.778894	-3.161027
N	-0.605360	3.159763	-4.964011
H	-0.682429	4.100575	-5.324885
H	-0.538230	2.392113	-5.621623

Point 14 θ = 230°

H	-2.702685	0.891087	-1.732546
C	-2.710952	0.334586	-0.800652
C	-2.680885	-1.091285	1.620270

C	-1.487460	0.050733	-0.159883
C	-3.889545	-0.093485	-0.225929
C	-3.876250	-0.790787	1.001679
C	-1.444733	-0.706273	1.038816
H	-4.835660	0.125157	-0.711362
H	-4.812854	-1.083044	1.465415
H	-2.685640	-1.596622	2.577925
C	1.008782	-0.404927	1.061598
C	-0.156181	-0.990829	1.620650
C	2.073556	0.947853	-0.828205
H	2.112751	2.016967	-0.570805
H	1.902223	0.898552	-1.909429
C	3.395809	0.280301	-0.434261
H	4.230210	0.852347	-0.852005
H	3.449201	-0.726088	-0.869810
C	3.501278	0.201421	1.089770
H	3.451144	1.214797	1.509252
H	4.466273	-0.216598	1.393298
C	2.372751	-0.657062	1.683801
H	2.331330	-0.468619	2.765824
H	2.622409	-1.722637	1.565574
N	-0.051766	-1.833475	2.691044
H	0.866110	-1.821849	3.115567
C	-0.673281	-3.167959	2.776924
H	-1.240665	-3.382720	1.870375
H	-1.339492	-3.246519	3.641910
H	0.114746	-3.919851	2.877699
C	0.890602	0.341727	-0.111415
N	-0.312552	0.526009	-0.688898
H	-0.362643	1.056790	-1.575520
C	-0.598211	2.905146	-3.674014
H	-0.744260	3.800067	-3.046721
O	-0.470206	1.774439	-3.197722
N	-0.574720	3.172369	-4.987835
H	-0.689694	4.112641	-5.339506
H	-0.450840	2.417639	-5.651872

Point 15 $\theta = 220°$

H	-2.691124	0.884092	-1.736607
C	-2.701124	0.321773	-0.808203
C	-2.671975	-1.115397	1.602517
C	-1.477095	0.028991	-0.172452
C	-3.881369	-0.101066	-0.233598
C	-3.867851	-0.802937	0.990416
C	-1.432869	-0.737907	1.021034
H	-4.827235	0.125597	-0.715814

H	-4.803979	-1.091556	1.457323
H	-2.684717	-1.624533	2.556965
C	1.021794	-0.423712	1.039309
C	-0.138861	-1.033300	1.591087
C	2.076158	0.955913	-0.835042
H	2.097842	2.024628	-0.574089
H	1.909410	0.907964	-1.917089
C	3.406936	0.306878	-0.439705
H	4.234272	0.896279	-0.847321
H	3.479494	-0.694550	-0.883850
C	3.505212	0.215258	1.083996
H	3.436355	1.223352	1.513327
H	4.474757	-0.190831	1.389246
C	2.386678	-0.666649	1.662256
H	2.338215	-0.493276	2.746788
H	2.653204	-1.726882	1.529770
N	-0.002531	-1.887169	2.641279
H	0.932032	-1.912334	3.024465
C	-0.731719	-3.146334	2.852299
H	-1.280500	-3.428386	1.952072
H	-1.429487	-3.080881	3.693580
H	-0.003723	-3.930936	3.074130
C	0.899023	0.329440	-0.125792
N	-0.305684	0.510179	-0.702989
H	-0.359915	1.048116	-1.584351
C	-0.603955	2.919765	-3.666641
H	-0.754022	3.807831	-3.030520
O	-0.472122	1.784964	-3.201719
N	-0.580198	3.200578	-4.977796
H	-0.698482	4.143925	-5.319960
H	-0.452848	2.453109	-5.649320

Point 16 $\theta = 210°$

H	-2.679648	0.884365	-1.740579
C	-2.693051	0.313757	-0.817271
C	-2.668612	-1.142292	1.578966
C	-1.469741	0.010982	-0.184812
C	-3.875683	-0.107055	-0.246790
C	-3.863707	-0.817893	0.971088
C	-1.425600	-0.768244	1.002023
H	-4.820506	0.128028	-0.726991
H	-4.800069	-1.106310	1.437617
H	-2.690619	-1.658619	2.528160
C	1.030455	-0.444999	1.017304
C	-0.126703	-1.076147	1.560259
C	2.076965	0.964134	-0.838654

H	2.083506	2.031391	-0.571135
H	1.914491	0.921086	-1.921606
C	3.414602	0.329872	-0.443267
H	4.235931	0.935069	-0.839754
H	3.503691	-0.665688	-0.897490
C	3.505339	0.222662	1.079824
H	3.418574	1.224480	1.520434
H	4.478798	-0.172752	1.386667
C	2.396266	-0.682264	1.640121
H	2.341618	-0.527449	2.727368
H	2.678529	-1.736481	1.490473
N	0.038633	-1.944415	2.588733
H	0.985122	-1.997249	2.936372
C	-0.770103	-3.117786	2.933140
H	-1.342036	-3.461304	2.068951
H	-1.453437	-2.920027	3.765776
H	-0.089847	-3.917025	3.236813
C	0.904855	0.317735	-0.138741
N	-0.300884	0.497990	-0.714860
H	-0.358264	1.044432	-1.590210
C	-0.607403	2.936353	-3.659717
H	-0.760206	3.819547	-3.017428
O	-0.473227	1.798711	-3.202847
N	-0.583155	3.226751	-4.968912
H	-0.703453	4.172231	-5.304380
H	-0.453425	2.484421	-5.645642

Point 17 $\theta = 200°$

H	-2.670167	0.889749	-1.744927
C	-2.687682	0.307376	-0.829043
C	-2.669868	-1.179569	1.545378
C	-1.466017	-0.003534	-0.197326
C	-3.872699	-0.119832	-0.269119
C	-3.863284	-0.847183	0.938116
C	-1.422742	-0.797757	0.980932
H	-4.815826	0.121619	-0.749472
H	-4.800256	-1.144433	1.397810
H	-2.701628	-1.710211	2.485083
C	1.034974	-0.468218	0.994323
C	-0.120162	-1.114541	1.531019
C	2.075745	0.969689	-0.842563
H	2.072163	2.034508	-0.565539
H	1.915313	0.935230	-1.926162
C	3.418072	0.343501	-0.451101
H	4.235003	0.961191	-0.837301
H	3.518027	-0.645618	-0.916959

C	3.504478	0.218068	1.070749
H	3.406149	1.213155	1.523982
H	4.480460	-0.172062	1.376386
C	2.402078	-0.704743	1.614632
H	2.344475	-0.568127	2.704313
H	2.695220	-1.753688	1.447867
N	0.069548	-1.995087	2.540799
H	1.024289	-2.064036	2.860339
C	-0.791315	-3.072153	3.028594
H	-1.390629	-3.491815	2.217722
H	-1.450634	-2.743075	3.839033
H	-0.144677	-3.860344	3.420349
C	0.907581	0.306368	-0.151685
N	-0.299265	0.490910	-0.724372
H	-0.359062	1.047314	-1.592826
C	-0.607307	2.961318	-3.647582
H	-0.758757	3.839865	-2.998591
O	-0.474665	1.820144	-3.199431
N	-0.582797	3.261736	-4.954611
H	-0.701872	4.209898	-5.282838
H	-0.454269	2.524386	-5.636979

Point 18 $\theta = 190°$

H	-2.662267	0.896187	-1.751920
C	-2.684520	0.297402	-0.846764
C	-2.674747	-1.237871	1.494261
C	-1.465645	-0.017816	-0.211714
C	-3.871483	-0.149144	-0.307360
C	-3.865339	-0.904596	0.881741
C	-1.423677	-0.829846	0.955766
H	-4.812100	0.094708	-0.791376
H	-4.802925	-1.225853	1.323690
H	-2.717067	-1.796020	2.416082
C	1.036098	-0.495524	0.968225
C	-0.119019	-1.145903	1.505958
C	2.073200	0.965603	-0.852984
H	2.066941	2.027583	-0.565392
H	1.910966	0.941715	-1.936606
C	3.417560	0.339117	-0.470144
H	4.232531	0.963277	-0.850052
H	3.519879	-0.644644	-0.946666
C	3.504733	0.197402	1.050060
H	3.403506	1.187150	1.514213
H	4.481751	-0.193401	1.351515
C	2.405110	-0.734548	1.584008
H	2.348256	-0.609922	2.675226

H	2.702836	-1.780385	1.405303
N	0.089005	-2.026681	2.510259
H	1.051531	-2.107122	2.801126
C	-0.800302	-2.991435	3.152008
H	-1.413621	-3.516644	2.415773
H	-1.445122	-2.524353	3.904093
H	-0.172096	-3.727143	3.657914
C	0.907643	0.291484	-0.167946
N	-0.300845	0.486521	-0.732903
H	-0.362860	1.055262	-1.592960
C	-0.603612	3.001840	-3.620216
H	-0.749341	3.871747	-2.958388
O	-0.476031	1.853716	-3.188767
N	-0.579987	3.320936	-4.922869
H	-0.694563	4.274348	-5.237187
H	-0.456383	2.592851	-5.616006

Point 19 $\theta = 180°$

H	-2.656083	0.919453	-1.749047
C	-2.681793	0.291928	-0.863674
C	-2.676293	-1.332443	1.414436
C	-1.466301	-0.025951	-0.223345
C	-3.868178	-0.196008	-0.361047
C	-3.863232	-1.004441	0.792128
C	-1.424759	-0.867044	0.924454
H	-4.805848	0.047829	-0.850720
H	-4.799157	-1.374958	1.197555
H	-2.725444	-1.945200	2.299214
C	1.036856	-0.527923	0.940435
C	-0.120848	-1.169550	1.486763
C	2.072795	0.954416	-0.865277
H	2.076623	2.011827	-0.561423
H	1.901943	0.948417	-1.947822
C	3.414764	0.311887	-0.502315
H	4.232058	0.933753	-0.880995
H	3.504519	-0.666745	-0.991673
C	3.511902	0.151400	1.015214
H	3.422907	1.136737	1.491159
H	4.487578	-0.251236	1.305211
C	2.408255	-0.776855	1.547846
H	2.357691	-0.656843	2.639913
H	2.699698	-1.823402	1.362986
N	0.095074	-2.032307	2.505334
H	1.064160	-2.127981	2.767053
C	-0.806997	-2.858216	3.302795
H	-1.401880	-3.528694	2.676286

H	-1.468658	-2.254492	3.932257
H	-0.187368	-3.472297	3.958673
C	0.907694	0.276801	-0.182742
N	-0.303494	0.494745	-0.731964
H	-0.367421	1.080959	-1.579992
C	-0.602127	3.062460	-3.576539
H	-0.734518	3.924187	-2.901366
O	-0.481732	1.907222	-3.162344
N	-0.585983	3.399688	-4.874731
H	-0.693975	4.358479	-5.174690
H	-0.474429	2.680396	-5.579008

Point 20 $\theta = 170°$

H	-2.655345	0.937440	-1.741085
C	-2.676584	0.268573	-0.886422
C	-2.654259	-1.489672	1.289986
C	-1.463142	-0.041121	-0.238115
C	-3.852887	-0.294060	-0.441608
C	-3.837624	-1.183823	0.650067
C	-1.416985	-0.920000	0.880608
H	-4.788500	-0.060324	-0.940052
H	-4.761897	-1.640096	0.989404
H	-2.691565	-2.190357	2.107530
C	1.043954	-0.572636	0.906646
C	-0.119777	-1.180723	1.477502
C	2.079552	0.918357	-0.892009
H	2.111521	1.969661	-0.569504
H	1.891037	0.935531	-1.971496
C	3.412175	0.239770	-0.562512
H	4.237003	0.845294	-0.951242
H	3.468013	-0.735800	-1.062779
C	3.534295	0.063816	0.951376
H	3.480688	1.047951	1.435102
H	4.504770	-0.365595	1.219508
C	2.417571	-0.838855	1.501940
H	2.381122	-0.705948	2.593010
H	2.686196	-1.892852	1.326512
N	0.081455	-1.982067	2.548937
H	1.051271	-2.108104	2.794330
C	-0.842038	-2.605647	3.493087
H	-1.364986	-3.462565	3.055996
H	-1.569072	-1.885665	3.878417
H	-0.248599	-2.968933	4.334154
C	0.912474	0.250293	-0.203475
N	-0.303201	0.505276	-0.725758
H	-0.369697	1.115894	-1.556393

C	-0.610785	3.157410	-3.486123
H	-0.723321	3.997563	-2.780855
O	-0.494729	1.988011	-3.112192
N	-0.613210	3.537130	-4.772581
H	-0.716686	4.506289	-5.038941
H	-0.520213	2.840581	-5.501971

Point 21 $\theta = 160°$

H	-2.665449	0.937915	-1.730135
C	-2.676198	0.244365	-0.895185
C	-2.626086	-1.592239	1.217965
C	-1.460438	-0.058600	-0.248109
C	-3.840573	-0.364448	-0.479616
C	-3.810409	-1.300029	0.573658
C	-1.406492	-0.960999	0.849873
H	-4.777873	-0.138335	-0.978427
H	-4.722729	-1.804305	0.875322
H	-2.640706	-2.339757	1.995516
C	1.051606	-0.611654	0.881657
C	-0.113993	-1.204028	1.460037
C	2.083263	0.899183	-0.902349
H	2.125048	1.945224	-0.564379
H	1.888057	0.933991	-1.980249
C	3.412879	0.205655	-0.591790
H	4.239458	0.809621	-0.979241
H	3.456932	-0.763719	-1.105041
C	3.545728	0.009183	0.918856
H	3.503664	0.987664	1.415083
H	4.515122	-0.430758	1.173428
C	2.426350	-0.891694	1.467281
H	2.395769	-0.769253	2.559585
H	2.686349	-1.945794	1.281331
N	0.064774	-1.984914	2.551705
H	1.030523	-2.141947	2.796921
C	-0.875866	-2.409760	3.587626
H	-1.385234	-3.344454	3.329366
H	-1.616099	-1.632462	3.790474
H	-0.302998	-2.581317	4.501467
C	0.916203	0.227961	-0.216888
N	-0.302304	0.504437	-0.721976
H	-0.370799	1.132607	-1.539567
C	-0.617292	3.211883	-3.423856
H	-0.717945	4.037689	-2.700106
O	-0.504026	2.034252	-3.075629
N	-0.630543	3.618433	-4.701971
H	-0.731125	4.593524	-4.946945

H	-0.548554	2.936878	-5.446693

Point 22 θ = 150°

H	-2.675313	0.929079	-1.728585
C	-2.677894	0.223786	-0.903477
C	-2.609364	-1.648872	1.180808
C	-1.459416	-0.077709	-0.261033
C	-3.835284	-0.404843	-0.496574
C	-3.796117	-1.360095	0.539626
C	-1.400376	-0.992747	0.824491
H	-4.774895	-0.181168	-0.992146
H	-4.702734	-1.882515	0.827319
H	-2.607031	-2.414594	1.942464
C	1.055168	-0.647121	0.861258
C	-0.110344	-1.238548	1.433627
C	2.084714	0.891196	-0.901350
H	2.120789	1.933232	-0.550542
H	1.892762	0.938607	-1.979384
C	3.416583	0.199756	-0.594965
H	4.241399	0.813346	-0.970861
H	3.467527	-0.761962	-1.121751
C	3.545300	-0.018365	0.913323
H	3.494593	0.952147	1.424279
H	4.516766	-0.455577	1.164634
C	2.429847	-0.935194	1.442433
H	2.396046	-0.838345	2.536946
H	2.694064	-1.983718	1.233384
N	0.044947	-2.029267	2.524998
H	1.006741	-2.219495	2.764512
C	-0.885049	-2.271679	3.631291
H	-1.424018	-3.218788	3.521165
H	-1.602434	-1.453587	3.722691
H	-0.302063	-2.321393	4.554042
C	0.917962	0.207164	-0.227989
N	-0.301075	0.492924	-0.726391
H	-0.369956	1.133991	-1.534333
C	-0.622980	3.237907	-3.386596
H	-0.724424	4.053318	-2.651278
O	-0.505846	2.055803	-3.054959
N	-0.639894	3.662020	-4.658857
H	-0.743385	4.640171	-4.890065
H	-0.557319	2.991137	-5.413156

Point 23 θ = 140°

H	-2.683239	0.921795	-1.731257
C	-2.680255	0.208941	-0.912706
C	-2.601297	-1.685710	1.155237

C	-1.459387	-0.096377	-0.276639
C	-3.834240	-0.426716	-0.505962
C	-3.790669	-1.392598	0.521402
C	-1.397748	-1.021338	0.798601
H	-4.776233	-0.200905	-0.996033
H	-4.695938	-1.919541	0.805129
H	-2.586276	-2.459840	1.909946
C	1.055247	-0.681229	0.843755
C	-0.109812	-1.279195	1.401412
C	2.085766	0.888177	-0.892715
H	2.109438	1.926490	-0.529938
H	1.902678	0.946417	-1.971810
C	3.421482	0.205422	-0.582525
H	4.243418	0.833032	-0.941144
H	3.487685	-0.747661	-1.123095
C	3.537982	-0.035289	0.923600
H	3.469710	0.925807	1.450173
H	4.512374	-0.464558	1.177239
C	2.428830	-0.974992	1.424064
H	2.386922	-0.910975	2.520344
H	2.702923	-2.014723	1.186482
N	0.018694	-2.090926	2.486207
H	0.975924	-2.320126	2.712780
C	-0.871943	-2.160417	3.653222
H	-1.445173	-3.093130	3.678926
H	-1.561027	-1.314004	3.662244
H	-0.257602	-2.114047	4.556158
C	0.918687	0.187544	-0.237129
N	-0.299295	0.477944	-0.734210
H	-0.367026	1.130108	-1.533911
C	-0.630529	3.251077	-3.362480
H	-0.739250	4.058878	-2.619873
O	-0.504952	2.066797	-3.041515
N	-0.648662	3.686585	-4.630745
H	-0.759297	4.665997	-4.853192
H	-0.559912	3.023283	-5.391041

Point 24 $\theta = 130°$

H	-2.696203	0.917990	-1.733889
C	-2.688887	0.199044	-0.920721
C	-2.603372	-1.712389	1.135886
C	-1.465737	-0.113651	-0.292750
C	-3.841451	-0.436969	-0.509527
C	-3.795638	-1.409794	0.512434
C	-1.402437	-1.048124	0.772755
H	-4.785945	-0.205931	-0.992310

H	-4.701816	-1.934577	0.797349
H	-2.577940	-2.491583	1.886759
C	1.047755	-0.713296	0.827353
C	-0.116129	-1.321553	1.366180
C	2.080346	0.889620	-0.879768
H	2.087793	1.924100	-0.505389
H	1.909082	0.958127	-1.960234
C	3.420580	0.219127	-0.561268
H	4.238584	0.863178	-0.899069
H	3.506964	-0.724218	-1.115901
C	3.520814	-0.045223	0.942320
H	3.430390	0.905150	1.484887
H	4.498326	-0.464021	1.201364
C	2.419720	-1.010788	1.409129
H	2.366970	-0.982388	2.505970
H	2.707118	-2.039443	1.141510
N	-0.014201	-2.159229	2.441379
H	0.937280	-2.436825	2.641405
C	-0.829000	-2.070845	3.666511
H	-1.395749	-2.990904	3.841949
H	-1.522796	-1.231361	3.602778
H	-0.166626	-1.905584	4.521206
C	0.912944	0.170426	-0.245144
N	-0.303373	0.462826	-0.743080
H	-0.369313	1.125539	-1.534936
C	-0.627682	3.258516	-3.347981
H	-0.743066	4.062403	-2.602196
O	-0.499752	2.073061	-3.031886
N	-0.640627	3.699670	-4.614206
H	-0.753300	4.679736	-4.832785
H	-0.545629	3.040180	-5.377083

Point 25 $\theta = 120°$

H	-2.702196	0.914871	-1.749633
C	-2.695977	0.189333	-0.942356
C	-2.614545	-1.743704	1.097886
C	-1.474868	-0.128872	-0.312953
C	-3.848728	-0.451078	-0.538179
C	-3.805003	-1.435074	0.474341
C	-1.415507	-1.071714	0.744350
H	-4.792282	-0.216968	-1.021308
H	-4.711591	-1.964943	0.748490
H	-2.580768	-2.534718	1.837184
C	1.031718	-0.746247	0.815853
C	-0.134910	-1.349065	1.343917
C	2.076592	0.875493	-0.869799

H	2.079340	1.906035	-0.484525
H	1.914496	0.955303	-1.950903
C	3.415415	0.204104	-0.546275
H	4.234540	0.854502	-0.868778
H	3.509768	-0.732012	-1.111754
C	3.502899	-0.078967	0.954891
H	3.403943	0.863805	1.509205
H	4.479646	-0.497575	1.217053
C	2.401453	-1.054978	1.397787
H	2.343304	-1.053213	2.494136
H	2.690551	-2.076768	1.107300
N	-0.061763	-2.203831	2.419254
H	0.882349	-2.528893	2.590856
C	-0.759851	-1.950262	3.695539
H	-1.050750	-2.898122	4.156300
H	-1.654595	-1.352845	3.524638
H	-0.108843	-1.402511	4.387191
C	0.904430	0.149591	-0.251929
N	-0.308209	0.449445	-0.750851
H	-0.369314	1.123848	-1.534205
C	-0.625196	3.278555	-3.314041
H	-0.748954	4.070840	-2.557338
O	-0.492304	2.089169	-3.014383
N	-0.633966	3.737620	-4.573683
H	-0.750970	4.720113	-4.778784
H	-0.531357	3.089732	-5.345494

Point 26 $\theta = 110°$

H	-2.711592	0.913364	-1.764538
C	-2.707471	0.183855	-0.960858
C	-2.634892	-1.758761	1.075216
C	-1.487923	-0.144487	-0.333538
C	-3.862673	-0.450951	-0.554999
C	-3.824124	-1.437276	0.456885
C	-1.432759	-1.095497	0.716679
H	-4.806066	-0.209564	-1.034864
H	-4.735346	-1.958045	0.733218
H	-2.598084	-2.550041	1.814394
C	1.010431	-0.773858	0.807586
C	-0.156752	-1.386386	1.311884
C	2.066534	0.873949	-0.850066
H	2.057955	1.899975	-0.452840
H	1.917450	0.965500	-1.932101
C	3.405790	0.207739	-0.516644
H	4.223904	0.868919	-0.819065
H	3.515497	-0.719519	-1.093861

C	3.475472	-0.095961	0.981581
H	3.361018	0.837608	1.548452
H	4.452276	-0.510053	1.250531
C	2.377113	-1.088120	1.394428
H	2.309463	-1.114964	2.489333
H	2.674360	-2.100570	1.080800
N	-0.106931	-2.262627	2.384996
H	0.829972	-2.627963	2.520353
C	-0.668778	-1.866313	3.694699
H	-0.712052	-2.749096	4.336473
H	-1.680065	-1.477854	3.572338
H	-0.057985	-1.095146	4.182020
C	0.891000	0.135503	-0.254178
N	-0.317369	0.434689	-0.759815
H	-0.373533	1.117784	-1.537186
C	-0.616328	3.282994	-3.299546
H	-0.752117	4.069776	-2.539275
O	-0.480897	2.092164	-3.005868
N	-0.613686	3.749551	-4.556189
H	-0.733131	4.732747	-4.756596
H	-0.499681	3.106934	-5.330840

Point 27 $\theta = 100°$

H	-2.722491	0.909576	-1.780860
C	-2.719765	0.178230	-0.978881
C	-2.656379	-1.765132	1.061844
C	-1.501171	-0.159946	-0.355280
C	-3.877890	-0.446803	-0.565813
C	-3.845224	-1.429207	0.451257
C	-1.449800	-1.118205	0.689088
H	-4.821628	-0.197450	-1.040952
H	-4.762393	-1.933925	0.737610
H	-2.618042	-2.548373	1.809769
C	0.988477	-0.793569	0.803314
C	-0.177581	-1.424693	1.276382
C	2.054075	0.883132	-0.822442
H	2.029250	1.904501	-0.413856
H	1.920967	0.985751	-1.905576
C	3.394820	0.226508	-0.474926
H	4.210142	0.901229	-0.753982
H	3.525165	-0.690685	-1.063888
C	3.443729	-0.099202	1.019767
H	3.309500	0.823860	1.599461
H	4.420997	-0.506240	1.297593
C	2.350893	-1.110618	1.398355
H	2.270418	-1.167878	2.490654

H	2.660268	-2.111770	1.061387
N	-0.151135	-2.319087	2.348495
H	0.767401	-2.745059	2.433306
C	-0.559249	-1.812703	3.679216
H	-0.549675	-2.648779	4.381798
H	-1.574700	-1.414671	3.632544
H	0.107642	-1.021822	4.048166
C	0.876473	0.128363	-0.252130
N	-0.327375	0.421306	-0.769340
H	-0.378740	1.110374	-1.542763
C	-0.613096	3.276540	-3.301544
H	-0.764967	4.062344	-2.543396
O	-0.472152	2.086716	-3.005647
N	-0.597644	3.742432	-4.558128
H	-0.722323	4.724569	-4.760647
H	-0.468799	3.100385	-5.330954

Point 28 $\theta = 90°$

H	-2.731687	0.895888	-1.808802
C	-2.732123	0.165380	-1.006081
C	-2.681387	-1.771366	1.045764
C	-1.516677	-0.175488	-0.378249
C	-3.892822	-0.454032	-0.591398
C	-3.867351	-1.429320	0.433642
C	-1.470737	-1.136528	0.664910
H	-4.835028	-0.202483	-1.068481
H	-4.789357	-1.921943	0.725553
H	-2.642833	-2.543520	1.805158
C	0.962121	-0.805915	0.805818
C	-0.203866	-1.449557	1.253318
C	2.038334	0.892128	-0.793892
H	2.001861	1.908270	-0.373136
H	1.918239	1.007239	-1.877261
C	3.379276	0.240317	-0.436841
H	4.192830	0.925029	-0.695953
H	3.524570	-0.667410	-1.036900
C	3.411901	-0.106653	1.053681
H	3.264821	0.806705	1.645603
H	4.388522	-0.511503	1.336949
C	2.321653	-1.130887	1.403182
H	2.234847	-1.217772	2.492144
H	2.636037	-2.121878	1.041861
N	-0.200435	-2.350539	2.333835
H	0.685440	-2.850477	2.361439
C	-0.432485	-1.755993	3.671569
H	-0.409027	-2.560124	4.410252

H	-1.421687	-1.292576	3.701164
H	0.315132	-0.996554	3.939134
C	0.858406	0.124605	-0.246207
N	-0.340173	0.409951	-0.777419
H	-0.385971	1.103128	-1.548480
C	-0.610699	3.271682	-3.300138
H	-0.780067	4.053821	-2.541990
O	-0.464124	2.082005	-3.005640
N	-0.580926	3.741149	-4.554927
H	-0.710842	4.722808	-4.756564
H	-0.435689	3.102413	-5.327620

Point 29 $\theta = 80°$

H	-2.734907	0.870114	-1.850154
C	-2.741261	0.143675	-1.043794
C	-2.708400	-1.776659	1.027129
C	-1.531980	-0.191057	-0.401299
C	-3.904357	-0.475299	-0.635175
C	-3.888171	-1.439657	0.401019
C	-1.493543	-1.148621	0.646650
H	-4.842557	-0.228870	-1.122771
H	-4.813967	-1.925570	0.692253
H	-2.672926	-2.533823	1.801384
C	0.933810	-0.809547	0.817723
C	-0.234015	-1.457729	1.248213
C	2.020518	0.903336	-0.762759
H	1.978636	1.911902	-0.324411
H	1.907269	1.036932	-1.844647
C	3.361516	0.249963	-0.407796
H	4.173958	0.942125	-0.650062
H	3.514005	-0.646522	-1.022791
C	3.386559	-0.123700	1.076413
H	3.237102	0.778424	1.684841
H	4.361817	-0.534223	1.356329
C	2.295040	-1.154215	1.400882
H	2.216316	-1.280006	2.485172
H	2.601963	-2.133469	1.002937
N	-0.257955	-2.348381	2.350209
H	0.573311	-2.937283	2.323511
C	-0.302001	-1.691632	3.678444
H	-0.269620	-2.472015	4.442013
H	-1.246655	-1.151093	3.783871
H	0.521215	-0.984580	3.850155
C	0.838658	0.125269	-0.234374
N	-0.353671	0.401712	-0.781968
H	-0.393266	1.097247	-1.552116

C	-0.610013	3.269429	-3.293387
H	-0.799075	4.044916	-2.533144
O	-0.456002	2.079252	-3.003941
N	-0.565452	3.746835	-4.544542
H	-0.702113	4.728399	-4.742241
H	-0.401790	3.114421	-5.318774

Point 30 $\theta = 70°$

H	-2.730012	0.838014	-1.901303
C	-2.745285	0.119836	-1.087715
C	-2.736402	-1.770736	1.012429
C	-1.545235	-0.200930	-0.421483
C	-3.910996	-0.501397	-0.690449
C	-3.906787	-1.448886	0.361658
C	-1.516449	-1.147940	0.637410
H	-4.842694	-0.266474	-1.195904
H	-4.835975	-1.930773	0.648834
H	-2.708935	-2.506758	1.806737
C	0.905893	-0.800900	0.839223
C	-0.265671	-1.446149	1.261432
C	2.001589	0.923889	-0.726852
H	1.957988	1.922284	-0.265693
H	1.889652	1.081436	-1.805507
C	3.343764	0.266024	-0.384510
H	4.154567	0.965437	-0.611039
H	3.498918	-0.616323	-1.018946
C	3.368357	-0.141162	1.090701
H	3.223668	0.746857	1.720726
H	4.342158	-0.562740	1.359274
C	2.273471	-1.174638	1.391130
H	2.215932	-1.351141	2.467670
H	2.563024	-2.137363	0.942795
N	-0.322522	-2.318077	2.388637
H	0.415306	-3.017778	2.305966
C	-0.171075	-1.650786	3.702176
H	-0.155950	-2.426928	4.470811
H	-1.042477	-1.014435	3.881881
H	0.730534	-1.032360	3.801294
C	0.818834	0.135554	-0.215297
N	-0.366081	0.401306	-0.781650
H	-0.398883	1.096481	-1.553094
C	-0.611972	3.265196	-3.293755
H	-0.822422	4.036300	-2.534752
O	-0.448197	2.076056	-3.004669
N	-0.553390	3.746033	-4.542854
H	-0.698555	4.726404	-4.740486

H	-0.369690	3.117565	-5.315825
Point 31 θ = 60°			
H	-2.715425	0.793110	-1.966566
C	-2.741942	0.091849	-1.138632
C	-2.761007	-1.741694	1.010839
C	-1.554101	-0.201941	-0.438915
C	-3.909512	-0.533308	-0.753921
C	-3.919076	-1.450517	0.324599
C	-1.535720	-1.125775	0.640629
H	-4.832342	-0.320184	-1.284671
H	-4.851150	-1.928195	0.609579
H	-2.746955	-2.442154	1.836521
C	0.881629	-0.766074	0.872282
C	-0.294347	-1.400744	1.298093
C	1.982336	0.958951	-0.696203
H	1.944154	1.947526	-0.213618
H	1.864303	1.138533	-1.770559
C	3.325677	0.293212	-0.374901
H	4.136143	0.994297	-0.597579
H	3.473394	-0.579932	-1.023662
C	3.359151	-0.135952	1.093375
H	3.229920	0.743761	1.738275
H	4.330904	-0.571957	1.346242
C	2.257519	-1.162917	1.388834
H	2.226342	-1.373473	2.457766
H	2.522571	-2.115388	0.904758
N	-0.385299	-2.260036	2.438164
H	0.152229	-3.111990	2.280847
C	-0.036141	-1.685830	3.751143
H	-0.184176	-2.467762	4.500146
H	-0.732133	-0.872402	3.976469
H	0.984865	-1.298186	3.851678
C	0.800064	0.165280	-0.191177
N	-0.376072	0.411844	-0.780947
H	-0.402726	1.099107	-1.560063
C	-0.617447	3.255087	-3.310570
H	-0.852045	4.022825	-2.555306
O	-0.441099	2.068316	-3.018531
N	-0.544837	3.736728	-4.558517
H	-0.701001	4.714884	-4.758776
H	-0.338649	3.111101	-5.328123
Point 32 θ = 50°			
H	-2.689064	0.774207	-2.000264
C	-2.734450	0.091139	-1.157944
C	-2.788123	-1.669543	1.024328

C	-1.562103	-0.157539	-0.414640
C	-3.906029	-0.544376	-0.805371
C	-3.935406	-1.420628	0.300334
C	-1.553662	-1.062600	0.674938
H	-4.812785	-0.360716	-1.373129
H	-4.868577	-1.892790	0.589866
H	-2.859037	-2.319229	1.890676
C	0.857036	-0.581564	0.984288
C	-0.306094	-1.292811	1.376360
C	1.951894	1.057693	-0.650998
H	1.970124	2.054764	-0.185978
H	1.805357	1.218119	-1.724583
C	3.273615	0.339873	-0.359457
H	4.109507	0.971523	-0.676477
H	3.331161	-0.587023	-0.944742
C	3.358349	0.032936	1.134859
H	3.320082	0.976966	1.694811
H	4.314409	-0.438656	1.384160
C	2.216043	-0.885705	1.599483
H	2.163575	-0.833064	2.688690
H	2.456169	-1.932573	1.361186
N	-0.272935	-2.275153	2.327081
H	-1.091688	-2.865730	2.316300
C	0.332146	-2.193032	3.666753
H	-0.272079	-2.806122	4.338748
H	0.324487	-1.166524	4.044142
H	1.353955	-2.580292	3.685377
C	0.766831	0.301675	-0.098428
N	-0.397860	0.488634	-0.745881
H	-0.417947	1.128470	-1.558420
C	-0.623460	3.204654	-3.443575
H	-0.863617	4.011621	-2.731739
O	-0.468122	2.032698	-3.090646
N	-0.519344	3.625425	-4.712369
H	-0.659737	4.594292	-4.962624
H	-0.304623	2.960980	-5.446115

Point 33 $\theta = 40°$

H	-2.685649	0.772110	-2.011888
C	-2.739275	0.098460	-1.162489
C	-2.811319	-1.634493	1.038467
C	-1.570544	-0.151507	-0.413965
C	-3.917525	-0.521976	-0.805606
C	-3.955948	-1.383945	0.310271
C	-1.570272	-1.043905	0.684672
H	-4.821521	-0.336722	-1.377213

H	-4.893286	-1.844416	0.605073
H	-2.894289	-2.272435	1.912482
C	0.845309	-0.572138	0.997265
C	-0.321924	-1.282359	1.389480
C	1.941937	1.058181	-0.649504
H	1.942018	2.064195	-0.203797
H	1.802737	1.196825	-1.727138
C	3.270459	0.365390	-0.334143
H	4.100490	1.006396	-0.647775
H	3.350354	-0.567454	-0.907268
C	3.338407	0.076879	1.164051
H	3.272915	1.025336	1.713968
H	4.298747	-0.374453	1.433783
C	2.207124	-0.859477	1.618898
H	2.149393	-0.808660	2.707311
H	2.469515	-1.899958	1.376834
N	-0.321355	-2.248811	2.349020
H	-1.159568	-2.809751	2.359463
C	0.398557	-2.287153	3.628900
H	-0.161863	-2.946580	4.294608
H	0.443087	-1.297066	4.091648
H	1.408740	-2.690348	3.528977
C	0.758786	0.299393	-0.094501
N	-0.402099	0.484175	-0.749937
H	-0.416717	1.116705	-1.567642
C	-0.612719	3.181951	-3.470169
H	-0.854765	3.993940	-2.764646
O	-0.460537	2.012248	-3.108967
N	-0.502677	3.594505	-4.741311
H	-0.640797	4.561900	-4.998378
H	-0.285928	2.925016	-5.469834

Point 34 $\theta = 30°$

H	-2.690605	0.787676	-2.004315
C	-2.749913	0.123077	-1.148189
C	-2.834332	-1.584627	1.069756
C	-1.580725	-0.136312	-0.403540
C	-3.935814	-0.474519	-0.778215
C	-3.980298	-1.323093	0.347135
C	-1.586027	-1.017900	0.702678
H	-4.840287	-0.280928	-1.346285
H	-4.922580	-1.765297	0.653859
H	-2.925176	-2.211293	1.951217
C	0.837161	-0.567170	1.005195
C	-0.333270	-1.276126	1.398954
C	1.931756	1.060903	-0.649776

H	1.896449	2.081321	-0.239371
H	1.809127	1.160890	-1.733874
C	3.271826	0.416416	-0.289071
H	4.089188	1.079370	-0.590070
H	3.398032	-0.521684	-0.845174
C	3.306767	0.149416	1.213835
H	3.186987	1.099534	1.751709
H	4.274778	-0.262238	1.517600
C	2.199763	-0.827021	1.640687
H	2.125235	-0.791906	2.728493
H	2.503490	-1.852628	1.385379
N	-0.357274	-2.240006	2.354859
H	-1.215903	-2.767413	2.382070
C	0.462402	-2.427771	3.556767
H	-0.053787	-3.157829	4.183014
H	0.557305	-1.499666	4.128051
H	1.454287	-2.822338	3.329382
C	0.752586	0.295825	-0.092736
N	-0.406606	0.481562	-0.751608
H	-0.416807	1.105777	-1.575137
C	-0.594030	3.144445	-3.516482
H	-0.828703	3.972991	-2.827871
O	-0.453971	1.981002	-3.131531
N	-0.478476	3.530182	-4.795694
H	-0.606725	4.493476	-5.072475
H	-0.267832	2.843903	-5.510226

Point 35 $\theta = 20°$

H	-2.693876	0.800405	-1.996579
C	-2.758118	0.147184	-1.132095
C	-2.853732	-1.530404	1.106660
C	-1.587345	-0.123713	-0.393976
C	-3.951950	-0.422485	-0.744223
C	-4.001842	-1.255307	0.392235
C	-1.598283	-0.991799	0.722105
H	-4.857730	-0.218668	-1.306598
H	-4.949170	-1.675648	0.713758
H	-2.950714	-2.144535	1.996392
C	0.832964	-0.567700	1.008274
C	-0.341086	-1.271629	1.406621
C	1.927908	1.052738	-0.657958
H	1.852204	2.089007	-0.295381
H	1.829542	1.102595	-1.748228
C	3.276777	0.466813	-0.238053
H	4.078986	1.153777	-0.525625
H	3.458064	-0.477233	-0.768401

C	3.268342	0.229397	1.270205
H	3.083015	1.180687	1.787101
H	4.241747	-0.132364	1.617214
C	2.192368	-0.792289	1.666194
H	2.093273	-0.773097	2.752592
H	2.545309	-1.799348	1.402541
N	-0.383145	-2.232283	2.360837
H	-1.261872	-2.722971	2.410540
C	0.517235	-2.567371	3.467767
H	0.035009	-3.364208	4.036890
H	0.668582	-1.717064	4.139309
H	1.482304	-2.939393	3.121810
C	0.751557	0.284295	-0.097627
N	-0.406563	0.470869	-0.758904
H	-0.412925	1.085844	-1.589001
C	-0.578316	3.102681	-3.559205
H	-0.806780	3.943427	-2.883348
O	-0.446661	1.944418	-3.156567
N	-0.460236	3.468089	-4.844274
H	-0.581759	4.427903	-5.135741
H	-0.255084	2.769383	-5.548260

Point 36 $\theta = 10°$

H	-2.696024	0.808981	-1.989200
C	-2.764417	0.167091	-1.116581
C	-2.869307	-1.482818	1.141204
C	-1.592256	-0.113979	-0.384337
C	-3.964694	-0.376807	-0.712279
C	-4.018918	-1.195767	0.433814
C	-1.608430	-0.968081	0.742125
H	-4.871509	-0.164120	-1.269670
H	-4.970046	-1.597818	0.767251
H	-2.971020	-2.088612	2.036263
C	0.830051	-0.570520	1.009575
C	-0.348024	-1.265373	1.416169
C	1.928095	1.035959	-0.670656
H	1.816571	2.086047	-0.361415
H	1.856887	1.032228	-1.764449
C	3.280303	0.507198	-0.190425
H	4.068314	1.214080	-0.468772
H	3.512067	-0.442791	-0.689506
C	3.227353	0.304185	1.322190
H	2.980682	1.256415	1.811030
H	4.201595	-0.007934	1.712334
C	2.182370	-0.756705	1.694762
H	2.055778	-0.745843	2.778858

H	2.582673	-1.746054	1.434275
N	-0.400251	-2.218022	2.374897
H	-1.298119	-2.666755	2.461222
C	0.565112	-2.687752	3.371948
H	0.106419	-3.538417	3.879297
H	0.782015	-1.923035	4.123706
H	1.494256	-3.030403	2.916797
C	0.752570	0.268961	-0.105247
N	-0.405340	0.456526	-0.767231
H	-0.408834	1.062359	-1.603841
C	-0.563596	3.064220	-3.592109
H	-0.785540	3.912994	-2.924093
O	-0.439488	1.909081	-3.178622
N	-0.444379	3.416742	-4.880768
H	-0.559863	4.374540	-5.181162
H	-0.245060	2.709997	-5.578355

5.2.1.3 Tabulation of energies obtained in the constrained optimizations

Table 5.2. Energies resulting from the constrained optimization of **16**·H^+

θ (°)	Counterclockwise Rotation		Clockwise Rotation	
	Energy (E_h)	Relative Energy (kcal/mol)	Energy (E_h)	Relative Energy (kcal/mol)
0	-653.057632	2.7	-653.057632	2.7
10	-653.057411	2.8	-653.057411	2.8
20	-653.057108	3.0	-653.057108	3.0
30	-653.056654	3.3	-653.056654	3.3
40	-653.055949	3.7	-653.055949	3.7
50	-653.054812	4.5	-653.054812	4.5
60	-653.053062	5.6	-653.053062	5.6
70	-653.050600	7.1	-653.040626	13.4
80	-653.048782	8.2	-653.044322	11.0
90	-653.046447	9.7	-653.047637	9.0
100	-653.043583	11.5	-653.050626	7.1
110	-653.040536	13.4	-653.053202	5.5
120	-653.037835	15.1	-653.055430	4.1
130	-653.057710	2.6	-653.057710	2.6
140	-653.059519	1.5	-653.059519	1.5
150	-653.060650	0.8	-653.060650	0.8
160	-653.061186	0.5	-653.061186	0.5
170	-653.061366	0.3	-653.061366	0.3
180	-653.061631	0.2	-653.061631	0.2
190	-653.061922	0.0	-653.061923	0.0
200	-653.061853	0.0	-653.061853	0.0
210	-653.061215	0.4	-653.061215	0.4
220	-653.059900	1.3	-653.059900	1.3
230	-653.057896	2.5	-653.057896	2.5
240	-653.055486	4.0	-653.038028	15.0
250	-653.053097	5.5	-653.041039	13.1
260	-653.050322	7.3	-653.044345	11.0
270	-653.047226	9.2	-653.047682	8.9
280	-653.044033	11.2	-653.050761	7.0
290	-653.041033	13.1	-653.053251	5.4
300	-653.054955	4.4	-653.054955	4.4
310	-653.056440	3.4	-653.056440	3.4
320	-653.057457	2.8	-653.057457	2.8
330	-653.057880	2.5	-653.057880	2.5
340	-653.057940	2.5	-653.057940	2.5
350	-653.057814	2.6	-653.057814	2.6
360	-653.057632	2.7	-653.057632	2.7

Table 5.3. Energies resulting from the constrained optimization of **12**·H^+

θ (°)	Counterclockwise Rotation		Clockwise Rotation	
	Energy (E_h)	Relative Energy (kcal/mol)	Energy (E_h)	Relative Energy (kcal/mol)
0	-497.015208	0.0	-497.015208	0.0
10	-497.014971	0.2	-497.014968	0.2
20	-497.014193	0.6	-497.014194	0.6
30	-497.012791	1.5	-497.012795	1.5
40	-497.010732	2.8	-497.010738	2.8
50	-497.008065	4.5	-497.008071	4.5
60	-496.989417	16.2	-497.004900	6.5
70	-496.990482	15.5	-497.001381	8.7
80	-496.992847	14.0	-496.997726	11.0
90	-496.995963	12.1	-496.994193	13.2
100	-496.999435	9.9	-496.991078	15.1
110	-497.002953	7.7	-496.988776	16.6
120	-497.006262	5.6	-496.987830	17.2
130	-497.009171	3.8	-497.009168	3.8
140	-497.011537	2.3	-497.011534	2.3
150	-497.013286	1.2	-497.013281	1.2
160	-497.014425	0.5	-497.014418	0.5
170	-497.015033	0.1	-497.015024	0.1
180	-497.015217	0.0	-497.015210	0.0
190	-497.015031	0.1	-497.015024	0.1
200	-497.014428	0.5	-497.014417	0.5
210	-497.013293	1.2	-497.013280	1.2
220	-497.011544	2.3	-497.011533	2.3
230	-497.009175	3.8	-497.009168	3.8
240	-496.987835	17.2	-497.006259	5.6
250	-496.988789	16.6	-497.002950	7.7
260	-496.991093	15.1	-496.999434	9.9
270	-496.994188	13.2	-496.995965	12.1
280	-496.997730	11.0	-496.992850	14.0
290	-497.001380	8.7	-496.990487	15.5
300	-497.004894	6.5	-496.989426	16.2
310	-497.008069	4.5	-497.008061	4.5
320	-497.010735	2.8	-497.010732	2.8
330	-497.012791	1.5	-497.012789	1.5
340	-497.014193	0.6	-497.014193	0.6
350	-497.014968	0.2	-497.014972	0.1
360	-497.015208	0.0	-497.015208	0.0

Table 5.4. Energies resulting from the constrained optimization of **1**·H^+

θ (°)	Counterclockwise Rotation		Clockwise Rotation	
	Energy (E_h)	Relative Energy (kcal/mol)	Energy (E_h)	Relative Energy (kcal/mol)
0	-613.758741	0.0	-613.758741	0.0
10	-613.758496	0.2	-613.758500	0.2
20	-613.757805	0.6	-613.757810	0.6
30	-613.756555	1.4	-613.756559	1.4
40	-613.754701	2.5	-613.754702	2.5
50	-613.752261	4.1	-613.752259	4.1
60	-613.734160	15.4	-613.749311	5.9
70	-613.735176	14.8	-613.745981	8.0
80	-613.737247	13.5	-613.742462	10.2
90	-613.740043	11.7	-613.739013	12.4
100	-613.743238	9.7	-613.735946	14.3
110	-613.746561	7.6	-613.733675	15.7
120	-613.749768	5.6	-613.732824	16.3
130	-613.752636	3.8	-613.752636	3.8
140	-613.754999	2.3	-613.754999	2.4
150	-613.756764	1.2	-613.756762	1.2
160	-613.757908	0.5	-613.757909	0.5
170	-613.758527	0.1	-613.758528	0.1
180	-613.758741	0.0	-613.758744	0.0
190	-613.758594	0.1	-613.758598	0.1
200	-613.758012	0.5	-613.758018	0.5
210	-613.756846	1.2	-613.756853	1.2
220	-613.755022	2.3	-613.755028	2.3
230	-613.752573	3.9	-613.752579	3.9
240	-613.732814	16.3	-613.749609	5.7
250	-613.734029	15.5	-613.746304	7.8
260	-613.736486	14.0	-613.742885	10.0
270	-613.739642	12.0	-613.739616	12.0
280	-613.743120	9.8	-613.736826	13.8
290	-613.746622	7.6	-613.734863	15.0
300	-613.749901	5.5	-613.734130	15.4
310	-613.752778	3.7	-613.752785	3.7
320	-613.755130	2.3	-613.755135	2.3
330	-613.756885	1.2	-613.756889	1.2
340	-613.758019	0.5	-613.758025	0.5
350	-613.758601	0.1	-613.758604	0.1
360	-613.758741	0.0	-613.758741	0.0

Table 5.5. Energies resulting from the constrained optimization of **13**·H^+

θ (°)	Counterclockwise Rotation		Clockwise Rotation	
	Energy (E_h)	Relative Energy (kcal/mol)	Energy (E_h)	Relative Energy (kcal/mol)
0	-730.447517	0.9	-730.447517	0.9
10	-730.448470	0.3	-730.448472	0.3
20	-730.448947	0.0	-730.448933	0.0
30	-730.448654	0.2	-730.448620	0.2
40	-730.447300	1.0	-730.447270	1.0
50	-730.444703	2.7	-730.444695	2.7
60	-730.440959	5.0	-730.440981	5.0
70	-730.436279	8.0	-730.426320	14.2
80	-730.433538	9.7	-730.427225	13.6
90	-730.430843	11.4	-730.430019	11.9
100	-730.428599	12.8	-730.433337	9.8
110	-730.427165	13.7	-730.436680	7.7
120	-730.439608	5.9	-730.439609	5.9
130	-730.442128	4.3	-730.442080	4.3
140	-730.444553	2.8	-730.444543	2.8
150	-730.446924	1.3	-730.446912	1.3
160	-730.448478	0.3	-730.448452	0.3
170	-730.448969	0.0	-730.448930	0.0
180	-730.448496	0.3	-730.448451	0.3
190	-730.447240	1.1	-730.447182	1.1
200	-730.445392	2.2	-730.445314	2.3
210	-730.443276	3.6	-730.443231	3.6
220	-730.441783	4.5	-730.441781	4.5
230	-730.440431	5.4	-730.440417	5.3
240	-730.438856	6.3	-730.438872	6.3
250	-730.436906	7.6	-730.426994	13.8
260	-730.434524	9.1	-730.428238	13.0
270	-730.432010	10.6	-730.430196	11.8
280	-730.429663	12.1	-730.432568	10.3
290	-730.427778	13.3	-730.432940	10.0
300	-730.426361	14.2	-730.437189	7.4
310	-730.439133	6.2	-730.441020	5.0
320	-730.443818	3.2	-730.443869	3.2
330	-730.445431	2.2	-730.445479	2.2
340	-730.445925	1.9	-730.445026	2.5
350	-730.445567	2.1	-730.446384	1.6
360	-730.447517	0.9	-730.447517	0.9

Table 5.6. Energies resulting from the constrained optimization of **14**·H^+

θ (°)	Counterclockwise Rotation		Clockwise Rotation	
	Energy (E_h)	Relative Energy (kcal/mol)	Energy (E_h)	Relative Energy (kcal/mol)
0	-536.299372	0.9	-536.299364	0.9
10	-536.300618	0.1	-536.300610	0.1
20	-536.300595	0.1	-536.300594	0.1
30	-536.299376	0.9	-536.299372	0.9
40	-536.297172	2.3	-536.297186	2.2
50	-536.294296	4.1	-536.294325	4.0
60	-536.290949	6.2	-536.290987	6.1
70	-536.287179	8.5	-536.281508	12.1
80	-536.283222	11.0	-536.283646	10.7
90	-536.279532	13.3	-536.286857	8.7
100	-536.276746	15.1	-536.290353	6.5
110	-536.293696	4.5	-536.293626	4.5
120	-536.296502	2.7	-536.296455	2.7
130	-536.298735	1.3	-536.298688	1.3
140	-536.300221	0.4	-536.300180	0.4
150	-536.300787	0.0	-536.300736	0.0
160	-536.300401	0.2	-536.300349	0.3
170	-536.299222	1.0	-536.299209	1.0
180	-536.297626	2.0	-536.297642	2.0
190	-536.299221	1.0	-536.299235	1.0
200	-536.300392	0.2	-536.300393	0.2
210	-536.300771	0.0	-536.300768	0.0
220	-536.300195	0.4	-536.300188	0.4
230	-536.298699	1.3	-536.298693	1.3
240	-536.296454	2.7	-536.296452	2.7
250	-536.293653	4.5	-536.293647	4.5
260	-536.290387	6.5	-536.276709	15.1
270	-536.286888	8.7	-536.279500	13.3
280	-536.283676	10.7	-536.283205	11.0
290	-536.281501	12.1	-536.287173	8.5
300	-536.290988	6.1	-536.290956	6.2
310	-536.294338	4.0	-536.294306	4.1
320	-536.297202	2.2	-536.297171	2.3
330	-536.299403	0.9	-536.299381	0.9
340	-536.300607	0.1	-536.300581	0.1
350	-536.300625	0.1	-536.296910	2.4
360	-536.299366	0.9	-536.299372	0.9

Table 5.7. Energies resulting from the constrained optimization of **15**·H^+

θ (°)	Counterclockwise Rotation		Clockwise Rotation	
	Energy (E_h)	Relative Energy (kcal/mol)	Energy (E_h)	Relative Energy (kcal/mol)
0	-692.350235	4.5	-692.350235	4.5
10	-692.349195	5.2	-692.351466	3.8
20	-692.354299	2.0	-692.354297	2.0
30	-692.356343	0.7	-692.356345	0.7
40	-692.357426	0.0	-692.357440	0.0
50	-692.357444	0.0	-692.357449	0.0
60	-692.356448	0.6	-692.356456	0.6
70	-692.354691	1.7	-692.354708	1.7
80	-692.352396	3.2	-692.347162	6.5
90	-692.349802	4.8	-692.349038	5.3
100	-692.347527	6.2	-692.351140	4.0
110	-692.346694	6.8	-692.353056	2.8
120	-692.354536	1.8	-692.354570	1.8
130	-692.355312	1.4	-692.355341	1.3
140	-692.354968	1.6	-692.354983	1.6
150	-692.353225	2.7	-692.353263	2.6
160	-692.349975	4.7	-692.350494	4.4
170	-692.349492	5.0	-692.349497	5.0
180	-692.349217	5.2	-692.349215	5.2
190	-692.349912	4.7	-692.349911	4.7
200	-692.353315	2.6	-692.353305	2.6
210	-692.356052	0.9	-692.356026	0.9
220	-692.357398	0.0	-692.357398	0.0
230	-692.357465	0.0	-692.357457	0.0
240	-692.356472	0.6	-692.356468	0.6
250	-692.354800	1.7	-692.354798	1.7
260	-692.352829	2.9	-692.347202	6.4
270	-692.350685	4.3	-692.348990	5.3
280	-692.348519	5.6	-692.351072	4.0
290	-692.346868	6.6	-692.352966	2.8
300	-692.354429	1.9	-692.354467	1.9
310	-692.355239	1.4	-692.355262	1.4
320	-692.355191	1.4	-692.355211	1.4
330	-692.354295	2.0	-692.354303	2.0
340	-692.352690	3.0	-692.352680	3.0
350	-692.351329	3.9	-692.351328	3.8
360	-692.350235	4.5	-692.350235	4.5

Table 5.8. Energies resulting from the constrained optimization of **17**

θ (°)	Counterclockwise Rotation		Clockwise Rotation	
	Energy (E_h)	Relative Energy (kcal/mol)	Energy (E_h)	Relative Energy (kcal/mol)
0	-822.976447	2.7	-822.976425	2.7
10	-822.976311	2.8	-822.976330	2.7
20	-822.976178	2.9	-822.976155	2.8
30	-822.975931	3.0	-822.975899	3.0
40	-822.975457	3.3	-822.975435	3.3
50	-822.974596	3.9	-822.974592	3.8
60	-822.973126	4.8	-822.958974	13.6
70	-822.971070	6.1	-822.962421	11.5
80	-822.969618	7.0	-822.965839	9.3
90	-822.967712	8.2	-822.968853	7.4
100	-822.965265	9.7	-822.971477	5.8
110	-822.962575	11.4	-822.973644	4.4
120	-822.960002	13.0	-822.975402	3.3
130	-822.977338	2.1	-822.977302	2.1
140	-822.978879	1.2	-822.978831	1.2
150	-822.979794	0.6	-822.979756	0.6
160	-822.980210	0.3	-822.980176	0.3
170	-822.980333	0.3	-822.980286	0.3
180	-822.980502	0.2	-822.980440	0.2
190	-822.980742	0.0	-822.980696	0.0
200	-822.980729	0.0	-822.980678	0.0
210	-822.980248	0.3	-822.980201	0.3
220	-822.979175	1.0	-822.979127	1.0
230	-822.977445	2.1	-822.977413	2.1
240	-822.975432	3.3	-822.960012	13.0
250	-822.973509	4.5	-822.962877	11.2
260	-822.971148	6.0	-822.965850	9.3
270	-822.968436	7.7	-822.968777	7.5
280	-822.965535	9.5	-822.971439	5.8
290	-822.962786	11.3	-822.973499	4.5
300	-822.974933	3.6	-822.974855	3.7
310	-822.976089	2.9	-822.975996	2.9
320	-822.976791	2.5	-822.976723	2.5
330	-822.976970	2.4	-822.976915	2.4
340	-822.976852	2.4	-822.976785	2.5
350	-822.976639	2.6	-822.976577	2.6
360	-822.976447	2.7	-822.976425	2.7

5.2.2 Calculation of rotational barriers.

The lowest energy conformation from the above conformational profiles was used as a starting geometry for a B3LYP/6-31G* optimization. Furthermore, a conformation near the peak of the energy profile curve was used as a starting geometry for a B3LYP/6-31G* transition state optimization. Both structures were confirmed using a frequency analysis (i.e. no imaginary frequencies found for the global minimum structure and one imaginary frequency found for the transition structure). Furthermore, the imaginary frequency was examined to insure that the transition state obtained was that for exocyclic nitrogen inversion. The resulting Cartesian coordinates were used in a PCM optimization at B3LYP/6-31G* using the default parameters of the PCM method as implemented in Gaussian 03[4] by incorporating the dielectric constant of the NMR solvent.

5.2.2.1 Cartesian coordinates for calculated rotational barriers

Protonated tacrine ($1 \cdot H^+$) with no solvent included:

Ground state structure

C	0.000605	-0.065744	-0.093255
C	-0.032610	-0.017873	1.327242
N	2.375605	0.008967	-0.013535
C	1.200551	-0.000062	2.081400
C	1.231199	-0.033061	-0.735379
C	2.420962	0.014536	1.363482
C	1.268060	0.006955	3.496611
H	4.581747	0.054199	1.457176
H	3.256679	0.040091	-0.515628
C	2.483493	0.030616	4.148883
H	0.362272	-0.013586	4.093980
H	2.515386	0.033340	5.233287
C	3.685619	0.049908	3.411640
H	4.638137	0.069455	3.931473
C	3.659423	0.041791	2.031655
C	1.384006	-0.048352	-2.236285
H	2.213795	0.610695	-2.522312
H	1.675699	-1.065008	-2.538986
C	-1.292234	-0.112220	-0.888033
H	-1.808189	0.854861	-0.784130
H	-1.961151	-0.868860	-0.454725
C	-1.091382	-0.427764	-2.379252
H	-0.913861	-1.503607	-2.505757
H	-2.012302	-0.194898	-2.922429
C	0.091027	0.354022	-2.956079

H	-0.077013	1.432555	-2.842272
H	0.199806	0.159505	-4.027233
N	-1.216114	0.009482	1.962789
H	-1.285887	0.064243	2.967067
H	-2.084721	0.020221	1.449774

Transition state structure 1

C	0.007941	-0.033681	-0.052647
C	0.001424	-0.043823	1.349600
N	2.383872	-0.013852	-0.005064
C	1.222994	-0.053040	2.085028
C	1.246663	-0.012912	-0.723375
C	2.451647	-0.037159	1.368692
C	1.274684	-0.072244	3.504038
H	4.617704	-0.025758	1.467925
H	3.263727	0.006359	-0.515164
C	2.490579	-0.075682	4.150702
H	0.336763	-0.083823	4.045622
H	2.527475	-0.091116	5.235136
C	3.700151	-0.058762	3.415125
H	4.648854	-0.061342	3.942647
C	3.690731	-0.038901	2.034771
C	1.382361	-0.006439	-2.225263
H	2.227048	0.631946	-2.514567
H	1.640961	-1.027635	-2.543763
C	-1.285950	-0.004679	-0.846631
H	-1.735779	0.993246	-0.735568
H	-2.002966	-0.703754	-0.401373
C	-1.106758	-0.320733	-2.339188
H	-0.959869	-1.400469	-2.474481
H	-2.025620	-0.060240	-2.873142
C	0.089428	0.435201	-2.924149
H	-0.049260	1.516762	-2.800092
H	0.182685	0.247651	-3.997865
N	-1.203512	-0.042320	2.112964
H	-1.787235	-0.846953	1.884315
H	-1.762144	0.788564	1.916939

Transition state structure 2

C	-0.015688	-0.037734	-0.107546
C	-0.044113	-0.034697	1.291596
N	2.361694	0.007076	-0.023931
C	1.170441	-0.021891	2.048360
C	1.236220	-0.014944	-0.758978
C	2.408528	0.002818	1.350444
C	1.214716	-0.025849	3.467230

H	4.572828	0.045574	1.472732
H	3.249126	0.028609	-0.520927
C	2.421535	-0.005839	4.131065
H	0.284904	-0.044919	4.024628
H	2.442957	-0.009755	5.215983
C	3.639229	0.020598	3.410699
H	4.581675	0.037009	3.948669
C	3.640768	0.025614	2.031140
C	1.396356	-0.036853	-2.257892
H	2.235330	0.609681	-2.546564
H	1.679609	-1.060569	-2.546709
C	-1.295326	-0.032010	-0.923239
H	-1.737291	0.971189	-0.847027
H	-2.018778	-0.699532	-0.448994
C	-1.085755	-0.394783	-2.399681
H	-0.921270	-1.476153	-2.500846
H	-1.998902	-0.164807	-2.957140
C	0.107736	0.361584	-2.990606
H	-0.050028	1.443917	-2.901088
H	0.224538	0.144006	-4.056419
N	-1.324291	-0.039807	1.918653
H	-1.451722	0.774499	2.518464
H	-1.456422	-0.867620	2.499092

Protonated tacrine (1·H$^+$) with DMSO solvation included:

Ground state structure

C	-1.002555	-0.052231	-0.701804
C	-1.044184	-0.005358	0.718873
N	1.374800	0.020436	-0.625212
C	0.193591	0.013354	1.469416
C	0.229834	-0.020021	-1.341504
C	1.412328	0.026520	0.749070
C	0.260457	0.022697	2.884409
H	3.571822	0.065290	0.832218
H	2.274091	0.050941	-1.126006
C	1.477849	0.046036	3.535800
H	-0.649084	0.007066	3.481821
H	1.509300	0.051081	4.623385
C	2.680184	0.063030	2.797468
H	3.636283	0.082621	3.317632
C	2.652634	0.053644	1.417302
C	0.379723	-0.035597	-2.842240
H	1.214028	0.619908	-3.123881
H	0.669684	-1.053918	-3.143234
C	-2.293171	-0.098014	-1.496953

H	-2.809691	0.869426	-1.392688
H	-2.965118	-0.850310	-1.059598
C	-2.092891	-0.414483	-2.986623
H	-1.908539	-1.490250	-3.112262
H	-3.015931	-0.183748	-3.529970
C	-0.910975	0.369036	-3.561447
H	-1.081559	1.447352	-3.440247
H	-0.800913	0.178375	-4.634595
N	-2.222833	0.019529	1.355784
H	-2.299091	0.067855	2.367322
H	-3.104072	0.032730	0.854763

Transition state structure 1

C	-1.004270	-0.013119	-0.675755
C	-1.017704	-0.020012	0.723021
N	1.372761	0.011566	-0.632868
C	0.206286	-0.028888	1.456672
C	0.237502	0.009198	-1.345433
C	1.431605	-0.012889	0.738052
C	0.264097	-0.048503	2.875408
H	3.595957	-0.002106	0.821257
H	2.273442	0.035366	-1.141449
C	1.481594	-0.053123	3.520329
H	-0.670808	-0.059908	3.425479
H	1.520289	-0.069326	4.607947
C	2.690149	-0.036434	2.781687
H	3.643259	-0.039964	3.307826
C	2.674257	-0.015591	1.402311
C	0.367236	0.013875	-2.846371
H	1.218539	0.644908	-3.132701
H	0.619866	-1.010875	-3.160536
C	-2.297106	0.012677	-1.468870
H	-2.749796	1.009419	-1.352468
H	-3.009898	-0.691280	-1.022687
C	-2.118914	-0.297845	-2.961735
H	-1.965820	-1.377157	-3.099867
H	-3.040258	-0.036409	-3.493817
C	-0.923059	0.461067	-3.542444
H	-1.062983	1.542149	-3.407934
H	-0.828967	0.279438	-4.618464
N	-2.228558	-0.014469	1.478662
H	-2.812133	-0.819411	1.222696
H	-2.783569	0.818644	1.250051

Transition state structure 2

C	-1.003721	-0.018654	-0.700189

C	-1.040497	-0.015711	0.695604
N	1.373867	0.027945	-0.619613
C	0.174687	-0.004520	1.451497
C	0.250812	0.005038	-1.349612
C	1.410687	0.020497	0.752515
C	0.217456	-0.011143	2.870508
H	3.573056	0.060169	0.864295
H	2.282705	0.052271	-1.113613
C	1.425575	0.005982	3.533786
H	-0.713602	-0.030289	3.430929
H	1.446513	-0.000209	4.621933
C	2.643660	0.032218	2.813103
H	3.589294	0.046097	3.352185
C	2.644147	0.040205	1.433796
C	0.407574	-0.019757	-2.847952
H	1.248817	0.625303	-3.133149
H	0.692963	-1.045029	-3.131183
C	-2.281523	-0.013829	-1.518439
H	-2.721872	0.991687	-1.451859
H	-3.005453	-0.681903	-1.044290
C	-2.070948	-0.383307	-2.992538
H	-1.896012	-1.464480	-3.085901
H	-2.986202	-0.160385	-3.552448
C	-0.878798	0.375715	-3.581744
H	-1.041945	1.457965	-3.488858
H	-0.760412	0.158283	-4.648781
N	-2.319447	-0.020233	1.329278
H	-2.406836	0.791465	1.951809
H	-2.412543	-0.847393	1.930933

Protonated 4-aminoquinaldine ($12 \cdot H^+$) with no solvent included:

Ground state structure

C	-1.714567	1.854405	-0.751939
C	-2.935628	1.208820	-0.743483
C	-3.018837	-0.161845	-0.425249
C	-1.876709	-0.873259	-0.118239
C	-0.607941	-0.245951	-0.116611
C	-0.547597	1.133985	-0.439796
C	0.631035	-0.924895	0.194214
C	1.834647	-0.188572	0.161922
C	1.848199	1.154586	-0.158045
N	0.678690	1.771817	-0.445795
C	3.096448	1.984875	-0.207436
N	0.654567	-2.228014	0.509054
H	-1.647275	2.910902	-0.996861
H	-3.837249	1.763004	-0.984072

H	-3.983474	-0.658141	-0.421860
H	-1.970508	-1.927244	0.122881
H	2.773803	-0.678947	0.391702
H	0.695216	2.758833	-0.680019
H	3.244670	2.407322	-1.208449
H	3.972384	1.383717	0.040968
H	3.039992	2.816912	0.504599
H	1.525586	-2.693228	0.724679
H	-0.179452	-2.794082	0.544832

Transition state structure 1

C	-1.721761	1.855653	-0.867046
C	-2.937090	1.197861	-0.867403
C	-3.028167	-0.166215	-0.503909
C	-1.901502	-0.871552	-0.139905
C	-0.636402	-0.230994	-0.126492
C	-0.568525	1.143317	-0.495949
C	0.571247	-0.900199	0.236692
C	1.771631	-0.198169	0.220257
C	1.818559	1.154685	-0.142478
N	0.667255	1.758663	-0.481378
C	3.079578	1.964582	-0.143922
N	0.481661	-2.275032	0.600265
H	-1.653706	2.903441	-1.146587
H	-3.834855	1.737973	-1.151378
H	-3.995986	-0.656843	-0.513651
H	-1.942948	-1.916774	0.142104
H	2.697808	-0.693444	0.491540
H	0.701773	2.739541	-0.747365
H	2.995951	2.854975	-0.774201
H	3.919357	1.364654	-0.504423
H	3.320463	2.290332	0.875907
H	1.052312	-2.855262	-0.014216
H	0.819345	-2.426193	1.550538

Transition state structure 2

C	-1.681258	1.789771	-0.945975
C	-2.876686	1.099253	-0.983147
C	-2.939913	-0.259652	-0.598269
C	-1.805642	-0.921058	-0.177849
C	-0.559086	-0.249305	-0.124959
C	-0.521736	1.118672	-0.517667
C	0.661997	-0.869283	0.300713
C	1.831479	-0.125554	0.317129
C	1.847453	1.221809	-0.073829
N	0.690970	1.777835	-0.467867

C	3.088667	2.059684	-0.070620
N	0.750641	-2.226922	0.715608
H	-1.631598	2.834261	-1.241590
H	-3.777945	1.606758	-1.311927
H	-3.890158	-0.782218	-0.635518
H	-1.855080	-1.963463	0.117201
H	2.749271	-0.602350	0.640239
H	0.701548	2.754330	-0.751410
H	2.900778	3.083015	-0.407412
H	3.846430	1.614251	-0.724665
H	3.513900	2.100492	0.938288
H	0.160903	-2.415920	1.525351
H	0.471066	-2.869405	-0.024828

Protonated 4-aminoquinaldine (12·H$^+$) with DMSO included:

Ground state structure

C	-1.713962	1.855867	-0.755766
C	-2.935391	1.210664	-0.745524
C	-3.019098	-0.160000	-0.424474
C	-1.876058	-0.871756	-0.116446
C	-0.608424	-0.243276	-0.117021
C	-0.544859	1.135695	-0.442299
C	0.629490	-0.927099	0.195376
C	1.831694	-0.185902	0.161321
C	1.840518	1.156020	-0.160939
N	0.675669	1.778988	-0.451712
C	3.095644	1.976131	-0.204004
N	0.658909	-2.224996	0.510915
H	-1.637241	2.914519	-1.002133
H	-3.839357	1.766965	-0.987499
H	-3.986191	-0.658538	-0.419203
H	-1.965365	-1.928634	0.128253
H	2.771466	-0.681689	0.393730
H	0.678491	2.778928	-0.693893
H	3.233527	2.421267	-1.196819
H	3.965811	1.358495	0.025652
H	3.046252	2.795622	0.523440
H	1.545135	-2.681842	0.724510
H	-0.170661	-2.810428	0.551533

Transition state structure 1

C	-1.721698	1.852472	-0.879210
C	-2.938816	1.200393	-0.881534
C	-3.033847	-0.162226	-0.511307
C	-1.908889	-0.867364	-0.139996
C	-0.641436	-0.231676	-0.124637

C	-0.568907	1.138764	-0.500017
C	0.565206	-0.900522	0.246918
C	1.760095	-0.196762	0.231378
C	1.803804	1.155613	-0.139855
N	0.660550	1.761206	-0.487018
C	3.075810	1.946463	-0.144026
N	0.488223	-2.276647	0.619386
H	-1.638264	2.901365	-1.162539
H	-3.836658	1.743219	-1.172314
H	-4.005206	-0.653141	-0.521549
H	-1.960309	-1.912648	0.146646
H	2.688361	-0.692126	0.510283
H	0.680481	2.756235	-0.766251
H	2.954722	2.908410	-0.650428
H	3.869831	1.380460	-0.641043
H	3.400081	2.135663	0.886806
H	1.110914	-2.823141	0.011161
H	0.871952	-2.389012	1.566147

Transition state structure 2

C	-1.676945	1.785083	-0.941436
C	-2.871433	1.093738	-0.975924
C	-2.931650	-0.265350	-0.589673
C	-1.795444	-0.925983	-0.171044
C	-0.550163	-0.251134	-0.122196
C	-0.514164	1.115629	-0.514797
C	0.672549	-0.869847	0.300166
C	1.835529	-0.121456	0.313173
C	1.842787	1.227546	-0.079093
N	0.691162	1.784386	-0.471140
C	3.090316	2.055245	-0.070240
N	0.754986	-2.232531	0.712201
H	-1.618309	2.832543	-1.236454
H	-3.776666	1.601562	-1.304199
H	-3.883743	-0.791546	-0.624217
H	-1.845384	-1.970880	0.125047
H	2.763792	-0.587699	0.633120
H	0.682819	2.775964	-0.764316
H	2.907379	3.072773	-0.426844
H	3.852164	1.589922	-0.705656
H	3.497098	2.106222	0.946258
H	0.123343	-2.400015	1.505002
H	0.425975	-2.849171	-0.040738

Protonated 9-azetidinyl-1,2,3,4-tetrahydroacridine (13·H$^+$) with no solvent included:

Ground state structure

C	-2.132505	2.610429	-1.582374
C	-3.438121	2.290651	-1.268516
C	-3.721547	1.113287	-0.551912
C	-2.696269	0.297158	-0.114687
C	-1.337931	0.610492	-0.379047
C	-1.088890	1.762469	-1.168872
C	-0.187824	-0.160025	0.082133
C	1.073050	0.040888	-0.583354
C	1.237151	1.175008	-1.362753
N	0.203939	2.033116	-1.555660
C	2.201389	-0.982702	-0.511640
C	3.240088	-0.804095	-1.627550
C	3.702666	0.651838	-1.689870
C	2.519673	1.548009	-2.070101
N	-0.298424	-1.035967	1.092616
C	0.738005	-1.607296	2.004073
C	-0.362554	-1.903952	3.046703
C	-1.392650	-1.300653	2.067891
H	-1.901857	3.495717	-2.169108
H	-4.246158	2.936604	-1.596916
H	-4.750915	0.839958	-0.344733
H	-2.952075	-0.617390	0.399025
H	0.368881	2.867379	-2.107770
H	1.767452	-1.987014	-0.573143
H	2.723603	-0.925172	0.450517
H	2.809337	-1.099540	-2.593525
H	4.085122	-1.473782	-1.438667
H	4.505595	0.783440	-2.421372
H	4.106011	0.955721	-0.715417
H	2.744049	2.604054	-1.867227
H	2.333957	1.475142	-3.151869
H	1.475952	-0.860343	2.308338
H	1.246404	-2.482735	1.596344
H	-0.255302	-1.354428	3.982730
H	-0.508991	-2.962630	3.263782
H	-2.136128	-2.009406	1.691703
H	-1.893188	-0.387468	2.403439

Transition state structure 1

C	-2.073761	2.643172	-1.474619
C	-3.249675	2.550100	-0.761161
C	-3.393424	1.583018	0.260549
C	-2.363204	0.719852	0.562332
C	-1.131469	0.777766	-0.146117

C	-1.019715	1.759996	-1.170418
C	-0.007700	-0.079885	0.111319
C	1.163423	0.045642	-0.656274
C	1.227237	1.031646	-1.659828
N	0.163746	1.827968	-1.866139
C	2.367021	-0.841527	-0.395354
C	3.398886	-0.830835	-1.531235
C	3.697946	0.599012	-1.990319
C	2.424169	1.244799	-2.552706
N	-0.008783	-1.064270	1.117980
C	-0.172032	-0.808180	2.577978
C	-0.828866	-2.206392	2.709964
C	-0.908367	-2.253236	1.162458
H	-1.954171	3.382258	-2.262432
H	-4.070726	3.223345	-0.985919
H	-4.326554	1.522877	0.811224
H	-2.492603	-0.012517	1.347048
H	0.237047	2.535618	-2.593012
H	2.018525	-1.856443	-0.189311
H	2.840883	-0.502585	0.536464
H	3.026804	-1.418624	-2.381380
H	4.314567	-1.322452	-1.188398
H	4.473732	0.612763	-2.761682
H	4.074114	1.193419	-1.147957
H	2.565733	2.319751	-2.725617
H	2.191204	0.801198	-3.532723
H	-0.842433	0.025442	2.824443
H	0.780366	-0.654431	3.095863
H	-1.782183	-2.239941	3.239870
H	-0.159583	-2.959009	3.130005
H	-0.484014	-3.133309	0.667701
H	-1.915146	-2.079244	0.760614

Transition state structure 2

C	-1.756509	3.235835	-1.203566
C	-2.842937	3.390351	-0.366598
C	-3.104690	2.451959	0.659845
C	-2.277344	1.366578	0.845947
C	-1.143300	1.175855	0.013551
C	-0.908911	2.128732	-1.013286
C	-0.243892	0.067961	0.166493
C	0.864674	-0.058877	-0.693894
C	1.048763	0.903401	-1.709257
N	0.182215	1.925394	-1.823771
C	1.919797	-1.139890	-0.513002
C	2.810576	-1.356280	-1.744010

C	3.340082	-0.023514	-2.275904
C	2.168687	0.860958	-2.721274
N	-0.541774	-0.826661	1.210361
C	-0.811438	-2.285347	1.131579
C	-0.357978	-2.400711	2.610439
C	0.196265	-0.957310	2.495504
H	-1.553779	3.950292	-1.996917
H	-3.506260	4.238960	-0.501302
H	-3.969606	2.590485	1.300532
H	-2.466016	0.632655	1.619673
H	0.348250	2.603764	-2.563057
H	1.448650	-2.081653	-0.229798
H	2.551659	-0.851397	0.339091
H	2.241823	-1.868841	-2.531409
H	3.639037	-2.018063	-1.472991
H	4.014253	-0.176347	-3.123889
H	3.917710	0.489350	-1.496399
H	2.504445	1.883281	-2.938709
H	1.749970	0.466292	-3.659581
H	-0.183489	-2.851609	0.432086
H	-1.860199	-2.511512	0.911605
H	0.376908	-3.177334	2.826493
H	-1.191294	-2.487615	3.309825
H	-0.112239	-0.235071	3.258954
H	1.288887	-0.917311	2.389848

Protonated 9-azetidinyl-1,2,3,4-tetrahydroacridine (13·H^+) with methanol included:

Ground state structure

C	-2.128973	2.609586	-1.578193
C	-3.434634	2.289727	-1.264496
C	-3.719798	1.108424	-0.552387
C	-2.695118	0.288564	-0.118567
C	-1.336635	0.603654	-0.381863
C	-1.084652	1.757604	-1.168230
C	-0.187791	-0.168898	0.076034
C	1.069322	0.035363	-0.588387
C	1.232168	1.173880	-1.365132
N	0.203189	2.031482	-1.558426
C	2.198405	-0.985597	-0.512224
C	3.238203	-0.805506	-1.626030
C	3.698715	0.651337	-1.682416
C	2.517172	1.545966	-2.066498
N	-0.299802	-1.050772	1.081903
C	0.739572	-1.607430	1.997641
C	-0.358912	-1.898102	3.043772
C	-1.389226	-1.292922	2.066822

H	-1.888296	3.496765	-2.163137
H	-4.244453	2.939959	-1.590567
H	-4.751725	0.833591	-0.344340
H	-2.954785	-0.629410	0.389625
H	0.364499	2.885928	-2.108573
H	1.766537	-1.991626	-0.571556
H	2.720270	-0.924329	0.450276
H	2.807257	-1.094857	-2.594699
H	4.083428	-1.476698	-1.436215
H	4.505863	0.786905	-2.410503
H	4.094491	0.950623	-0.702516
H	2.734940	2.603592	-1.863767
H	2.332402	1.473245	-3.148886
H	1.472117	-0.851477	2.295520
H	1.252335	-2.485433	1.598857
H	-0.246597	-1.346004	3.978732
H	-0.509217	-2.957747	3.258688
H	-2.146963	-1.994304	1.703452
H	-1.872315	-0.368321	2.399500

Transition structure 1

C	-2.064835	2.645746	-1.472536
C	-3.243236	2.553463	-0.763855
C	-3.392045	1.583624	0.255471
C	-2.363710	0.718552	0.561149
C	-1.128691	0.778220	-0.142636
C	-1.011807	1.759937	-1.166210
C	-0.004932	-0.077580	0.112675
C	1.159685	0.045327	-0.655616
C	1.223353	1.035308	-1.660137
N	0.167115	1.832469	-1.864079
C	2.361863	-0.844043	-0.396145
C	3.391126	-0.836436	-1.533852
C	3.692547	0.594041	-1.988037
C	2.421806	1.241544	-2.550224
N	-0.002645	-1.062471	1.125539
C	-0.183729	-0.801210	2.578551
C	-0.814525	-2.211735	2.711828
C	-0.893618	-2.253509	1.163757
H	-1.931533	3.383964	-2.262916
H	-4.065173	3.229940	-0.991001
H	-4.330008	1.521119	0.803856
H	-2.505633	-0.014552	1.344738
H	0.232786	2.557942	-2.599569
H	2.012876	-1.859523	-0.190893
H	2.840965	-0.503219	0.533128

H	3.010467	-1.416558	-2.386296
H	4.305629	-1.334787	-1.193211
H	4.470112	0.608721	-2.759329
H	4.066702	1.183855	-1.140392
H	2.560069	2.316523	-2.725092
H	2.183641	0.796457	-3.528985
H	-0.877065	0.016554	2.816314
H	0.760707	-0.623924	3.106257
H	-1.768324	-2.261654	3.241371
H	-0.128114	-2.952910	3.127865
H	-0.467051	-3.131155	0.663666
H	-1.903783	-2.081279	0.768058

Transition state structure 2

C	-1.741695	3.240152	-1.191125
C	-2.826691	3.397238	-0.353762
C	-3.095286	2.452073	0.665868
C	-2.275019	1.359172	0.843947
C	-1.141971	1.167622	0.010088
C	-0.900321	2.124514	-1.009682
C	-0.246779	0.055721	0.152614
C	0.854382	-0.069925	-0.708297
C	1.040323	0.902197	-1.719721
N	0.184995	1.927599	-1.825370
C	1.908130	-1.151663	-0.528820
C	2.813693	-1.355569	-1.750622
C	3.335808	-0.016469	-2.271955
C	2.160578	0.854084	-2.728331
N	-0.542378	-0.842446	1.198141
C	-0.787223	-2.301648	1.134447
C	-0.358378	-2.389965	2.623128
C	0.171269	-0.937775	2.495130
H	-1.524865	3.955141	-1.984200
H	-3.485789	4.254059	-0.482310
H	-3.961884	2.591040	1.309513
H	-2.474958	0.622185	1.614293
H	0.348444	2.629699	-2.568028
H	1.437201	-2.099275	-0.264422
H	2.529694	-0.870912	0.334275
H	2.254607	-1.865967	-2.547179
H	3.643995	-2.013547	-1.471088
H	4.021149	-0.160309	-3.114134
H	3.897171	0.499901	-1.481713
H	2.482837	1.878008	-2.957733
H	1.741127	0.444354	-3.660641
H	-0.138136	-2.871788	0.457334

H	-1.829490	-2.549333	0.900469
H	0.389420	-3.149633	2.859595
H	-1.202960	-2.481900	3.310095
H	-0.165709	-0.210446	3.243509
H	1.265705	-0.879429	2.409898

Protonated *N*,*N*-dimethylquinoline (14·H$^+$) with no solvent included:

Ground state structure

C	-3.155966	-4.266425	0.032891
C	-1.776049	-4.276146	-0.025264
C	-1.030002	-3.073362	-0.125723
C	-1.769509	-1.857119	-0.067389
C	-3.175528	-1.852885	-0.038544
C	-3.862587	-3.049835	-0.004347
H	-3.696289	-5.203237	0.120192
H	-1.262138	-5.223882	0.050509
C	0.426455	-3.005288	-0.189551
H	-3.707937	-0.905710	-0.020077
H	-4.947486	-3.048756	0.024904
C	0.251088	-0.598785	0.103386
C	1.021364	-1.731737	0.035331
H	0.687247	0.388711	0.199516
H	2.094636	-1.611986	0.059019
N	-1.089941	-0.656467	0.009327
N	1.211199	-4.076125	-0.432824
H	-1.629899	0.200551	0.047338
C	2.653606	-4.023525	-0.157683
H	3.018774	-5.048050	-0.066065
H	3.203315	-3.527674	-0.967896
H	2.847379	-3.512282	0.786847
C	0.810037	-5.238418	-1.240212
H	1.606370	-5.433501	-1.964780
H	0.680340	-6.134414	-0.623245
H	-0.105440	-5.032182	-1.792115

Transition state structure 1

C	-2.526454	-3.879774	1.815432
C	-1.383498	-4.048144	1.066176
C	-0.988315	-3.053775	0.133159
C	-1.806650	-1.890062	0.001676
C	-2.972669	-1.726377	0.771220
C	-3.321329	-2.717327	1.667170
H	-2.825756	-4.641743	2.527746
H	-0.758518	-4.927976	1.160866
C	0.185238	-3.172429	-0.670874
H	-3.582974	-0.834630	0.657879

H	-4.218982	-2.602257	2.266604
C	-0.319318	-1.029159	-1.664850
C	0.500894	-2.144916	-1.565486
H	-0.119985	-0.205835	-2.341482
H	1.384050	-2.202842	-2.190629
N	-1.418934	-0.928210	-0.904927
N	0.988364	-4.334940	-0.528711
H	-2.002287	-0.100861	-0.997242
C	1.023395	-5.163704	-1.746615
H	0.003938	-5.388838	-2.071313
H	1.568187	-4.692892	-2.581344
H	1.519914	-6.106283	-1.500726
C	2.332877	-4.045266	0.000214
H	2.250935	-3.469650	0.926151
H	2.818313	-4.997314	0.231307
H	2.972601	-3.493331	-0.707852

Transition state structure 2

C	-2.815262	-4.392816	0.380679
C	-1.482357	-4.281969	0.052854
C	-0.883054	-3.006507	-0.129292
C	-1.718253	-1.857965	0.041664
C	-3.080336	-1.978908	0.376864
C	-3.617116	-3.238311	0.543277
H	-3.258961	-5.373683	0.516574
H	-0.877423	-5.170450	-0.069280
C	0.497355	-2.816498	-0.470920
H	-3.692464	-1.089646	0.500800
H	-4.665885	-3.344379	0.801747
C	0.131373	-0.422102	-0.449379
C	0.974430	-1.512631	-0.623904
H	0.459843	0.605224	-0.558407
H	2.014933	-1.358356	-0.881709
N	-1.155105	-0.613086	-0.130685
N	1.425195	-3.866141	-0.667412
H	-1.754747	0.198556	-0.007581
C	1.850188	-4.602912	0.528238
H	1.131791	-5.363452	0.873303
H	2.793834	-5.106887	0.298018
H	2.034436	-3.902432	1.347560
C	1.262303	-4.671196	-1.883301
H	2.212616	-5.174357	-2.086264
H	0.475707	-5.439707	-1.818233
H	1.039997	-4.017920	-2.731664

Protonated *N*,*N*-dimethylquinoline (14·H$^+$) with methanol included:

Ground state structure

C	-3.148820	-4.270737	0.042882
C	-1.768685	-4.279014	-0.014916
C	-1.026331	-3.073873	-0.120280
C	-1.765605	-1.857698	-0.066405
C	-3.173733	-1.855589	-0.037822
C	-3.857819	-3.053704	0.001007
H	-3.688274	-5.211274	0.133797
H	-1.254115	-5.227407	0.067090
C	0.428009	-3.004025	-0.185988
H	-3.700465	-0.901953	-0.023166
H	-4.945952	-3.054951	0.030543
C	0.245862	-0.599924	0.092071
C	1.022145	-1.734307	0.025658
H	0.679723	0.393788	0.179655
H	2.096678	-1.605053	0.041960
N	-1.091053	-0.658983	0.005329
N	1.206548	-4.088156	-0.414981
H	-1.634799	0.216028	0.036682
C	2.644285	-4.039709	-0.136264
H	3.004565	-5.065972	-0.033557
H	3.201190	-3.551873	-0.947805
H	2.835439	-3.516162	0.802698
C	0.811133	-5.223136	-1.259014
H	1.608033	-5.393173	-1.990971
H	0.681099	-6.139279	-0.671336
H	-0.106019	-5.002395	-1.803320

Transition state structure 1

C	-2.533431	-3.877018	1.818448
C	-1.389120	-4.050451	1.071699
C	-0.988863	-3.059522	0.137164
C	-1.802702	-1.894980	0.001605
C	-2.971462	-1.726092	0.769684
C	-3.325810	-2.712369	1.666778
H	-2.836199	-4.639567	2.533641
H	-0.770880	-4.936339	1.175505
C	0.184539	-3.176071	-0.667721
H	-3.572595	-0.826203	0.644172
H	-4.226837	-2.593659	2.266232
C	-0.322935	-1.035920	-1.657621
C	0.501596	-2.155182	-1.558995
H	-0.123880	-0.208723	-2.336467
H	1.385741	-2.205095	-2.189730
N	-1.417562	-0.934799	-0.901920

N	0.992425	-4.344148	-0.525284
H	-2.007564	-0.088914	-1.001248
C	1.030236	-5.161984	-1.746186
H	0.009874	-5.387101	-2.069912
H	1.567895	-4.679788	-2.579972
H	1.534019	-6.105018	-1.511500
C	2.335414	-4.047042	-0.006646
H	2.252895	-3.471321	0.919824
H	2.833015	-4.995470	0.219345
H	2.965231	-3.485756	-0.717344

Transition state structure 2

C	-2.807059	-4.394706	0.379790
C	-1.473482	-4.284366	0.051929
C	-0.873853	-3.008588	-0.130434
C	-1.709143	-1.861155	0.040183
C	-3.072751	-1.982823	0.375479
C	-3.610333	-3.240817	0.542375
H	-3.249777	-5.379616	0.515627
H	-0.876793	-5.180166	-0.068024
C	0.504761	-2.808060	-0.472572
H	-3.676656	-1.083973	0.496746
H	-4.662175	-3.347858	0.801459
C	0.123406	-0.419483	-0.448311
C	0.975720	-1.508964	-0.625081
H	0.446419	0.614211	-0.556716
H	2.017243	-1.340789	-0.884063
N	-1.155521	-0.615755	-0.130583
N	1.442308	-3.860371	-0.671244
H	-1.765445	0.212918	-0.005688
C	1.843390	-4.606256	0.523454
H	1.112413	-5.360306	0.858397
H	2.784526	-5.122762	0.304317
H	2.022493	-3.908691	1.347027
C	1.260305	-4.671254	-1.877023
H	2.202752	-5.189389	-2.086436
H	0.464921	-5.430701	-1.801103
H	1.035370	-4.018810	-2.725957

Protonated *N*-methyltacrine (16·H$^+$) with no solvent included:

Ground state structure 1

C	-1.034307	-0.043035	-0.992942
C	-1.216572	-0.027683	0.429169
N	1.314392	0.083943	-0.682495
C	-0.053224	-0.137556	1.290424
C	0.245066	0.047007	-1.513234

C	1.229335	-0.043279	0.685064
C	-0.082485	-0.374943	2.690815
H	3.372605	-0.006110	0.952464
H	2.237923	0.169280	-1.092814
C	1.079489	-0.452224	3.431946
H	-1.022161	-0.535643	3.196126
H	1.023647	-0.644142	4.498340
C	2.333542	-0.293075	2.812248
H	3.243018	-0.343161	3.402454
C	2.410004	-0.098739	1.448411
C	0.550018	0.120222	-2.990164
H	1.376286	0.824527	-3.152466
H	0.916108	-0.866539	-3.310469
C	-2.237587	-0.063908	-1.921186
H	-2.769687	0.897792	-1.844809
H	-2.944183	-0.839308	-1.592048
C	-1.881043	-0.325740	-3.392952
H	-1.655915	-1.390954	-3.532291
H	-2.751944	-0.102973	-4.016958
C	-0.675927	0.511621	-3.823150
H	-0.891669	1.579269	-3.688692
H	-0.455256	0.361684	-4.884256
N	-2.480119	0.085745	0.883399
H	-3.185203	0.098682	0.160766
C	-2.999529	0.393796	2.215919
H	-3.992893	0.827852	2.087063
H	-2.368362	1.126815	2.722821
H	-3.099367	-0.502222	2.837497

Ground state structure 2

C	-1.031562	-0.039553	-0.768335
C	-1.094353	-0.009987	0.659685
N	1.338533	0.205522	-0.642256
C	0.147447	-0.039946	1.424037
C	0.209603	0.104132	-1.381574
C	1.372013	0.093403	0.728694
C	0.217765	-0.168298	2.834602
H	3.526866	0.229354	0.838787
H	2.220264	0.325423	-1.129356
C	1.428524	-0.156665	3.497096
H	-0.678582	-0.300264	3.432449
H	1.453024	-0.264635	4.576335
C	2.631368	-0.004435	2.779110
H	3.580103	0.009556	3.305858
C	2.606081	0.120114	1.405520
C	0.423713	0.128378	-2.877658

H	1.095667	0.961213	-3.125444
H	0.960097	-0.792326	-3.151157
C	-2.258861	-0.306212	-1.635378
H	-2.894741	0.585394	-1.687194
H	-2.856704	-1.092051	-1.162950
C	-1.909885	-0.734439	-3.067541
H	-1.511497	-1.757837	-3.066949
H	-2.826346	-0.752071	-3.665627
C	-0.881094	0.219104	-3.673927
H	-1.264548	1.247126	-3.650954
H	-0.682054	-0.023536	-4.722000
N	-2.250453	0.021116	1.353226
H	-2.143943	-0.024579	2.354901
C	-3.587094	0.469749	0.942330
H	-3.525553	1.366453	0.322281
H	-4.133803	0.723421	1.852211
H	-4.145994	-0.305623	0.415175

Transition state structure 1

C	-1.030436	0.198619	-0.949703
C	-1.177293	0.258146	0.445456
N	1.296418	-0.197443	-0.665344
C	-0.029397	0.141894	1.297313
C	0.248232	-0.043495	-1.492902
C	1.239766	-0.107442	0.705425
C	-0.068602	0.313495	2.707202
H	3.362638	-0.434057	0.999338
H	2.205501	-0.380773	-1.083402
C	1.077869	0.200316	3.461962
H	-1.009840	0.558551	3.182037
H	1.033149	0.340303	4.537135
C	2.319773	-0.088692	2.848734
H	3.212699	-0.181660	3.458610
C	2.408764	-0.234308	1.480317
C	0.515905	-0.196219	-2.969780
H	1.472543	0.281528	-3.219119
H	0.643564	-1.270129	-3.174583
C	-2.217663	0.383058	-1.875631
H	-2.456472	1.455872	-1.910717
H	-3.090702	-0.092246	-1.421581
C	-1.973388	-0.130612	-3.300653
H	-1.998449	-1.228714	-3.312497
H	-2.787463	0.208035	-3.948841
C	-0.623970	0.357177	-3.835878
H	-0.593190	1.454149	-3.832142
H	-0.470072	0.037857	-4.870939

N	-2.487428	0.421427	0.956153
H	-2.696782	1.367443	1.259488
C	-3.064691	-0.627427	1.808460
H	-4.119094	-0.385848	1.963325
H	-2.590262	-0.759493	2.789938
H	-3.017626	-1.582311	1.276817

Transition state structure 2

C	-1.036324	-0.276261	-0.924978
C	-1.165172	-0.217810	0.471421
N	1.285027	0.186740	-0.705689
C	-0.006703	-0.034594	1.295971
C	0.229305	-0.052725	-1.503871
C	1.249696	0.191821	0.668580
C	-0.024778	-0.104414	2.714904
H	3.369520	0.577735	0.907787
H	2.182503	0.364003	-1.150284
C	1.129819	0.080141	3.442668
H	-0.955787	-0.329138	3.219188
H	1.102529	0.015754	4.525575
C	2.357748	0.346288	2.791941
H	3.257087	0.497269	3.380436
C	2.425841	0.396493	1.415443
C	0.482468	-0.058580	-2.990476
H	1.217027	0.718023	-3.240855
H	0.950103	-1.021977	-3.244946
C	-2.245496	-0.504492	-1.814327
H	-2.864689	0.402268	-1.779331
H	-2.866483	-1.291747	-1.379098
C	-1.886797	-0.835892	-3.269684
H	-1.530979	-1.872587	-3.341668
H	-2.790405	-0.772612	-3.883698
C	-0.808828	0.111053	-3.802902
H	-1.154214	1.150679	-3.737797
H	-0.594576	-0.088439	-4.857007
N	-2.471068	-0.325071	1.006216
H	-2.695880	-1.246459	1.369025
C	-3.023350	0.784884	1.794763
H	-2.552937	0.956731	2.771965
H	-4.085603	0.582706	1.952644
H	-2.944605	1.707211	1.212085

Transition state structure 3

C	-1.023717	-0.025436	-0.799779
C	-1.097160	-0.253845	0.585620
N	1.347625	0.080085	-0.626697

C	0.098873	-0.336848	1.366655
C	0.244518	0.141945	-1.393495
C	1.356025	-0.158277	0.727107
C	0.093684	-0.576122	2.766459
H	3.513010	-0.079052	0.932940
H	2.247456	0.206808	-1.083903
C	1.279134	-0.640768	3.464572
H	-0.865098	-0.700698	3.254318
H	1.268700	-0.824951	4.533994
C	2.517522	-0.462326	2.802602
H	3.441938	-0.513992	3.369242
C	2.564729	-0.219056	1.444810
C	0.465751	0.338222	-2.874293
H	1.229998	1.111566	-3.028324
H	0.889128	-0.597277	-3.270338
C	-2.261330	0.006556	-1.679082
H	-2.746513	0.985827	-1.571549
H	-2.981399	-0.730598	-1.307617
C	-1.961538	-0.234099	-3.164963
H	-1.689104	-1.285130	-3.330028
H	-2.868495	-0.047754	-3.748154
C	-0.824136	0.676697	-3.633093
H	-1.092709	1.726729	-3.461621
H	-0.644856	0.565710	-4.706520
N	-2.317963	-0.419326	1.290381
H	-2.751415	-1.322064	1.113704
C	-3.286049	0.687431	1.306327
H	-3.794174	0.882589	0.353354
H	-2.774246	1.600388	1.623021
H	-4.044194	0.454068	2.058350

Transition state structure 4

C	-1.029951	-0.037290	-0.802257
C	-1.090502	0.295370	0.562248
N	1.346854	-0.087672	-0.653750
C	0.115318	0.441233	1.322115
C	0.235924	-0.225421	-1.397931
C	1.367716	0.239050	0.681128
C	0.124093	0.774866	2.702304
H	3.528161	0.209476	0.861930
H	2.242792	-0.224656	-1.115333
C	1.316571	0.904183	3.379410
H	-0.830046	0.919322	3.193668
H	1.315524	1.159283	4.434230
C	2.549853	0.701613	2.715147
H	3.479993	0.805171	3.265040

C	2.584223	0.369125	1.376094
C	0.435224	-0.577661	-2.851229
H	1.353041	-0.102782	-3.221082
H	0.599269	-1.664093	-2.914260
C	-2.275478	-0.090857	-1.672740
H	-2.643472	0.939227	-1.788983
H	-3.067482	-0.633696	-1.154770
C	-2.055929	-0.716522	-3.058459
H	-1.999571	-1.809375	-2.966362
H	-2.925122	-0.500640	-3.687333
C	-0.775229	-0.195754	-3.712669
H	-0.822057	0.894869	-3.825876
H	-0.647521	-0.615461	-4.714916
N	-2.299566	0.520329	1.267270
H	-2.713055	1.428849	1.080078
C	-3.281784	-0.555992	1.443245
H	-2.752804	-1.486272	1.666518
H	-3.950862	-0.730810	0.590259
H	-3.900124	-0.310009	2.311268

5.2.2.2 Tabulation of calculated rotational barrier results

Table 5.9. Absolute energies, thermodynamic correction factors, and calculated rotation barriers for the tacrine derivatives examined.

Compound	State	Energy (E_h)	Scaled ZPVE (E_h)	T (K)	$G_{corr}(T)$ (E_h)	G(T) (E_h)	$\Delta G(T)$ (kcal/mol)
12·H^+	Minimum	-497.015186	0.190405	313	0.152276	-496.862910	0.0
	Transition	-496.989404	0.189637	313	0.151933	-496.837471	16.0
	Transition	-496.987832	0.189488	313	0.151348	-496.836484	16.6
1·H^+	Minimum	-613.758750	0.255496	311	0.215550	-613.543200	0.0
	Transition	-613.734126	0.254457	311	0.214951	-613.519175	15.1
	Transition	-613.732783	0.254302	311	0.214719	-613.518064	15.8
13·H^+	Minimum	-730.448954	0.318540	225	0.290363	-730.158591	0.0
	Transition	-730.426725	0.317057	225	0.289027	-730.137698	13.1
	Transition	-730.426260	0.317065	225	0.289048	-730.137212	13.4
14·H^+	Minimum	-536.300746	0.219940	205	0.197619	-536.103127	0.0
	Transition	-536.281193	0.218496	205	0.196621	-536.084572	11.6
	Transition	-536.275669	0.218076	205	0.195980	-536.079689	14.7
16·H^+	Minimum	-653.061951	0.284240	298	0.244707	-652.817244	0.0
	Minimum	-653.057950	0.283609	298	0.243022	-652.814928	1.5
	Transition	-653.039428	0.282267	298	0.243378	-652.796050	13.3
	Transition	-653.037886	0.281783	298	0.242438	-652.795448	13.7
	Transition	-653.037791	0.281892	298	0.242651	-652.795140	13.9
	Transition	-653.037452	0.281953	298	0.242502	-652.794950	14.0

[a] These values include zero-point vibrational energy corrections. [b] Based on the lowest energy ground state structure.

Table 5.10. Absolute energies, thermodynamic correction factors, and calculated rotation barriers for the tacrine derivatives examined with the inclusion of ^{1}H NMR solvent through the PCM model.

Compound (Solvent)	State	Energy (E_h)	Scaled ZPVE (E_h)	T (K)	$G_{corr}(T)$ (E_h)	G(T) (E_h)	$\Delta G(T)$ (kcal/mol)
12·H^+ (d_6-DMSO)	Minimum	-497.098997	0.187919	313	0.149792	-496.949205	0.0
	Transition	-497.073747	0.187271	313	0.149090	-496.924657	15.4
	Transition	-497.073257	0.187281	313	0.149135	-496.924122	15.7
1·H^+ (d_6-DMSO)	Minimum	-613.838126	0.252843	311	0.212683	-613.625443	0.0
	Transition	-613.815326	0.251983	311	0.212292	-613.603034	14.1
	Transition	-613.814646	0.251889	311	0.212151	-613.602495	14.4
13·H^+ (CD_3OD)	Minimum	-730.518114	0.316311	225	0.288008	-730.230106	0.0
	Transition	-730.498950	0.314902	225	0.286817	-730.212133	11.3
	Transition	-730.498147	0.314793	225	0.286588	-730.211559	11.6
14·H^+ (CD_3OD)	Minimum	-536.376294	0.217815	205	0.195430	-536.180864	0.0
	Transition	-536.362035	0.216451	205	0.194584	-536.167451	8.4
	Transition	-536.356854	0.216060	205	0.194006	-536.162848	11.3

[a] These values include zero-point vibrational energy corrections.

References for Chapter 5

1. Michalson, E. T.; D'Andrea, S.; Freeman, J. P.; Szmuszkovicz, J. The synthesis of 9-(1-azetidinyl)-1,2,3,4-tetrahydroacridine. *Heterocycles* **1990,** 30, 415-25.

2. Abeywickrama, C.; Rotenberg, S. A.; Baker, A. D. Inhibition of protein kinase C by dequalinium analogues: Structure-activity studies on head group variations. *Bioorg. Med. Chem.* **2006,** 14, 7796-7803.

3. Brian, W. P.; Souther, B. L. New Derivatives of 9-Amino-1,2,3,4-tetrahydroacridine. *J. Med. Chem.* **1965,** 8, 143-144.

4. Frisch, M. J.; Trucks, G. W.; Schlegel, H. B.; Scuseria, G. E.; Robb, M. A.; Cheeseman, J. R.; J. A. Montgomery, J.; Vreven, T.; Kudin, K. N.; Burant, J. C.; Millam, J. M.; Iyengar, S. S.; Tomasi, J.; Barone, V.; Mennucci, B.; Cossi, M.; Scalmani, G.; Rega, N.; Petersson, G. A.; Nakatsuji, H.; Hada, M.; Ehara, M.; Toyota, K.; Fukuda, R.; Hasegawa, J.; Ishida, M.; Nakajima, T.; Honda, Y.; Kitao, O.; Nakai, H.; Klene, M.; Li, X.; Knox, J. E.; Hratchian, H. P.; Cross, J. B.; Adamo, C.; Jaramillo, J.; Gomperts, R.; Stratmann, R. E.; Yazyev, O.; Austin, A. J.; Cammi, R.; Pomelli, C.; Ochterski, J. W.; Ayala, P. Y.; Morokuma, K.; Voth, G. A.; Salvador, P.; Dannenberg, J. J.; Zakrzewski, V. G.; Dapprich, S.; Daniels, A. D.; Strain, M. C.; Farkas, O.; Malick, D. K.; Rabuck, A. D.; Raghavachari, K.; Foresman, J. B.; Ortiz, J. V.; Cui, Q.; Baboul, A. G.; Clifford, S.; Cioslowski, J.; Stefanov, B. B.; Liu, G.; Liashenko, A.; Piskorz, P.; Komaromi, I.; Martin, R. L.; Fox, D. J.; Keith, T.; Al-Laham, M. A.; Peng, C. Y.; Nanayakkara, A.; Challacombe, M.; Gill, P. M. W.; Johnson, B.; Chen, W.; Wong, M. W.; Gonzalez, C.; Pople, J. A. *Gaussian 03*, Gaussian, Inc.: Pittsburgh, PA, 2003.

Chapter 6. Conclusions and Future Directions

6.1 Re-optimization of the tacrine pharmacophore

Acetylcholinesterase (AChE) is an enzyme of the serine hydrolase family responsible for the termination of cholinergic neurotransmission. Selective, reversible inhibition of this enzyme forms the basis of the treatment of senile dementia due to Alzheimer's disease (AD). However, inhibition can present either therapeutic or toxic effects depending on the administered dose. Systemic inhibition of AChE is a well-known strategy to kill insects, and this work focused on means to control *Anopheles gambiae* (*Ag*), the African malaria vector mosquito.

Tacrine was the first AChE inhibitor approved for the treatment of AD related dementia. In Chapters 2 and 3, we discussed the re-optimization of the tacrine pharmacophore to develop a potent inhibitor that was highly selective for *Ag*AChE over the human enzyme. Beginning with modifications of the tacrine pharmacophore known to cause deleterious effects on mammalian AChE inhibition, 36 tacrine analogs were synthesized using the Friedländer condensation and subsequently assayed for human- and *Ag*AChE inhibition. One mildly potent inhibitor was obtained which exhibited nearly 110-fold selectivity for the mosquito enzyme. Dimerization of this lead compound afforded a highly potent inhibitor that was 1100-fold selective for the mosquito enzyme.

While the optimized tacrine dimer from Chapter 2 exhibited an excellent *in vitro* pharmacological profile, attempts to use the inhibitor as an effective pesticide were unsuccessful. Both WHO contact toxicity[1] and topical application studies[2] showed that the inhibitor was not toxic, suggesting that it could not be delivered to the CNS, where *Ag*AChE is localized. It is possible that these modified tacrine inhibitors are too polar (due to their basicities) to penetrate the lipophilic cuticle of the mosquito. Blood-brain-barrier permeability could pose significant challenges, as well. Also, it is possible that the metabolic pathways of the mosquito decompose the inhibitors before they can reach the neuronal AChE.

We envision two methods by which the first problem could be overcome. First, the PAS-binding portion of the dimer could be modified to incorporate a more lipophilic group. However, this method is not without possible challenges. The known inhibitors of AChE are all highly hydrophilic, and decreasing the polarity of the optimized dimer may greatly decrease the potency toward AChE inhibition. The second method to overcome the poor delivery of the

optimized dimer is through the use of a lipophilic delivery system. If the inhibitor were encapsulated in a relatively non-polar nanoparticle, which can decompose *in vivo*, one could envision penetration of the cuticle with the nanoparticle followed by AChE inhibition by the optimized dimer.

The second problem (metabolism) plagues both drug and pesticide development.[3] Metabolic deactivation of enzymatic inhibitors can be studied through the use of synergists, such as piperonyl butoxide (PBO), which deactivate the enzymes responsible for detoxification.[4] It would be interesting to perform the contact toxicity and topical application studies in the presence of synergists to rule out bio-deactivation of these inhibitors. Our group has performed these experiments for other AChE inhibitors with some success.

6.2 Rotational barriers of *N*-alkyltacrines

The alkyl-linked tacrine dimers, described above, are known to bind AChE with high affinity. Protein X-ray crystal structures of tacrine-containing homo- and heterodimers complexed to AChE possess a wide range of conformations of the alkyl chain relative to the ring system. Because structural evidence suggests that the *N*-alkyltacrine unit is protonated in its binding state, a wide range of conformational energies is expected, ranging from insignificantly low to high enough to be detrimental to binding potency. In Chapters 4 and 5, we discussed our efforts to experimentally and computationally determine the penalties of adopting the crystallographically-derived conformations. The conformational profile of *N*-methyltacrine, as calculated using B3LYP/6-31G*, was generated to estimate the energies associated with the crystallographically determined conformations. In these calculations, we determined that some of the crystallographically-derived conformations were associated with penalties in excess of 7 kcal/mol. To validate the model, the barriers of rotation for two tacrine derivatives and two quinoline derivatives were experimentally determined and compared to computationally-derived rotation barriers. In all four cases, we computationally modeled the experimental rotational barriers to within 2 kcal/mol. Including this error in the N-methyltacrine calculations, we can be sure that the crystallographically-derived conformations are associated with penalties of at least 5 kcal/mol. The results indicate that one cannot prudently exclude high energy conformations when performing virtual ligand screenings at the outset of inhibitor design.

As discussed in Chapter 4, Perola and Charifson[5] used molecular mechanics methods to show that ligands may bind proteins with conformational energies in excess of 9 kcal/mol. Because the free energy of binding for the protein/ligand complex is related to the conformational energy of the ligand, it is important to develop computational methods to predict the shape and conformational energy of the ligand bound to the enzyme. Also, the difference in free energy of binding for a 50 nM ligand and a 100 μM ligand is only 4.5 kcal/mol. Combined with the high conformational energies determined by Perola and Charifson (molecular mechanics methods), as well as those determined in this work (DFT methods), it is apparent that the conformational energy of the ligand is an extremely important component of the free energy of ligand binding. In order to predict even relative binding strengths with virtual ligand screening for protein-ligand complexes, it is important to develop methods by which these highly energetic conformations can be included, while not increasing the occurrence of false positive hits. Our work with high energy conformations of potent AChE inhibitors can be used as a starting point in the development of those methods.

References for Chapter 6

1. Guidelines for testing mosquito adulticides for indoor residual spraying and treatment of mosquito nets. Document WHO/CDS/NTD/WHOPES/GCDPP/2006.3. World Health Organization, Geneva.

2. Pridgeon, J. W.; Pereira, R. M.; Becnel, J. J.; Allan, S. A.; Clark, G. G.; Linthicum, K. J. Susceptibility of *Aedes aegypti*, *Culex quinquefasciatus Say*, and *Anopheles quadrimaculatus Say* to 19 pesticides with different modes of action. *J. Med. Entomol.* **2008,** 45, 82-87.

3. Hemingway, J.; Hawkes, N. J.; McCarroll, L.; Ranson, H. The molecular basis of insecticide resistance in mosquitoes. *Insect Biochem. Mol. Biol.* **2004,** 34, 653-665.

4. Paul, A.; Harrington, L. C.; Scott, J. G. Evaluation of novel insecticides for control of dengue vector *Aedes aegypti* (diptera: *Culicidae*). *J. Med. Entomol.* **2006,** 43, 55-60.

5. Perola, E.; Charifson, P. S. Conformational analysis of drug-like molecules bound to proteins: An extensive study of ligand reorganization upon binding. *J. Med. Chem.* **2004,** 47, 2499-2510.